



**Economic and Empirical Investigation of
Bioelectrochemical Systems for CO₂ utilization**

A thesis submitted to Newcastle University for the Degree of
Doctor of Philosophy

by

Xenia Christodoulou

School of Chemical Engineering and Advanced Materials
Newcastle University, United Kingdom

February 2017

Abstract

This thesis investigates economically and empirically the feasibility of CO₂ reduction into high grade chemicals using microbial electrosynthesis (MES). An economic evaluation was initially performed for MES and anaerobic fermentation (AF) for 100 tonnes per year (t/y) acetic acid production. MES and AF incurred high investment and production costs; however, integrating MES and AF decreased investment costs, doubled production rates, and set production cost at 0.24 £/Kg which is market competitive (0.48 £/Kg). Although integrating MES and AF processes showed to be cost effective, it generated no positive return across 15 years of operation. Similar analyses were used to evaluate MES as stand-alone process for the production of acetic, formic and propionic acids, methanol, and ethanol at higher production rates (1000 t/y). High returns were evaluated for formic acid (21%) and ethanol (14%) compared to the minimum requirements of the industry (11.60%) making these products economically attractive.

Experimentally, volatile fatty acid bioproduction was investigated in H-shape bioelectrochemical systems using *Shewanella Oneidensis* MR-1 as biocatalyst and CO₂ as a substrate on polarised carbon cloth electrodes. Biofilm and mediated driven systems were used to evaluate the influence of electron transfer on bioproduction. It was found that mediated systems (0.66 mmol/L) produced more volatile fatty acids than biofilm systems (0.53 mmol/L), suggesting that the use of mediators enhances electron transfer. Different polarizations (-0.2, -0.4, -0.6 and -0.8 V) were also evaluated on biofilm driven systems, revealing that volatile fatty acid production was not affected by polarization ($p=0.192$) and incurred low cathode capture (13-77%) and energy (0.0009-0.6%) efficiencies which suggests a biochemical process rather than respiration. This was later confirmed using extracted proteins from *Shewanella Oneidensis* MR-1 cells.

The effects of operating conditions (i.e. temperature and agitation) and biofilm development technique: open circuit (OCP) and closed circuit (CCP) potential, were further assessed for energy production. It was found that energy production increased with high temperature (30 °C) and slow agitation (90 rpm), as reflected by higher current generation (median = 12.05 µA), more live cells number (median= 2.3×10^6 cells), and better electrode bacterial coverage (median=35.29%). In addition, using OCP biofilms offered further advantages by reducing the lag phase (1-2 days). The effect of OCP and CCP biofilms operating at the best operating conditions found were then examined for chemical production. OCP and CCP biofilms resulted in the synthesis of different chemicals suggesting that the bacterial metabolism is dependent on the biofilm development conditions. These findings offer insights on MR-1 performance and reveal a bright opportunity towards the use and scale-up of MES for a technically and economically viable bioprocess.

Declaration

I, Xenia Christodoulou, declare that this thesis and the work presented in it are my own and have been generated by me as the result of my own original research.

Title of thesis

I confirm that:

1. This work was done wholly while in candidature for a research degree at this university; Newcastle University
2. No part of this thesis has been previously been submitted for a degree or any other qualification at this or any other University or institution.
3. Where I have consulted the published work of others, has always clearly attributed
4. I have acknowledged all main sources of help
5. Part of this work has been submitted for publications in scientific journals

A handwritten signature in black ink, appearing to read 'Xenia', with a long horizontal flourish extending to the right.

29/09/2016

Acknowledgement

I would like to express my sincere gratitude and special appreciation to my supervisor Dr. Sharon Velasquez-Orta for her continuous support during my Ph.D. study and related research, for her patience, motivation, encouragement and immense knowledge. Her guidance and feedback helped me in all the time of research and writing of this thesis and her advice on both research as well as on my career have been priceless. Her encouragement helped me to continue and finish my research and allowed me to grow as a research scientist. Besides my supervisor, I would like to thank the rest of my thesis supervision: Professor Ian Head and Professor Adam Harvey, for their insightful comments.

I gratefully acknowledge the funding I received towards my Ph.D. from the Engineering and Physical Sciences Research Council Ph.D. fellowship. This project would not be possible without it.

I would especially like to thank the lab technicians in Chemical engineering department, Rob Dixon and Paul Sterling, and the lab technicians in Civil Engineering department, David Race and Harry Drysdale, for their continuous support and help with carrying on experiments and with the analyses of my samples. Special thanks to Tracey Davey and Dr Trevor Booth for their help with screening microbiological samples. Also, huge thanks to Justine McGruther for always looking out for us and never let us miss a deadline.

A special thanks to my family. Words cannot express how grateful I am to my parents, my brother and sister and my parents-in law for all the sacrifices they have made on my behalf and for supporting me spiritually throughout writing this thesis and my life in general. I would also like to thank my friends who supported me in writing and incited me to strive towards my goal. At the end, I would like to express my appreciation to my beloved husband: Dr Ferran Galan, who spent sleepless nights with, for his endless patience and support in the moments when there was no one to answer my queries.

Nomenclature

Anaerobic fermentation	AF
Bioelectrochemical systems	BES
British pounds	£
British pounds per tonne	£/t
Carbon dioxide	CO ₂
Cathode capture efficiency	CCE
Closed circuit potential	CCP
Cyclic voltammetry	CV
Extracellular electron transfer	EET
Mega watts	MW
Microbial electrosynthesis	MES
Microbial fuel cell	MFC
Open circuit potential	OCP
Scanning electron microscopy	SEM
Silver / silver chloride electrode	Ag/AgCl
Standard deviation	STD
Standard hydrogen electrode	SHE
Thousand	k
Thousand tonnes per year	kt/y
Tonnes	t
Tonnes per year	t/y
Watts	W
Year	y

Table of Contents

Abstract	i
Declaration	ii
Acknowledgement	iii
Nomenclature	iv
List of publications	x
List of figures	xi
List of tables	xvi
Chapter 1: Introduction.....	1
1.1 Background.....	1
1.2 Motivation of study.....	3
1.3 Aim	4
1.4 Structure of thesis	5
Chapter 2: Literature review	6
2.1 Bioelectrochemical systems	6
2.1.1 Types of bioelectrochemical systems.....	6
2.2 Electrobiocommodities	8
2.3 Microbial electrosynthesis	9
2.3.1 Formate	10
2.3.2 Methane	10
2.3.3 Acetate	11
2.3.4 Other carbohydrates	12
2.4 Electron transfer mechanisms	13
2.5 Green chemistry and bioelectrochemical systems	16
2.6 Advantages and Challenges: Microbial electrosynthesis vs. bioprocesses.....	16
2.7 Electrochemical fundamentals linking to bioelectrochemical systems	19
2.7.1 Electrode reactions	20
2.7.2 Losses in the system.....	24
2.7.3 Cyclic voltammetry.....	27
2.7.4 Amperometric detection.....	29
Chapter 3: Microbial electrosynthesis and anaerobic fermentation: An economic evaluation for acetic acid production.....	31
3.1 Introduction	31
3.1.1 General hypothesis:	33
3.1.2 Objectives:.....	33

3.2	Theory and methodology	34
3.2.1	Process description and economic analysis based on investment and production costs 34	
3.2.2	Economic analysis based on fixed capital costs	36
3.2.3	Economic analysis based on variable costs	36
3.3	Process economics for bioprocess	38
3.3.1	Bioprocess integration and process economics advancement	38
3.3.2	Renewable energy utilisation and projected productivity levels	38
3.3.3	Economic return and financial risk evaluations	39
3.4	Results and Discussion	41
3.4.1	Fixed capital: equipment costs.....	41
3.4.2	Total Investment and operating costs.....	43
3.4.3	Acetic acid production costs	45
3.4.4	Integration of anaerobic fermentation and microbial electrosynthesis	46
3.4.5	Use of renewable energy, increase of acetic acid production rates and production of other chemicals	49
3.4.6	Pay-back and discounted cash flow rate of return	51
3.5	Conclusions	54
Chapter 4: Comparison of biofilm and mediator driven systems for microbial electrosynthesis using <i>Shewanella Oneidensis</i> MR-1.....		55
4.1	Introduction	55
4.1.1	General hypothesis:	58
4.1.2	Objectives:.....	58
4.2	Materials and methods	59
4.2.1	Growth and inoculum of electroactive culture:.....	59
4.2.2	Experimental set-up and operation of bioelectrochemical cells:	60
4.2.3	Bacterial growth and conditioning period	62
4.2.4	Biosynthesis: CO ₂ as electron acceptor for bioproduction	63
4.2.5	Electrochemical analyses	63
4.2.6	Scanning electron microscopy	65
4.2.7	Calculations and analytical measurements.....	65
4.3	Results and discussion:.....	67
4.3.1	Start-up and operation of BESs	67
4.3.2	Biosynthesis using CO ₂ in BESs	73
4.3.3	Working electrode performance.....	75

4.4	Conclusion:	77
Chapter 5:	Investigation of bioproduction using <i>Shewanella</i> cells	78
5.1	Introduction	78
5.1.1	General hypothesis:	79
5.1.2	Objectives:	79
5.2	Materials and methods:	81
5.2.1	Growth and inoculum of electroactive culture:	81
5.2.2	Experimental set-up and operation of bioelectrochemical cells:	81
5.2.3	Bioproduction	82
5.2.4	Investigation of bioproduction pathway:	83
5.2.5	Electrochemical analyses:	84
5.2.6	Chemical analyses	85
5.2.7	Electrode analyses:	85
5.2.8	Calculations:	86
5.3	Results and Discussion:	89
5.3.1	Start-up and operation of BES:	89
5.4	Effect of set potential on metabolic pathway and bioproduction	93
5.4.1	Performance of <i>Shewanella Oneidensis</i> MR-1:	93
5.4.2	BES performance and efficiency:	98
5.4.3	CO ₂ reduction: Thermodynamics description	100
5.5	The effect of metabolic pathway on bioproduction	100
5.5.1	Role of proteins in CO ₂ reduction pathway:	101
5.6	Hypothesized pathway of bioproduction	104
5.7	Conclusion:	105
Chapter 6:	Effect of temperature, agitation and biofilm development techniques on the performance of bioelectrochemical systems for energy and chemical production	106
6.1	Introduction	106
6.1.1	General hypothesis	107
6.1.2	Objectives	107
6.2	Materials and methodology	108
6.2.1	Experimental set-up of BESs	108
6.2.2	Experimental set-up using polyHIPEs electrodes	110
6.2.3	Cathode: Experimental set-up using carbon cloth electrodes	111
6.2.4	Statistical analysis	111
6.2.5	Electrochemical analyses	112

6.2.5.1	Biofilm growth and conditioning period	112
6.2.6	Biofilm analysis.....	112
6.3	Results and discussion.....	113
6.3.1	Effect of operating temperature, agitation and electrode pre- treatment on anode performance.....	113
6.4	Anodic biofilm growth.....	115
6.4.1	Shewanella Oneidensis MR-1 cultivation on PolyHipe anodes and reactor performance	118
6.4.2	Effect of electrode pre- treatment on cathode performance and chemical production	121
6.5	Conclusions	126
Chapter 7:	Conclusions & Future work	127
7.1	Conclusion	127
7.1.1	Economic evaluation for acetic acid production using MES	127
7.1.2	Investigation of bioproduction.....	128
7.1.3	Investigation of factors affecting energy and chemical production	128
7.2	Summary	129
7.3	Future research	129
References.....		131
Appendices.....		147
A1 - Operating costs.....		147
A2 – Investment and production costs		148
A3 – Selectivity and conversion rates		167
A4: Energy and acetic acid production costs		167
A5: Energy values and costs.....		168
A6: Mass flow rates.....		169
B1: Growth curves in aerobic conditions		177
B2: Medium compositions		178
B3: Growth curves in different anaerobic mediums.....		181
C1 – Bioproduction at -0.2 V polarization		182
C2 – Bioproduction at -0.4 V polarization		183
C3 – Bioproduction at -0.6 V polarization		184
C4 – Bioproduction at -0.8 V polarization		185
C5 – Total organic carbon and volatile fatty acid bioproduction.....		186
C6 – Live/Dead analysis.....		186

D1: Mann Whitney U-test and p-values.....	187
D2: Electrochemical analysis.....	187
D3: Two way interaction tests: Temperature & agitation	188
D4: Two way interaction tests: Temperature & oxygen exposure	189
D5: Two way interaction tests: Agitation & oxygen exposure.....	190

List of publications

1. **X. Christodoulou** and S.B Velasquez-Orta. (2016) 'Microbial electrosynthesis and anaerobic fermentation: An economic evaluation of acetic acid production from CO₂ and CO', *Environmental Engineering & Science*, 50 (20), pp. 11234–11242.
2. **X. Christodoulou**, T. Okoroafor, S.B Velasquez-Orta and S. Parry. Carbon dioxide use in microbial electrosynthesis: advancements, sustainability and economic feasibility. *Accepted for publication in Journal of CO₂ utilization*.
3. **X. Christodoulou**, S.B Velasquez-Orta and I. Head. Investigation of bioproduction using *Shewanella* cells. *Bioresource Technology*. *In preparation*.
4. **X. Christodoulou** and S.B Velasquez-Orta. Effect of temperature, agitation and electrode treatments on the performance of bioelectrochemical systems and biofilm development. *Bioresource Technology*. *In preparation*.
5. S.B Velasquez-Orta, R. Ferschy and **X. Christodoulou**. Sediment microbial fuel cells for continuous in-situ monitoring of water pollution. *In preparation*.

List of figures

Figure 2.1: Schematic representation of a microbial fuel cell	7
Figure 2.2: Schematics of direct and indirect electron transfer by (a) bacterial contact, (b) direct electron transfer using nanowires and (c) indirect electron transfer using mediators. The electrode is presented in grey and the bacteria in pink. <i>S</i> symbolizes the substrate, <i>I</i> the intermediate reactions, <i>M</i> the mediator, e^- the electrons and ox and red symbolize the oxidation and reduction reactions respectively (Adapted from: Huang <i>et al.</i> , 2011).....	14
Figure 2.3: Electron transfer channel in <i>Shewanella Oneidensis</i> MR-1 (Adapted from: Pirbadian <i>et al.</i> (2014a))	15
Figure 2.4: Schematics on electrochemical reactions on a working electrode in an electrochemical cell. (1) Mass transport to the electrode surface, (2) electrochemical reaction at the electrode surface, (3) electron transfer, (4) mass transfer to the bulk solution and (5) electrolyte transport (Adapted from: Zhao <i>et al.</i> , 2009).....	21
Figure 2.5: Schematics of proposed pathways of electron transfer from bacteria to an electrode surface in a bioelectrochemical system using (a) direct electron transfer and (b) indirect electron transfer (Adapted from: Zhao <i>et al.</i> , 2009). (a) (1) direct electron transfer using active sites of extracellular enzymes, (2) Distant bacteria incapable of electron transfer, (3) direct electron transfer using nanowires. (b) (1) indirect electron transfer using metabolites and mediators and (2) indirect electron transfer from distant released metabolites and mediators (mass transfer).....	23
Figure 2.6: Representation of the losses in bioelectrochemical systems (Adapted from: Rismani-Yazdi <i>et al.</i> , 2008)	24
Figure 2.7: (a) forward voltage sweep (oxidation) and back scan (reduction). (b) Resulting cyclic voltamogram showing reversible redox activity with peak currents and peak potentials. E_{pC} is the cathode potential, E_{pA} is the anode potentials, ipC is the cathodic peak current and ipA is the anodic peak current.	28
Figure 2.8: Amperometric detection scan showing the biofilm development state; (a) lag phase, (b) early state of biofilm development and (c) steady state biofilm.	30
Figure 3.1: Bioprocess flowsheet of acetic acid production for a 100 t/y plant. (A) Process flowsheet schematic of microbial electrosynthesis and anaerobic fermentation with main equipment. Code letters and numbers; S: separator, R: reactor, C: rectification column, 1: Microbial electrosynthetic reactor (or anaerobic fermenter), 2: bacterial filter, 3: rectification of water-acetic acid (acetic acid purification), 4: CO ₂ separation. (B) Mass fraction representation throughout the flowsheet. Stream numbers show the mass fraction of the reactants, products and biocatalysts.	35
Figure 3.2: Integrated process flowsheet for the production of acetic acid of 200 t/y plant. (A) Process flowsheet schematic of the integration of anaerobic fermentation and microbial electrosynthesis	

with main equipment. Code letters and numbers; S: separator, R: reactor, C: rectification column, 1: anaerobic fermenter, 2: microbial electrosynthesis reactor, 3: bacterial filter, 4: rectification of water-acetic acid (acetic acid purification), 5: CO₂/N₂/O₂/CO separator. (B) Mass fraction representation throughout the flowsheet. Stream numbers show the mass fraction of the reactants, products and biocatalysts..... 48

Figure 3.3: Cumulative cash flow over time of MES as stand-alone process for the production of ethanol and formic acid (1000 t/y). 52

Figure 4.1: Extracellular electron transfer pathways in bioelectrochemical systems of direct (a) and indirect (b and c) pathways (Adapted from: Rabaey and Rozendal, 2010). The zoom in shows the Mtr Pathway of electron transfer of *Shewanella Oneidensis* MR-1 (Adapted from: Pirbadian *et al.*, 2014b) 56

Figure 4.2: Flow chart of the methodology showing the steps followed in the experimental design . 59

Figure 4.3: Experimental set-up of a bioelectrochemical system in H-shape cells..... 61

Figure 4.4: Schematic experimental set-up and operation of the bioelectrochemical cells showing different contacts of the bacterial cells and the electrode. Direct cell contact with the electrode is shown by (a) and (b) and indirect cell contact with the electrode is shown by (c) (Adapted from: Rabaey and Rozendal, 2010). 62

Figure 4.5: Schematic experimental set-up and operation of the bioelectrochemical cells for biosynthesis (Adapted from: Rabaey and Rozendal, 2010) 63

Figure 4.6: Current generation over time of (A) Mediated Systems and Blank System 1 and (B) Biofilm Systems and Blank System 2. The black star (*) indicates the addition of bacteria and the green star (*) indicates the addition of lactate (1g/L). All systems were operating at a +0.2 V vs. (Ag/AgCl) polarized potential. The experiment was performed in duplicates..... 68

Figure 4.7: Redox activity voltammetry associated with (A) Mediated Systems and Blank System 1 and (B) Biofilm Systems and Blank System 2 with *Shewanella Oneidensis* MR-1. The blanks' voltammetry is shown as a baseline. The arrows indicate the occurred peaks. 69

Figure 4.8: Bioproduction performance of (A) Mediated System and (B) Biofilm System for volatile fatty acids. 73

Figure 4.9: The caclulated carbon fraction present in solution after 48 hours of operation for the Mediated and Biofilm System. 74

Figure 4.10: Cyclic voltammograms of (A) Mediated System and Blank System 1 and (B) Biofilm System and Blank System 2 after 48 hours of biosynthesis in bioelectrochemical systems at a scan rate of 0.005 V/s..... 75

Figure 4.11: Linear sweep voltammetry scans of (A) Mediated System and Blank System 1 and (B) Biofilm System and Blank System 2 at a scan rate of 0.005 V/s. 75

Figure 4.12: Scanning electron microscopy of Mediated System solution (A) and electrode (B) and Biofilm System electrode (C), (D), (E) and (F).....	76
Figure 5.1: Current generation over time of bioelectrochemical systems with their replicates during biofilm formation using <i>Shewanella Oneidensis</i> MR-1. The black star (*) indicates the addition of lactate (1g/L). All bioelectrochemical systems were operating at a +0.2 V vs. (Ag/AgCl) potential. Subfigures A-D are referred to a group that will be polarized with different polarization potentials (A: -0.2V, B: -0.4 V, C: -0.6 V and D: -0.8 V) after biofilm development for bioproduction monitoring. ...	90
Figure 5.2: Redox activity voltammetry associated with bioelectrochemical systems with <i>Shewanella Oneidensis</i> MR-1. The abiotic cell voltammetry is shown as a baseline. Subfigures A-D are referred to a group that will be polarized with different polarization potentials after biofilm development for bioproduction monitoring. At -0.2 V: BES 1-2, at -0.4 V: BES 3-4, at -0.6 V: BES 5-8 and at -0.8 V: BES 9-10. The arrows indicate the observed peaks.....	92
Figure 5.3: Acetate production from biotic microbiological experiments using <i>Shewanella Oneidensis</i> MR-1, CO ₂ as an electron acceptor and H ₂ as an electron donor with no polarization potentials at 30°C (n=3).....	94
Figure 5.4: (A) Formate and (B) acetate reduction; reactants and products balances in biotic microbiological experiments using <i>Shewanella Oneidensis</i> MR-1 and H ₂ as an electron donor at 30°C (n=3).	95
Figure 5.5: Biotic potentiostatically controlled experiments using <i>Shewanella Oneidensis</i> MR-1 with H ₂ as an electron donor and (A) formate and (B) acetate as electron acceptors at 30 °C (n=3).	96
Figure 5.6: Redox activity voltammetry associated with BESs with <i>Shewanella Oneidensis</i> MR-1 using acetate as substrate. The abiotic cell voltammetry is shown as a baseline. E _j stands for the calculated redox potential of BES 1 and BES 2 using coordinated colours. The experiment was performed at 30 °C.	97
Figure 5.7: (A) Total organic carbon and (B) volatile fatty acids data versus different polarizations. BESs 1-4 are referred to a group that was polarized with different polarization potentials (1: -0.2 V, 2: -0.4 V, 3: -0.6 V and 4: -0.8 V).	97
Figure 5.8: Acetate production from biotic microbiological experiments using dead <i>Shewanella Oneidensis</i> MR-1, CO ₂ as an electron acceptor and H ₂ as an electron donor at 30 °C (n=3).....	101
Figure 5.9: (A) Amperometric detection of MES 1 and 2 for electrochemical activity of proteins with CO ₂ . Polarization was performed at -0.8 V vs. Ag/AgCl. The arrows indicate the additions of proteins extracted from <i>Shewanella Oneidensis</i> MR-1 cells and CO ₂ . (B) Cyclic voltammetry of BESs with extracted proteins from <i>Shewanella</i> cells after with CO ₂ . (C) First derivative originated from the cyclic voltammetry in subfigure (B). The arrows indicate the resulted reduction peak. All electrochemical experiments were performed at pH 7.	102

Figure 5.10: (A) Acid and alcohol concentration before and after CO ₂ addition using different concentrations of proteins measured as equivalent to bacterial concentration (CFU/mL). (B) Acid concentration 10 and 30 minutes after applying a potential. The polarized potential used was -0.8 V vs. (Ag/AgCl) and the pH was measured stable at 7.	103
Figure 5.11: Hypothesized pathway of bioproduction using <i>Shewanella Oneidensis</i> MR-1.....	104
Figure 6.1: Schematics on bioelectrochemical systems' overall dimensions and operation.....	108
Figure 6.2: Schematic on hydrodynamic method set-up	109
Figure 6.3: Controls of biofilm development at OCP: (A) Day 0, (B) Day 3, (C) Day 5, (D) Day 7, (E) Day 10 and (F) Day 12	110
Figure 6.4: Steps of the anode electrode preparation; (A) biofilm growth on anode electrode, (B) electrode preparation, (C) bioelectrochemical system set-up	111
Figure 6.5: Current generation over time using <i>Shewanella Oneidensis</i> MR-1 and a polarization potential of +0.2 V (vs. Ag/AgCl); At 90 rpm and 30 °C: A and B, at 90 rpm and 15 °C: C and D, at 140 rpm and 30 °C: E and F, at 140 rpm and 15 °C: G and H. The stars (*) indicate the addition of substrate (lactate). The pH of all reactors was set at 7 with an electrical conductivity of approximately 9 mS/cm.	113
Figure 6.6: Effect of operating conditions in lag-phase and electric current generation. Left: Box plots of temperature conditions (n=8). Centre: Box plots of agitation rates (n=8). Right: Box plots of OCP treatment (n=8). The star (*) indicates the significant pairwise difference (p < 0.05).	114
Figure 6.7: Redox activity associated with <i>Shewanella Oneidensis</i> MR-1 in MFCs and Fluid mechanic reactors at different operating conditions; At 90 rpm and 30 °C: A and B, at 90 rpm and 15 °C: C and D, at 140 rpm and 30 °C: E and F, at 140 rpm and 15 °C: G and H. The arrows indicate the identified peaks at pH 7 and electrical conductivity of approximately 9 mS/cm.....	115
Figure 6.8: Scanning electron microscopy of MFC and Fluid mechanic reactors at different operating conditions. (A) MFC at 90 rpm and 30 °C, (B) Fluid mechanics at 90 rpm and 30 °C, (C) MFC at 140 rpm and 30 °C and (D) Fluid mechanics at 140 rpm and 30 °C. (E) MFC at 90 rpm and 15 °C, (F) Fluid mechanics at 90 rpm and 15 °C, (G) MFC at 140 rpm and 15 °C and (H) Fluid mechanics at 140 rpm and 15 °C.	116
Figure 6.9: Effect of operating conditions in electrode coverage. Box plots of temperature, agitation and OCP treatment (n=8). The star (*) indicates the significant pairwise difference (p < 0.05).	116
Figure 6.10: Live Dead analyses of MFC and Fluid mechanic reactors at different operating conditions. (A) MFC at 90 rpm and 30 °C, (B) Fluid mechanics at 90 rpm and 30 °C, (C) MFC at 140 rpm and 30 °C and (D) Fluid mechanics at 140 rpm and 30 °C. (E) MFC at 90 rpm and 15 °C, (F) Fluid mechanics at 90 rpm and 15 °C, (G) MFC at 140 rpm and 15 °C and (H) Fluid mechanics at 140 rpm and 15 °C.	117

Figure 6.11: Effect of operating conditions in live and dead cells number. Left: Box plots of temperature conditions (n=8). Centre: Box plots of agitation rates (n=8). Right: Box plots of OCP treatment (n=8). The star (*) indicates the significant pairwise difference ($p < 0.05$).	118
Figure 6.12: (A) Amperometric detection of PolyHIPE electrodes at +0.2 V (vs. Ag/AgCl). (B) Cyclic voltammetry of PolyHIPE electrode at a scan rate of 0.001 V/s.	119
Figure 6.13: Scanning electron microscopy on PolyHIPE electrodes; (A) MFC 1 and (B) MFC 2. Confocal microscopy on PolyHIPE electrodes: (C) MFC 1 and (D) MFC 2.	120
Figure 6.14: Current generation over time using <i>Shewanella Oneidensis</i> MR-1 and a polarization potential of -0.8 V (vs. Ag/AgCl) at 90 rpm and 30 °C at (A) CCP (n=3) and (B) OCP (n=3) systems. The colour coordinated stars indicate the addition of CO ₂	121
Figure 6.15: Redox activity associated with <i>Shewanella Oneidensis</i> MR-1 in (A) CCP and (B) OCP systems at different at 90 rpm and 30 °C. The colours coordinated arrows indicate the identified peaks at pH 7. The arrows indicate the identified peaks.	122
Figure 6.16: Total organic carbon production from CCP (n=3, STD = 30.04) and OCP (n=3, STD = 25.32) biofilm systems after 48 hours of operation using CO ₂ as a reactant.	123
Figure 6.17: Scanning electron microscopy on biofilm development on cathode electrodes using; (A) CCP and (B) OCP. Confocal microscopy on biofilm development on cathodes using; (C) CCP and (D) OCP.	125
Figure 9.1 : <i>Shewanella Oneidensis</i> MR-1 growth curves in Luria broth medium under aerobic conditions. The experiment was performed in quadruplicates (n=4).	177
Figure 9.2: <i>Shewanella Oneidensis</i> MR-1 growth curves in three different anaerobic growth mediums. Each experiment was performed in quadruplicates (n=4).	181

List of tables

Table 2-1: Electrochemical half reaction reduction potentials of CO ₂ and free energies based on pH 7	78
Table 2-2: Comparison between fermentation and microbial electrosynthesis processes.....	17
Table 3-1: Acetic acid process, reaction conditions and chemical and bacterial catalyst costs. Chemical catalysts costs were taken from ^a Smejkal <i>et al.</i> (2005) and ^b Soliman <i>et al.</i> (2012). ^c Bacteria catalysts costs were estimated from (ATCC, 2015).....	37
Table 3-2: Energy costs per MWh from different technologies.....	39
Table 3-3: Main reactions occurring in MES for producing different products	40
Table 3-4: Major purchased equipment costs for acetic acid production via methanol carbonylation (200 kt/y), ethane direct oxidation (200 kt/y), AF (100 t/y), MES (100 t/y) and integrated process (200 t/y).....	42
Table 3-5: Investment operating costs and production costs of acetic acid price for methanol carbonylation (200 kt/y), ethane direct oxidation (200 kt/y), AF (100 t/y) and MES (100 t/y) and the integrated processes (200 t/y). The total and detailed variable costs are also shown.	43
Table 3-6: Investment and operating costs of formic and propionic acids and methanol and alcohol using microbial electrosynthesis (1000 t/y).	50
Table 4-1: Electrochemical parameters of the redox reaction potentials vs. Ag/AgCl obtained by the CV scans at a scan rate of 0.005 V/s.	71
Table 4-2: Possible electrochemical potentials vs. Ag/AgCl, at pH 7, of possible reactions occurring in Mediated and Biofilm Systems.....	72
Table 5-1: Experimental design showing the conditions and parameters used for each experimental set.....	82
Table 5-2: Experimental design for chemical production using extracted proteins.....	84
Table 5-3: Molar conversion factors of product formation via MES.....	86
Table 5-4: Gibbs free energy and enthalpy of formation of products formed via MES.....	87
Table 5-5: Electrochemical parameters of the redox reaction potentials vs. Ag/AgCl obtained by the CV scans at a scan rate of 0.001 V/s	93
Table 5-6: Cathode capture efficiency values for bioproduction obtained from CO ₂ reduction using <i>Shewanella Oneidensis</i> MR-1	98
Table 5-7: Energy efficiency values for products derived from CO ₂ reduction using <i>Shewanella Oneidensis</i> MR-1 in H-shape bioelectrochemical systems.....	98
Table 5-8: Maximum theoretical energy efficiency obtained from products derived via MES	99
Table 5-9: Carbon conversion rates into organic compounds at different polarizations	99
Table 9-1: Variables details of chemical processes; methanol carbonylation and ethane direct oxidation, and biological processes; MES and AF	147

Table 9-2: Example of Lang factors calculation for acetic acid production (100 t/y) via MES using the purchased equipment cost.....	166
Table 9-3: Selectivity and conversion rates.....	167
Table 9-4: Energy costs per MWh from different technologies and acetic acid production costs (£/kg) of the Integrated process.....	167
Table 9-5: Energy values of MES	168
Table 9-6: Energy values of anaerobic fermentation and Integrated process.....	168
Table 9-7: Investment, operating and production costs and rate of return of formic and propionic acids and methanol and alcohol using MES (1000 t/y) including full utility costs. Chemical such as: acetic, formic and propionic acids, and alcohols; methanol and ethanol were assessed for plant capacities of 1000 t/y.....	168
Table 9-8: Mass flow rates of MES plant for acetic acid production (100 t/y)	169
Table 9-9: Mass flow rates of AF plant for acetic acid production (100 t/y)	170
Table 9-10: Mass flow rates of integrated process (MES and AF) plant for acetic acid production (200 t/y).....	171
Table 9-11: Mass flow rates of MES plant for acetic acid production (1000 t/y)	172
Table 9-12: Mass flow rates of MES plant for formic acid production (1000 t/y)	173
Table 9-13: Mass flow rates of MES plant for propionic acid production (1000 t/y)	174
Table 9-14: Mass flow rates of MES plant for methanol production (1000 t/y).....	175
Table 9-15: Mass flow rates of MES plant for ethanol production (1000 t/y).....	176
Table 9-16: Medium A.....	178
Table 9-17: Medium B.....	178
Table 9-18: Medium C.....	179
Table 9-19: Vitamin mix	179
Table 9-20: Mineral mix	179
Table 9-21: Amino acids mix	180
Table 9-22: Total organic carbon and volatile fatty acids analyses based on different polarizations	186
Table 9-23: Live/Dead cells count before and after CO ₂ addition	186
Table 9-24: Mann Whitney U-test of operating conditions and electrode pre-treatment effect on lag phase, electric current generation, live/dead cells count and electrode coverage. The 'p' values and Wilcoxon test values are at a confidence level of 95% ($\alpha=0.05$)	187
Table 9-25: Peaks identified from cyclic voltammetry.....	187

Chapter 1: Introduction

1.1 Background

Carbon dioxide (CO₂) is naturally present in the atmosphere as a result of the biogeochemical cycle where carbon exchanges occur among animals, plants, soil, oceans and the atmosphere (NOAA, 2010). Although CO₂ is produced from a range of natural sources, anthropological activity has increased its rate of accumulation in the atmosphere since the beginning of the industrial revolution (NRC, 2010). Deforestation and the produced human-related CO₂ result in the incapability of balancing the biogeochemical cycle and generate air pollution.

Human-related CO₂ has accounted for over than 90% of emissions in the environment during the last 27 years (WEO, 2015). These emissions are mainly a product of the global energy demand. Fossil fuels combustion, such as coal, natural gas and oil, is the main source of energy production and accounts for over than 80% energy-related CO₂ emissions. In addition the demand of chemical production is globally increasing. From 2000 to 2010, the global chemical production has grown 54% (GCO, 2013). Chemical processes responsible for these productions are very often produced by-products and release further CO₂ emissions to the environment.

The increase of CO₂ emissions has also resulted to the temperature increase globally (IPCC, 2007). The National and Atmospheric Administration Climatic Data Centre reported that the average global temperature has risen one degree since the pre-industrial levels, and it will still continue rising by at least 0.6 degrees in the hypothetical case that greenhouse gas emissions end. Since 1880, the year 2012 has been the tenth warmest year globally from the time when the records began (NOAA, 2012). The year 2015 was the warmest in the 136 year recording period and has increased the temperature by 0.86 degrees above the 20th century average (NOAA, 2015).

The need to reduce CO₂ emissions and stop the global temperature increase as well as the ongoing increasing demand of energy (41% by 2035, (BP, 2014)) and chemical production (60% by 2035, (GCO, 2013)) are stimulating the use of CO₂ as a feedstock material for new resources and business opportunities (Centi and Perathoner, 2009).

A promising technology, bioelectrochemistry, has been developed that merges together biological resources and the principles of electrochemistry. Bioelectrochemistry has gained a lot of interest after findings that certain bacteria extracellularly transfer electrons to solid state electrodes. Bioelectrochemistry is accommodated in so-called bioelectrochemical systems (BES); an emergent source of renewable energy which converts organic and inorganic waste

into electricity and/or chemical products (Rabaey *et al.*, 2010). BES usually consist of an anode and a cathode which are separated by a cation or proton exchange membrane. While an electrode reduction occurs in the anode compartment, an electrode oxidation occurs in the cathode compartment. These redox reactions are driven by electroactive biocatalysts; bacteria, at the solid state electrodes which are connected through an electrical circuit that defines the cell's mode.

BES can be divided based on its applications which include microbial fuel cells, microbial desalination cells, microbial solar cells and microbial electrolysis cells. In microbial fuel cells, bacteria function as catalysts to oxidize organic and/or inorganic matter to produce energy and convert it into electrical energy (Logan *et al.*, 2006). In microbial desalination cells, desalination occurs alongside with energy/hydrogen recovery (Cao *et al.*, 2009b). In microbial solar cells, electrical energy and/or chemicals are produced *in situ* by integrating photosynthetic and electroactive bacteria (Strik *et al.*, 2011). In microbial electrolysis cells, bacteria reduce organic or inorganic compounds with the use of external energy to produce chemicals using bioelectrocatalytic processes (Rabaey and Rozendal, 2010).

Processes that explore the use of CO₂ emissions as a carbon source for producing chemicals and processes that can use biological resource for the production of energy can be found in the field of green chemistry, also referred as sustainable chemistry. BES fit within the requirements of the green chemistry principles. BES are operated under mild conditions (designed for energy efficiency), use bacteria as catalysts (less hazardous chemical synthesis), combine all materials used in the reactor into the final product (atom economy) and finally use CO₂ as a renewable feedstock which is not only economically practicable but also treats and prevents waste (prevention of waste and use of renewable feedstock) (Anastas and Warner, 1998). These points place BES technology as a feasible solution to contribute on meeting the 2050 emission reduction target.

Within the technologies under development, microbial electrosynthesis has shown the feasibility to reduce CO₂ and water into usable carbohydrates (Nevin *et al.*, 2010; Marshall *et al.*, 2012), grounding a theoretical alternative route of chemical production. Microbial electrosynthesis is conducted in microbial electrolysis cells. Few studies have shown chemical production using a range of microorganisms (Nevin *et al.*, 2011; Marshall *et al.*, 2013). This has triggered an increasing interest on how microorganisms deal with supplied power and how they interact with the electrodes (Rabaey *et al.*, 2010), as well as what biological pathways are being used.

1.2 Motivation of study

Several studies have investigated how to improve BES; however, microbial electrosynthesis has been largely unexplored. Furthermore, the effect of different parameters on the production of chemicals is still unknown.

The motivation of this study is to assess the feasibility of the microbial electrosynthesis route for the production of energy and/or chemicals using *Shewanella Oneidensis* MR-1 (MR-1) and to investigate the process optimization by evaluating the effect of different parameters (i.e. mixing rate, electrode treatments and biofilm formation). In earlier studies, it has not been investigated whether MR-1 is capable of using CO₂ to produce chemicals and how this process affects bioproduction and the bacterial cell itself. The proof of concept in this field will help to clarify the impact of this pathway on the process performance. In addition, testing different cell properties (i.e. proteins), microbial electrosynthesis process can be further determined. In order to accomplish this, an empirical description of microbial electrosynthesis will be performed.

Finally, the production of chemicals from anaerobic fermentation and microbial electrosynthesis has not been economically assessed because of the early stage of the technologies' development. Bioprocesses face barriers due to (a) slow growth of bacteria, (b) low levels of the acid produced and (c) difficulty to separate acids in the downstream process. These barriers state the difficulty of the bioprocesses to be economically competitive with chemical synthesis processes under current market conditions. Scaling-up MES has not been proven yet. Therefore, an economic analysis will be calculated based on microbial electrosynthesis as an acetic acid production route including the assessment of required productivities at the given investment costs; reactor, electrodes, reaction medium and bacteria costs. This will help to determine the overall process performance and outline information for the production of chemicals as well as identify the limiting process parameters.

1.3 Aim

The overall aim of this PhD thesis is to economically evaluate and empirically investigate bioproduction from CO₂ in BES as well as to evaluate biofilm development. This is pursued according to four specific studies where each one has its own aim and objectives as follows:

Aim 1: To economically evaluate microbial electrosynthesis as an acetic acid route to determine its feasibility to compete with already existing processes

Objectives:

1. To evaluate **investment** and **production costs** of microbial electrosynthesis and anaerobic fermentation compared to industry relevant methanol carbonylation and ethane direct oxidation
2. To **integrate** anaerobic fermentation and microbial electrosynthesis processes to **optimize** production costs
3. To evaluate **investment** and **production costs of other** possible **chemicals** produced from MES
4. To assess the **profitability** of the designed plants

Aim 2: To demonstrate that *Shewanella Oneidensis* MR-1 is a feasible system for the production of biochemical compounds using CO₂ as substrate and electron transport facilitated either by a mediator or a biofilm.

Objectives:

1. To cultivate ***Shewanella Oneidensis* MR-1** cells and evaluate their growth in different mediums.
2. To evaluate the performance of *Shewanella Oneidensis* MR-1 in BES using either a **biofilm** or a **mediator based electron transport**.
3. To determine the feasibility of **bioproduction from CO₂** in a BES using *Shewanella Oneidensis* MR-1 and a biofilm or mediator based electron transport.

Aim 3: To study bioproduction from CO₂ using *Shewanella Oneidensis* MR-1 in BES using different polarization potentials

Objectives:

1. To evaluate the performance of *Shewanella Oneidensis* MR-1 in BES using **biofilm based electron transport**.

2. To evaluate the feasibility of **bioproduction from CO₂** in a BES using *Shewanella Oneidensis* MR-1 under different polarizations.
3. To study the effect of set potential on **metabolic pathway** and bioproduction.
4. To determine the ability of **bacterial cell properties** to contribute in bioproduction.
5. To draw a **hypothesised pathway** for the production of chemicals from CO₂ using *Shewanella Oneidensis* MR-1.

Aim 4: To evaluate how the biofilm growth affects current density and to determine appropriate biofilm growth conditions for energy and chemical production

Objectives:

1. To cultivate *Shewanella Oneidensis* MR-1 cells and evaluate their growth using different **temperatures, mixing rates and oxygen exposure**.
2. To enhance and evaluate the performance of *Shewanella Oneidensis* MR-1 biofilm in BES using **polymers**
3. To determine the most **favourable conditions** of biofilm growth
4. To test the most favourable conditions in BES for **cathodic biofilm** formation and **biochemical production**.

1.4 Structure of thesis

This thesis is divided into seven chapters. Chapter 2 explains how BES works, how microbial electrosynthesis process occurs and how the microbial electron transport process occurs. Chapter 3-6 are individual studies; each study has its own introduction, methodology, results and discussion and conclusion sections. Chapter 3 demonstrates an economic evaluation of microbial electrosynthesis compared to biological and chemical processes for the production of acetic acid and other possible products. Chapter 4 describes how a biofilm and a mediator based electron transport system affects current density and biochemical production. Chapter 5 investigates how different polarization affects bioproduction and what bacterial cell properties can affect it. Chapter 6 shows the most appropriate conditions and pre-treatments for a biofilm growth and chemical production. A final conclusion is given in Chapter 7, along with recommendations for future studies to further improve and understand biofilm growth and bio-energy production as well as biochemical production using microbial electrosynthesis in BES.

Chapter 2: Literature review

2.1 Bioelectrochemical systems

BES are an emergent source of renewable energy by converting organic and inorganic waste into electricity and/or chemical products (Rabaey *et al.*, 2010). BES consists of an anode and a cathode which are separated by a cation or proton exchange membrane. While an electrode reduction occurs at the anode, an electrode oxidation occurs at the cathode. The separation between oxidation and reduction reactions results in a large range of applications with low economic cost. Both reactions are driven by biocatalysts; either bacteria or enzymes (Osman *et al.*, 2011), at the solid state electrodes which are connected through an electrical circuit that defines the cell's mode.

2.1.1 Types of bioelectrochemical systems

BES can be divided based on its applications. In a microbial fuel cell microorganisms, such as bacteria, function as catalysts to oxidize organic and inorganic matter in order to produce energy and convert it into electrical energy (Logan *et al.*, 2006; Pham *et al.*, 2006; Du *et al.*, 2007). Figure 2.1 shows a representation of a traditional microbial fuel cell. The oxidation of organic and/or inorganic matter occurs by bacteria in the anode and results to electrons and protons production. The electrons are transferred to a terminal electron acceptor such as oxygen and solid state electrodes. These electron acceptors are then reduced by the produced electrons. In parallel, the produced protons at the anode are moved to the cathode through an exchange proton membrane which separates the anode from the cathode. Microbial fuel cells are receiving attention, scientific (Pant *et al.*, 2010) and commercial (Pant *et al.*, 2011), as their potential for alternative energy production, wastewater treatment and bioremediation of contaminated environments (Kim *et al.*, 2004; Liu *et al.*, 2004; Gregory and Lovley, 2005; Rabaey *et al.*, 2005b; Aulenta *et al.*, 2008; Lovley, 2008; Puig *et al.*, 2011; Pant *et al.*, 2012; Lefebvre *et al.*, 2013).

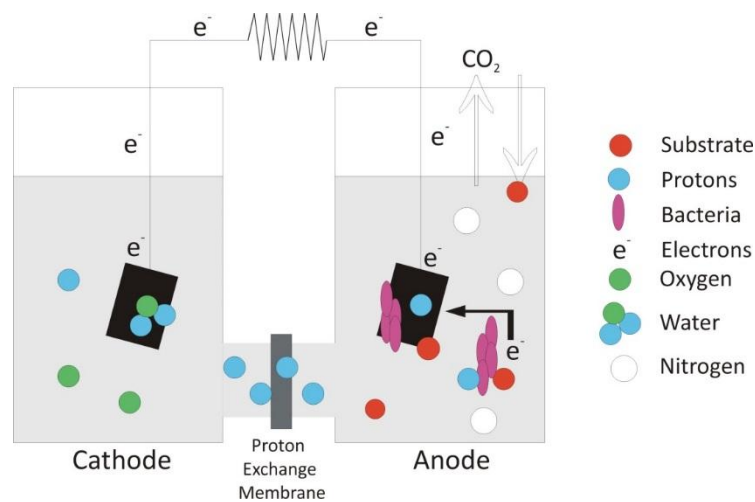


Figure 2.1: Schematic representation of a microbial fuel cell

An approach of using BES as a desalination technology alongside with energy and/or hydrogen production has recently been introduced by Cao *et al.* (2009b) and was further investigated later on (Mehanna *et al.*, 2010; Jacobson *et al.*, 2011; Saeed *et al.*, 2015). As in microbial fuel cell, a desalination cell uses bacteria to oxidize substrate and transformed it into electricity. This results in a potential gradient across the anode and cathode which drives the desalination process and produces energy in the form of hydrogen (Wang and Ren, 2013). Microbial solar cell systems have also gained attention for the optimization of electrical energy and/or chemicals production *in situ* by integrating photosynthetic and electroactive bacteria (Strik *et al.*, 2010; Strik *et al.*, 2011; Strycharz-Glaven *et al.*, 2013).

Finally, microbial electrolysis cell, uses power to achieve a certain process or product formation (Rabaey *et al.*, 2010). While microbial fuel cells produce electrical energy from the microbial oxidation of compounds, microbial electrolysis cells reverse this process to product formation by applying an electric current. Its research is focused on microbe-electrode interactions for driving microbial processes with electrons supplied from electrodes (Thrash and Coates, 2008). Microbial electrolysis cell technology results in a wide range of applications spanning from bioremediation of organic, metal and nitrate contaminated water to production of fuels and chemicals (Gregory and Lovley, 2005; Aulenta *et al.*, 2008; Lovley, 2008; Rozendal *et al.*, 2008b; Cheng *et al.*, 2009; Strycharz *et al.*, 2010; Pant *et al.*, 2012).

During the last decade of research and public attention, microbial fuel cell systems increased the energy production levels and optimized the wastewater treatment (Aelterman *et al.*, 2008; Logan, 2010; Pant *et al.*, 2010). However, the cost of the cathode materials is very important for microbial fuel cell performance. The use of microbial cathodes (biocathodes) reduces the economic excess and increases the environmental sustainability of microbial fuel cell systems.

Biocathodes use biocatalysts to accept electrons from the cathode substrate and enables the use of alternate electrons resulting to a wide range of microbial fuel cells' utilities and present potential opportunities for the microbially catalysed conversion of electrical current into various products (Huang *et al.*, 2011).

2.2 Electrobiocommodities

Electrobiocommodities refer to the fuels and chemicals that are produced by microorganisms which utilise electrical energy as energy source and CO₂ as a substrate (Table 2-1) (Lovley and Nevin, 2013). This new concept is so-called as an artificial form of photosynthesis when renewable energy sources are used (Lovley, 2011). These electrobiocommodities show an opportunity to drive our fuel economy into electricity economy.

Table 2-1: Electrochemical half reaction reduction potentials of CO₂ and free energies based on pH 7

Redox pair	Product formation	Standard potential, E^0 (V vs. SHE)	Standard Gibbs free energy, ΔG^0 (kJ)
CO_2/CH_2O	Carbohydrate	-0.43	41.5
CO_2/CH_4	Methane	-0.25	24.1
CO_2/CH_3OH	Methanol	-0.39	37.5
CO_2/CH_3COO^-	Acetate	-0.29	28.0
CO_2/CH_3CH_2OH	Ethanol	-0.33	31.8
$CO_2/C_2H_5COO^-$	Propionate	-0.29	28.0

There are a number of methods that electricity can provide low potential electrons to microorganisms to enable them for CO₂ reduction, cell growth and maintenance. An approach includes the use of organic molecules (neutral red) as electron shuttles (or mediators) for accepting electrons from electrodes (this approach will be discussed later at 2.4 sections). This method is not preferred because of the additional cost, chemical instability and toxicity (Rabaey and Rozendal, 2010; Lovley, 2011). Another option is the generation of electron donors from microbial respiration (such as ammonia) but the fact of a high potential electron acceptor, higher than CO₂, for supporting the cell growth results to inefficiencies (Khunjar *et al.*, 2012). Water is one more strategy for electrobiocommodities production and is chosen for its inexpensive and abundant properties. Sulphide and organic wastes are potential electron producing sources as well (Rabaey and Rozendal, 2010).

The possibility of providing electrons directly to microorganisms offers a new approach where microorganisms are able of consuming electrons (electrotrophs) and reducing CO₂ in a more efficient way.

2.3 Microbial electrosynthesis

The use of a microbial anode combined with a chemical cathode has already shown the feasibility of hydrogen production in microbial electrolysis cell (Rozendal *et al.*, 2006b). Microbial electrolysis cell is a relatively new method for hydrogen production from fermentation end products, i.e. acetate (Ditzig *et al.*, 2007; Sun *et al.*, 2009). A microbial electrolysis cell operates oppositely than microbial fuel cells. In microbial electrolysis cell, the cathode is anaerobic and there is no generation of current. Therefore, a small external power source is supplied to the system which allows the hydrogen production at the cathode through the reduction of protons (Logan *et al.*, 2008). For example, hydrogen gas can be produced by water electrolysis using a polarization potential of -1.2 V (vs. SHE). On the other hand, hydrogen gas can be produced in a cathode using a -0.41 V (vs. SHE) which is much less than what is required for splitting water (Logan *et al.*, 2008). However, using acetate as an oxidation substrate and bacteria, can generate an anode potential of -0.28 V (vs. SHE) meaning that a required amount of -0.13 V will need to be added externally. This amount of added energy is approximately 89% less compared to water electrolysis due to the thermodynamics of organic matter degradation.

The ability of using biocathodes for the production of usable chemicals introduces a range of applications from bioremediation to bioproduction and carbon fixation. Even though the bioremediation process has been the most commonly studied application (Gregory and Lovley, 2005; Clauwaert *et al.*, 2007b; Aulenta *et al.*, 2008), recently researchers have focused on microbial electrolysis cells and its ability to reduce CO₂ into usable chemicals (Logan *et al.*, 2008; Lovley, 2008; Cheng *et al.*, 2009). Microbial electrosynthesis is related to microbial electrolysis cells. Both systems use bacterial interactions in anaerobic cathodes; however no generation of current occurs. Therefore, a small external power source is needed to be supplied to the system which allows the hydrogen production at the cathode through the reduction of protons (Logan *et al.*, 2008). In microbial electrolysis cells, the external power source is used to supplement the electric current produced by the bacteria. In microbial electrosynthesis, electrons are exclusively supplied by the external power source. These electrons are then used by the microorganisms for CO₂ reduction. Microbial electrosynthesis has firstly gained a lot of attention for the conversion of CO₂ to methane (Clauwaert *et al.*,

2008; Parameswaran *et al.*, 2010) and acetate (Nevin *et al.*, 2010); however, nowadays researchers are investigating the formation of other carbohydrates.

2.3.1 Formate

Microbial electrosynthesis has been used for producing building blocks of larger molecules using intermediary biocatalyst from CO₂, i.e. formate and acetate, followed by other microorganisms. Peters *et al.* (1999) has showed formate production using different cultures (*Acetobacterium woodii*, *Acetobacterium carbinolicum*, *Sporomusa ovate*, *Eubacterium limosum* and *Desulfovibrio vulgaris*) and added H₂ where it was realised that not only the bacteria could produce formate on a ratio of 0.5 mM formate per 10 kPa H₂, but also could use it as an energy source for growing. Over time, the product formation shifted from formate to acetate for *Acetobacterium carbinolicum* and to methane for *Methanobacterium formicum*. Zhao *et al.* (2012) also observed the production of formate when he used a series-connected microbial fuel cell to reduce CO₂ in situ using the energy generated from the degradation of the carbon substances in the anodes. They achieved a 0.092 mM per litre per hour formate production and a coulombic efficiency of 64.8% when 12.7 mM of CO₂ was produced in the anodic part and recycled back to the cathode.

2.3.2 Methane

The production of methane rather than H₂ gas in biocathodes using CO₂ is more desirable as it can be used in the gas infrastructure and can be stored transported and converted to syngas. Cheng *et al.* (2009) used a pure culture of *Methanobacterium palustre* and a polarization potential of -0.500 to -0.800 V (vs. SHE) with saturated CO₂ solution and demonstrated a production of 200 mM of methane per day with a consumption of approximately 210 mM of CO₂. On the other hand, Villano *et al.* (2010), used a methanogenic mixed culture and produced 0.055 mmol per day. In these study polarization potentials more negative than -0.650 V (vs. SHE) were used with a carbon paper cathode. Jiang *et al.* (2013) showed the ability of a mixed culture biofilm obtained from a sewage treatment plant to accept electrons from the electrode and to reduce CO₂ to methane and acetate at potentials more negative than -0.950 V (vs. SHE). They demonstrated that with a high cathode surface area (49 cm²), a saturated solution of ultrapure CO₂ and a polarization potential of -1.150 V (vs. SHE), methane and acetate were produced at 5.32 mM and 1.56 mM per day, respectively. van Eerten-Jansen *et al.* (2015) studied methane production using mixed cultures. They observed that methane

was bioelectrochemically produced indirectly using hydrogen and acetate as intermediates at potentials equal or lower to -0.700 V (vs. SHE). They discussed the feasibility of acetate and formate production from CO₂ via direct electron transfer or indirectly via bioelectrochemically produced hydrogen as well as the possibility of the electrochemical reduction of CO₂ to formate and its consequently use to produce other end products. Siegert *et al.* (2015) used anaerobic sludge and anaerobic bog sediments where a maximum sustained methane production rate was achieved at 8 mM and 11 mM, respectively, with a saturated solution of CO₂ (gas ratio of N₂:CO₂ at 80:20) showing the importance of using hydrogenotrophic methanogens for the formation of methane. As a new approach to upgrade biogas, Batlle-Vilanova *et al.* (2015) used mixed culture bacteria from an anaerobic digester with the dominant genus of *Methanobacterium* in both batch and continuous systems to endeavour biogas upgrading processes. Using microbial electrosynthesis, methane was produced at 5.12 mM per day for batch systems and 15.33 mM per day for continuous systems using 99.9% CO₂ gas. The production was achieved at a coulombic efficiency of 75.3% and 68.9 % for batch and continuous systems, respectively, showing the capability of microbial electrosynthesis technology to be used as biogas upgrading process.

2.3.3 Acetate

Nevin *et al.* (2010) showed the feasibility of CO₂ and water reduction into acetate using a pure culture of an acetogenic bacterium *Sporomusa ovate* using electrons derived from graphite electrodes when a continuous flow-through mode system under a mixture of N₂:CO₂ (80:20) was introduced (0.1 ml/min; dilution rate of 0.03 h⁻¹). A coulombic efficiency of 85% was achieved with acetate concentration of 2 mM. It was also observed that *Sporomusa ovate* produced small amounts of 2-oxobutyrate from CO₂. This study triggered the increasing interest on how microorganism deal with supplied power and how they interact with the electrodes (Rabaey and Rozendal, 2010). In this line, Nevin *et al.* (2011) reported that not only *Sporomusa ovate* is capable of microbial electrosynthesis but other species including two other *Sporomusa* species; *Sporomusa silvacetica*, *Sporomusa sphaeroides* and *Clostridium ljungdahlii*, *Clostridium aceticum* and *Moorella thermoacetica*. Blanchet *et al.* (2015) used *Sporomusa ovata* and increased the acetate production two times compared to Nevin *et al.* (2010). This increase was due to the use of hydrogen and its contribution to the metabolic pathway for CO₂ conversion. *Sporomusa ovata* gained a lot of interest and attention as an efficient microbial catalyst for microbial electrosynthesis operation. Tremblay *et al.* (2015) treated *Sporomusa ovata* with CO₂ and H₂ during growth stage and showed their effect on acetate production.

Acetate was increase 6.5 times compared to the untreated culture and resulted to the highest rate production up to date of 866.7 mM per day reaching a coulombic efficiency of 94.7%. Other researchers have shown that hydrogen, acetate and methane were simultaneously produced when an autotrophic mixed culture from a brewery waste was utilised when using a polarization potential of -0.590 V (vs. SHE) and a periodically flushed system with 100% CO₂ in a continuous system (Marshall *et al.*, 2012; Marshall *et al.*, 2013). These subsequent studies improved the acetate production at 7 mM and 17.25 mM per day, respectively. Patil *et al.* (2015) achieved a 25 mM per day acetate production when he used a mixed culture which was enriched using the simple approach of several culture transfers in H₂:CO₂ conditions at different ranges. In this study, a current of -5 amperes was used rather than a polarization potential with a 58.5 % of electron recovery. A high acetate production up to date was achieved by Jourdin *et al.* (2015b) at a value of 11400 mM per day with a 94% of CO₂ conversion and an achieved titre of 180 mM per day. With even higher proton availability (-1.1 V vs. SHE), it was shown that 99% conversion was possible with an acetate production reaching at 22148 mM per day (Jourdin *et al.*, 2016a) and highlighting the importance of H₂ within the system (Blanchet *et al.*, 2015). This high production specificity was achieved by a well acclimatised and enriched mixed culture combined with a new electrode material synthesized using electrophoretic deposition technique. These results show promising perspectives for the industrialize use of microbial electrosynthesis. Mohanakrishna *et al.* (2015) has also shown that maximum acetate production (90 mM) was occurred at -0.8 V vs. (SHE) with acetogenic bacteria at 30% maximum efficiencies.

2.3.4 Other carbohydrates

Longer chain carbohydrates were also produced from CO₂, such as butyrate (Ganigué *et al.*, 2015). Ganigué *et al.* (2015) achieved a maximum production of butyrate at 1.82 mM per day in hydrogen driven environment using a mixed culture biofilm dominated by the genus of *Clostridium*. Li *et al.* (2012) demonstrated that after genetically modifying *Ralstonia eutropha* H16, were capable to obtain longer chain alcohols such as isobutanol (1.2 mM) and 3-methyl-1-butanol (0.6 mM) promoting the opportunity of producing desired products by manipulating microorganisms.

The importance of formate production is of its use in pharmaceutical, paper and pulp syntheses. Acetate on the other hand is a chemical widely used a raw material for many petrochemical intermediates and products. Even that a number of carbohydrates were produced using CO₂ and a range of microorganisms as well as polarization potentials, the

production rates and the final obtained concentrations are still low. Thus major improvements for the optimization are essential for using microbial electrosynthesis for CO₂ reduction to larger applications.

2.4 Electron transfer mechanisms

For assessing how bacteria deal with electrical current, it is important to understand how electrons may be transported from the electrode to the cell. Electron transfer from the electrode to the cell occurs directly or indirectly (Huang *et al.*, 2011; Rabaey *et al.*, 2011). However, while a plethora of studies have investigated the performance of electron transfer mechanisms in bioanodes, electron transfer in biocathodes is poorly understood (Lovley, 2008; Pant *et al.*, 2012; Kracke *et al.*, 2015).

Direct electron transfer requires a physical contact between the bacterial cell membrane and the cathode electrode surface in order for the electrons to move (Figure 2.2a). These mechanisms rely on the existence of a biofilm or on a single cell layer on the electrode surface (Bond and Lovley, 2003). Biofilms have been previously observed on cathodes reducing nitrates however based on bioproduction only pre grown biofilms have been obtained as far (Gregory *et al.*, 2004; Nevin *et al.*, 2010; Viridis *et al.*, 2011). Direct electron transfer using nanowires can also be a type of electron transfer mechanism where bacteria use appendages to conduct electrons (Figure 2.2b) (Gorby *et al.*, 2006). This mechanism was seen in *Shewanella* when was exposed to low oxygen concentrations or anaerobic conditions. These nanowires which previously thought to be pilus-like based structure was now shown, using in vivo fluorescence measurements, that it is an extension of the outer membrane and periplasm including the contact of the cytochromes responsible for extracellular electron transfer (Pirbadian *et al.*, 2014a).

Direct electron transfer mechanism has been reported with pure cultures such as *Geobacter* or mixed cultures using fumarate, nitrate, tetrachloroethene, CO₂, O₂, Cr (VI) and U (VI) as electron acceptors (Gregory and Lovley, 2005; Dumas *et al.*, 2008; Strycharz *et al.*, 2008; Cao *et al.*, 2009a; Tandukar *et al.*, 2009). Pure culture of *Shewanella putrefaciens*, which is a gram-negative bacterium, has shown that it can use an outer membrane bound redox compound for transferring electrons while reducing oxygen (Fredrickson *et al.*, 2008; Freguia *et al.*, 2010) where it has been shown that gram-negative *Geobacter Sulfurreducens* uses a different electron mechanism (Dumas *et al.*, 2008). Although most of the bacteria used in biocathodes are reported to be gram-negative, some gram-positive bacteria can also perform direct

electron transfer expanding the potential capability among the bacteria (Cournet *et al.*, 2010). Beside pure cultures, direct electron transfer has also been reported with mixed cultures biocathodes (Clauwaert *et al.*, 2007a; Cao *et al.*, 2009a; Aulenta *et al.*, 2010).

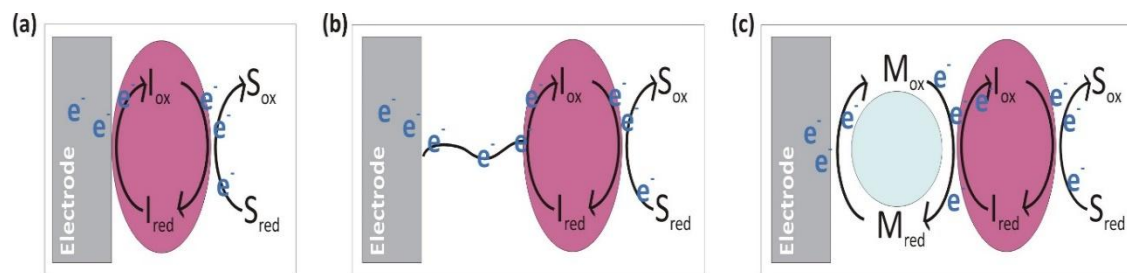


Figure 2.2: Schematics of direct and indirect electron transfer by (a) bacterial contact, (b) direct electron transfer using nanowires and (c) indirect electron transfer using mediators. The electrode is presented in grey and the bacteria in pink. *S* symbolizes the substrate, *I* the intermediate reactions, *M* the mediator, e^- the electrons and ox and red symbolize the oxidation and reduction reactions respectively (Adapted from: Huang *et al.*, 2011)

Although some microorganisms need physical contact with the electrode to transfer electrons others do not as they excrete redox active compounds to perform indirect electron transfer (Figure 2.2c). Bacterial cells use either added (exogenous) or self-excreted (endogenous) shuttle compounds for extracellular electron transfer (Velasquez-Orta *et al.*, 2010; Huang *et al.*, 2011). Electron shuttles are molecules able of catalysing redox reactions, chemically stable and not easily biodegradable. In the indirect electron transfer, electrons are transferred inside the cell to the cell surface using a pathway of redox active proteins and low molecular weight compounds. The electrons are then passed to cytochromes or potentially shuttles in the periplasm or outer membrane. Soluble shuttles can then diffuse into the medium and pass on the electrons to suitable external electron acceptors (insoluble iron oxides or anode) (Chang *et al.*, 2006; Nielsen *et al.*, 2010; Rabaey *et al.*, 2010).

It has been shown by a number of studies that the addition of mediators such as *thionine*, *methyl viologen*, *2-hydroxy-1,4-naphtoquinone*, *neutral red*, *methylene blue*, *humic acids* and *anthraquinone-2,6-disulphonic acid* (Bennetto *et al.*, 1983; Roller *et al.*, 1984; Newman and Kolter, 2000; Sund *et al.*, 2007; Thrash *et al.*, 2007) allows current production in microbial fuel cells. Despite the benefits of the exogeneous mediators, there are few drawbacks that place a barrier for future applications of biocathode microbial electrolysis cells; they are short-lived, toxic, and unsustainable and introduce additional cost (Huang and Angelidaki, 2008).

Bacteria such as *Acinetobacter cacloaceticus* was reported to exploit self-excreted redox compound, similar to an electron shuttle named *pyroloquinoline quinine*, for extracellular electron transfer in microbial cathodic oxygen reduction (Laurinavicius *et al.*, 2004; Rabaey *et*

al., 2008; Freguia *et al.*, 2010). Furthermore, *Gamma proteobacteria* such as *Pseudomonas aeruginosa* and *Shewanella Oneidensis* MR-1 have shown that they were able to produce their own electron shuttles (Rabaey *et al.*, 2005a; Marsili *et al.*, 2008; Von Canstein *et al.*, 2008). Watanabe *et al.* (2009) suggested that extracellular substances are always involved in BES that accommodate microbial communities. Thus, it is essential for the efficiency of the system to understand the properties of the electron mediators in biocathodes (such as chemical structures, water solubility etc.).

The electron transfer channel used in electroactive bacteria (Figure 2.3), it has been proven to consist of multiheme c-type cytochromes as a key component in gram-negative bacteria (Reguera *et al.*, 2005; Gorby *et al.*, 2006; Shi *et al.*, 2007b). Although the mechanisms of electron transfer between cathodic electrodes and bacteria have attracted a significant amount of attention, the interactions between the electrons derived from the electrodes and the terminal electron acceptors require further research. However, recently it has been discussed the possibility of the same electron transfer channel used for microbe to electrode interaction (anode) is used for electrode to microbe interaction (cathode) as well (Choi and Sang, 2016).

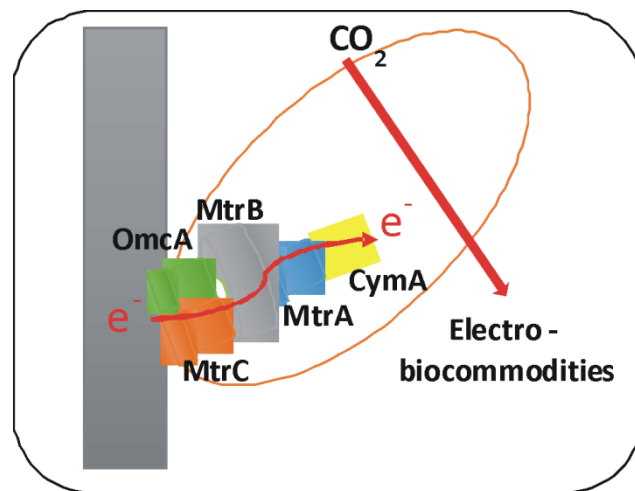


Figure 2.3: Electron transfer channel in *Shewanella Oneidensis* MR-1 (Adapted from: Pirbadian *et al.* (2014a))

Biofilm development is highly relevant for BES operation. Different operating conditions (including electrode materials) affect the electron transfer mechanisms and thus influence the energy and/or chemical production based on the application. In terms of microbial fuel cells, voltage generation and coulombic efficiencies showed to be two times higher when high temperature (30 °C) was used instead of lower temperatures (15 and 20 °C) (Feng *et al.*, 2009). Biofilm development and BES performance can also be affected by different flow rates according to Ieropoulos *et al.* (2010). Based on microbial electrosynthesis operation, electrode

materials proved to be essential for high production of chemicals when using nano-porous electrodes (Jourdin *et al.*, 2015b). However, only few studies have revealed appropriate operating conditions for biofilm development to monitor wastewater.

2.5 Green chemistry and bioelectrochemical systems

BES are designed for energy efficiency as they are operating under mild conditions; 25 °C and 1 atmospheric pressure. The use of bacteria as catalysts instead of chemical catalysts promotes a sustainable process for a non-hazardous chemical synthesis. Finally the use of CO₂ as a renewable feedstock is not only economically practicable but also treats the CO₂ waste in the atmosphere. In addition, since microbial electrosynthesis has been endorsed as an artificial form of photosynthesis, oxygen remains the main by-product confirming the prevention of any greenhouse gas waste (Anastas and Warner, 1998). BES are an efficient technology with high atom economy processes which are important for sustainable development. These facts place BES technology as a feasible solution to meet the 2050 emission reduction target (CCC, 2015).

2.6 Advantages and Challenges: Microbial electrosynthesis vs. bioprocesses

The last five years, published studies have shown that microbial electrosynthesis is an exciting and promising technology for bioproduction with lots of opportunities and challenges (Sadhukhan *et al.*, 2016). However, other bioprocesses, such as fermentation, have also shown great improvement. Sugar fermentation has proven a promising technology for the production of bioproducts and is dominating in bio-industry becoming another competitor to microbial electrosynthesis apart from the traditional chemical production routes (Jang *et al.*, 2012). Syngas fermentation is another possible chemical production route that performs as a competitor to microbial electrosynthesis (Worden *et al.*, 1997).

Microbial electrosynthesis is at its early stage but it has proven its feasibility and shown advantages to overcome fermentation processes in terms of chemical, technical and economic advantages for lab production and scale-up applications although few challenges are present as well (Sadhukhan *et al.*, 2016). In order to discuss the advantages and challenges of each process, their benefits and limitations must be exposed. Table 2-2 shows the comparison between fermentation and microbial electrosynthesis processes.

Table 2-2: Comparison between fermentation and microbial electrosynthesis processes

Microbial electrosynthesis	Sugar Fermentation	Syngas fermentation
+ Use of CO ₂ as substrate which offers a reduction in greenhouse gases	- Use of organic substrate (availability depends on location and the size of plant or supply)	+ Use a mixture of CO/H ₂ and very often includes CO ₂
+ CO ₂ is funded (£0)	- Organic substrate prices vary on type, location and purity	- Syngas prices vary
+ CO ₂ is available in atmosphere, seawater and solid minerals	-CO ₂ production as by-product	+ Syngas is produced from many sources (i.e. natural gas, coal, biomass, hydrocarbon feedstock, by steam reforming, by dry reforming or partial oxidation)
- CO ₂ is available in low atmospheric conditions per unit land surface	+ most organics are highly soluble	- CO ₂ is not always present in syngas mixture
+ independent of arable land	+/- requirement of arable land if high quality of substrate is needed	+/- requirement of arable land if high quality of substrate is needed
+ CO ₂ in solution serves as a buffer (pH balancing)	- pH varies and might be unfavourable for bioproduction based on the type of substrate	- CO ₂ in solution serves as a buffer. CO inhibits the growth of methanogens
- nutrient requirement for bacteria growth	- nutrient requirement for bacteria growth	- nutrient requirement for bacteria growth
- extensive energy requirement	+ less electrons needed as substrate is partially reduced	+/- energy requirements depends on the syngas production route
+ electricity produced can be stored as H ₂	- lose of energy	- lose of energy
- low bioproduction rates	+ high production rates	- low production rates
+ operates in anaerobic conditions which limits extensive biomass growth	- oxidative fermentation requires sufficient air/oxygen supply	+ operates in anaerobic conditions which limits extensive biomass growth
- sensitive to redox balancing & specific product formation	- extensive biomass growth (limits production rates)	- sensitive to redox balancing & specific product formation
+ use of solid state electrodes provides strengthens the electron donor/acceptor	+ waste derived organics have negative value thus processing offers net profit	
+ biocatalytic performance can be monitored by the electrode current output	+/- bacterial performance is monitored by spectroscopic methods	+/- bacterial performance is monitored by spectroscopic methods

+ final product depends on the chosen bacteria		+ final product depends on the chosen bacteria
--	--	--

Using CO₂ as a substrate offers a number of advantages over other choices. CO₂ is an abundant source as it is available in the atmosphere, oceans and soils and the cost can be considered subsidized by government funding as a pilot project for Carbon Capture and Utilization. CO₂ is being produced by several chemical processes and by the combustion of fossil fuels. This results to a complete independence of arable land. CO₂ can also provide buffering effects in the reactors media. Its use can contribute in the carbon removal from the atmosphere and have a positive impact on greenhouse gas levels. However, using such a substrate also has its disadvantages. CO₂ requires a large amount of electrons for the synthesis of organic compounds due to its thermodynamic stability. Also, for activating the pathway for an autotrophic growth within the cell energy is needed. Both from an economic and environmental point of view, efficient electron use is a main concern. In this line, it can be noted that the use of renewable energy can solve this matter. However, bioelectrochemical hydrogen production offers further advantages on energy storing and reuse. Also, mixed culture biofilms with a mixed metabolism can perform bioproduction in a more feasible way (lithoautotrophic production). Another solution to reduce energy input is the use of redox mediators (Rabaey *et al.*, 2011).

On the other hand, fermentation processes, use organic substrates which vary in price (at a range of £380 per tonne) (Cheung *et al.*, 2000), availability, location and purity but require limited electrons for bioproduction as the organic substrates are already partially reduced. Furthermore, fermentation results in the production of by-products such as CO₂ which contributes to greenhouse gases. Even that most of organic substrates are highly soluble and can facilitate dosing, in bioproduction processes, they change the pH which might be unfavourable for bioproduction and will required the need of buffer solution. With fermentation, high rates of bioproduction are possible, however when anaerobic fermentation is used the production of oxygen can limit the processes and the bacterial substrate selectivity resulting to a lower production rate. On the other hand oxidative fermentation requires extensive use of oxygen supply which results to extensive biomass growth and thus decreases the production rates. Here, microbial electrosynthesis overcomes fermentation processes as it operates in anaerobic conditions and avoids the use of oxygen presenting economical, chemical and technical advantages which also accounts for full scale-up applications and industrial intake (Angenent and Rosenbaum, 2013). In addition, the lack of oxygen limits the biomass growth and in return, it increases product yields. However, all anaerobic processes are

sensitive to redox balancing and specific product formation is challenging as it highly depends on balanced removal or supply of reducing equivalents. In this line, microbial electrosynthesis uses solid state electrodes which can provide a stable and sustainable solution as they can manipulate the strength of the electron donor/acceptor through an applied electrode potential (this concept will be discussed in section 2.7). Moreover, the performance of the bacterial and the process can be monitored through the electrode current output.

Syngas fermentation on the other hand, depends on syngas production from industrial processes; natural gas, coal, biomass, hydrocarbon feedstock, by steam reforming, by dry reforming or partial oxidation. Syngas is a waste gas containing mainly CO and H₂ (raw syngas contains high amounts of CO₂) and the production cost varies from £19.70 - £72.45 per thousand cubic meters (Pei *et al.*, 2016). Similarly to microbial electrosynthesis, syngas fermentation process requires nutrient addition for bacteria growth and results in low production rates.

Although that the key challenges for microbial electrosynthesis is to reduce energy requirements, achieve efficient growth of the bacteria and to ensure sufficient specificity of product formation and high production rates, other disciplines areas place a barrier to optimization. The electrode surface structure and chemistry is at a very early stage and the bacteria interaction is strongly depended on it. Electrode materials need further research to identify low costs materials for scalability which relates further to reactor sizes and microbial reaction rates. Pilot plants on BES are vital to deliver key information for larger scale application and operation for microbial electrosynthetic conversions (Logan, 2010). The economic viability of the process has not been proven yet and such a study needs to take place for exposing limiting parameters and help on the optimization of the process.

2.7 Electrochemical fundamentals linking to bioelectrochemical systems

Electrochemistry is the study of the interaction between electricity and chemical reactions. In terms of BES, electrochemical fundamentals and techniques are important for the characterization of the system. Using this field, the metabolic states of bacteria can be investigated. The following session will briefly explain the fundamental concepts relevant to this study.

2.7.1 Electrode reactions

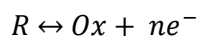
In this study all experiments are conducted in 3-electrode H-shape electrochemical cells containing a working electrode, a counter electrode and a reference electrode. The working electrode is the electrode of investigation and is populated by bacteria. The reference electrode defines a potential with a known point of reference and allows the potential of the working electrode to be measured without passing current through it. The counter electrode is where the opposite reaction occurs and allows the current to pass. For example, if an oxidation reaction occurs at the working electrode, the reduction reaction that uses the same magnitude of current is sustained at the counter electrode. Thus there is not any current flow between the working and reference electrode. Therefore, changes in the working electrode potential can be evaluated accurately.

In a BES a reduction and an oxidation reaction occurs, also called redox reactions (Equation 2.1 and Equation 2.2, respectively). Ox symbolizes the compound that is being reduced, R symbolizes the compound that has been oxidized and e^- symbolizes the electrons.

Equation 2.1



Equation 2.2



As previously discussed (in section 2.4), the working electrode that is populated with bacteria has been reported to transfer electrons in three ways; (a) directly via bacterial contact (outer membrane cytochromes), (b) directly via nanowires and (c) indirectly via mediators. These mechanisms are involved with transferring electrons from the bacteria to the electrode at the electrode surface using redox reactions.

The electrode reaction can be affected by the charged species as they differ at the electrode surface and the bulk solution and can take place in a number of steps as shown in Figure 2.4 (Bard and Faulkner, 2001). The rate of a redox reaction can be affected from the mass transport of O'' species from bulk solution to the interface of the electrode surface area where the reaction occurs. At the electrode surface other elementary steps might occur such as adsorption, desorption, protonation and decomposition steps ($O'' \leftrightarrow O', R'' \leftrightarrow R'$), that might not involve the redox reaction that follows electron transfer ($Ox + ne^- \leftrightarrow R$). After the completion of the redox reaction, the reduction products, R' , are transported back from the

electrode to the bulk solution. And the last step is the transport of the electrolyte which includes ions and chemical species (migration) (Zhao *et al.*, 2009).

Mass transfer may include (a) diffusion from concentration gradients, (b) migration due to an electric field and (c) convection due to the presence of mechanical agitation. In order to mitigate the mass transfer issues, in electrochemical experiments, a buffer solution can be used (>100 mM) and lack of stirring or agitation (Bretschger *et al.*, 2007).

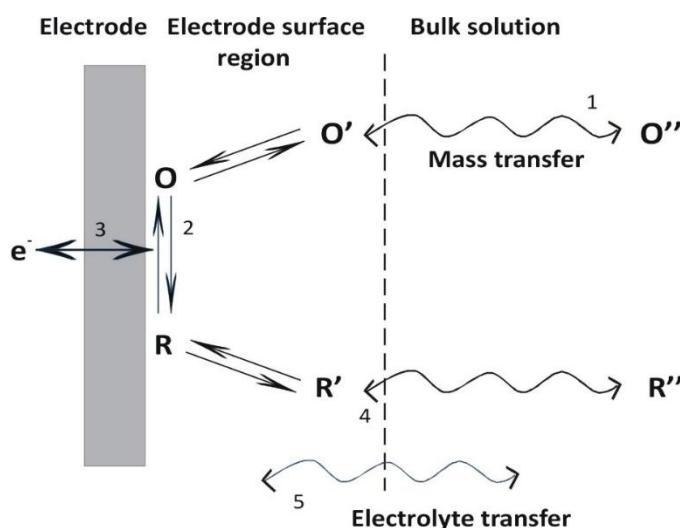


Figure 2.4: Schematics on electrochemical reactions on a working electrode in an electrochemical cell. (1) Mass transport to the electrode surface, (2) electrochemical reaction at the electrode surface, (3) electron transfer, (4) mass transfer to the bulk solution and (5) electrolyte transport (Adapted from: Zhao *et al.*, 2009)

If a biofilm is assumed on the working electrode some considerations have to be taken into account for extracellular electron transfer. A proposed pathway for direct and indirect electron transfer is shown in Figure 2.5. The biofilm formation on the electrode surface is essential for the operation of a BES. Live and dead cells are taken into account for regeneration of the biofilm. During an electrochemical reaction with the electrode several steps can be occurred. Transport of the substrate from the bulk solution to the biofilm region, transport of the substrate in biofilm region, present metabolisms inside the bacteria, direct electron transfer between the biofilm and the electrode using i.e. the active sites of extracellular enzymes of the bacteria, transport of the metabolites, mediators and the reaction products and finally transport of electrolyte (inc. ions and chemical species).

The substrate that is transferred from the bulk solution is consumed by the living cells in the biofilm resulting to the generation of electrons from the active enzyme site. These electrons are collected by the anode via extracellular cytochromes. When the biofilm thickness is bigger

than the electrode surface region, the position of the enzymes is very important for electron transfer processes. Direct electron transfer can only occur if the active enzyme site is close to the electrode. If bacteria are distant from the electrode surface then electron transfer process cannot occur. When however, bacteria can produce nanowires, then they can use them as electrical conductive appendages to complete electron transfer. Indirect electron transfer can occur when electroactive metabolites or mediators are produced by the cell which they can be used for electron transfer. Two different mechanisms can take place in this case. When the cells are in contact with the electrode, the metabolites and mediators released from the bacterium are on the electrode surface and can proceed with chemical and/or surface reactions. And, when the metabolites and mediators are released away from the electrode surface (by the suspended cells in the bulk solution), mass transport will also occur.

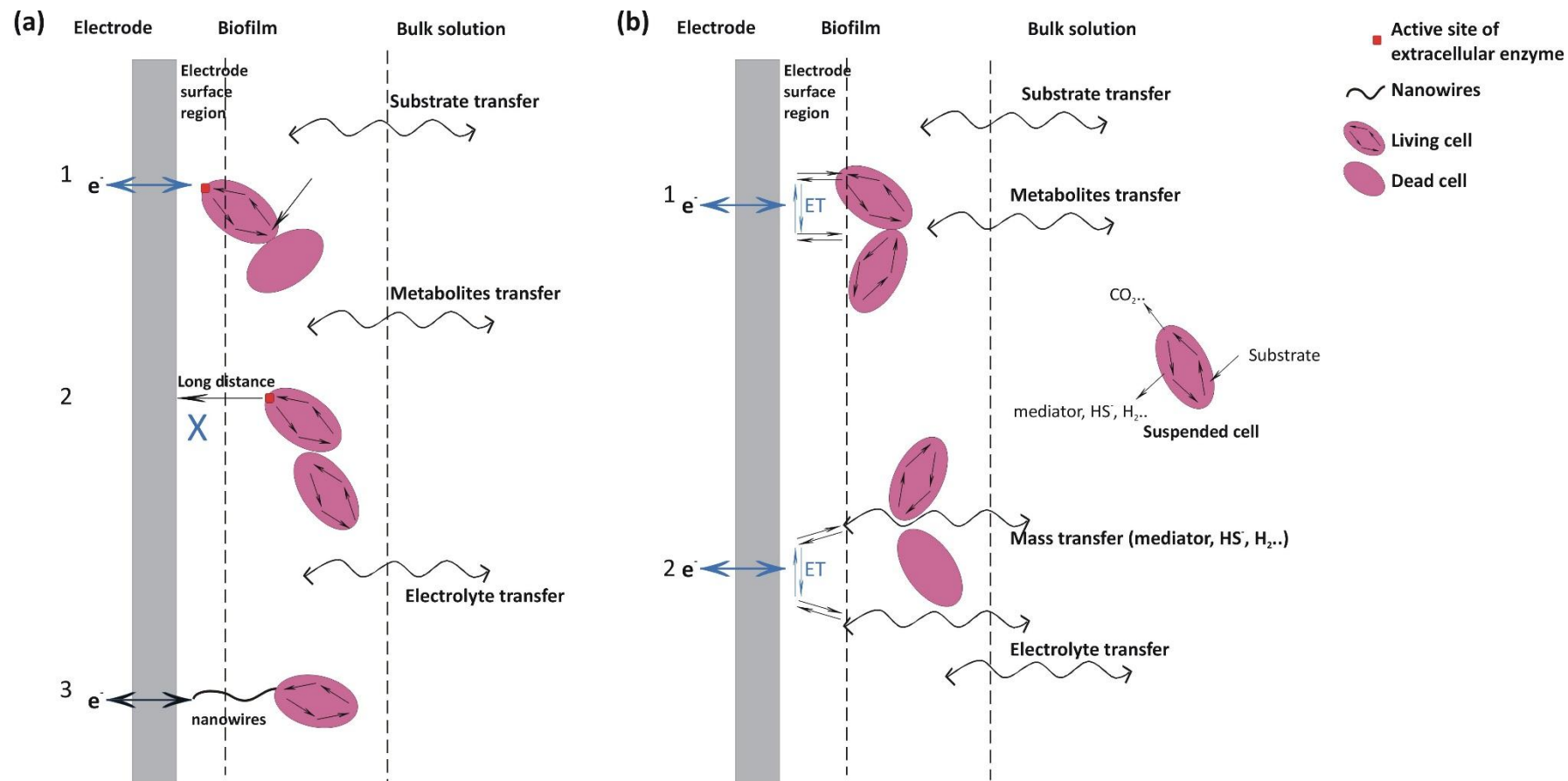


Figure 2.5: Schematics of proposed pathways of electron transfer from bacteria to an electrode surface in a bioelectrochemical system using (a) direct electron transfer and (b) indirect electron transfer (Adapted from: Zhao *et al.*, 2009). (a) (1) direct electron transfer using active sites of extracellular enzymes, (2) Distant bacteria incapable of electron transfer, (3) direct electron transfer using nanowires. (b) (1) indirect electron transfer using metabolites and mediators and (2) indirect electron transfer from distant released metabolites and mediators (mass transfer)

2.7.2 Losses in the system

Theoretically, less energy should be needed to drive a microbial electrosynthetic process where the energy derived from the microbial conversion should be high. However, practically the energy derived and needed is less and more respectively based on three major irreversible losses in BES; activation losses, ohmic losses and mass transport losses (Figure 2.6) (Logan *et al.*, 2006; Rabaey *et al.*, 2010; Huang *et al.*, 2011). In order to understand the reason that BES do not perform ideally is crucial to consider these losses in the systems.

For the activation losses, the current depends on the kinetics of the reduction that takes place at the cathode. A portion of cathode potential is lost in order to overcome the activation barrier every time there is current drawn. This loss is called activation loss. As more current is taken from the cell, the activation losses are increasing which results to a lower cell potential (Rinaldi *et al.*, 2008; Rismani-Yazdi *et al.*, 2008; Rozendal *et al.*, 2008a). As in the chemical fuel cells, the biological cells occur similarly thus the magnitude of the cathodic activation losses depends on the kinetics of the reduction. The decrease of the activation barrier and the increase of the interface area, temperature or oxidant concentration can improve the kinetics of BES and decrease the activation losses.

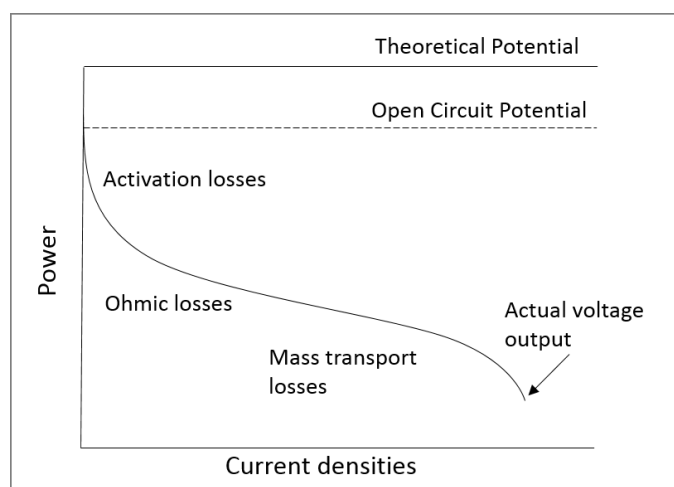


Figure 2.6: Representation of the losses in bioelectrochemical systems (Adapted from: Rismani-Yazdi *et al.*, 2008)

For the ohmic losses, the loss is referred to the voltage that is required to drive the electrons and protons transport processes. The ohmic losses are declared of medium current densities and the operating voltages decrease linearly as current increases, following the Ohm's law. Decreasing the resistance from the electrodes, electrolytes and interconnection will lower the internal resistance and will drive the electrons and protons transport processes positively resulting to an improvement of the BES performance.

The mass transport loss is based on the voltage required to drive the mass transport processes at the cathode. The mass transport losses occur at high current densities, due to the reactant depletion or product accumulation, and the magnitude increases with increasing current density. By maintaining high bulk concentrations and even distributions of oxidant across cathode chambers and by optimizing the operating conditions of the BES, electrode materials and cathode compartment geometry, the mass transport losses can be reduced.

Biocathode studies for current production reports based on the role of microbial catalysis of the abiotic cathodes showed that the apparent decrease in activation losses at oxygen reducing biocathodes proves that bacteria act as true catalysts (Chen *et al.*, 2008; Freguia *et al.*, 2008; You *et al.*, 2009; Erable *et al.*, 2010). On the other hand, to progress future biocathodes for BES applications though, parameters such as comparative performance, cost, duration, selectivity and stability of biocatalysts must be assessed (Rismani-Yazdi *et al.*, 2008). The power densities from an abiotic cathode cannot be directly compared with another abiotic cathode because of the effects of multiple parameters; reactor architecture, electrode spacing, solution conductivity and anodic specific bacteria or mixed cultures (Logan, 2009; Yi *et al.*, 2009; Kim *et al.*, 2010). Electrode materials, solution chemistry and reactor architecture also affect the performance of the biocathodes. Consequently, comparisons of biocathodes must be carried out using the same conditions of reactor architecture, anodic conditions and solution chemistry (Clauwaert *et al.*, 2007a; You *et al.*, 2009; Huang *et al.*, 2010).

In addition, the formation of a biofilm is also important in the development of the electrode potential in BES as power current densities can be affected from it. Rabaey *et al.* (2008) compared the power densities from mixed and pure cultures (*A. cacloaceticus*, *Sphingobacterium multivorum* and a designated isolate similar to *Beta-proteobacteria* Uncultured clone C11r0) forming electrochemically active biofilms using oxygen as electron acceptor showing that isolates produce less power than the mixed culture. Erable *et al.* (2010) also showed similar results between 30 pure cultures and one mixed culture. It was assumed that synergetic effects occurred in the mixed culture biofilm or a more productive exoelectrotroph was present in the mixed culture but not in the pure cultures. Other potential reasons are caused because of underdeveloped biofilm under pure culture conditions, surface modifications or pH change that could contributed on the lower power generation (Rabaey *et al.*, 2008). Behera *et al.* (2010) reported the role of biofilm thickness on the cathodic electrode. Exoelectrogenic anode biofilms were reported of higher current production from thicker anodic biofilms of *Geobacter sulfurreducens* (Nevin *et al.*, 2008). Cathodic biofilm thickness can however affect the power generation in a different way. Behera *et al.* (2010) observed that

power generation was decreasing with an increasing thickness of the cathode biofilm on both of the materials used; graphite plate and stainless steel mesh.

Furthermore, Yang *et al.* (2000) stated that the surface roughness of the cathodic electrode is important for the performance of the cathode. The surface roughness can affect the structural heterogeneity of the biofilm. Subsequently, the biofilm activities and the mass transfer dynamics are influenced resulting on affecting the open circuit potential of the attachment surface. A rough surface supports bacterial adhesion and colonization for biofilm formation (Tang *et al.*, 2007). Nguyen *et al.* (2007) observed that a more compact and homogenous biofilm of *Leptothrix duscophora* SP-6 was grown on a smoother initial electrode surface of glassy carbon and stainless steel. Likewise, Dumas *et al.* (2008) showed that under a polarization of -0.60 V (vs. Ag/AgCl), stainless steel achieved 25 times higher power density than graphite and also showed excellent electrokinetic properties for processing fumarate reduction using *Geobacter sulfurreducens* as a pure culture.

Electrode surface area is one more essential parameter that can affect the reactor's performance. The increase of the surface area of the cathodic electrode in a biocathode microbial electrolysis cell will consequently increase the amount of biocatalysts and thus will decrease the activation overpotential. This will lead to an increase of cathode potential and power production (Logan, 2009). Huang *et al.* (2010) used a higher cathodic specific area than Tandukar *et al.* (2009) achieving higher energy production and higher Cr (VI) reduction rate. The performance of the reactor can be optimized for more viable applications of this technology by reducing the start-up time for biocathodes as well (Clauwaert *et al.*, 2007b). An applied cathodic potential can accelerate the start-up of current and can increase the performance of biocathodes using oxygen as an electron acceptor (Thrash and Coates, 2008; Liang *et al.*, 2009).

The pH changes is a general problem in BES which results to acidification at the anode compartment (by microbial fuel oxidation) and alkaline production at the cathode compartment (oxygen reductions) (Rozendal *et al.*, 2006a; Clauwaert *et al.*, 2008; Rozendal *et al.*, 2008a; Harnisch *et al.*, 2009; Sleutels *et al.*, 2009). Changes in the pH can influence the microorganisms in the cathode. The charge changes the surface properties of the cell inside the biofilm (cell surface hydrophobicity, net surface electrostatic charge, cell surface shape and polymers, cell morphology, cell size at cell division, time to division as well as biofilm structure) affecting the biocatalytic activity (Busalmen and De Sánchez, 2005; Luo *et al.*, 2005). The need of buffer is also necessary in biocathodes for pH control, specifically for biocathodes working at high rate. A recent strategy for pH control is the development of a reversible bio-electrode

that performs anodic and cathodic reactions. The protons produced at the anode are used to reduce oxygen at the same compartment, rather than be transported in the cathode through a membrane, without producing any persistent and inhibitory pH control problem (Cheng *et al.*, 2010; Strik *et al.*, 2010). The use of anodes effluent in cathode, bipolar membranes, membrane less operations and loop operations can be considered as other strategies (Freguia *et al.*, 2008; Viridis *et al.*, 2008; Clauwaert *et al.*, 2009).

The role of carbon source and the effects of carbon limited conditions in biocathode must also be taken into account as they can affect the solution chemistry for biocathodes. Inorganic carbon has been used as a carbon source for cathodophilic bacteria growth, in aerobic and anaerobic biocathode microbial fuel cells (Shea *et al.*, 2008; Tandukar *et al.*, 2009; Huang *et al.*, 2010). These autotrophic biocathodes (autotrophs use light to produce organic compounds) resulted to some implications based on system start up time and operation due to the fact that the autotrophic growth is slower than the heterotrophic growth. Organics crossover from anode to cathode through a membrane (occurring due to electro-osmosis and molecular diffusion) leads to implication contributing to lowering the abiotic cathode potential, changing the surface structure and deactivation of the catalyst. Subsequently, the system's performance and the columbic efficiencies are affected (Zuo *et al.*, 2007; Chae *et al.*, 2008; Rismani-Yazdi *et al.*, 2008; Harnisch *et al.*, 2009). Feeding an aerobic biocathode using the anodic effluent results in excessive chemical oxygen demand to enter the biocathodes and contribute to the growth of aerobic heterotrophs (heterotrophs cannot fix carbon and uses organic carbon for growth). The cathode is then turning into an aerobic heterotrophic biofilm resulting in restriction of the oxygen reduction reaction and prevention of electricity generation. In the meantime, the right amount of heterotrophs at the cathode can use the oxygen to hydrolyse and oxidize the biodegradable chemical oxygen demand effluent from the anode indicating the ability of removing certain organics in the biocathode (Freguia *et al.*, 2008; Liang *et al.*, 2009; Behera *et al.*, 2010).

2.7.3 Cyclic voltammetry

Cyclic voltammetry is an electrochemical technique that analyses the underlying redox activity on the surface of the working electrode. Cyclic voltammetry can determine whether the redox reactions are reversible or irreversible redox couples. In BES, cyclic voltammetry can be used to study the mechanism of electrode interactions between the biomass and the electrode surface. It can also be used to identify the potential of the main electrochemical reactions

involved with extracellular electron transfer and it can evaluate the performance of the bacteria as catalysts (Bard and Faulkner, 2001).

Cyclic voltammetry consists in applying a voltage to the working electrode which gradually varies the voltage through time while current changes are recorded. The voltage varies forward and backwards in a fixed voltage range (using a potentiostat). Figure 2.7b shows a resulting cyclic voltammogram. The curve that has occurred from the forward scan is the oxidation curve (anodic peak) and the curve occurred from the backward scan is the reduction curve (cathodic curve) according to the reaction from Equation 2.1 and Equation 2.2, respectively.

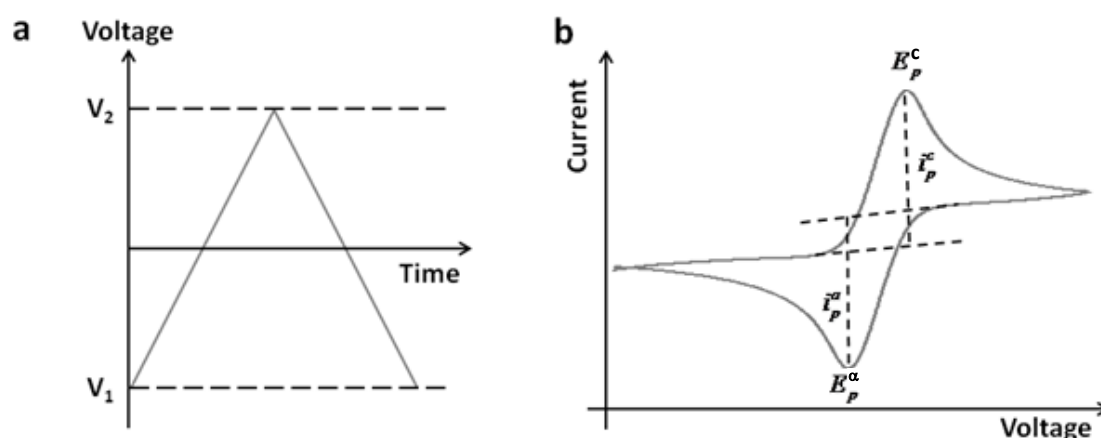


Figure 2.7: (a) forward voltage sweep (oxidation) and back scan (reduction). (b) Resulting cyclic voltammogram showing reversible redox activity with peak currents and peak potentials. E_p^c is the cathode potential, E_p^a is the anode potentials, i_p^c is the cathodic peak current and i_p^a is the anodic peak current.

For understanding this behaviour, the influence of the voltage must be considered. The Nernst equation predicts the relationship between the concentration and voltage (Equation 2.3).

Equation 2.3

$$E = E^0 + \frac{RT}{nF} \ln \frac{[C_R^0]}{[C_O^0]}$$

E is the applied potential and E^0 is the standard electrode potential, n is the number of electrons, F is the Faraday constant ($96,484 \text{ C mol}^{-1}$), R is the gas constant (8.314) and T is the temperature in Kelvins (K). The standard potential of a cyclic voltammogram can be calculated from the average of the peak potentials (Equation 2.4).

Equation 2.4

$$E^0 = \frac{E_p^a + E_p^c}{2}$$

The standard potential can compare the energetics of different systems and it is specific for the system studied but not for the concentration used. Kinetics can also be obtained using cyclic voltammetry (Equation 2.5).

Equation 2.5

$$\Delta E = E_p^a - E_p^c$$

These parameters can be used for mechanistic and kinetic analysis electron transfer processes at electrodes when are recorded in different rate.

Redox reactions can also be described thermodynamically using the Gibbs free energy equation. For a spontaneous reaction, Gibbs free energy is negative with a positive reaction potential and for a non-spontaneous reaction, Gibbs free energy is positive with a negative reaction potential.

Equation 2.6

$$\Delta G^o = \Delta H^o - T\Delta S^o$$

Where ΔH is the change in enthalpy of formation and ΔS is the change in entropy. The Gibbs free energy it can then be related to the cell voltage of a redox reaction using Equation 2.7.

Equation 2.7

$$\Delta G = -nFE$$

2.7.4 Amperometric detection

Amperometric detection is the polarization technique used in this study. This measurement starts from an open circuit potential. If an anode is operated, the potentiostat applies a potential from open circuit potential towards zero and positive potentials (Bard and Faulkner, 2001). An example of an Amperometric detection scan is presented in Figure 2.8. The potential is applied and held constant and current is being measured and recorded. Usually, a BES starts at potential near to zero indicating no electron transfer within the system (Figure 2.8a). In the presence of a feedstock, the current starts increasing (Figure 2.8b). This fact suggests the

occurrence of electron transfer to the electrode. Finally, a steady state biofilm is indicated by a repeatable maximum current supporting that the biofilm has evolved to its maximum potential (Figure 2.8c). Using a BES, it is difficult to measure appropriate steady state polarization curves for a number of reasons. Bacterial communities keep evolving with time and the communication with the electrode is a dynamic relationship. The concentration of electrochemically active metabolites keeps changes within the biofilm. Also, as it is being discussed previously, the mechanisms of extracellular electron transfer changes with each biofilm and electrode configuration. The same principle is applied if a cathode is operated; however the applied potential is at negative values.

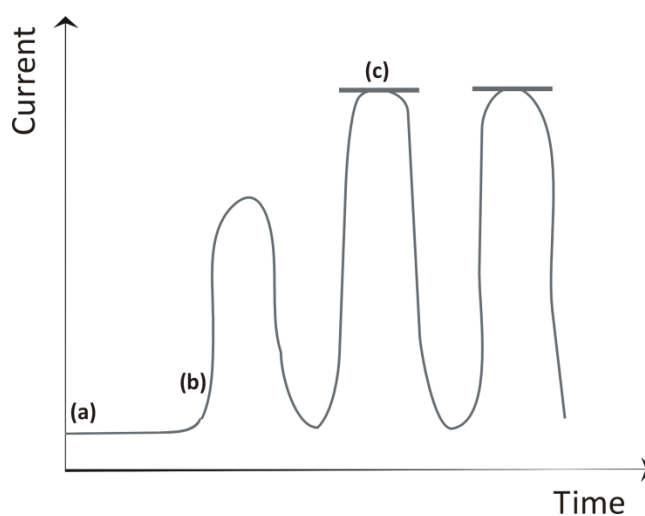


Figure 2.8: Amperometric detection scan showing the biofilm development state; (a) lag phase, (b) early state of biofilm development and (c) steady state biofilm.

Chapter 3: Microbial electrosynthesis and anaerobic fermentation: An economic evaluation for acetic acid production

3.1 Introduction

Chemicals have had a fivefold increase in global demand from 1980 to 2010 and it is projected to reach 3,500 Billion USD by 2020 in developed countries only (Massey and Jacobs, 2011). As a result, energy demand and greenhouse gas emissions are growing exponentially (DECC, 2015). Acetic acid is one of the most valuable chemicals as it is an essential raw material for many petrochemical intermediates and products. Its derivatives and applications include latex emulsion resins for paints, adhesives, paper coatings, textile finishing agents, cellulose acetate fibres, cigarette filter tow and cellulosic plastics (MMSA, 2013). Acetic acid's global demand is expected to grow by 4.9% per year and reach 16 million tonnes by 2020 (Mordor Intelligence, 2015). Acetic acid is mainly synthesized chemically via methanol carbonylation, acetaldehyde oxidation, oxidation of naphtha and n-butane, fermentation of hydrocarbons, and ethane direct oxidation (Sano *et al.*, 1999; Hosea *et al.*, 2005; Soliman *et al.*, 2012).

Acetic acid was first produced biologically by oxidative fermentation using ethanol as a raw material and *Acetobacter* bacteria as a catalyst (Hromatka and Ebner, 1949). This process has become the conventional route for producing vinegar and it accounts for the 5% of worldwide production. Synthetically, acetic acid is currently obtained using five main processes. Methanol carbonylation is the most widely used process for large scale production and is responsible for the 65% of the world's stock (Soliman *et al.*, 2012). The high pressure and high temperature process of methanol carbonylation was later optimized by Monsanto process (Patent US 3769329, 1973). Monsanto processes operating conditions were then optimized through a newer the Cativa Process (Jones, 2000). The acetaldehyde oxidation is the second most important manufacturing method which can be produced from butane or naphtha oxidation or by ethylene hydration (Sano *et al.*, 1999). Prior to methanol carbonylation commercialization, acetaldehyde oxidation was the first process used and it was responsible for about 30% of the acetate produced worldwide (Yoneda *et al.*, 2001). The ethylene oxidation process replaced most of the acetaldehyde process and became competitive with methanol carbonylation in small plants (100-250 kt/y) which accounts to 30% of the worldwide production. Ethylene oxidation (Hoecht-Wacker process) uses a single stage conversion rather than the two stages required in acetaldehyde oxidation (Yoneda *et al.*, 2001). The most recent acetic acid chemical

route was introduced in 2002 and is known as ethane direct oxidation. Here acetic acid is produced using ethane as raw material (Q. Smejkal *et al.*, 2005). The partial oxidation of ethane became very attractive for acetic acid production as ethane costs as low as £0.75/(kJ/Kg) as commercialized in Saudi Arabia by ARAMCO (Soliman *et al.*, 2012).

However, all these processes form a significant amount of by-products making their separation and recovery complex and expensive (Sano *et al.*, 1999; Yoneda *et al.*, 2001). As corrosive chemical catalysts are used, reaction vessels are made of expensive materials (Yoneda *et al.*, 2001). Furthermore, they demand high temperature and pressure conditions which require considerable energy and cause CO₂ emissions (Chenier, 2002). Hence, the development of alternative production routes from renewable feedstock capable of reducing hazardous substances while meeting acetic acid's demand is highly desired.

Anaerobic fermentation (AF) is a bioprocess capable of reducing carbon monoxide and water into acetic acid using *Clostridium* bacteria, but it releases CO₂ (Jia *et al.*, 2007). Suitably, studies on microbial electrosynthesis (MES) have shown the feasibility of reducing CO₂ and water into acetic acid using acetogenic bacteria (Nevin *et al.*, 2010; Nevin *et al.*, 2011; Li *et al.*, 2012; Marshall *et al.*, 2012; Marshall *et al.*, 2013). Although the biological conversion of gaseous substrates into chemicals by using microorganisms as biocatalysts shows great potential, both bioprocesses (i.e. AF and MES) are limited by energy demand and low production rates which cap their efficiency.

Currently, methanol carbonylation is the most important process for large scale acetic acid production as it is responsible for the 65% of the world's stock. On the other hand, ethane direct oxidation became very attractive for acetic acid production as ethane costs as low as £0.75 per million BTU and is commercialized in Saudi Arabia from 2012 (Soliman *et al.*, 2012; BMI Research, 2014). Economic evaluations between methanol carbonylation and ethane oxidation demonstrated that methanol carbonylation requires higher investment costs compared to ethane oxidation caused by the special materials used for the construction of the plant (Smejkal *et al.*, 2005). Despite that, production costs of methanol carbonylation were lower mainly due to conversion rates (higher product formation). The features of ethane direct oxidation showed its capability to compete with methanol carbonylation and allowed reduction projections using process design optimization (Soliman *et al.*, 2012).

There is no comprehensive evaluation on investment and production costs for bioprocesses, however; an economic analysis on lysine production from sucrose was recently published on bulk electricity prices for MES compared to fermentation (Harnisch *et al.*, 2015). It was

demonstrated that a sensible market potential for MES could be anticipated if higher yields up to 24.7 mM are achieved per reactor (Total yield \approx 444 mM). Additionally, an estimation of a commercial electricity price was evaluated on acetate production from CO₂ using MES showing a compatible with the current market (Marshall *et al.*, 2013). However, as in Harnisch *et al.* (2015), no other costs such as capital and fully operating costs were taken into account. In regards to AF, no economic evaluation was found other than using AF of organic wastes to generate renewable energy; i.e. biogas (Gebrezgabher *et al.*, 2010) where it was shown that using reverse osmosis as a green fertilizer would lower environmental burden but incur high investment costs. These findings confirm the importance of performing economic evaluations on new technologies.

To the author's knowledge, the production of acetic acid via bioprocesses using gaseous substrates has not been economically assessed because of the early stage of the technologies' development. In this study, we evaluate investment and production costs of acetic acid bioproduction via MES and AF compared to methanol carbonylation and ethane direct oxidation. We further assess the economic viability and profitability of integrating MES as a recycle plant for AF. In addition, investment and production costs as well as the pay-back period and discounted cash flow rate of return of MES for the production of acetic, formic and propionic acids, methanol and ethanol for a larger capacity plant are also evaluated and optimized by the use of renewable energy.

3.1.1 General hypothesis:

MES could be cost-competitive and environmental beneficial for the production of acetic acid using microorganisms as biocatalysts and carbon dioxide as a raw material.

3.1.2 Objectives:

1. To evaluate the **investment** and **production costs** of MES and AF compared to conventional routes; methanol carbonylation and ethane direct oxidation
2. To **integrate** AF and MES processes to **optimize** the production costs
3. To evaluate **investment** and **production costs of other** possible **chemicals** produced from MES
4. To assess the **economic return** and **financial risk** of all designed plants

3.2 Theory and methodology

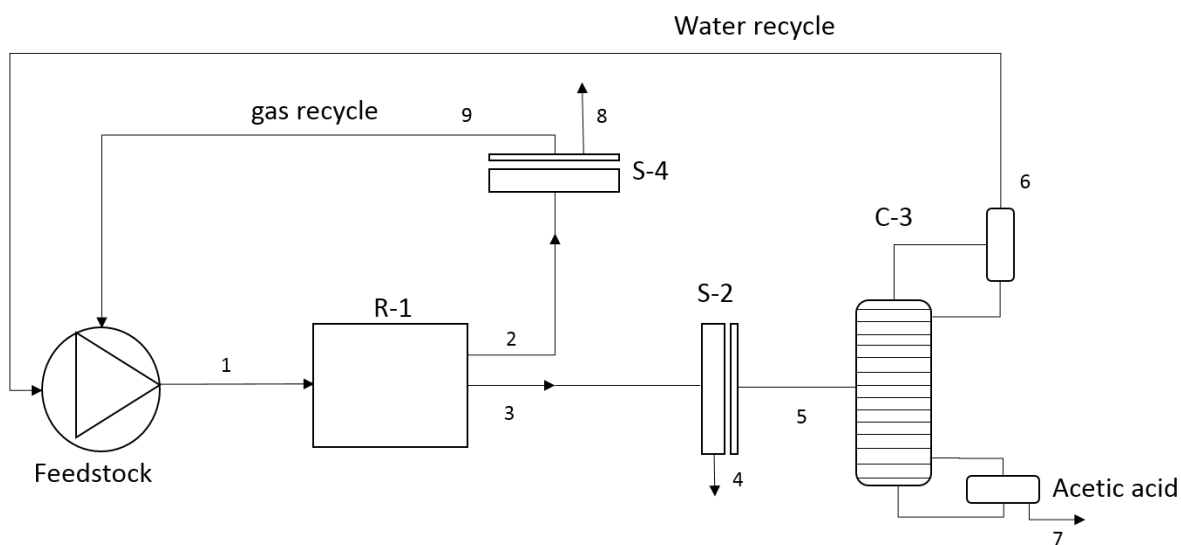
3.2.1 Process description and economic analysis based on investment and production costs

The analysis for MES and AF was calculated based on a plant producing 100 tonne per year (t/y) as per productivity rates reported in the literature (Jia *et al.*, 2007; Marshall *et al.*, 2013). A recent study in MES showed a 11.4 moles per day production of acetic acid with a 94% conversion rates by increasing product specificity with well – acclimatized and enriched microbial cultures along with the use of an optimized electrode material (Jourdin *et al.*, 2015b). The study used sodium carbonates as a source of carbon indirectly derived from CO₂ instead of gaseous CO₂ as used here. Using sodium carbonates will add up operating costs as capturing CO₂ and processing it into carbonates requires process steps embedding high temperatures and raw materials such as sodium chloride and ammonia (by Solvay process) (Kiefer, 2002). This route is not evaluated here but should also be assessed in the future.

Figure 3.1A illustrates a flowsheet of MES and AF plants which includes major equipment excluding storage tanks. Figure 3.1B shows the process mass fraction throughout the flowsheet. Liquid reaction medium and gaseous substrates, CO₂ in case of MES and CO for AF, are mixed prior their entry to the reactor and are fixed to 30°C. For MES, the reactants enter the large scale single chamber bioelectrochemical systems which include the biocatalyst in the form of a biofilm on electrodes. The biofilm was assumed to be developed prior the MES start-up using wastewater as the bacterial source. The reaction occurs by applying a specific potential, -0.393 V vs. SHE (Marshall *et al.*, 2013), to achieve the preferred product. In this case, assuming that only CO₂ is being converted to acetic acid, with the occurrence of water and O₂, the liquid mixture is moved to a biocatalyst separator where any remaining biocatalyst is filtered and collected. A vacuum pump was used to draw the output gas mixture from the reactor to the membrane to separate O₂ from CO₂. The CO₂/O₂ selectivity of the membrane was assumed to be 50% with a capture efficiency of 99% (Bounaceur *et al.*, 2006; Brunetti *et al.*, 2010). Any CO₂ excess will be recycled back to the reactor where any O₂ production would be released in the atmosphere. After the removal of the biocatalyst, the liquid mixture will undergo distillation to separate water from acetic acid. A total number of four reactors were assumed to work in batches. Each batch would last for 3.66 days with a total targeted flowrate of ca. 16,652 M (1 tonne production per batch) of acetate. The coulombic efficiency of the MES reactors were estimated to be 69% (Marshall *et al.*, 2013). Similar process is used for AF using large scale bioreactors. Assuming the conversion of CO to acetate and CO₂, the liquid

mixture is moved to the biocatalyst separator followed by distillation. Any excess of CO is recycled back to the bioreactor.

(A)



(B)		1	2	3	4	5	6	7	8	9
MES	CO ₂	25%	48.5%	-	-	-	-	-	-	100%
	Acetic acid	-	-	19%	-	20%	-	100%	-	-
	H ₂ O	75%	-	79%	-	80%	100%	-	-	-
	Dead bacteria	-	-	2%	100%	-	-	-	-	-
	O ₂	-	51.5%	-	-	-	-	-	100%	-
AF	CO	66%	33%	-	-	-	-	-	-	100%
	Acetic acid	-	-	98%	-	100%	-	100%	-	-
	H ₂ O	34%	-	-	-	-	-	-	-	-
	CO ₂	-	66%	-	-	-	-	-	100%	-
	Dead bacteria	-	-	2%	100%	-	-	-	-	-

Figure 3.1: Bioprocess flowsheet of acetic acid production for a 100 t/y plant. (A) Process flowsheet schematic of microbial electrosynthesis and anaerobic fermentation with main equipment. Code letters and numbers; S: separator, R: reactor, C: rectification column, 1: Microbial electrosynthetic reactor (or anaerobic fermenter), 2: bacterial filter, 3: rectification of water-acetic acid (acetic acid purification), 4: CO₂ separation. (B) Mass fraction representation throughout the flowsheet. Stream numbers show the mass fraction of the reactants, products and biocatalysts.

The analysis for methanol carbonylation and ethane direct oxidation was calculated based on a plant producing 200 thousand tonnes per year (kt/y) which run a continuous process as described in Smejkal *et al.* (2005). All the values in the study were converted to UK pounds per tonne (£/t) for reliable comparisons unless stated differently.

3.2.2 Economic analysis based on fixed capital costs

Estimation of purchased equipment costs for methanol carbonylation (BP - Cativa process) and ethane direct oxidation were projected from Smejkal *et al.* (2005) and Soliman *et al.* (2012) respectively. For bioprocesses, the price of major equipment was estimated using an educational software cost estimator tool (McGraw-Hill Higher Education, 2003). Costs of standby equipment, storage and surge tanks were not within the scope of this economic analysis and were excluded. Equipment cost analysis for MES included the electrode (£380 per half a tonne of carbon granulars) based on Marshall *et al.* (2013). Fixed capital costs were estimated by summing up the bare erected and external costs (e.g. piping, instrumentation etc.) using Lang factors (Sinnott, 2005), and operating costs were calculated as detailed in Appendix A1 - Table 0-1. The working capital accounts for receivable, operating expenses cash and taxes and was estimated as 5% of the fixed capital cost. To obtain the total investment cost, operating and working capital costs were summed up.

3.2.3 Economic analysis based on variable costs

The amount of raw materials was calculated using the main reaction assuming that the formation of by-products is insignificant (Table 3-1). Equipment cost was converted to 2015 prices using CPI index. Raw material costs were estimated using prices for year 2015. Selectivity and conversion rates of chemical processes were used as in Smejkal *et al.* (2005) and Soliman *et al.* (2012), whereas the rates for bioprocesses were used as in Jia *et al.* (2007) and Marshall *et al.* (2013) (see Appendix A3 – Table 0-3).

Table 3-1: Acetic acid process, reaction conditions and chemical and bacterial catalyst costs. Chemical catalysts costs were taken from ^a Smejkal *et al.* (2005) and ^b Soliman *et al.* (2012). ^c Bacteria catalysts costs were estimated from (ATCC, 2015).

Processes	Main reaction	Reaction conditions			Catalyst costs (£)	References
		°C	Atm	ΔG (kJ/mol)		
Methanol Carbonylation	$CH_3OH + CO \xrightarrow{[Ir(CO_2)I_3]^-} CH_3COOH$	190	30-40	-52.28	20,334,582 ^a	(Cheng and Kung, 1994; Smejkal <i>et al.</i> , 2005)
Ethane Oxidation	$CH_3CH_3 + 1.5O_2 \xrightarrow{[MoVNbPd]} CH_3COOH + H_2O$	277	20	-515.25	2,603,268 ^b	(Soliman <i>et al.</i> , 2012)
AF	$4CO + 2H_2O \xrightarrow{Biocatalyst} CH_3COOH + 2CO_2$	30	1	-152.20	350 ^c	(Jia <i>et al.</i> , 2007; Henstra and Stams, 2011)
MES	$2CO_2 + 6H_2O + 8e^- \xrightarrow{Biocatalyst} CH_3COOH + 4H_2O + 2O_2$	30	1	874.82	350 ^c	(Marshall <i>et al.</i> , 2013)

Glucose fermentation runs continuously without need for bacteria enhancement and it was expected that AF and MES will perform the same (Chandrasekaran, 2012). Thus, biocatalysts were included as onetime costs in raw materials (Table 3-1). However, their capabilities of storage and reproducibility at minimum cost should also be noted.

The economic analysis on utilities (i.e. electricity and cooling water) was based only on the main reaction for product formation. The main reaction of the chemical processes and AF is exothermic thus cooling water was used as their utility value. To calculate the temperature of the reactor, Table 3-1 and Equation 3.1 were used. The process temperature was assumed as 25°C for the chemical processes and AF. It was assumed that the reactors' inlet and outlet were maintained isothermally at operating temperatures.

Equation 3.1

$$Q = \Delta H_R = \Delta H_R(T_1) + \int_{T_1}^{T_2} \Delta C_p dT$$

Where Q is the heat required or given out, ΔH_R is the heat of reaction, C_p is the heat capacity, T_1 is the starting temperature and T_2 is the reaction temperature (Table 3-1). To calculate the amount of cooling water required to control the reaction Equation 3.2 was used.

Equation 3.2

$$\text{Heat load } (q) = q_h = q_c$$

Where q_h is the rate of heat loss by hot fluid equal to $m_h C_{p,h} \Delta T_h$, m_h is the mass flowrate, $C_{p,h}$ is the mass heat capacity constant and ΔT is the difference in the temperature. Where q_c is the rate of heat gain by cold fluid equal to $m_c C_{p,c} \Delta T_c$.

The utility of MES was calculated as the energy needed to activate and control the reaction. The operating temperature of MES was evaluated at 30 °C from -37 °C, due to CO₂ storage requirements. The energy needed for this was also taken into account. The energy balance of the reaction was calculated based on the Coulombic efficiency given by Marshall *et al.* (2013), the amount of electrons (Table 3-1) needed for the conversion of CO₂ to acetic acid and the activation energy (V).

The Gibbs free energy was calculated using Equation 2.6.

3.3 Process economics for bioprocess

3.3.1 Bioprocess integration and process economics advancement

AF and MES processes were merged together. MES was used to recycle CO₂ produced from AF and increase acetic acid production. Variable, fixed and capital investment costs were re-evaluated using the procedure as described in section 3.2.2 and 3.2.3.

3.3.2 Renewable energy utilisation and projected productivity levels

Different energy sources were used to calculate energy costs of the integrated process. Initially, natural gas was used to provide energy to the integrated process. However other energy sources were evaluated such as onshore wind, nuclear, coal, offshore wind and solar photovoltaics (Arthur, 2014) in order to reduce investment and production costs. Costs used are shown in Table 3-2. Domestic wastewater was also evaluated as an alternative renewable energy source. The energy production was calculated using a wastewater load equivalent to a community of 279 thousand people as described in Logan (2008). However, since MES showed a great potential for becoming an alternative route for the production of not only acetic acid

but a range of other chemicals, its optimization was essential. Thus, its potential was assessed using renewable energy to reduce production costs.

Table 3-2: Energy costs per MWh from different technologies

Energy sources	Cost (£/MWh)
Onshore wind	80
Gas	130
Nuclear	105
Coal	128-184
Offshore wind	147
Solar photovoltaics	171

3.3.3 Economic return and financial risk evaluations

The revenue generated by the plant came from the sales of acetic acid. The cost of products annually was expressed as:

Equation 3.3

$$Production\ cost\ (\text{£}/kg) = \frac{Operating\ costs\ (\text{£}\ per\ year)}{Total\ amount\ of\ product\ (kg\ per\ year)}$$

The plant was assumed to operate for 15 years. Tax allowance was assumed to be 20% of the invested capital in year 1 and 80% of previous tax amount thereafter. The corporation tax was assumed 20% based on UK tax rates (UK gov, 2016). The operating costs were assumed constant over the projects' life. The economic return measured pay-back period and discounted cash flow rate of return. The discounted cash flow rate of return was calculated as follows:

Equation 3.4

$$\sum_{n=15}^{n=0} \frac{Estimated\ net\ cash\ flow\ in\ year\ 15}{(1 + r')^n} = 0$$

Where r' is the discount rate (interest rate).

Similar methods and technical options were considered when methanol, ethanol, propionic and formic acids were evaluated for 1000 t/y production using MES. The reaction balances and process parameters are shown in Table 3-3. For the energy balances, the values taken for acetic and formic acids are based on experimental data which derived their activation energy. However, for propionic acid, methanol and ethanol values, the theoretical data was used as none of these products' formation has yet been investigated directly from CO₂.

Table 3-3: Main reactions occurring in MES for producing different products

Product	Main reaction	Theoretical potential (V vs. SHE)	ΔG° (KJ/mol)	Empirical potential (V vs. SHE)	References
Acetic acid	$2CO_2 + 6H_2O + 8e^- \xrightarrow{\text{Biocatalyst}} CH_3COOH + 4H_2O + 2O_2$	-0.290	874.82	-0.393	(Marshall <i>et al.</i> , 2013)
Formic acid	$CO_2 + 2H_2O + 2e^- \xrightarrow{\text{Biocatalyst}} HCOOH + H_2O + 0.5O_2$	-0.430	269	-0.203	(Reda <i>et al.</i> , 2008; Marshall <i>et al.</i> , 2013; Srikanth <i>et al.</i> , 2014)
Propionic acid	$3CO_2 + 10H_2O + 6e^- \xrightarrow{\text{Biocatalyst}} CH_3CH_2COOH + 7H_2O + 3.5O_2$	-0.290	1509	NA	(Marshall <i>et al.</i> , 2013; CEAE, 2014)
Methanol	$CO_2 + 3H_2O + 6e^- \xrightarrow{\text{Biocatalyst}} CH_3OH + H_2O + 1.5O_2$	-0.390	702.45	NA	(Xu <i>et al.</i> , 2006; CEAE, 2014)
Ethanol	$2CO_2 + 9H_2O + 18e^- \xrightarrow{\text{Biocatalyst}} CH_3CH_2OH + 6H_2O + 3O_2$	-0.335	1325	NA	(Blanchet <i>et al.</i> , 2015)

All calculations were performed in Matlab software and are shown in Appendix A2.

3.4 Results and Discussion

3.4.1 Fixed capital: equipment costs

Equipment costs of MES (498.30 £/t) and AF (418.32 £/t) were comparable as they use similar equipment (Table 3-4). However, the increased cost of MES from AF was observed due to electrode costs and large mixing tanks. The MES system evaluated did not use any proton exchange membrane but this would have represented additional costs (£6,870/m²) (Sigma Aldrich, 2016). Electrode and membrane research is essential for decreasing costs; future work insights should investigate development of high performance carbon electrodes and membrane durability at minimum costs (Holtmann *et al.*, 2014). In terms of the electrode material, positive characteristics, for sustainable operation, are: high electrical conductivity, strong bio-compatibility, chemical stability and large surface area. In this line, recent publications by Jourdin *et al.* (2015) showed that chemical production was improved ten times due to extended bacterial colonization on 3D electrodes highlighting the importance of high surface area. Furthermore, it is crucial that the electrodes and membranes are obtained from the same region as import and transport contributes 10-20% to their costs. As a result of low production rates and a large amount of reaction medium needed, based on reaction balances (Table 3-1), MES required larger reactors (total reactor size: 1.8 m³) and mixing tanks (total reactor size: 2 m³) than AF (total reactor size: 0.6 m³) which lead to additional costs.

Table 3-4: Major purchased equipment costs for acetic acid production via methanol carbonylation (200 kt/y), ethane direct oxidation (200 kt/y), AF (100 t/y), MES (100 t/y) and integrated process (200 t/y).

	Cost (£)				
	Methanol Carbonylation (Smejkal <i>et al.</i> , 2005)	Ethane direct oxidation (Smejkal <i>et al.</i> , 2005)	AF	MES	Integrated process
Main process major equipment					
Compressor	2,201,380	5,234,185	-	-	-
Pre-Heater	113,374	75,582	-	-	-
Reactor	425,158	132,270	17,262	13,821	17,262
Cooler	-	302,334	-	-	
Mixing tank	-	-	7,621	15,242	21,541
Tank	1,322,717	80,281	-	-	-
Distillation column	1,150,834	1,794,578	13,251	13,251	13,251
Catalyst separator	8,434,525	-	1,998	1,998	1,998
Gas separator	56,669	47,224	1,700	1,700	2,000
Recycle	-	-	-	-	13,821
Electrodes	-	-	-	3,818	3,818
Total (£):	13,700,000	7,600,000	41,832	49,830	75,013
Total (£/ton):	68.5	38	418.32	498.30	375.06

Bioprocesses did not require expensive equipment, as they can be fabricated of stainless steel. The material choice is an important parameter for the plants development to ensure long time operation. For example, methanol carbonylation used Hastelloy alloy as equipment material due to the use of high corrosive catalyst mixture ($Rh(CO)_x$) in the process. This option made the total purchase equipment costs of methanol carbonylation (£13.7 million) overpriced in relation to ethane direct oxidation (£7.6 million), AF (£41.8k) and MES (£49.8k). On the other hand, ethane direct oxidation required an expensive compressor when the production capacity was as high as 200 kt/y (Smejkal *et al.*, 2005) making it the main contributor to the purchase equipment cost. Acetic acid purification process of chemical processes were 86 (£1.15 million) and 135 (£1.79 million) times more expensive, respectively, than bioprocesses (£13.2 k) mainly due to the unit size (Patent US 5160412, 1991). Another benefit of bioprocesses, is the use of filtration systems (£1,998), for separating the biocatalyst, which showed to be 4220 times cheaper than the catalyst separator used for methanol carbonylation (£8.4 million). In addition, in bioprocesses, a membrane system (£1700) was used for gas separation which was 33 and 28 times less expensive than the conventional gas separators used in methanol

carbonylation (£56.6 k) and ethane direct oxidation (£47.2 k), respectively. However, showing the cost in relation to unit capacity per tonne (Table 3-4) made the bioprocesses most expensive as a result of the low production rates. In this study, it was assumed for bioprocesses, that one batch would last for 3.66 days (88 hours) for the production of 1 tonne. Maximizing productivities by increasing residence time could contribute to a further reduction in equipment costs.

3.4.2 Total Investment and operating costs

Total investment costs for acetic acid production via MES (1,904 £/t) and AF (1,598 £/t) were about 85% more expensive than methanol carbonylation (261 £/t) and ethane direct oxidation (258.50 £/t) (Table 3-5). The plant size and number of equipment is critical for the economics of a process as it is directly related to the investment costs. By increasing the productivities of MES and AF, the investment costs would decrease substantially as the same equipment could be used for larger production quantities.

Table 3-5: Investment operating costs and production costs of acetic acid price for methanol carbonylation (200 kt/y), ethane direct oxidation (200 kt/y), AF (100 t/y) and MES (100 t/y) and the integrated processes (200 t/y). The total and detailed variable costs are also shown.

	Costs (£)				
	Methanol Carbonylation	Ethane direct oxidation	AF	MES	Integrated process
Total Investment cost (£/t):	261	258.5	1,598	1,904	1,435
Operating cost (£/t):	267	115	4147	1,378	2,390
Detailed variable cost:					
Raw material (£/t)	127	63	2,927	168	1547
Utilities (£/t)	0.67	2.41	213.1	242	227
(Bio)catalyst (£/t)	102	13.01	3.30	3.50	3.40
Total variable cost (£/t):	229.67	78.42	3143.4	413.5	1,777.4
Total Fixed cost (£/t):	37.33	36.58	380.6	1,052	608.75
Acetic acid production costs (£/kg):	0.26	0.11	4.14	1.37	0.24

Operating costs of bioprocesses were very costly compared to chemical processes (Table 3-5). Operating costs are divided into variable (i.e. raw material, utility and ((bio)catalyst costs) and fixed (e.g. maintenance, operating labour etc.) costs. Using CO₂ as a raw material for MES for the production of acetic acid can be considered as negligible cost. The cost of buying CO₂ starts from as low as 2.38 £ per metric tonne according to Global CCS Institute; with small changes based on its source (ammonia producers, pipelined CO₂, power, steel and cement plants) and thus can be considered negligible or as a cost subsidized by government (Styring et al., 2014). In fact, the cost of releasing CO₂ emissions (12-22 £ per metric ton by 2020 and reached up to 29-88 £ per metric ton) should be included, in the future, as a utility cost to support incoming legislation (Synapse Energy Economics, 2016). Therefore, companies producing CO₂ should directly absorb the costs of using in processes such as the MES. Thus water became the main contributor to raw material costs (168 £/t) in MES. On the contrary, for other processes, water costs were negligible compared to other raw materials used. Raw material costs of AF (2,927 £/t) were 46 times more expensive than ethane direct oxidation (63 £/t), 30 times more than methanol carbonylation (127 £/t) and 17 times more than MES (168 £/t). AF uses gaseous carbon monoxide and water as raw materials. Carbon monoxide was the main contributor to the raw material costs of AF as it cost 25 times (18.95 £/t) more than water (0.76 £/t) and is needed 4 times more, in quantity, than methanol carbonylation based on reactions (Table 3-1). The carbon offset policies do not apply for carbon monoxide as it has insignificant contributions to the greenhouse gas effect. However, this should be altered as carbon monoxide emissions can have an indirect impact to the environment (Shindell *et al.*, 2006). Methanol carbonylation was the most expensive acetic acid production *chemical* route as it used methanol (183.40 £/t) and carbon monoxide. Methanol costs 10 times more than carbon monoxide, resulting in the highest raw material cost. Ethane direct oxidation showed cheaper raw material costs than methanol carbonylation and AF. This is because ethane direct oxidation uses oxygen (33.62 £/t) and ethane (20.17 £/t) as its main raw materials which were almost 2 times higher than carbon monoxide and 9 times less expensive than methanol. This made ethane direct oxidation the cheapest chemical route.

Regarding utilities used for product formation, MES uses CO₂ as the main raw material which is thermodynamically stable and it requires a significant amount of electrons for the synthesis of organic compounds i.e. acetic acid, thus covering more than half (242 £/t) of the variable costs (413.5 £/t) (Rabaey *et al.*, 2011). On the other hand, AF was found to be the most expensive process for utility costs (213.1 £/t). The amount of cooling water used in AF was 318 and 88 times more compared to methanol carbonylation (0.67 £/t) and ethane direct oxidation (2.41 £/t), respectively. Decreasing the utility costs of MES equivalent to chemical processes would

make the technology more competitive. The MES reaction energy barrier does not allow for a further significant reduction on the energetic demand but costs may be depleted by exploring the use of renewable energies to drive reactions as initially discussed by Nevin *et al.* (2010).

Biocatalysts cost showed to be negligible due to their nature of reproducibility and ability of long term storage in laboratories. In contrast, chemical plants have catalyst costs added every year due to catalyst design. Methanol carbonylation had the highest cost based on catalysts as it required a mixture of iridium, ruthenium, methyl acetate and methyl iodide which are expensive and less available. The use of biocatalysts offers unique characteristics over chemical catalysts (Johannes *et al.*, 2006). Their high selectivity is a key advantage as it can reduce side reactions and simplify downstream processes. Biocatalysts also offer environmental benefits compared to chemical catalysts as they operate under mild conditions (temperature range of 20°C – 40°C and typically in a pH range of 5-8) and completely degrade in the environment.

Chemical processes had the cheapest fixed costs around 37 £/t; 10 and 28 times less than AF (380 £/t) and MES (1,052 £/t), respectively. In addition, it was revealed that 60% of MES' operating costs were covered by fixed costs suggesting that the maintenance and operating labour of the plant had a higher cost than the actual process. In this line, further detailed evaluation should be performed to explain this trend. In contrast, the fixed cost of AF was only 12% from the total operating cost, mainly due to the raw material costs (2,927 £/t).

3.4.3 Acetic acid production costs

Methanol carbonylation and ethane direct oxidation have a production cost of 0.26 and 0.11 £/kg, respectively (Table 3-5). According to the latest purchasing prices, the commercial acetic acid price was set at 0.48 £/kg in December 2015 (APIC, 2015). Production costs of acetic acid were 1.8 times lower for methanol carbonylation and 4.36 times lower for ethane direct oxidation than the commercial price, revealing the advantages of their use in industry. On the other hand, the acetic acid production costs for AF and MES were calculated at 4.14 and 1.37 £/kg, respectively which is 88% and 33% more expensive than the commercial price. In this analysis only the energy costs from the reactor were considered. For a more detailed production cost, distillation column energy costs should be considered as energy requirements for acetic acid and water separation always incur in high energy needs. Taking this into account the production costs of acetic acid through MES and AF increases to £6.55 and £9.34 per tonne, respectively (a complete energy balance is showed in Appendix A5). As production costs were highly related to operating costs, a high production cost was expected for bioprocesses.

For this reason, in this current state, bioprocesses are currently inappropriate to serve as acetic acid production plants and compete with the already existing technologies. However, the optimization of such processes in terms of productivity levels and energy management might improve their feasibility.

3.4.4 Integration of anaerobic fermentation and microbial electrosynthesis

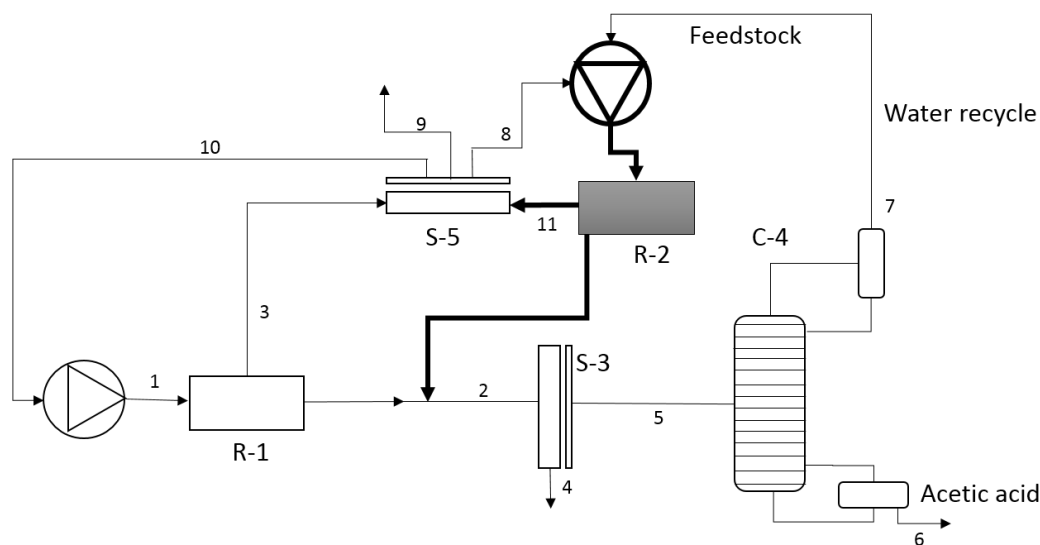
Low production rates restrict the commercial application of MES and AF. Producing small volumes of acetic acid per year results in an expensive product, compared to the commercial routes, as the price is calculated in terms of annual production cost (variable, fixed costs and sales expenses) over production rate (i.e. 1 t/y). Increasing production rates at this point of research is a technical challenge. In addition, competing with methanol carbonylation that produces 200 kt/y is not possible. One way to achieve increased product yields in MES is by using several reactors in series, as shown in the case of microbial fuel cells for energy production (Aelterman *et al.*, 2006). Doing this for MES would require a significant amount of land and electrode material, as in this study, one system can only produce 17.25 mM per day (Marshall *et al.*, 2013), which is unfeasible (i.e. thus the use of bioreactor-like reactors). Therefore, MES research should focus on optimising the actual conversion rate by looking into different aspects (such as microorganisms and their product specificity, electrode materials and reactor designs). AF can easily increase its conversion rates by providing higher residence times using larger reactors. This allows AF to be scaled up easier compared to MES due to the nature of MES technology (larger reactors increase the difficulty to sustain a biofilm on the electrodes). Additionally, to further improve the process economics, selling of other byproducts from bioprocesses should be experimentally analysed and economically explored.

AF has a better potential of scale up than MES. However, it produces CO₂ as a byproduct which is released to the atmosphere contributing to greenhouse gas emissions. Even though MES cannot compete economically with existing processes, its ability of using CO₂ as raw material allows it to serve as a recycle plant. Integrating MES with AF, could offer complementary advantages and increase the production rates as well as avoiding the release of CO₂, increase the process efficiency and result in lower investment costs as the same refining equipment will be used for both. Since MES is not only capable of producing acetic acid from CO₂ but a range of other carbohydrates, this principle could be applied to any plant that produces CO₂ (Cheng *et al.*, 2009; Villano *et al.*, 2010; Nevin *et al.*, 2011; Li *et al.*, 2012; Marshall *et al.*, 2013). Reusing the CO₂ stream in chemical reactions has been previously applied for the production

of syngas, hydrogen etc (Ng *et al.*, 2013; Sadhukhan *et al.*, 2015). MES integration could help AF to achieve a full polygeneration potential (Sadhukhan *et al.*, 2016).

Figure 3.2 shows the integrated process. AF was the first stage of the process where liquid water was mixed and preheated at 30°C together with gaseous carbon monoxide and pumped into the anaerobic fermenter. Assuming that only the conversion of carbon monoxide to acetic acid occurred, the mixture went through the membrane gas separator (i.e. CO₂/N₂/O₂/CO) (Duan *et al.*, 2014) where the by-product, CO₂, and excess of carbon monoxide were separated followed by recycle; carbon monoxide was recycled back to the fermenter and the CO₂ was used as raw material. The CO₂ would enter the mixing tank to be prepared and mixed with water prior its entrance in the MES reactor. The MES reactor also included electrodes and the biocatalyst in the form of biofilm. The liquid mixture from both fermenter and MES reactor was filtered to remove any remaining within the mixture. After removing bacteria, the liquid mixture underwent distillation to separate acetic acid and water. Part of the water production would be then recycled to the fermenter as raw material. By integrating the bioprocesses, the production yield automatically doubles as each of the process would produce 100 t/y of acetic acid.

(A)



(B)	(%)	1	2	3	4	5	6	7	8	9	10	11
Integrated process	CO ₂	-	-	66	-	-	-	-	100	-	-	48.5
	Acetic acid	-	31	-	-	30	100	-	-	-	-	-
	H ₂ O	34	65	-	-	70	-	100	-	-	-	-
	Dead bacteria	-	4	-	100	-	-	-	-	-	-	-
	O ₂	-	-	-	-	-	-	-	-	100	-	51.5
	CO	66	-	33	-	-	-	-	-	-	-	100

Figure 3.2: Integrated process flowsheet for the production of acetic acid of 200 t/y plant. (A) Process flowsheet schematic of the integration of anaerobic fermentation and microbial electrosynthesis with main equipment. Code letters and numbers; S: separator, R: reactor, C: rectification column, 1: anaerobic fermenter, 2: microbial electrosynthesis reactor, 3: bacterial filter, 4: rectification of water-acetic acid (acetic acid purification), 5: CO₂/N₂/O₂/CO separator. (B) Mass fraction representation throughout the flowsheet. Stream numbers show the mass fraction of the reactants, products and biocatalysts.

The advantage of integrating both bioprocesses is the use of the same downstream equipment and the increase of productivity rates. By using this approach, the investment cost (1,435 £/t) was reduced almost 23% and 14% compared to MES (1,904 £/t) and AF (1,598 £/t) as alone processes, respectively. This was mainly because of the increase in production rates (200 t/y). On the other hand, the operating costs of the integrated process (2,390 £/t) decreased 42% compared to AF (4,147 £/t) and increased 61% compared to MES (1,447 £/t) as the two alone processes are now sharing material and energy costs for downstream processes. This made the final acetic acid production costs to significantly decrease and set the production cost at 0.24 £/kg (Table 3-5) becoming compatible with the conventional routes and the current market

(0.48 £/kg). Further reductions in raw material costs may be achieved by using the water produced from the MES process to be recycled back to the fermenter or the MES reactor. As mentioned before, for the production costs, only the reactors energy costs were taken into account, however, adding the energy costs from the distillation column (since the distillation would consist of the highest energy costs in this processes due to the separation of acetic acid and water), the production costs were then set at 0.49 £/kg (the complete energy balance and mass flow rates are showed in Appendix A4 and A5). This production cost was two times more than the cost without accounting the distillation column energy costs showing the importance of including total utility costs.

3.4.5 Use of renewable energy, increase of acetic acid production rates and production of other chemicals

The evaluation of the integrated process was confirmed as a cheapest production route compared to AF and MES as stand-alone processes. However, since MES showed a great potential for becoming an alternative route for the production of not only acetic acid but a range of other chemicals, its optimization was essential. Thus, its potential was assessed using renewable energy to reduce production costs.

Here, the introduction of renewable energy is vital not only for reducing energy costs but also for the development of a sustainable process. In recent years, there has been an increasing global support of green energy. According to the European Wind Energy Association (2014), onshore wind energy was the cheapest. Based on renewable energy uses, onshore wind energy showed a minor reduction in energy costs by 2.7% setting the price at 0.23 £/kg showing no major benefits over the use of natural gas (results using other energy sources are shown in Appendix A4).

Similarly, using wind energy to cover the energy costs for MES as a stand-alone process reduced the acetic acid production cost 6.9% and set it at 1.35 £/t which still remains costly compared to the market. Another source of energy that could be used is wastewater. Bioelectrochemical systems have a wide range of application including treating wastes by applying an electrical power to achieve a product (e.g. MES) or by performing redox reactions to directly produce electrical power (microbial fuel cells, MFC). An MFC configuration can be used to treat wastewater and harvest the energy in the anode and conduct a MES process in the cathode. Along, with the energy produced, other products can be obtained such as hydrogen gas which can be sold as a by-product to increase the earnings of the plant. It was

found that 411 MW per year could be produced from a domestic wastewater which covered the entire cathode energy needs and reduced the acetic acid production cost by 16.6% reaching 1.20 £/Kg; making this source of energy more attractive than wind energy. However, increasing production rates and reducing fixed costs would still be needed in the MES process to achieve production costs compatible to the market price.

The use of MES for producing a diverse array of chemicals was also explored and shown in Table 3-6 for larger plant capacities of 1000 t/y. Chemicals such as formic and propionic acid and methanol and ethanol were assessed, including acetic acid. The production costs were evaluated with and without the use of energy derived from wastewater to justify the importance of using other energy sources. The investment cost for producing formic acid was found to be the cheapest (434,700 £/y) due to the use of smaller reactor size (total size: 7.8 m³) compared to methanol (total reactor size: 50 m³) and ethanol (total reactor size: 36 m³) that had the largest investment costs. Consequently, the purchased equipment cost was highly affected by the size of reactors. The larger the reactor, the higher the cost and thus the higher the purchased equipment cost. Methanol and ethanol were using more and larger reactors due to the allowance of only 10% of product formation for preventing the biocatalyst's death.

Table 3-6: Investment and operating costs of formic and propionic acids and methanol and alcohol using microbial electrosynthesis (1000 t/y).

	Total investment cost (£)	Operating cost (£/year)	Purchased equipment cost (£)	Production cost (£/Kg)	Production cost using wastewater (£/kg)	Market price (£/kg) (ICIS, 2016)
Acetic acid	1009300	523270	264070	0.52	0.46	0.48
Formic acid	434700	207170	113740	0.21	0.16	0.38
Propionic acid	1063800	486690	279050	0.48	0.41	1.01
Methanol	2074100	962270	542680	0.96	0.90	0.23
Ethanol	2149200	1113800	562320	1.11	0.88	1.06

The operating costs were also evaluated. Formic, acetic and propionic acids are currently produced from biological and chemical production routes using a diversity of raw materials. An example are the use of carbon monoxide and methanol for acetic acid production or methyl formate for formic acid production (Cheung et al., 2000; Reutemann and Kieczka, 2000) achieving a maximum cost of 380 £ per tonne of raw material. In the case of formic acid

synthesis, the cost can be lowered significantly if the raw materials (methanol) are produced in house or recovered from the processes. Using CO₂ as a raw material for MES for the production of biocarboxylates and bioalcohols can be considered as free of charge, revenue stream or utility cost. As explained in section 3.4.2, CO₂ can be considered as a minor or subsidized cost. Here, since all processes use CO₂ free of cost, water, energy and fixed operating costs become the main costs elements. Looking on the thermodynamic properties of CO₂ reduction to organic acids and bioalcohols, a rough indication was given on feasibility and energy consumption. Additionally, based on reaction balances (Table 3-3) ethanol, methanol and acetic acid were expected of high operating costs. Similarly to the purchased equipment cost, ethanol and methanol were driven by the fact that only 10% of alcohol was allowed to be produced per batch thus the need of more feedstock and energy utilisation. Acetic acid, on the other hand, uses a larger amount of energy (1839 MW) compared to formic (310 MW) and propionic (825 MW) acids allowing them to be the most appropriate products derived from MES. Ethanol was resulted to be the most energy demanded product set at 4600 MW which is 93 and 82% more compared to formic and propionic acids, respectively. Acetic acid was also shown to use more energy than formic and propionic acid making these two the most desirable products evaluated. These results indicate that producing bioalcohols using MES is less economically feasible than producing organic acids as also shown in (ElMekawy *et al.*, 2016).

The most beneficial products resulted from the production costs analysis were formic and propionic acids with (0.16 and 0.41 £/Kg, respectively) and without (0.21 and 0.48 £/Kg, respectively) renewable energy source, suggesting their capability to compete with the current market (Table 3-6) offering a bright opportunity in their chemical industry. This analysis indirectly suggests that bioprocesses will have better opportunities to be scaled-up for industrial intake if high value chemicals are targeted (e.g. pharmaceuticals) which will reduce the obstacles of competing with large scale chemical plants.

3.4.6 Pay-back and discounted cash flow rate of return

For the investment to be financially viable, the return over the life of the plant must exceed the original capital investment. A statement of annual cash flow over time is shown in Figure 3.3. This return was measured in terms of pay-back period and discounted cash flow rate of return.

MES for the production of methanol, the MES as a stand-alone process for acetic acid production (100 t/y plant), AF (100 t/y plant) and the integrated process for acetic acid production (200 t/y plant) produced no positive return across 15 years of operation mainly due

to the high operating costs and the low revenue, calculated on current market prices of each product. These results suggest that the capital outlay would not be paid back as the processes would not produce any net positive revenue streams across a 15 year period. Similarly no positive returns were found for MES stand-alone processes for acetic and propionic acids, and methanol. On the other hand, MES stand-alone process for formic acid and ethanol production were estimated to have pay-back period of approximately 2 and 7 years, respectively (Figure 3.3). A short pay-back time is vital for new processes as it indicates a shorter time to recover fixed capital investments, which reduced financial risk.

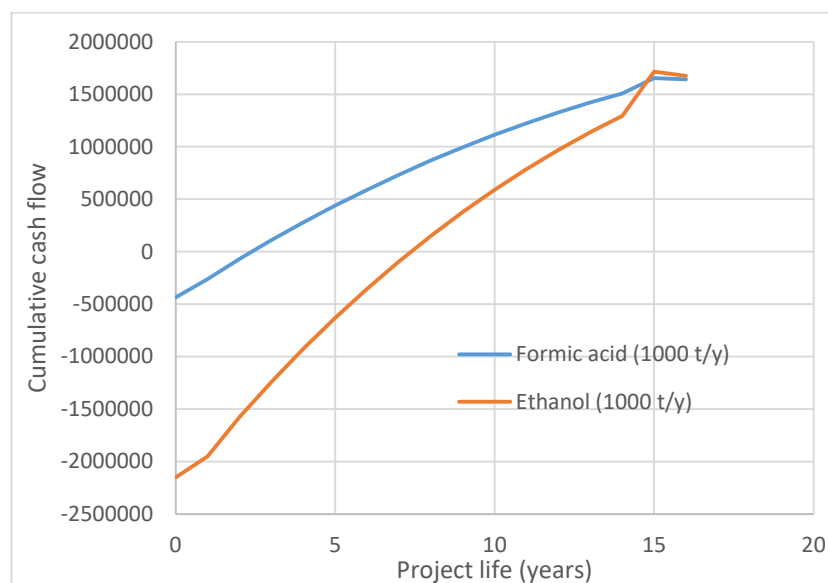


Figure 3.3: Cumulative cash flow over time of MES as stand-alone process for the production of ethanol and formic acid (1000 t/y).

The cumulative cash flow evaluation revealed that producing formic acid and ethanol using MES would offer cumulative cash flows as high as £1,640,000 and £1,670,000, respectively, at the end of the project's life. MES stand-alone process for the production of formic acid and ethanol showed a positive discounted cash flow rate of return and suggested that the plants would generate a maximum rate of *ca.* 45 and 15%, respectively. This indicates that these processes could be economically viable. In addition, based on the chemical manufacturing sector of CSI market (2016), formic acid and ethanol would offer returns far in excess of the requirements of the industry (11.60%). This makes the processes economically attractive. On the other hand, the methanol process showed a 0.0% of discounted cash flow rate of return.

Table 3.6 was based on the utilities of the MES reactor. Apart from the MES reactor and as discussed in section 3.4.3, the rectification and gas separator units were also energy intensive

(energy values and mass flow rates are shown in detail in Appendix A4 and A5). Including those energy costs, none of the investigated products showed to be economically feasible to compete with the current market. To optimise all production costs and also to make the bioalcohol production via MES attractive, renewable energy (i.e. energy derived from wastewater) was used to cover energy costs and considered these values as the net impact, and therefore reduce production costs (values are shown in Appendix A5). After using wastewater to cover energy costs, only formic acid (0.30 £/kg) and ethanol (0.88 £/kg) showed economic feasibility to compete with the current market as the price is presently set at 0.38 and 1.09 £/kg, respectively. MES for the production of methanol, acetic and propionic acids produced no positive return across 15 years of operation, mainly due to the high operating costs and low revenue, both calculated based upon current market prices of each product. These results suggested that the capital outlay would not be paid back as the process would not generate any net positive revenue streams across a 15-year period. Pay-back period was estimated to start on the 15th year for all investigated MES projects. The discounted cash flow rate of return of the MES for formic acid and ethanol was also evaluated and suggested that the plants would generate a maximum rate of *ca.* 21 and 14%, respectively. This indicates that these two processes could be economically viable based on the chemical manufacturing sector of CSI market (2016).

These results suggest that MES as a production route using bioelectrochemical conversions would become more attractive if high-energy value molecules with high market value are targeted. The market of the assessed chemicals is in scale of 100 thousand tonnes to million tonnes with acetic acid to have the largest market volume as it is used as a raw material for many petrochemical intermediates (MMSA, 2013). Market saturation is an important limitation in establishing a business case and in defining the production strategy for a targeted chemical. Propionic and formic acids showed to be the most interesting assessed chemicals from both their use and the economic point of view. However, their global production stands at 350 thousand (ICIS Chemical Business, 2007) and 610 thousand (ICIS Chemical Business, 2006) tonnes per year, respectively. A strategy that can be applied in order for MES to become part of industry as a production route, is to achieve a full atom economy. The produced water and oxygen from these process already contribute to a better atom economy and they can also be sold to contribute to the process revenue.

3.5 Conclusions

An economic analysis of MES and AF for acetic acid production has been presented. The use of gaseous substrates and especially CO₂ offers environmental benefits over the chemical processes, but embeds high costs. High energy demand (i.e. for MES) and low production rate resulted to expensive investment and production costs of bioprocesses compared to chemical processes. On the other hand, MES' low raw material costs showed an advantage over AF and the chemical process. The research findings of this study have provided evidence that MES and AF cannot stand as alone processes; however, an integration between them can give complementary advantages on economics by reducing production costs, avoiding CO₂ emission in the environment, and increasing overall process efficiency performance by widening the production rates. Further, the evaluation of other chemicals showed that formic and propionic acids can be the cheapest products derived from MES as stand-alone processes compared to acetic acid, methanol and ethanol mainly due to the less energy and feedstock demand. In addition, using energy derived from wastewater sources to cover part of the energy costs reduced the production costs. The economic return of the MES process for acetic, formic and propionic acids and ethanol production showed a high discounted cash flow rate of return suggesting their high economic viability. Conversely, the return of MES and AF as well as their integration for acetic acid production for lower production rates confirmed them as economically risky projects favouring the larger scale plants. The results of this study also revealed that focusing on the production of high value products of small demand would lead MES to an appropriate compatible process. MES, as a technology, not only helps decrease green-house gas emissions but can also reduce production costs and strengthen our economy. This offers a bright opportunity towards the use and scale up of MES.

Chapter 4: Comparison of biofilm and mediator driven systems for microbial electrosynthesis using *Shewanella Oneidensis* MR-1

4.1 Introduction

Shewanella Oneidensis MR-1 belongs to the genus *Shewanella* and is one of over 40 species discovered up to date (Hau and Gralnick, 2007a; Marshall *et al.*, 2013). *Shewanella Oneidensis* MR-1 is a gram-negative proteobacterium capable of aerobic and anaerobic respiration. *Shewanella Oneidensis* MR-1 cells are usually rod shaped of 2-3 μm in length and 0.4-0.7 μm in diameter (Oak Ridge National Laboratory). These facultative bacteria were discovered to be capable to swim with the aid of single polar flagellum in marine sediments of Lake Oneida (USA) in 1988 (Venkateswaran *et al.*, 1999). The *Shewanella* genus is characterised to have psychrotolerance, mild halophilicity and the ability to reduce a number of inorganic and organic compounds for respiration (Hau and Gralnick, 2007a). Their respiratory versatility and potential applicability to biotechnological processes such as metal remediation and energy production in bioelectrochemical systems (BES) had built an increased interest (Myers and Nealson, 1988; Lies *et al.*, 2005; Lovley, 2006; Ruebush *et al.*, 2006; Weber *et al.*, 2006; Logan, 2009; Watson and Logan, 2010).

Their ability to respire insoluble solutions like manganese and iron in oxide mineral forms is a particular controversy. The same ability allows the bacterium to respire carbon electrodes. However, solid metal and carbon respiration requires distinct mechanisms for electron transfer from intracellular electron donors to extracellular electron acceptors. A number of studies have been performed to understand the electron mechanism pathways of *Shewanella Oneidensis* MR-1 (Shi *et al.*, 2007a; Fredrickson *et al.*, 2008). The reported mechanisms use either direct or indirect pathways to facilitate extracellular electron transfer (EET) pathways. Direct pathways transfer electrons to soluble ions using direct contact to an electron acceptor using outer membrane cytochromes (Shi *et al.*, 2007a). Studies have also shown the ability of the bacterium to produce and utilise nanowires (Gorby *et al.*, 2006; El-Naggar *et al.*, 2010) for electron transfer and cell surface polysaccharides (Kouzuma *et al.*, 2010). Indirect pathways transfer electrons using electron shuttles such as flavins (Marsili *et al.*, 2008; Von Canstein *et al.*, 2008).

Shewanella Oneidensis MR-1 is extensively used as a model microorganism in BES research and the first application that was used in was in microbial fuel cells. A microbial fuel cell is a type of BES in which microorganisms function as biocatalysts to oxidize organic and inorganic matter

in order to produce an electrical current (Pham *et al.*, 2006; Du *et al.*, 2007). Metal remediation and energy production from *Shewanella Oneidensis* MR-1 has been accommodated in BES using the EET pathways. Electron transfer from the electrode to the bacterial cell occurs directly or indirectly (Huang *et al.*, 2011; Rabaey *et al.*, 2011). Figure 4.1 shows the EET pathways used in BESs and the cytochromes used for the electron transfer.

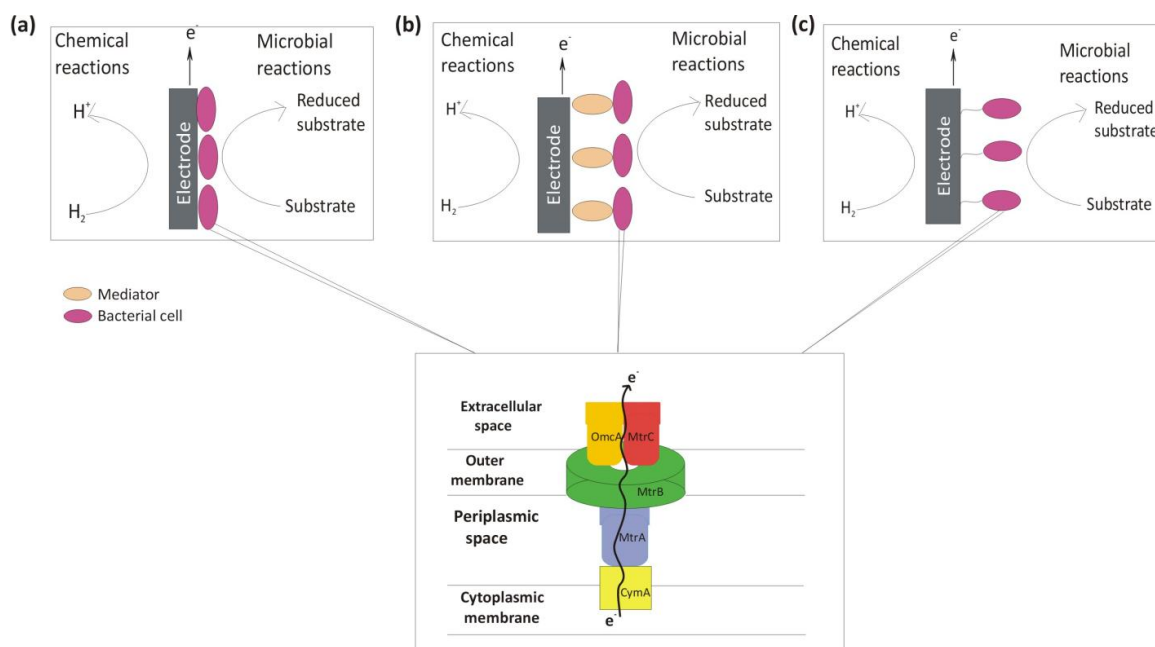


Figure 4.1: Extracellular electron transfer pathways in bioelectrochemical systems of direct (a) and indirect (b and c) pathways (Adapted from: Rabaey and Rozendal, 2010). The zoom in shows the Mtr Pathway of electron transfer of *Shewanella Oneidensis* MR-1 (Adapted from: Pirbadian *et al.*, 2014b)

Direct electron cell transfer requires a physical contact between the bacterial cell and the electrode surface to allow electron transfer. These individual mechanisms rely on the existence and grow of biomass in the form of biofilm on the electrode surface (Bond and Lovley, 2003). Studies have shown that *Shewanella Oneidensis* MR-1 strains in the presence of oxygen, form relatively large biofilms using an outer membrane bound redox compound for transferring electrons while reducing oxygen (Fredrickson *et al.*, 2008; Freguia *et al.*, 2010) and while the removal of oxygen from the environment drives biomass detachment (Thormann *et al.*, 2004; Thormann *et al.*, 2005; Thormann *et al.*, 2006). This fact shows the ability of *Shewanella Oneidensis* MR-1 to form large biofilms under anaerobic conditions and the capacity of the bacterial cells to produce high current densities in comparison with aerobic biofilms.

Although, several studies have shown the need of certain microorganisms to physically contact the electrode to transfer electrons, other studies have shown that the bacterial cells can perform EET with the help of shuttle compounds called mediators using indirect EET (Figure

4.1) (Velasquez-Orta *et al.*, 2010; Huang *et al.*, 2011). Mediators are chemically stable molecules able to catalyse redox reactions; however some exogeneous redox compounds used can be toxic to the bacterial cells. *Shewanella Oneidensis* MR-1 has shown the feasibility of self-excreting its own mediators (i.e. flavins) for the reduction of Fe (III) oxides (Von Canstein *et al.*, 2008). Marsili *et al.* (2008) detected the excretion of flavins by the *Shewanella* species and confirmed their electron mediator activity in electrochemical half cells. *Shewanella Oneidensis* MR-1 was also thought to excrete compounds that could restart menaquinone biosynthesis mutants (Newman and Kolter, 2000). This was later demonstrated that those compounds were intermediates of quinone biosynthesis which were released by lysed cells (Myers and Myers, 2004). Using mediators the electron pathway has as following. Electrons are transferred to the cell surface through a redox active proteins pathway within the cell. Then the electrons pass to the mediators in the cell periplasm or outer membrane. These mediators are then diffuse in solution and pass the electrons to suitable terminal external acceptors such as insoluble Fe (III) oxides and solid state electrodes. It is been shown that the addition of mediators such as thionine, 2-hydroxy-1,4-naphtoquinone, neutral red, methyl viologen and methylene blue (Bennetto *et al.*, 1983; Roller *et al.*, 1984) increase the current production in microbial fuel cells.

Apart from the use of the cytochromes and mediators for EET, *Shewanella Oneidensis* MR-1 have also been shown to synthesise electrically conductive appendages known as bacterial nanowires (Gorby *et al.*, 2006). Gorby *et al.* (2006) saw this mechanisms using a scanning electron microscope in *Shewanella* when was exposed to low oxygen concentrations or anaerobic conditions. These nanowires which previously thought to be pilus-like based structure was now shown, using in vivo fluorescence measurements, that it is an extension of the outer membrane and periplasm including the contact of the cytochromes responsible for EET (Pirbadian *et al.*, 2014b). Pirbadian *et al.* (2014b) also showed that the outer membrane MtrC and OmcA located next to these membrane extensions directly supports one of the two models of electron transport through the nanowires.

Microbial electrosynthesis (MES), as a novel application for chemical production has gained large interest. This process is used for the bioproduction of valuable products from sediment, polluted water and CO₂ (Gregory and Lovley, 2005; Clauwaert *et al.*, 2007a; Nevin *et al.*, 2010). MES is used for firstly producing building blocks from CO₂ (i.e. formate), followed by the formation of longer chain molecules (inc. acids and alcohols) using intermediary biocatalyst. Few studies have been done up to date where different microorganisms and different electrode materials were used to improve the carbohydrates formation rate. Methane and

acetate were the main products in a range of electron consumption efficiencies and production rates. Recent studies have shown that the choice of microorganisms, the electrode material and the reactor design are essential for optimizing the hydrocarbons production using MES (Li *et al.*, 2011; Li *et al.*, 2012; Jourdin *et al.*, 2015b; Tremblay *et al.*, 2015; Jourdin *et al.*, 2016a; Jourdin *et al.*, 2016b).

Shewanella Oneidensis MR-1 is a model bacterium used in BES and is becoming a well-known microorganism usually used to obtain energy to be used in wastewater treatment or in monitoring devices. Along with the energy production in BES, *Shewanella* cells naturally produce hydrocarbons. Wackett and Gralnick (2012) clarified the main protein responsible for fuel production. *Shewanella Oneidensis* MR-1 was used indirectly with a co-culture of *Synechococcus* for the production of fuels. The process is in two-steps where the first microbe *Synechococcus*, a *Cyanobacterium*, takes sunlight, CO₂ and water to form carbohydrates such as glucose which is a food molecule for *Shewanella Oneidensis* MR-1. *Shewanella Oneidensis* MR-1 cells then convert the glucose into complex hydrocarbons. These hydrocarbons can be further processed into vehicle fuels. Having said this, and the ability of *Shewanella Oneidensis* MR-1 of respiring a diverse array of compounds and perform different pathways of EET drives us to study its ability for bioproduction in BES using CO₂ as electron acceptor and a polarization potential as electron donor.

4.1.1 General hypothesis:

A bioelectrochemical process using *Shewanella Oneidensis* MR-1 could be a feasible system for the production of biochemical compounds using CO₂ as substrate and electron transport facilitated either by a mediator or a biofilm.

4.1.2 Objectives:

1. To cultivate ***Shewanella Oneidensis* MR-1** cells and evaluate their growth in different mediums.
2. To evaluate the performance of *Shewanella Oneidensis* MR-1 in BES using either a **biofilm** or a **mediator based electron transport**.
3. To determine the feasibility of **bioproduction from CO₂** in a BES using *Shewanella Oneidensis* MR-1 and a biofilm or mediator based electron transport.

4.2 Materials and methods

Figure 4.2 shows the methodology in the form of a flow chart in three steps; (a) bacterial growth in fermentation vessels, (b) BES monitoring and (c) biochemical production. Bacterial cells were grown in fermentation vessels until high density was achieved. The cells were then subcultured into the BES for bacterial condition period or biofilm growth. In parallel the BESs were monitored using a number of electrochemical and chemical processes. For Mediated System, the biochemical production performed after ensuring the system reached limiting carbon environment using volatile fatty acids analyses where for biofilm system, the biochemical production was performed once the electrochemical analyses showed accumulation of biomass on the electrode.

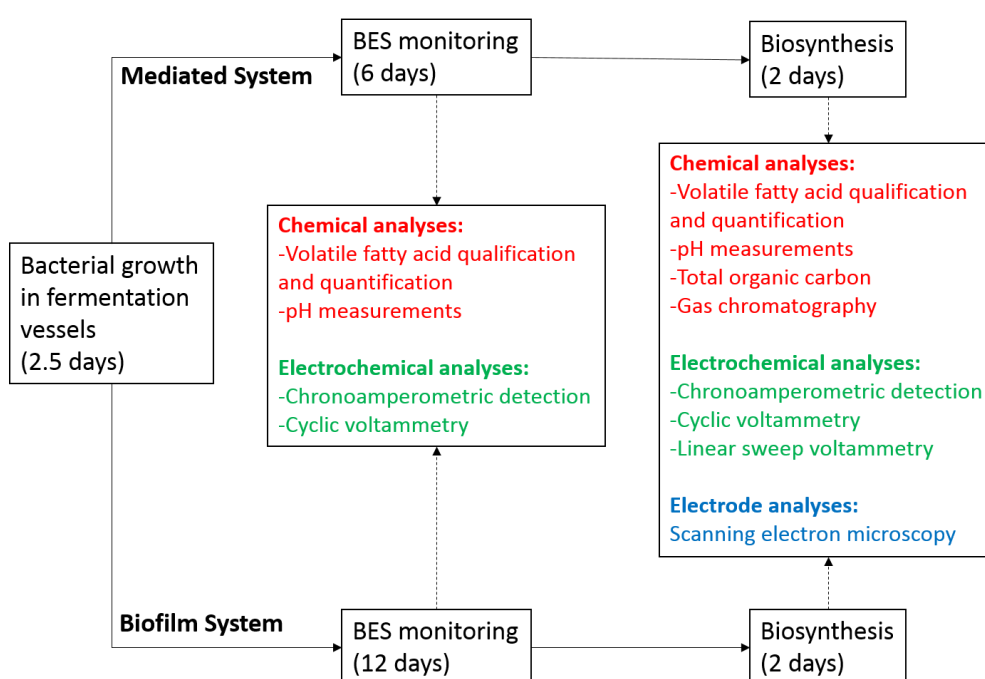


Figure 4.2: Flow chart of the methodology showing the steps followed in the experimental design

4.2.1 Growth and inoculum of electroactive culture:

4.2.1.1 Aerobic bacterial growth in fermentation vessels using different mediums:

Frozen stocks of *Shewanella Oneidensis* MR-1 (ATCC 700550) stored in glycerol solution at -80°C were inoculated in Luria broth (LB) medium and incubated aerobically at 150 rpm and 30°C for 56 hours corresponding to exponential growth/early stationary phase and an optical density (OD_{600}) of 1 (see Appendix B1).

4.2.1.2 Anaerobic bacterial growth in fermentation vessels using different media:

A volume of 1 mL from the aerobic bacterial growth was subcultured in three different anaerobic defined minimal mediums to evaluate bacterial growth. The anaerobic growth

media were labelled medium A, B and C and prepared as described previously (Meshulam-Simon *et al.*, 2007; Marsili *et al.*, 2008; Pinchuk *et al.*, 2010) (see Appendix B2). In addition 5% (v/v) of vitamin mix (see Appendix B2 - Table 0-19) and 5% (v/v) of mineral mix (see Appendix B2 - Table 0-20) were added from sterile filtered stock solutions to the growth media. HEPES (1M) was used to adjust to a final pH of 7.4. A volume of 0.05% of casamino acids was added to help the growth of cells. In order to set anaerobic conditions, the systems were purged with N₂ for 30 mins. The gases were passed through a filtration mechanism to avoid contamination. All the solutions and equipment were sterilised and/or autoclaved prior use.

Based on the growth curve obtained from the anaerobic growth, medium A was chosen to be used in the BESs (see Appendix B3 - Table 0-16). Prior to inoculation of the culture in BES, the solution was centrifuged (10 min, 10 000 rpm); washed twice and re-suspended in 5 mL of medium A.

4.2.2 Experimental set-up and operation of bioelectrochemical cells:

Six identical H-shaped BES made of glass were set up with an anode and a cathode chamber of 80 mL and headspace of 30 mL (Figure 4.3). The anode and cathode chambers were separated by a proton exchange membrane (Nafion 117, Sigma Aldrich, UK). The reactors were stirred using a magnetic stirrer to maintain uniform flow and the temperature was maintained at room temperature (25 ± 2 °C). The reactors were equipped with working and counter electrodes made of carbon cloth (4 cm², wet proofed 20%, Fuel Cell Earth, US). The electrodes were previously immersed in ethanol for 48 hours to prevent contamination in the cells, and a reference electrode of Ag/AgCl (+0.197 V vs. Standard Hydrogen electrode, Basi, UK). The electrodes were connected using titanium wire through rubber stoppers to ensure the system was close.

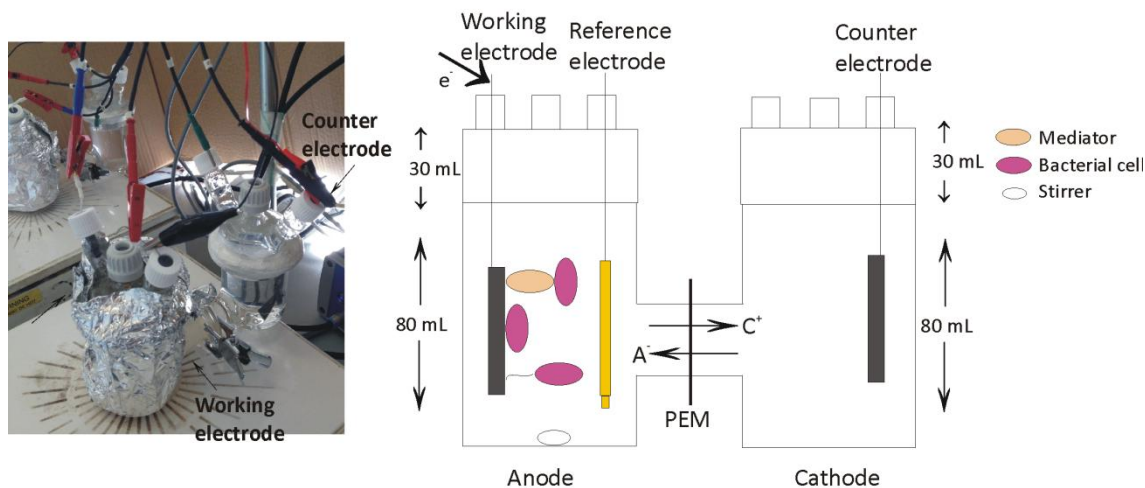


Figure 4.3: Experimental set-up of a bioelectrochemical system in H-shape cells

A volume of 80 mL of anaerobic medium A was introduced in the anode and cathode chambers of the BESs while sparging with N_2 to achieve complete anaerobic conditions for the prevention of the cells to use oxygen as an electron acceptor. *Shewanella Oneidensis* MR-1 cells were subcultured into four of the six H-shape cells as two cells were used as the blanks. The conditions used for each cell are the following:

Cell 1 & 2 - Mediated System: Riboflavin (0.0025 g/L, 2.5 μmol) was added as a mediator to facilitate electron transport as it has been shown in the literature. The anode electrode was polarized at +0.200 V (vs. Ag/AgCl, PSTrace, PalmSens) to act as an electron acceptor and lactate was used as an electron donor.

Cell 3 & 4- Biofilm System: No mediator was added and the system was given enough time and monitoring in order to ensure the growth of a biofilm. The anode electrode was polarized at +0.200 V (vs. Ag/AgCl, PSTrace, PalmSens) to act as an electron acceptor and lactate was used as an electron donor.

Cell 5- Blank System 1: No bacteria were inoculated in this reactor and it contained the growth medium, lactate and riboflavin. The anode electrode was polarized at +0.200 V (vs. Ag/AgCl, PSTrace, PalmSens) to act as an electron acceptor.

Cell 6 – Blank System 2: No bacteria were inoculated in this reactor and it only contained the growth medium and lactate. The anode electrode was polarized at +0.200 V (vs. Ag/AgCl, PSTrace, PalmSens) to act as an electron acceptor.

Figure 4.4 illustrates the experimental set-up and operation of the BES showing the direct and indirect contact of the bacterial cells with the electrode.

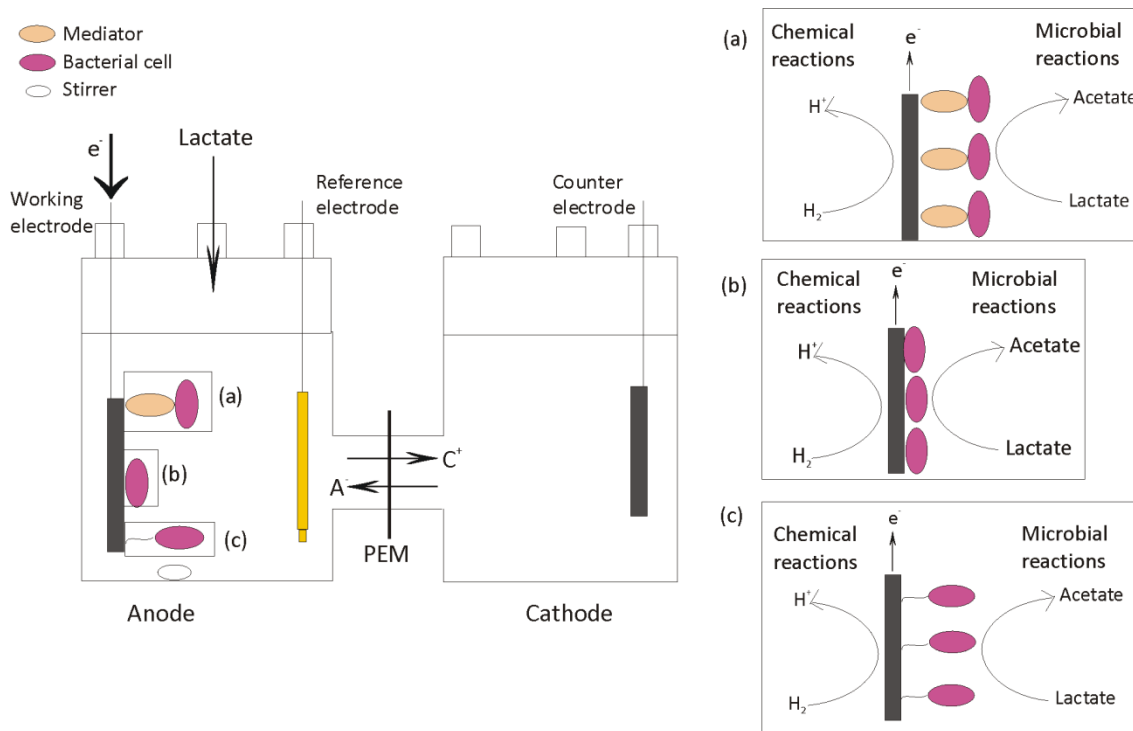


Figure 4.4: Schematic experimental set-up and operation of the bioelectrochemical cells showing different contacts of the bacterial cells and the electrode. Direct cell contact with the electrode is shown by (a) and (b) and indirect cell contact with the electrode is shown by (c) (Adapted from: Rabaey and Rozendal, 2010).

4.2.3 Bacterial growth and conditioning period

During the growth of bacteria in BES, lactate (1 g/L) was used as electron donor and the electrode as electron acceptor. In the Mediated Systems the BES were left for conditioning until the bacterial growth reached $\times 10^8$ CFU/mL (this value was the maximum obtained in previous fermentation experiments using a haemocytometer). After the bacterial growth, the Mediated system was allowed to reach a limiting carbon environment by depleting the lactate in the system as well as the acetate which was a product from lactate fermentation while the Biofilm system was left to develop a biofilm. The anode was polarized at +0.200 V (vs. Ag/AgCl) during the bacterial growth. In the biofilm systems, a concentration of 1 g/L of lactate was used frequently to enhance the biofilm where the anode electrode was polarized at +0.200 V (vs. Ag/AgCl, PStace, PalmSens) to act as an electron acceptor. The solution in the anode chamber was replaced with fresh solution after achieving steady state to ensure that no nutrients were present in the solution.

4.2.4 Biosynthesis: CO₂ as electron acceptor for bioproduction

The anode electrode was converted to cathode electrode by polarizing the potential at a negative potential of -0.200 V (vs. Ag/AgCl). Prior the polarization, the Mediated systems were allowed to reach limiting carbon environment. For the Biofilm systems, the solution was also replaced with fresh one to remove nutrients and possible carbon sources in solution. CO₂ was then used as the only electron acceptor by purging the cathode chamber for 3 mins at a flowrate of 10 mL/min. The headspace was also flushed with CO₂ gas for 3 mins at the same flowrate. The gases passed through a filtration mechanism to avoid contamination. Figure 4.5 shows the experimental set-up of the bioelectrochemical cells in biosynthesis conditions.

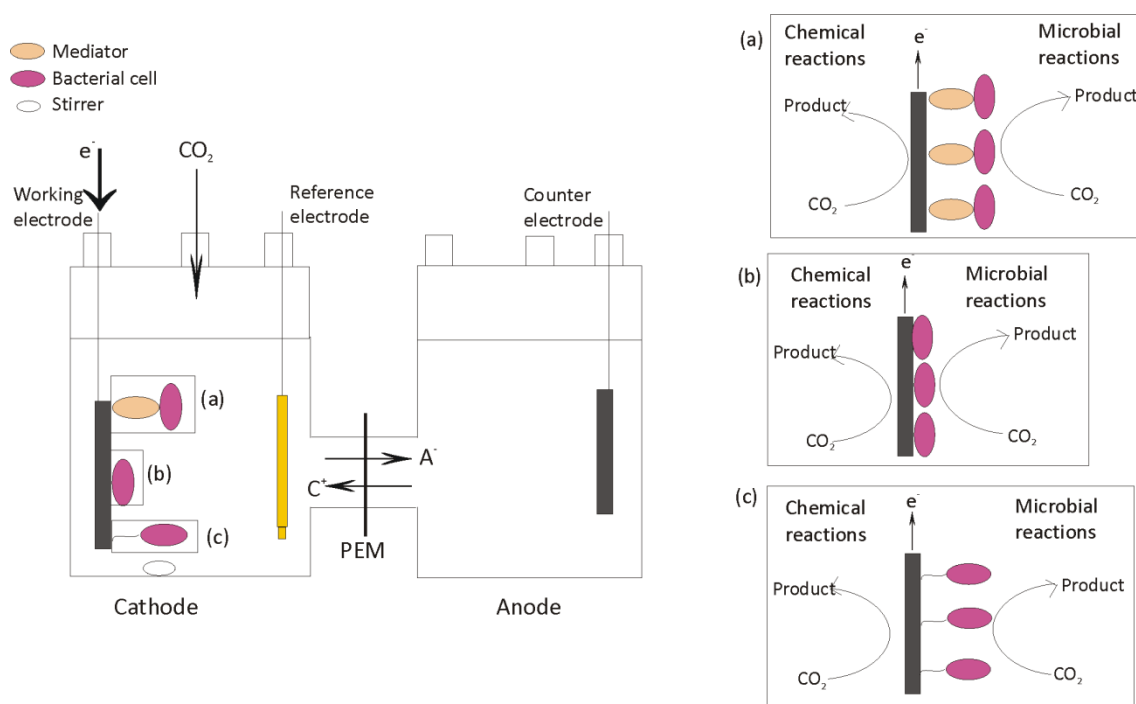


Figure 4.5: Schematic experimental set-up and operation of the bioelectrochemical cells for biosynthesis (Adapted from: Rabaey and Rozendal, 2010)

4.2.5 Electrochemical analyses

4.2.5.1 Bacterial growth and conditioning period

The electrochemical experiments were conducted in the H-shape cells using a 3 electrode system containing a reference electrode (Ag/AgCl wire within a saturated solution of NaCl (3M)) and carbon cloth (4 cm² of surface area) as working and counter electrodes wired with titanium wire as current collectors. All measurements and applied potential experiments were done on a PSTrace potentiostat. Cyclic voltammograms were measured from -0.800 to 0.400 V

(vs. Ag/AgCl) at a scan rate of 0.005 V/s. Slow scan is used to prevent damage of the cells. In this report, we evaluate the biological systems which require the initial scans of cyclic voltammetry to avoid the effect of electrode polarization on the electrode bound protein metabolism. Thus, cyclic voltammograms reported here, refer to the second scans. Polarization curves were measured during bacterial growth based on the current obtained over time under potentiostatic polarization. Furthermore, the results reported are representative of experiments performed in duplicates.

4.2.5.2 CO₂ as electron acceptor

The cyclic voltammograms were recorded from open circuit voltage conditions and the voltage was changed from -1.200 to 0 V (vs. Ag/AgCl) during bioproduction at a scan rate of 0.005 V/s. Slow scans were used to prevent damage of the cells. As mentioned previously, cyclic voltammograms reported here, refer to the second scans. Polarization curves were measured during biosynthesis based on the current obtained over time under potentiostatic polarization. Furthermore, the results reported are representative of experiments performed in duplicates. After the 48 hours of biosynthesis, linear sweep voltammetry tests were applied from -1.200 to 0.0 V (vs. Ag/AgCl) to test the ability of the microorganisms to accept electrons from the electrode.

4.2.5.3 Chemical Analyses

Gaseous and liquid samples were taken every 2 hours for a period of 12, 16, 20, 24 and finally 48 hours.

4.2.5.4 Liquid and gas analysis

Liquid and gas samples were taken to analyse bioproduction. The liquid samples were analysed for volatile fatty acids using a Dionex ICS-1000 with an AS40 auto sampler liquid chromatography system. The column was an Ionpac ICE-AS1, 4 × 250 mm analytical column with a flow rate of 0.16 mL/min, an eluent of 1.0 mM heptafluorobutyric acid solution and a cation regenerant solution used for the AMMS-ICE II Suppressor of a 5 mM tetrabutylammonium hydroxide. The injection loop was 10 µL. Also, liquid samples were analysed for total organic carbon using a Shimadzu 5050A Total organic carbon analyser, with an ASI-5000A auto sampler. The carrier gas was zero grade air, and the inorganic catalyst solution was 25% phosphoric acid.

The gaseous samples were analysed using Varian 450-GC. The gas chromatographer was equipped with 2 ovens, 5 columns and 3 detectors (2 TCDs and 1 FID). One oven housed 3 columns (Hayesep T 0.5m x1/8" ultimet, Hayesep Q 0.5m x1/8" ultimet and Molsieve 13X

1.5m x1/8" ultimet) to detect permanent gases. The second oven housed a CP-SIL 5CB FS 25X.25 (.4) column for hydrocarbons and a CP-WAX 52CB FS 25X.32 (1.2) for alcohols.

Only the last sample at 48 hours was analysed for hydrocarbons and alcohols due to the limitation of sample solution.

4.2.6 Scanning electron microscopy

Scanning electron microscopy (SEM) was used to visualize features of the biomass on the electrode and in solution. Carbon cloth electrodes with biofilm were fixed with 2.5% glutaraldehyde solution in phosphate buffer, dehydrated in increasing ethanol concentrations (25, 50, 75 and 100%) and subjected to critical point drying using an automated critical point dryer. The samples were sputter-coated with gold and examined by SEM (Cambridge Stereoscan 240 SEM, UK). In the experiments where mediators were used, cells were also present in the medium thus, the solutions were also used for SEM.

4.2.7 Calculations and analytical measurements

The cyclic voltammograms (CVs) were performed as non-turnover conditions to study the microbial oxidation and reduction of the substrate and subsequent possible electron transfer. The formal potential of a redox couple was calculated using Equation 4.1 (Bard and Faulkner, 2001).

Equation 4.1

$$E^j = \frac{E_{pA} + E_{pC}}{2}$$

Where E_{pA} is the anodic potential and E_{pC} is the cathodic potential. Using non-turnover conditions allow us to study all redox-active compounds at the electrode and the formal potential of possible EET. Further analysing the CVs, different parameters can be evaluated like peak separation (Equation 4.2) (Bard and Faulkner, 2001).

Equation 4.2

$$\Delta E_p = E_{pA} + E_{pC}$$

These parameters can be used for mechanistic and kinetic analysis electron transfer processes at electrodes when are recorded in different rate. In this study we have only calculated the rate of reaction using Equation 4.3 (Bard and Faulkner, 2001).

Equation 4.3

$$\Delta E_p = E_{pA} + E_{pC} = \frac{59}{n} mV$$

The number of electrons involved in the reduction and oxidation process separately observed using Equation 4.4 (Bard and Faulkner, 2001).

Equation 4.4

$$z = \frac{56.5}{E_p + E_{p/2}}$$

Where $E_{p/2}$ is the half peak potential calculated from the mean of the anodic and cathodic potentials.

4.3 Results and discussion:

4.3.1 Start-up and operation of BESs

Figure 4.6A shows the electric current during the addition of bacteria, riboflavin and lactate (1g/L) of the bioanode for the Mediated Systems. Riboflavin was added as a mediator to optimize the electron transfer within the bacteria and the substrate. Both cells were potentiostatically controlled at an oxidizing value of +0.200 V vs. (Ag/AgCl) to enhance the anode start-up. *Shewanella Oneidensis* MR-1 cells were inoculated after 10 minutes from the start-up of the BES. After 4 hours of the inoculation of *Shewanella Oneidensis* MR-1, lactate (1 g/L) was added in the anode compartment. A lactate spike was observed, for both systems, and the electric current immediately increased from 1 to approximately 2 μA . The absence of a lag-phase suggests the presence of electro-active culture and its ability to switch from using oxygen to use the carbon cloth anode as terminal electron acceptor in their metabolism. The electric current remained stable for approximately one day until lactate exhaustion when the current dropped down to 1 μA . Lactate (1g/L) was added in the anode chamber and the current resumed after one day and it gradually reached a maximum of 8 μA after 2 days and then dropped at 2 μA . The biomass reached a steady state after 4 days. Lactate was added two more times, and the same effect was repeated with the electric current to reach 10 μA . This indicated that system had reached the steady state phase. The electric current was then started to drop suggesting the need of substrate in the system.

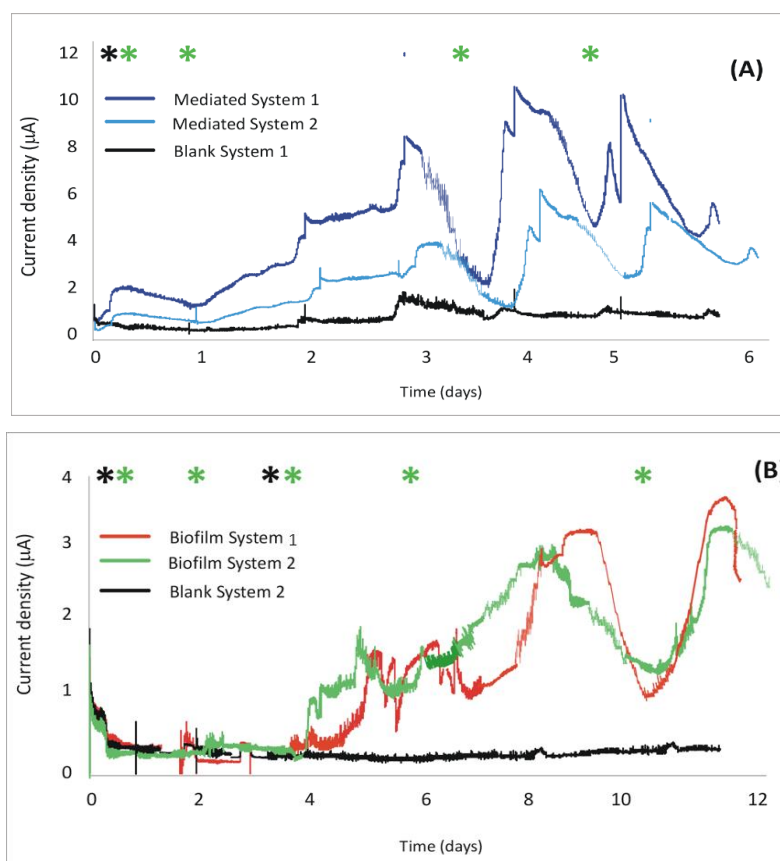


Figure 4.6: Current generation over time of (A) Mediated Systems and Blank System 1 and (B) Biofilm Systems and Blank System 2. The black star (*) indicates the addition of bacteria and the green star (*) indicates the addition of lactate (1g/L). All systems were operating at a +0.2 V vs. (Ag/AgCl) polarized potential. The experiment was performed in duplicates.

Figure 4.6B shows the electric current generation over time for Biofilm Systems and Blank System 2. Biofilm system and Blank System 2 were potentiostatically polarised at an oxidizing value of +0.200 V vs. (Ag/AgCl) during this time course. Similarly, *Shewanella Oneidensis* MR-1 cells were inoculated 10 minutes after the start-up of the Biofilm Systems followed by lactate addition (1 g/L). The electric current remained stable around 0.5 µA for approximately 2 days for both Biofilm Systems and Blank System 2. Lactate (1 g/L) was then added in the anode compartment to enhance the anode start-up where no respond was observed. The solution of the anode compartment was then replaced with fresh one, including fresh bacterial cells and lactate (1 g/L). The electric current was then immediately increased and reached 2 µA for the Biofilm Systems, where the Blank System remained stable at 0.5 µA. After almost one day, the current dropped to 1 µA and lactate (1 g/L) was added again. The Biofilm Systems immediately showed the lactate spike and increased the electric current to a maximum of 3 µA. The current remained stable for approximately 12 hours and then dropped back to 1 µA. Lactate (1 g/L) was added for the last time and a repetitive electric current peek was produced around 3.5 µA suggesting that the Biofilm Systems reached a steady state.

The Mediated Systems showed almost four times better responds of electric current than the Biofilm System. These results suggest that because the Mediated Systems were using a mediator (i.e. riboflavin), they tend to produce higher electric current densities and better use of the substrate from the bacteria. In addition, the Mediated Systems showed to condition twice times faster than the Biofilm System suggesting that the exogeneous mediator not only can increase the electric current generation but can also reduce the lag phase or conditioning time.

The reproducibility of the produced current density showed to vary for Mediated system 1 & 2 and Biofilm system 1 & 2 can be explained as a result of heterogeneity of the population and the potential for a subpopulation of cells in less active metabolic state causing activity level and biochemical processes to occur differently (Davey and O'Toole, 2000; Tolker-Nielsen and Molin, 2000; Teal *et al.*, 2006).

Subsequent analytical methods were used for elucidating the effect of changes in the local redox environment in respect to biofilm formation for Biofilm Systems and to the bacterial cells in solution for Mediated Systems. The CV scans were performed as non-turnover conditions. Using non-turnover conditions allow us to study all redox-active compounds of the substrate at the electrode and the formal potential of possible extracellular electron transfer. Figure 4.7 shows the CV scans of Mediated Systems and Biofilm Systems.

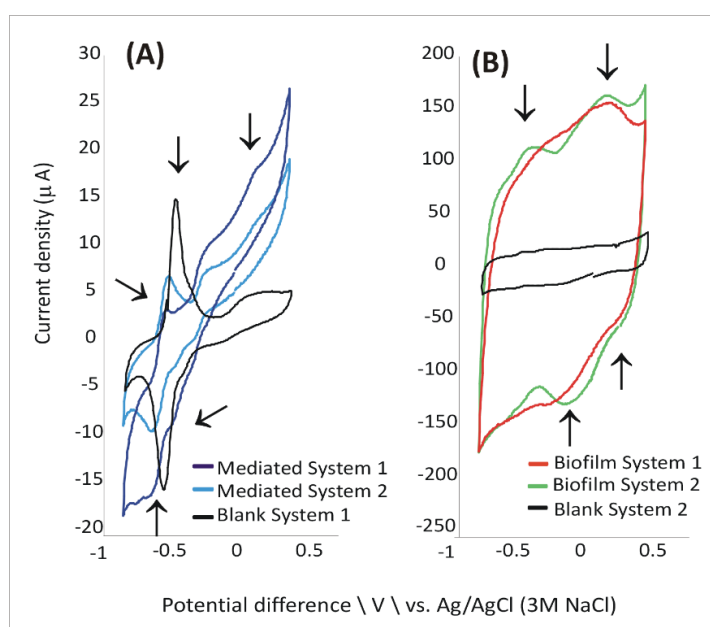


Figure 4.7: Redox activity voltammetry associated with (A) Mediated Systems and Blank System 1 and (B) Biofilm Systems and Blank System 2 with *Shewanella Oneidensis* MR-1. The blanks' voltammetry is shown as a baseline. The arrows indicate the occurred peaks.

Figure 4.7A Blank System 1 shows the electrochemical characteristics of riboflavin determined by CV scans. The concentration of riboflavin used in this experiment was based on micro molar amounts which are very often reported in microbial fuel cell studies (Velasquez-Orta *et al.*, 2010). The CV scans of both Mediated System and Blank System 1 show symmetrical response of anodic and cathodic sweeps indicating the reversibility behaviour of the redox reactions. The redox potential of riboflavin was around -0.505 and -0.500 V (vs. Ag/AgCl, Table 4-1) for all the CV scans of Mediated System and Blank System 1. This redox potential agrees with the standard thermodynamic potential of the flavin molecule (Walsh, 1980) with a shift to the left. These results confirm that the CV can be used to qualify the electrochemical response of riboflavin. A reversible redox peak around -0.280 V (vs. Ag/AgCl, Table 4-1) was also detected in Mediated System with a measured pH of 6.7. If the pH of the solutions gets more acidic (pH<7) the peak tends to be shifted to the right. Thus, the peak identified could be referred to *Shewanella Oneidensis* MR-1 redox potential and lactate to acetate redox potential. Meitl *et al.* (2009) suggested that the proteins MtrcA and OmcA on the bacterium membrane can be shaped at the same position and likely replace each other due to the similar redox potential they have (Table 4-2). Also, they reported that *Shewanella Oneidensis* MR-1 has a tendency of forming the redox peak at a close position to the proteins resulting to one peak that sums up the current from the proteins and the electrode. This suggests that the peak identified around -0.280 V (vs. Ag/AgCl) is possibly a sum up peak from the OmcA, MtrC, and lactate to acetate and the electrode. As the bacterial growth becomes more extend over time, the presence of extracellular electron transfer mechanism appears around -0.45 V (vs. Ag/AgCl). This electrode reduction flow is characteristic to a mediator (Marsili *et al.*, 2008). This mediator is possibly the exogeneous riboflavin added in the system suggested from the catalytic feature corresponding to the potential similar with that of riboflavin's.

Table 4-1: Electrochemical parameters of the redox reaction potentials vs. Ag/AgCl obtained by the CV scans at a scan rate of 0.005 V/s.

	E_{pA} (V)	E_{pC} (V)	E_j (V)	Absolute z (mV)	pH
				z	
Mediated System	-0.500 (± 0.05)	-0.510 (± 0.05)	-0.505 (± 0.05)	11.3	6.9
	-0.250 (± 0.05)	-0.310 (± 0.05)	-0.280 (± 0.05)	1.88	6.7
	+0.220 (± 0.05)	0.280 (± 0.05)	-0.030 (± 0.05)	0.23	6.7
Blank System 1	-0.500	-0.500	-0.500	0	7
Biofilm System	-0.500	-0.400	-0.45	1.13	6.7
	+0.050 (± 0.05)	+0.00 (± 0.05)	+0.025 (± 0.05)	2.26	6.7
	-0.410	-0.610	-0.510	0.56	6.5
	+0.180	-0.200 (± 0.05)	-0.010	0.30	6.5
Blank System 2	-	-	-	-	7

Figure 4.7B shows the CV scans from Biofilm System and Blank System 2. The CV scans of Biofilm System seem to maintain a redox peak around -0.450 to -0.510 V (vs. Ag/AgCl, Table 4-1) which agrees with the redox potential of riboflavin (Table 4-2). *Shewanella Oneidensis* MR-1 was found to produce its own mediators (Marsili *et al.*, 2008; Von Canstein *et al.*, 2008) of flavin molecules. This fact and the detected peak suggest the excretion of flavin molecules from the bacteria in the system. However, the peak is slightly shifted to the right most probably to the pH changes. Another peak was also detected around 0.025 V (vs. Ag/AgCl, Table 4-1) over time. This potential comes into agreement with the NAD^+ to NADH energy molecule. The CV scans of Blank System 2 did not show any peak. Also, the CV scans obtained for Biofilm System also suggest evidence for the accumulation of biomass on the electrode surface area, based on a higher current density relative to the Blank System 2 scans.

Table 4-2: Possible electrochemical potentials vs. Ag/AgCl, at pH 7, of possible reactions occurring in Mediated and Biofilm Systems

		<i>E</i> ⁰ (V)	References
Mediator	Riboflavin	-0.219	(Albertas Malinauskas, 2008)
		-0.450	(Velasquez-Orta <i>et al.</i> , 2010)
Cell proteins	MtrC	-0.149	(Meitl <i>et al.</i> , 2009)
		-0.163	(Eggleston <i>et al.</i> , 2008)
		-0.267	(Hartshorne <i>et al.</i> , 2007)
	OmcA	-0.189	(Meitl <i>et al.</i> , 2009)
		-0.201	"
		-0.160	(Eggleston <i>et al.</i> , 2008)
Bacteria	<i>Shewanella Oneidensis</i> MR-1	-0.173	(Meitl <i>et al.</i> , 2009)
		-0.214	"
		-0.136	(Kim <i>et al.</i> , 2002)
		-0.183	(Cho and Ellington, 2007)
Substrate	<i>Lactate/acetate</i>	-0.226	(White, 1999)
	<i>Lactate + NAD⁺ → Acetate + NADH</i>	+0.151	"
Energy molecules	<i>NAD⁺/NADH</i>	-0.034	"
Electrochemical reactions	$\frac{1}{2} O_2 + 2H^+ + e^- \rightarrow H_2O$	1.013	(Bard, 1985)
	$2H^+ + 2e^- \rightarrow H_2$	-0.224	"

Table 4-1 shows the electrochemical parameters of the peaks derived from the CV scans. Although the riboflavin and lactate redox reactions involve two electrons, the actual redox responses obtained from the CV were valued in a range of 0.23-11.3 and indicated a considerably low Faradic conversion of the compounds. The number of electrons appeared to be higher in Mediated System than Biofilm System suggesting that the electron transfer in Mediated System is more efficient.

To ensure that no carbon atoms were available in the systems and to continue with the biosynthesis experiment, different attempts were taken. During the bacterial growth in the systems and until the biomass reaches steady state, Mediated System was allowed to reach a limiting carbon environment by depleting the lactate in the system as well as the acetate which was a product of lactate fermentation. Total organic carbon and volatile fatty acid analyses results showed no source of carbon atoms were present in solution. The solution in the anode compartment of Blank System 1 was replaced with fresh one to ensure no possible electron acceptors are present in solution.

For Biofilm System, the solution in the anode compartment was replaced with fresh one to remove all electron acceptors or carbohydrate sources. This ensures that no nutrients or carbon atoms were available in solution and that the system reached a carbon limiting environment.

All the biosynthesis experiments hereafter described were carried out after the culture had reached a stable performance (i.e. after 7 days for Mediated system and after 12 days for Biofilm System).

4.3.2 Biosynthesis using CO₂ in BESs

Figure 4.8 shows the bioproduction of *Shewanella Oneidensis* MR-1 culture used for MES during the 48 hours of operation using CO₂ as electron acceptor and the carbon cloth electrode as electron donor with a polarized potential of -0.200 V vs. (Ag/AgCl). All systems were purged with CO₂ gas before polarization. The first sample (time 0) was taken few minutes after polarization. Figure 4.8A show bioproduction of Mediated System. Acetic acid was a primary bioproduct detected during biosynthesis starting at 0.03 mmol/L and reaching a maximum of 0.66 mmol/L after 4 hours of operation. The acetic acid values fluctuated from 0.03096 - 0.6625 mmol/L throughout the experiment. Formic acid was qualified continuously during the experiment and quantified from 0.0044-0.17 mmol/L. Furthermore, butyric and propionic acids traces were identified sporadically around 0.0045 mmol/L. Figure 4.8B show bioproduction of Biofilm System and Blank System 2. The Biofilm System showed to produce acetic acid only after 20 hours of operation at 0.5386 mmol/L. No carbohydrates were observed for Blank System 1 and 2. The occurrence of different chemical produced might be a result of heterogeneity as discussed earlier in section 4.3.1.

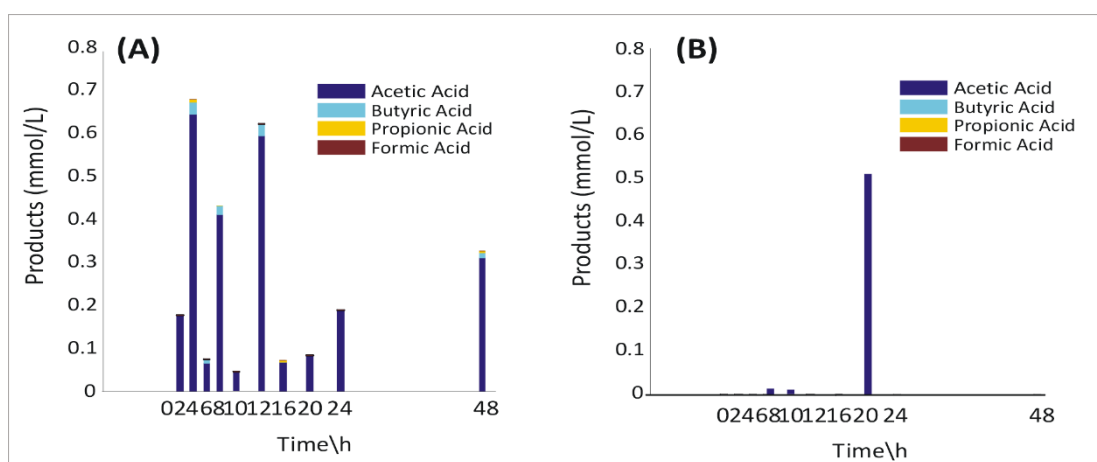


Figure 4.8: Bioproduction performance of (A) Mediated System and (B) Biofilm System for volatile fatty acids.

In addition, the total organic carbon and gas chromatography of all systems were analysed after 48 hours of operation. Due to the small volume of reactor only small amount of liquid can be collected. Thus only the samples taken at 48 hours were used for the gas chromatographer. Figure 4.9 shows the amount of carbon fraction in solution for Mediated System and Biofilm System. The Mediated System showed *ca.* 18% of carbon fraction with main product to be ethane. Acetic acid and PIPES (pH controller) were also part of the carbon fraction in low concentrations of 0.5 and 5%, respectively. The Biofilm System did not show any, however, 5% of the carbon fraction was qualified as PIPES. The Blank System 1 and 2 did not show any carbon fractions apart from the reactant, CO₂. The biosynthesis results derived from the chemical analyses suggest the capability of *Shewanella Oneidensis* MR-1 to biosynthesise hydrocarbons directly from CO₂.

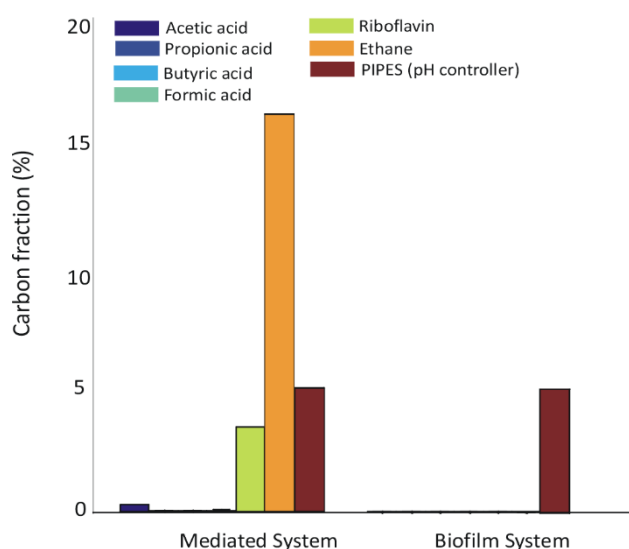


Figure 4.9: The cacluated carbon fraction present in solution after 48 hours of operation for the Mediated and Biofilm System.

Consequent analytical methods were used to elucidate the effect of changes in the local redox environment in respect to biofilm formation for Biofilm System and to the bacterial cells in solution for Mediated System. Figure 4.10 shows the CV scans recorded after 48 hours of biosynthesis. Figure 4.10 (A) shows the CV scans form Mediated Systems and Blank System 1 and (B) from the Biofilm System and Blank System 2. Blank Systems are used as the abiotic controls and user as the baselines. The Mediated System CV scan shows the reversible riboflavin peak at -0.45 V (vs. (Ag/AgCl) as discussed earlier in Start-up and performance of the anodes section. Even that the Biofilm System CV scans did not show any peaks, the CV scan

can be used to elucidate the biomass accumulation on the electrode based on the higher current density measured than the Blank System 2.

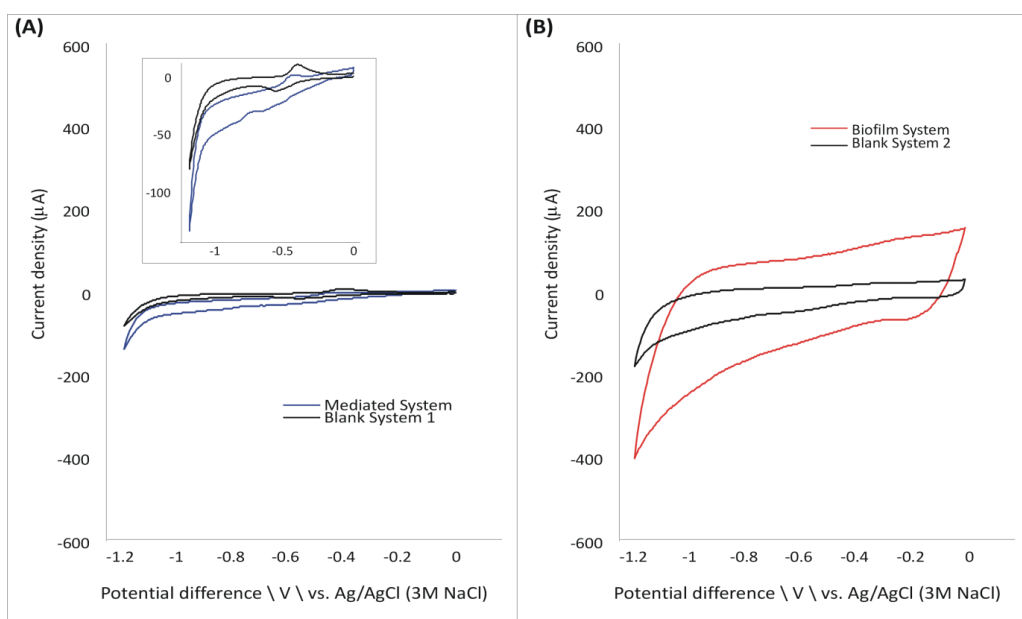


Figure 4.10: Cyclic voltammograms of (A) Mediated System and Blank System 1 and (B) Biofilm System and Blank System 2 after 48 hours of biosynthesis in bioelectrochemical systems at a scan rate of 0.005 V/s.

4.3.3 Working electrode performance

To verify the ability of *Shewanella Oneidensis* MR-1 to directly accept electrons from a polarized carbon cloth electrode, we recorded linear sweep voltammetry scans. Figure 4.11 shows the linear sweep voltammetry scans after 48 hours of biosynthesis. For both, Mediated System and Biofilm System the current density produced was higher than the ones from the abiotic controls (i.e. Blank system 1 and Blank System 2 respectively).

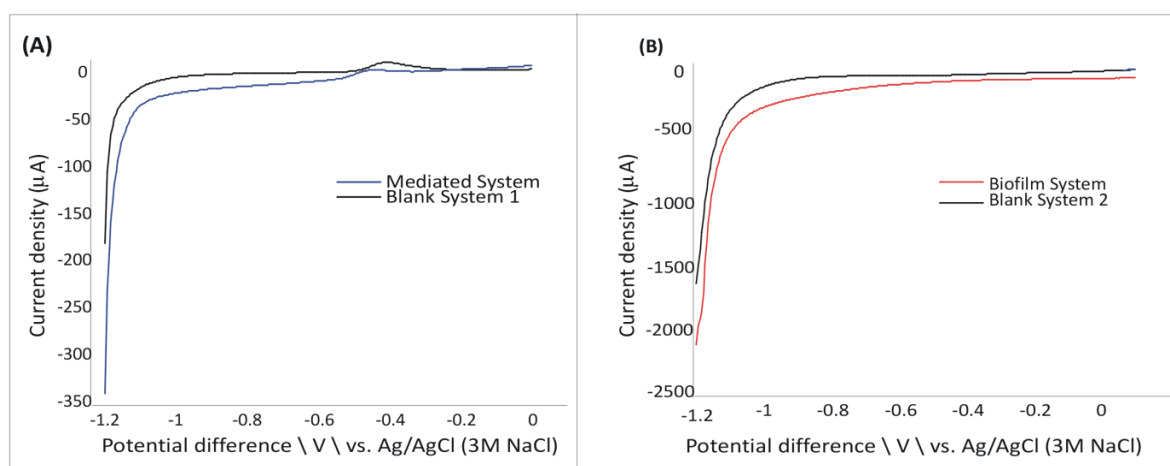


Figure 4.11: Linear sweep voltammetry scans of (A) Mediated System and Blank System 1 and (B) Biofilm System and Blank System 2 at a scan rate of 0.005 V/s.

To further verify the existence of electrogenic bacteria on the electrode and in solution, samples were taken after potentiostatic experiments and subjected to scanning electron microscopy analysis. Figure 4.12 shows the scanning electron microscopy of Mediated System solution and electrode surface and Biofilm System electrode surface. For both systems, bacteria morphology is homogeneous with rod shape cells correlating to *Shewanella Oneidensis* MR-1 cells suggesting of a pure culture biofilm and growth in solution.

In all scanning electron microscopy analyses, it is visible the formation of pilus-like nanowires which are proved to be electrically conductive appendages (Gorby *et al.*, 2006). *Shewanella Oneidensis* MR-1 is capable of nanowire production in low oxygen or anaerobic conditions with low concentration of electron acceptors. This allows us to re-ensure the anaerobic conditions from the cells. Cloudy-like substance is also present on the electrode. This substance is most possibly polysaccharide molecules excreted by the bacterial cells to help the adhesion of the cells on the electrode working as 'glue'. Polysaccharide molecules were also showed to help on the electric current generation.

The fact of low electric current produced could be due to the lack of uniformity of the biofilm. Consequently, this could be linked to the low concentration of by-product formation.

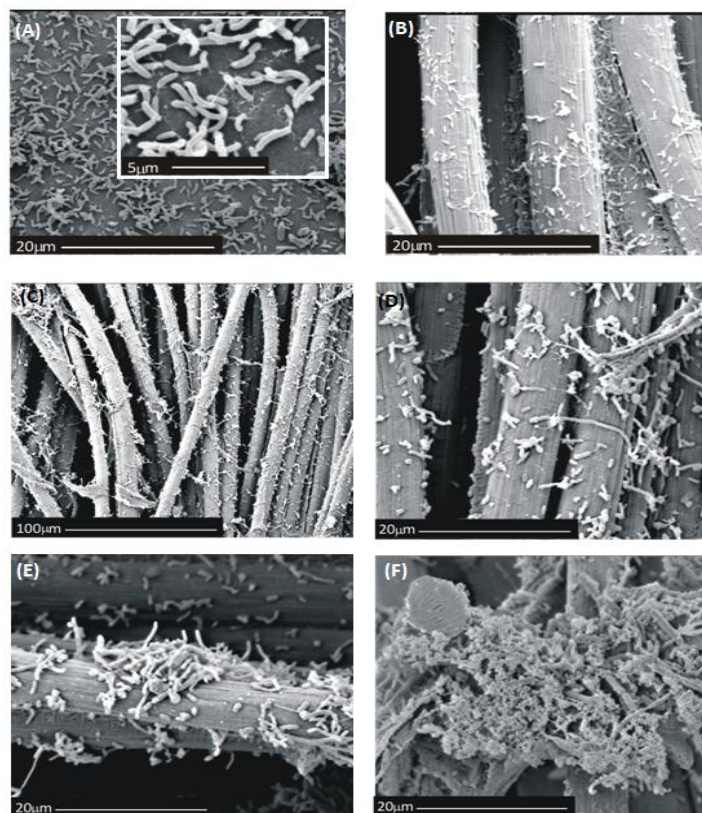


Figure 4.12: Scanning electron microscopy of Mediated System solution (A) and electrode (B) and Biofilm System electrode (C), (D), (E) and (F).

4.4 Conclusion:

This study confirmed that a Mediated System using *Shewanella Oneidensis* MR-1 produces 10 times higher electric current densities and has better use of the substrate from the bacteria suggesting that the use of mediators affects the electric density output. In addition, CV scans showed a clear catalytic activity of the Mediated System. The CV scans of Biofilm System showed evidence of resistance on the electrode which it was linked to biofilm growth. Calculations also showed a better Faradaic conversion of the compounds in the Mediated systems in terms of electron distribution suggesting that the use of mediators can optimise the reactions. The results of biosynthesis presented acetic acid to be the main product in both Mediated and Biofilm Systems suggesting the use of electricity as electron donor and CO₂ as electron acceptor for the production of carbohydrates. Traces of formic, propionic and butyric acids were present suggesting the formation of other products. The Mediated system also showed of ethane production. These findings suggest the capability of *Shewanella Oneidensis* MR-1 to biosynthesize hydrocarbons from CO₂. The electrode analyses based on electrochemical techniques confirmed the existence of bacteria for both Mediated and Biofilm Systems where the scanning electron microscopy analysis verified the homogenous morphology of bacteria on the electrode surface and solution.

Chapter 5: Investigation of bioproduction using *Shewanella* cells

5.1 Introduction

The *Shewanellae* genus is included in the family of *Shewanellaceae* of marine bacteria and is facultative anaerobic (Satomi, 2013). *Shewanellae* are found in marine environment, deep sea, marine organisms, iced fish, proteinaceous foods, and sometimes clinical samples. Many *Shewanella* species are known to have unique metabolic characteristics. For instance, *Shewanellae* can respire a diverse array of electron acceptors and can adapt in extreme and varied environments making their growth in laboratories simple. In addition, they are amenable to genetic manipulation (Hau and Gralnick, 2007b). These characteristics have attracted interest for the use of *Shewanellae* genus in biotechnology and industry.

Shewanellae are dissimilatory metal reducing bacteria and are good candidates for bioremediation of pollutants applications as a result of their inherent ability to respire a broad range of electron acceptors (Hau and Gralnick, 2007b). *Shewanella Oneidensis* MR-1 has shown great metabolic versatility as it is being used widely as a model to study anaerobic respiration of metals, including dissimilatory reduction of manganese, iron oxide, and other metal compounds as well as other extracellular electron acceptors and electrogenesis (Gorby *et al.*, 2006). Moreover, *Shewanella Oneidensis* MR-1 (Karpinets *et al.*, 2010), *Shewanella putrefaciens* (Wildung *et al.*, 2000; Liu *et al.*, 2002) and *Shewanella algae* (Wildung *et al.*, 2000) show to reduce cobalt (Gorby *et al.*, 1998) and/or technetium, radionuclides produced from nuclear reactor operations and from nuclear weapons testing, and have been suggested to be used in remediation of cobalt and technetium contaminated environments and waste streams. Other species of *Shewanellae* can reduce chromium, mercury and arsenic (Nealson and Scott, 2005). Even that using *Shewanellae* for bioremediation strategies is promising (Lovley, 2003), their use outside in the lab have not been put into practice due to technical difficulties and lack of understanding how the bacteria would behave in other environments (soil and groundwater) than their primary habitat (aquatic) (Hau and Gralnick, 2007b).

Shewanella Oneidensis MR-1 (Petrovskis *et al.*, 1994; Ward *et al.*, 2004), *Shewanella putrefaciens* 200 (Picardal *et al.*, 1995) and *Shewanella algae* (Workman *et al.*, 1997) are also known for their dehalorespiration characteristics; use of halogenated organic products as terminal electron acceptors. Although the potential of using these bacteria in chlorinated organic pollutants remediation applications is stimulating, toxic chemicals are transformed into equally toxic chemicals which then remain in the environment (Petrovskis *et al.*, 1994).

A characteristic that is only present in *Shewanellae* marine bacteria is the degradation of cyclic nitramines (Zhao *et al.*, 2004). Then again, most *Shewanellae* species related to the marine environment, i.e. *Shewanella baltica* MAC1, can biochemically produce polyunsaturated fatty acid and thus result in the production of omega 3 fatty acid which has shown major benefits in human health (Amiri-Jami and Griffiths, 2010; Amiri-Jami *et al.*, 2014). On the other hand, *Shewanella* microbes such as *Shewanella putrefaciens*, do not synthesize any polyunsaturated fatty acid but are capable of producing a range of volatile sulphides and can reduce trimethylamine oxide (TMAO) to trimethylamine (TMA) (i.e. fishy smell), becoming important in the food industry (Satomi, 2013).

The first application of *Shewanella* microbes was in BESs where energy was produced by oxidizing inorganic and/or organic matter and mentioned in Logan *et al.* (2006). Another application is their use as power sources for long-term, monitoring devices for environment and water treatment (Lowy *et al.*, 2006). Moreover, Wackett and Gralnick (2012) are exploring the possibility of hydrocarbon fuel cells generation using *Shewanella* microbes along with a mixed culture. Other potential application is the production of advanced biofuels and chemicals production via cross-metathesis (Jenkins *et al.*, 2015) as *Shewanella* species have a high content of oligomers which makes them a good candidate for performing cross-metathesis (Tranier *et al.*, 2002).

The ability of *Shewanellae* species to respire a diverse array of substrates but also to perform a range of biochemical processes makes them a suitable choice for bioproduction investigation using CO₂. *Shewanella Oneidensis* MR-1 has shown great potential as it is used widely in BESs for remediation and energy production and showed the ability of accepting and donating electrons. This led us to further examine its ability of CO₂ reduction in BESs and gain insights into the metabolism for chemical production.

5.1.1 General hypothesis:

Shewanella Oneidensis MR-1 is capable of reducing CO₂ to volatile fatty acids using different polarization potentials by either respiration or biochemical processes.

5.1.2 Objectives:

- To evaluate the performance of *Shewanella Oneidensis* MR-1 in BES using **biofilm based electron transport**.
- To evaluate the feasibility of **bioproduction from CO₂** in a BES using *Shewanella Oneidensis* MR-1 under different polarizations.
- To study the effect of set potential on **metabolic pathway** and bioproduction.

- To determine the ability of **bacterial cell properties** to contribute in bioproduction.
- To draw a **hypothesised pathway** for the production of chemicals from CO₂ using *Shewanella Oneidensis* MR-1.

5.2 Materials and methods:

Shewanella Oneidensis MR-1 biofilm was developed in H-shaped BESs and tested for bioproduction using CO₂ as the substrate at different polarizations. Subsequently, acetate and formate were used as substrates to elucidate the occurrence of bioproduction and to determine a one-step or multi-step process. Then, cathode capture and energy efficiencies were calculated to evaluate how well the substrate and energy is being converted into products. Consequently, extracted proteins from *Shewanella Oneidensis* MR-1 were used to reveal whether the occurred process is a result of a respiration or biochemical process.

5.2.1 Growth and inoculum of electroactive culture:

Frozen stocks of *Shewanella Oneidensis* MR-1 (ATCC 700550) stored in glycerol solution at -80°C were inoculated in Luria broth (LB) medium and incubated aerobically at 140 rpm and 30°C for 56 hours corresponding to exponential growth/early stationary phase. Bacterial cells were harvested by centrifugal (10 min, 10 000 rpm), washed three times and re-suspended in 5 mL of anaerobic medium made of 0.225g K₂HPO₄, 0.225g KH₂PO₄, 0.46g NaCl, 0.225g (NH₄)₂SO₄ and 0.117g MgSO₄ per litre.

5.2.2 Experimental set-up and operation of bioelectrochemical cells:

Ten H-shaped BESs made of glass were set up with an anode and a cathode chamber of 80 mL and headspace of 30 mL. The anode and cathode chambers were separated by a proton exchange membrane (Nafion 117, Sigma Aldrich, UK). The reactors were stirred using a magnetic stirrer to maintain uniform flow and the temperature was maintained at the laboratory's temperature (16 ± 4 °C). The reactors were equipped with working and counter electrodes made of carbon cloth (4 cm², wet proofed 20%, Fuel Cell Earth, US) and a reference electrode of Ag/AgCl (+0.197 V vs. Standard Hydrogen electrode, Basi, UK). The carbon cloth electrodes were previously immersed in ethanol for 24 hours to prevent contamination in the cells and then washed in autoclaved deionised water over night. The electrodes were connected using titanium wire through rubber stoppers to ensure the system was close.

A volume of 80 mL of anaerobic medium was introduced in the anode and cathode chambers of the BESs while sparging with N₂ for 30 mins to achieve complete anaerobic conditions. The gases passed through a filtration mechanism to avoid contamination. All the solutions and equipment were sterilised and/or autoclaved prior use. *Shewanella Oneidensis* MR-1 cells were subcultured into the anode compartments along with lactate (1g/L) as an electron donor. All systems were given enough time for monitoring in order to ensure growth of a biofilm. The anode electrodes were polarized at +0.200 V (vs. Ag/AgCl, PSTrace, PalmSens) to act as an

electron acceptor. Four abiotic BESs were set up and operated in similar ways as mentioned above but without the use of any microorganisms.

5.2.3 Bioproduction

5.2.3.1 CO₂ as electron acceptor

The anode electrodes were converted to cathodes by changing the applied potential from positive to a range of negative potentials. Table 5-1 shows the experimental design that was followed to perform the current study. Prior the polarization at each potential, the anode solution of the BESs was replaced with fresh one to remove any remaining nutrients and possible carbon sources in solution. CO₂ was then used as the only electron acceptor by purging the cathode chamber for 3 mins at a flowrate of 10 mL/min to remove any oxygen in the reactor prior adding the CO₂-saturated reaction medium. The headspace was also flushed with CO₂ gas for 3 mins at the same flowrate. All gases passed through a filtration mechanism to avoid contamination. Abiotic experiments were also performed following the same procedure.

Table 5-1: Experimental design showing the conditions and parameters used for each experimental set.

Conditions	Substrate	Cell viability	Polarization potential (V vs. Ag/AgCl)	Repeats
Biotic potentiostatically controlled experiments	CO ₂	Live	-0.2 V	2
			-0.4 V	2
			-0.6 V	4
			-0.8 V	2
Abiotic potentiostatically controlled experiments	CO ₂	None	-0.2 V	5
			-0.4 V	5
			-0.6 V	5
			-0.8 V	5
Biotic potentiostatically controlled experiments	Acetate	Live	-0.6 V	2
Biotic potentiostatically controlled experiments	Formate	Live	-0.6 V	2
Abiotic potentiostatically controlled experiments	Acetate	None	-0.6 V	2
Abiotic potentiostatically controlled experiments	Formate	None	-0.6 V	2
Biotic microbiological experiments	CO ₂ , H ₂	Live	None	3
Biotic microbiological				3

experiments	CO ₂ , H ₂	Dead	None	
Biotic microbiological experiments	Formate, H ₂	Live	None	3
Biotic microbiological experiments	Formate, H ₂	Dead	None	3
Biotic microbiological experiments	Acetate, H ₂	Live	None	3
Biotic microbiological experiments	Acetate, H ₂	Dead	None	3
Abiotic experiments	CO ₂ , H ₂	None	None	3
Abiotic experiments	Formate, H ₂	None	None	3
Abiotic experiments	Acetate, H ₂	None	None	3

5.2.3.2 Formate and acetate as electron acceptors

Abiotic and biotic H-shape cells were set up and run using formate and acetate as electron acceptors (Table 5-1) following similar procedures as stated previously. The anode and cathode chambers were filled with 80 mL of anaerobic medium previously spurge with N₂ for 30 mins through a filtration mechanism to avoid contamination. A polarised potential of -0.6 V was applied during the operation of the experiments.

5.2.3.3 Biotic microbiological experiments

Microbiological control experiments were set up and run in serum bottles without the use of any electrochemical technique (Table 5-1). The serum bottles were filled with 80 mL of anaerobic medium preciously spurge with N₂ for 30 mins. Where appropriate; CO₂ and H₂ was spurge for additional 10 mins at a flowrate of 10 mL/min. All serum bottles were sealed with caps containing rubber stoppers to prevent any gas leakage and/or contamination. The filtration mechanism, glassware and serum caps/stoppers where previously autoclaved to avoid any contamination.

5.2.4 Investigation of bioproduction pathway:

5.2.4.1 Total protein extraction from *Shewanella Oneidensis* MR-1 cells

Protein extraction was achieved through cell lysis to give soluble protein fraction. The bacterial cell pellets were incubated with native lysis buffer supplemented with lysozyme and Benzonase Nuclease enzymes for disrupting the cell wall and digest nucleic acids (Qproteome Bacterial protein kit, Qiagen, USA). The cells were incubated with the lysis buffer and was centrifuged at low temperatures (-4 °C) to separate cell debris and insoluble protein. The supernatant was then taken and mixed with chilled acetone at a ratio of 1:4 to precipitate the protein. After incubation in dry ice for 15 mins, the solution was centrifuged at -4 °C. The pellet

was then labelled as the protein fraction. The proteins were then used as biocatalysts in H-shaped BESs at the same set up as mention previously and following the experimental design shown in Table 5-2.

Table 5-2: Experimental design for chemical production using extracted proteins

Conditions	Substrate	Polarization potential (vs. Ag/AgCl)	Repeats
Electrochemical experiments with proteins	CO ₂	-0.8 V	5
Electrochemical experiments with proteins	None	-0.8 V	2
Electrochemical experiments (no proteins)	CO ₂	-0.8 V	5
Proteins (no polarization)	CO ₂	-0.8 V	2

5.2.5 Electrochemical analyses:

5.2.5.1 Bacterial growth and conditioning period

The potentiostatically controlled experiments were conducted in H-shape cells using a 3 electrode system containing a reference electrode (Ag/AgCl wire within a saturated solution of NaCl (3M)) and carbon cloth (4 cm² of surface area) as working and counter electrodes wired with titanium wire as current collectors. All measurements and applied potential experiments were done on a PSTrace potentiostat. Cyclic voltammograms were measured from -0.800 to 0.400 V (vs. Ag/AgCl) at a scan rate of 0.001 V/s. Slow scan was used to prevent damage of the cells. In this report, we evaluate biological systems which require the initial scans of cyclic voltammetry to avoid the effect of electrode polarization on the electrode bound protein metabolism. Thus, cyclic voltammograms reported here, refer to the second scans. Amperometric detection curves were measured during bacterial growth based on the current obtained over time under potentiostatic polarization.

5.2.5.2 Bioproduction

Cyclic voltammograms (CVs) were recorded from open circuit voltage conditions and the voltage was changed from -1.200 to 0 V (vs. Ag/AgCl) at a scan rate of 0.001 V/s. For the potentiostatically controlled experiment using formate and acetate as a substrate, the CVs were performed at the same scan rate as previously at the range of 0.4 to -0.8 V (vs. Ag/AgCl).

5.2.6 Chemical analyses

The liquid samples were analysed for volatile fatty acids using a Dionex ICS-1000 with an AS40 auto sampler liquid chromatography system. The column was an Ionpac ICE-AS1, 4 × 250 mm analytical column with a flow rate of 0.16 mL/min, an eluent of 1.0 mM heptafluorobutyric acid solution and a cation regenerant solution used for the AMMS-ICE II Suppressor of a 5 mM tetrabutylammonium hydroxide. The injection loop was 10 µL. The total organic carbon in the liquid samples was analysed using a Shimadzu 5050A Total organic carbon analyser, with an ASI-5000A auto sampler. The carrier gas was zero grade air, and the inorganic catalyst solution was 25% phosphoric acid. Samples for alcohol content analysis were performed with a GC, Shimadzu GC-2010plus equipped with BID detector and a Zebron™ ZB-WAXplus.

Bioproduction using CO₂: Liquid samples were taken every 2 hours for a period of 12, 14 and finally 24 hours including a sample at time zero (i.e. immediate sampling after CO₂ was added).

Bioproduction using formate and acetate: Liquid samples were taken every one day for a period of days, including a sample at day zero (i.e. immediate sampling after substrates were added).

Bioproduction using proteins: Liquid samples were taken after 30 mins of operation. CO₂ was assumed to be added at time zero where a sample was immediately taken and labelled as time zero.

5.2.7 Electrode analyses:

5.2.7.1 Scanning electron microscopy (SEM)

SEM was used to visualize features of the biomass on the electrode and in solution. Carbon cloth electrodes with biofilm were fixed with 2.5% glutaraldehyde solution in phosphate buffer, dehydrated in increasing ethanol concentrations (25, 50, 75 and 100%) and subjected to critical point drying using an automated critical point dryer. The samples were sputter-coated with gold and examined by SEM (Cambridge Stereoscan 240 SEM, UK). In the experiments where mediators were used, the solutions were also used for SEM.

5.2.7.2 Live/Dead analysis

Live/Dead analysis was used to observe the condition of the bacterial cells on the electrode. The carbon cloth electrodes were immersed in filtered deionised water which contained two stains; SYTO9 for live cells and propidium iodide for dead cells (FILMTRACER™ LIVE/DEADR biofilm viability kit, Thermo Fisher, UK). The samples were incubated at room, temperature for 30 mins and then washed with filtered deionized water to remove excess of dye. The samples

were examined by confocal microscopy (Leica TCS SP2 UV, Software LCS 2.61, Leica Microsystems, GmbH, Heidelberg) with magnification lens 63x/1.32.

5.2.8 Calculations:

The CVs were performed as non-turnover conditions to study the microbial oxidation and reduction of the substrate and subsequent possible electron transfer. The formal potential of a redox couple was calculated using Equation 5.1.

Equation 5.1

$$E^j = \frac{E_{pA} + E_{pC}}{2}$$

Where E_{pA} is the anodic potential and E_{pC} is the cathodic potential. Using non-turnover conditions allow us to study all redox-active compounds at the electrode and the formal potential of possible extracellular electron transfer.

The molarities of volatile fatty acids produced were calculated as shown in Equation 5.2.

Equation 5.2

$$mol = \frac{ppm}{1000} \times molar\ mass$$

Cumulative equivalents recovered as formic, acetic, propionic and valeric acids were calculated from their measured amounts (μmol), considering the molar conversion factors for estimating how many electrons are being converted into mass (Table 5-3).

Table 5-3: Molar conversion factors of product formation via MES

Products	Molar conversion factors
Formic acid	2 $\mu\text{eq } \mu\text{mol}^{-1}$
Acetic acid	8 $\mu\text{eq } \mu\text{mol}^{-1}$
Valeric acid	8 $\mu\text{eq } \mu\text{mol}^{-1}$
Propionic acid	6 $\mu\text{eq } \mu\text{mol}^{-1}$

The cathode capture efficiency (CCE) represents the product recovery from current and was calculated as shown below;

Equation 5.3

$$CCE (\%) = \left(\frac{\mu eq_{product}}{\mu eq_i} \right) \times 100$$

The cumulative electric charge (μeq_i) that was transferred at the electrodes was calculated by integrating the current (μA) over time and dividing for the Faraday's constant ($F=96485 \text{ Ceq}^{-1}$) (see Equation 5.4).

Equation 5.4

$$\mu eq_i = \frac{\int_B^A I}{F}$$

The energy efficiency relative to the electrical input was calculated as:

Equation 5.5

$$\eta_E (\%) = \frac{W_{products}}{W_{IN}}$$

Where $W_{products} = n_{products} \times \Delta G_{product}$ is the energy recovered (kJ) as product, calculated from the total amount of product produced (mol) and the molar Gibbs free energy of product reduction from carbon dioxide (Table 5-4).

Table 5-4: Gibbs free energy and enthalpy of formation of products formed via MES

Products	ΔG^0 (kJ/mol)	ΔH^0 (kJ/mol)
$CO_2 + H_2O + 2e^- \rightarrow HCOO^- + OH^-$	-1.3	-666.5
$2CO_2 + 6H_2O + 8e^- \rightarrow CH_3COOH + 8OH^-$	-77.364	-480
$5CO_2 + 18H_2O + 8e^- \rightarrow C_5H_{10}O_2 + 26OH^-$	-246.204	-514.6
$3CO_2 + 10H_2O + 6e^- \rightarrow C_3H_6O_2 + 14OH^-$	-149.646	-471.1

W_{IN} is the electrical energy added to the system calculated in Equation 5.6. C is the total Coulombs calculated by integrating the current over time and E_{app} (V) is the applied voltage.

Equation 5.6

$$W_{IN} = C \times E_{app}$$

The maximum theoretical energy efficiency (η_{EL}) was calculated of the process based on the electrical energy input (W_{EL}). Acetate energy is calculated as $W_{Acetate} = \Delta H_{Acetate} Q_{r_{cat}} / Fn$,

using the enthalpy of liquid acetate (Table 5-4), $n = 8$ as the number of transferred electrons and assuming a cathodic recovery of $r_{cat} = 100\%$. This maximum theoretical energy efficiency can be defined as:

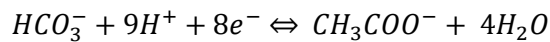
Equation 5.7

$$\eta_{EL} = \frac{W_{Acetate}}{W_{EL}} = \frac{0.06}{U_{app}}$$

Since the amount of acetate produced is dependent on the current, the charge terms cancel out resulting to the maximum energy efficiency that depends only on the applied voltage. For this case, where U_{app} is equal to -0.2, -0.4, -0.6 and -0.8 V. The maximum theoretical energy efficiency was calculated for all compounds found. The values used are shown in Table 5-4.

In order to examine the limitation of the system and the possible cause of the resulted chemical production, the thermodynamics of the main reaction were analysed. Thermodynamically, the electrochemical reduction of carbonates (HCO_3^-) to acetate is described in Equation 5.8.

Equation 5.8



This reaction is possible at potentials lower than its equilibrium (i.e. 0.187 vs. Standard Hydrogen Electrode, SHE) (Logan *et al.*, 2006) derived as shown below.

Equation 5.9

$$E_{CO_2/acetate}^{0'} = E_{CO_2/acetate}^0 - \frac{RT}{nF} \ln \frac{[CH_3COOH^-]}{[HCO_3^-]^2 [H^+]^9}$$

Where $E_{CO_2/acetate}^0$ is the standard potential of the redox pair CO_2 to acetate, T is the temperature (298 K), R is the gas constant ($8.314 \text{ J mol}^{-1} \text{ K}^{-1}$), n is the number of electrons, F is the Faraday constant (96485 C mol^{-1}) and $[CH_3COOH^-]$, $[HCO_3^-]$ and $[H^+]$ are the concentrations (mol L^{-1}). The $[H^+]$ concentration were calculated using the pH of the solution which it was measured at 6.7. The $[HCO_3^-]$ concentration was assumed as equilibrium with a pK of $10^{-6.3}$ (i.e. 1.03 mM) (Blanchet *et al.*, 2015).

5.3 Results and Discussion:

5.3.1 Start-up and operation of BES:

Figure 5.1 shows the electric current during biofilm development in the anode chamber using *Shewanella Oneidensis* MR-1 cells and lactate (1g/L) as the substrate. The figure is divided in four subfigures, each referred to a group that would be polarized with different polarization after biofilm development to study bioproduction. All cells were potentiostatically controlled at an oxidizing value of +0.200 V vs. (Ag/AgCl) to enhance the anode start-up. *Shewanella Oneidensis* MR-1 cells and lactate were inoculated after 10 minutes from the start-up of the BESs. In Figure 5.1(A), BES1 & 2 responded similar to the abiotic cell, after the first addition of lactate, showing the presence of lag phase which indicates the conditioning of the bacterial cells. Around the sixth day, the medium was replaced with fresh one and lactate was added. A lactate spike was observed for BES1 and gradually increased up to 5.8 μA for approximately 10 days. On the other hand, BES2 showed an electric current increased on the fifteenth day with a maximum electric current of 4.7 μA . The current was decreased for both BESs around 2.5 μA suggesting the depletion of substrate. An additional lactate concentration (1 g/L) was added and the electric current was increased to a maximum of 8 μA for both BESs and decreased around 3.5 – 4 μA . Lactate was added for the last time and the electric current instantly increased from around 4 to 10 μA . This was assumed as the steady state phase of this group of BESs which were considered ready for bioproduction.

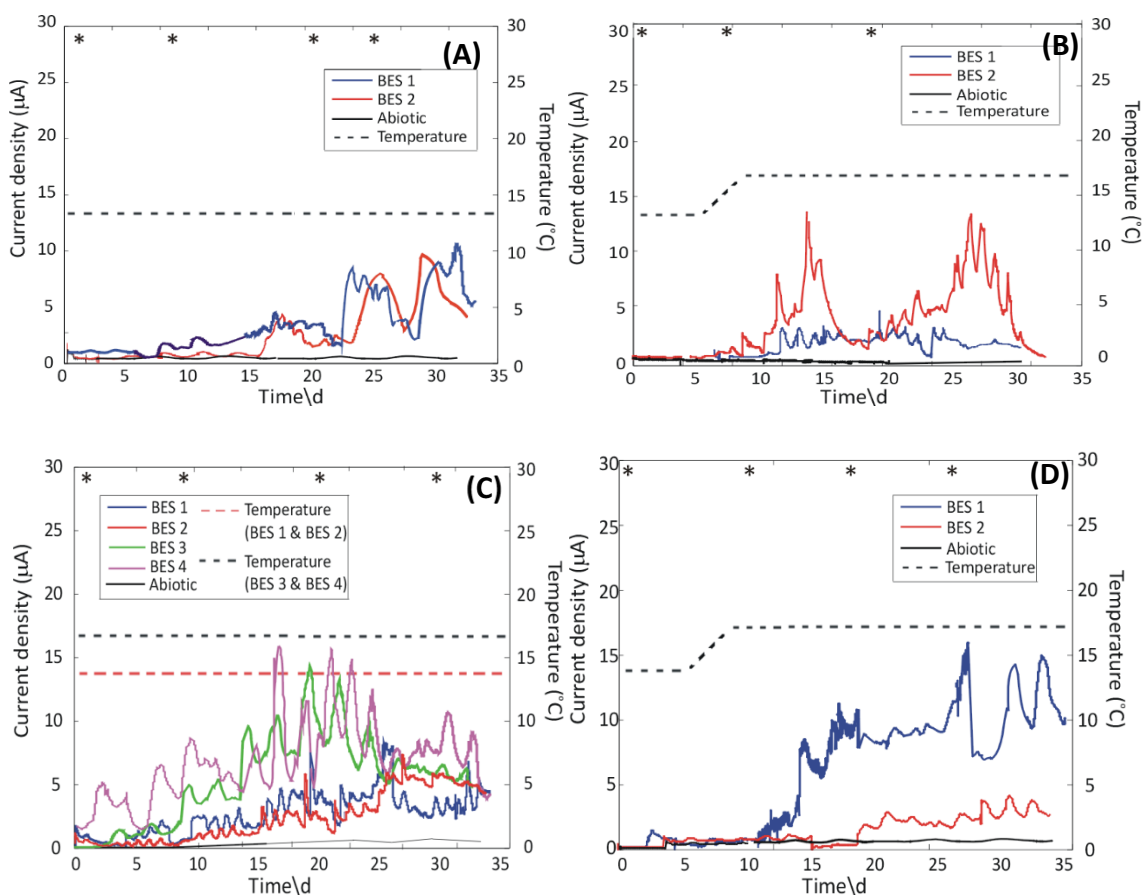


Figure 5.1: Current generation over time of bioelectrochemical systems with their replicates during biofilm formation using *Shewanella Oneidensis* MR-1. The black star (*) indicates the addition of lactate (1g/L). All bioelectrochemical systems were operating at a +0.2 V vs. (Ag/AgCl) potential. Subfigures A-D are referred to a group that will be polarized with different polarization potentials (A: -0.2V, B: -0.4 V, C: -0.6 V and D: -0.8 V) after biofilm development for bioproduction monitoring.

In Figure 5.1(B), both BESs also showed a lag phase of approximately four days after bacteria inoculation and lactate addition confirming their conditioning stage. During the conditioning period, the electric current was measured around 1 - 2 μA for the BESs and 0.1 - 0.5 μA for the abiotic cell. The difference in the electric currents between the BESs and abiotic cell suggested the presence of the electroactive culture in BESs. Lactate was added in the anode chamber on the fifth day and the current increased and reached a maximum of 11 μA for BES1 and 4 μA for BES2 after five days and then gradually decreased to 3 μA for both BESs suggesting the exhaustion of lactate. The abiotic cell remained constant around 0.1 – 0.5 μA . Lactate was added one last time and the current resumed immediately and reached around 13 μA for BES1 and around 3 – 4 μA for BES2 suggesting that both BESs reached an early steady state stage and were conditioned for bioproduction. This is shown by the electric current which repeatedly reached around 11 μA for two cycles which shows the steady state phase of the biofilm. The electric current was then started to drop suggesting the need of substrate in the

system. For the abiotic cell the current remained stable throughout the experiment at around 0.1 – 0.5 μA .

In Figure 5.1(C), the electric current of four replicates was observed as a different group. BES1 & 2 showed an identical time course of electric current production which started after 5 days of lactate addition and bacteria inoculation. The current increased from 1 to 3 μA and dropped after 3 days suggesting the depletion of lactate. Lactate was then added and the current resumed to 3 μA immediately and reached to a maximum of 15 μA after fifteen days. The current dropped again indicating the exhaustion of substrate. BES3 and 4 showed absence of lag phase which suggests the presence of electro-active culture and its ability to switch from using oxygen to use the carbon cloth anode as terminal electron acceptor in its metabolism. For BES1 the current remained stable around 10 – 13 μA for 10 days and then reached 18 μA after the addition of lactate where it gradually decreased to 8 μA . Lactate was added for the last time and the current resumed after five days. For BES2 the absence of lag phase was also observed and the depletion of lactate was shown earlier than BES1. The current resumed after the addition of lactate and reached around 6 μA where it remained for fifteen days. The current was then dropped suggesting the complete exhaustion of substrate. During this time course the abiotic cell remained stable around 0.5 to 1 μA .

In Figure 5.1(D), the last pair of BESs is shown. As in all the subfigures, here the presence of lag phase is also observed which lasted for approximately four days. After addition of lactate at day zero, the current was slightly increased from 0.1 to 1 μA for BESs where for the abiotic cell it remained stable at 0.1 μA . On the fifth day, after using an additional amount of lactate the current resumed around 8 μA for BES1. BES2 did not show any response suggesting the possibility of an extended lag phase. After three days, lactate was added and the current resumed for both BESs and reached a maximum of 18 μA for BES1 and 4 μA for BES2.

The average lag phase resulting from Figure 5.1 was calculated at 7.6 days (STD=5.10 days, n=10) suggesting the time *Shewanella Oneidensis* MR-1 requires to condition. This is supported by the Abboud *et al.* (2005) study where it was found that below 20 °C temperature, *Shewanella* cells display a long lag phase of almost 4.5 days. The temperature of the lab was measured between 15-18 °C which confirms the above statement. Having low temperatures, not only the lag phase of the bacterial cells is affected but also the growth due to the fall of enzymatic activity within the cells. Thus this fact explains the low current densities observed throughout the experiments.

Subsequent analytical methods were used for elucidating the effect of changes in the local redox environment in respect to biofilm formation for all the bioanodes. The CV scans were performed as non-turnover conditions. Using non-turnover conditions allowed us to study all redox-active compounds of the substrate at the electrode and the formal potential of possible extracellular electron transfer. The CV scans showed in Figure 5.2 are at the end of the conditioning period. Abiotic scans are also shown as a baseline.

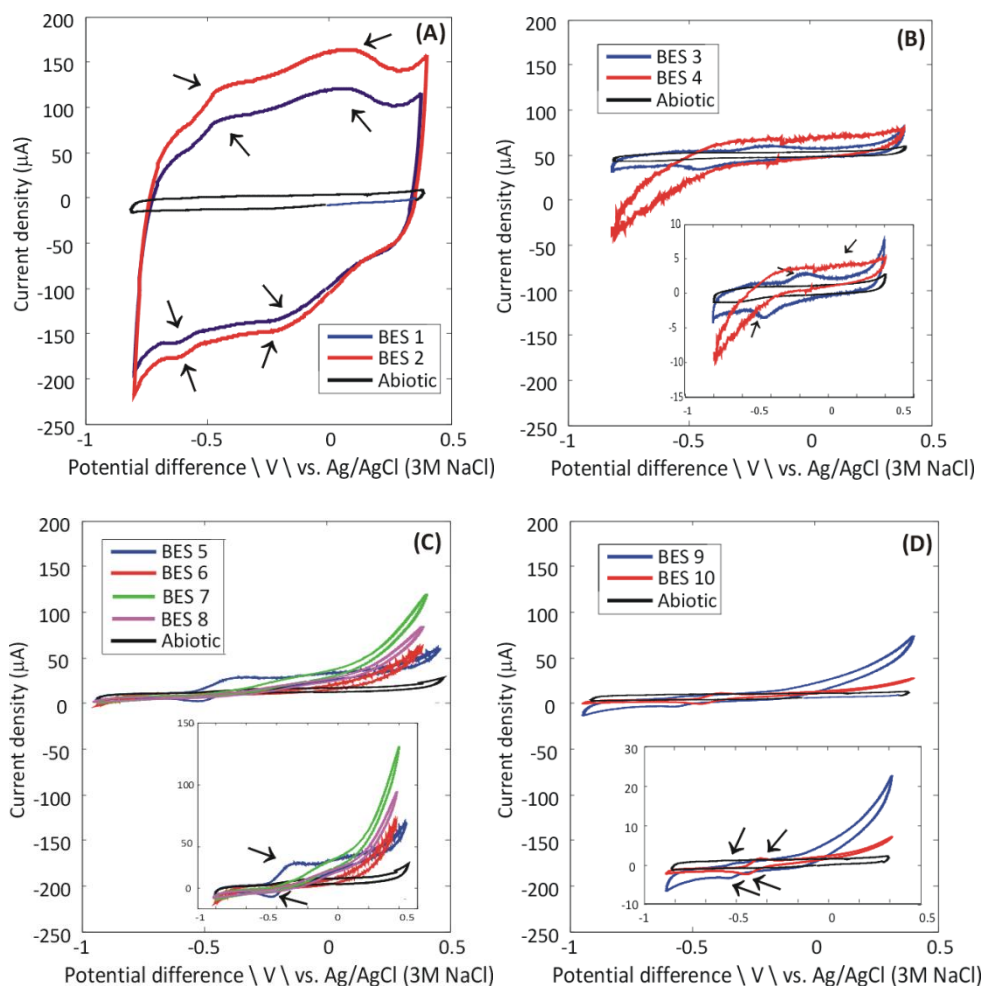


Figure 5.2: Redox activity voltammetry associated with bioelectrochemical systems with *Shewanella Oneidensis* MR-1. The abiotic cell voltammetry is shown as a baseline. Subfigures A-D are referred to a group that will be polarized with different polarization potentials after biofilm development for bioproduction monitoring. At -0.2 V: BES 1-2, at -0.4 V: BES 3-4, at -0.6 V: BES 5-8 and at -0.8 V: BES 9-10. The arrows indicate the observed peaks.

Figure 5.2(A) – (D) shows redox activity with symmetrical response of anodic and cathodic sweeps which indicates the reversibility behaviour of the redox reactions. Two redox potentials were identified in Figure 5.2(A); at -0.465 and -0.035 V (vs. Ag/AgCl, Table 5-5). The redox potential at -0.465 V (vs. Ag/AgCl) agrees with the standard thermodynamic potential of the flavin molecule (Walsh, 1980), excreted by *Shewanella Oneidensis* MR-1 (Marsili *et al.*, 2008; Von Canstein *et al.*, 2008) with a shift to the right due to pH implications (pH<7, Table

5-5). The second redox potential found was not correlated with any known possible redox potential. A similar redox peak was also identified in Figure 5.2(B). The CV scans obtained in Figure 5.2(A) also suggest evidence for the accumulation of biomass on the electrode surface area, based on a higher current density.

Figure 5.2(C) – (D) showed a redox potential between the ranges of -0.314 to -0.391 V (vs. Ag/AgCl, Table 5-5) which suggests that the peak of lactate to acetate (White, 1999) and the proteins MtrcA (Hartshorne *et al.*, 2007) and OmcA on the bacterium membrane were shaped at the same position and likely replace each other due to the similar redox potential they have (Meitl *et al.*, 2009). This suggests that the peak identified around these potentials is possibly a sum up peak from the OmcA, MtrC, and lactate to acetate and the electrode. An extent increase of the current density for BESs compared to the abiotic cells was also observed in Figure 5.2 which suggests that as the bacterial growth increases, the presence of extracellular electron transfer mechanism increase the current density production.

Table 5-5: Electrochemical parameters of the redox reaction potentials vs. Ag/AgCl obtained by the CV scans at a scan rate of 0.001 V/s

	E_{pA} (V)	E_{pC} (V)	E_j (V)	pH
(A) BES1 & 2	-0.320	-0.610	-0.465	6.7
	+0.210	-0.280 (± 0.05)	-0.035	6.7
(B) BES1 & 2	0.046	-0.24	-0.097	6.6
(C) BES1, 2, 3 & 4	-0.201 (± 0.10)	-0.428 (± 0.002)	-0.314	6.5
(D) BES1 & 2	-0.366 (± 0.10)	-0.416 (± 0.07)	-0.391	6.5

5.4 Effect of set potential on metabolic pathway and bioproduction

5.4.1 Performance of *Shewanella Oneidensis* MR-1:

Biotic microbiological experiments using *Shewanella Oneidensis* MR-1 cells alone with CO₂ and H₂ as the electron donor were performed in order to examine the capability of the microorganism to use CO₂ as an electron acceptor. Product formation using biotic microbiological experiments is presented in Figure 5.3. Acetate production was observed after one day of CO₂ addition at a maximum of 20 μ mol supporting the use and reduction of CO₂. Similar experiments, without the use of H₂, did not produce volatile fatty acids suggesting a microbial electrosynthetic route where acetic acid is possibly biologically synthesised.

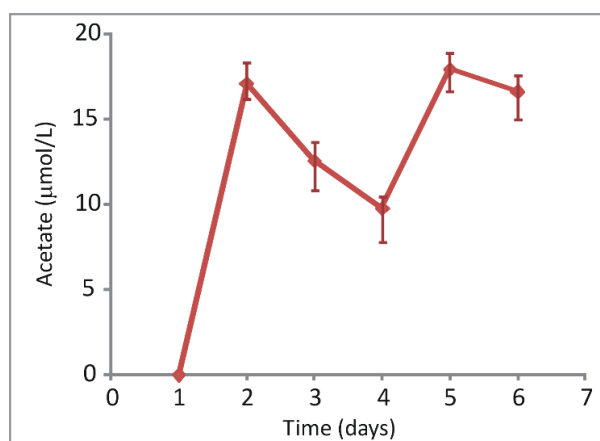


Figure 5.3: Acetate production from biotic microbiological experiments using *Shewanella Oneidensis* MR-1, CO₂ as an electron acceptor and H₂ as an electron donor with no polarization potentials at 30°C (n=3).

To study the ability of the inoculated microorganisms to produce acetate and/or other compounds using CO₂ in BESs, the cathode potentials were set at four values; -0.2, -0.4, -0.6 and -0.8 V vs. (Ag/AgCl). In the presence of a biofilm, acetate was the primary product at -0.2 V sporadically with a maximum of 53.86 µmol concentration after 24 hours (data shown in Appendices C1-C4). When the polarization was increased to -0.4 V, the acetate production was found at 40 µmol after 24 hours of operation. Formate was also produced after 6 hours around 39 µmol. Using the -0.6 V polarization, the time production of acetate was further improved starting after 2 hours of operation and reaching a more constant profile with acetate concentrations varying from 9.80–26.50 µmol. Other compounds such as formate and valerate were also present in solution at 2.74-7.30 µmol throughout the experiment and 383.8 µmol after 18 hours of operation, respectively. At the highest polarization, -0.8 V, acetate was produced periodically around 12.8-36.4 µmol throughout the 24 hours of operation. Formate and propionate were also found alongside with acetate production at a concentration of 11-43.45 µmol after 2 hours of operation and 204.11-270.9 µmol after 6 hours of operation, respectively.

In order to further analyse the data obtained from the experiments and the possibility of a multi-step reaction, additional analyses were carried out using acetate and formate as substrates. Microbiological vessels were set up using H₂ as an electron donor and formate and acetate as an electron acceptor to evaluate whether *Shewanella* cells can respire or catalyse these substrates. Figure 5.4 shows the analysis of a triplicate experiment where it reveals the ability of the bacteria to reduce formate and acetate using H₂ as an electron donor. Formate and acetate reduction concentrations were calculated and found within the ranges of 1000 – 2000 and 3000 – 5000 µmol, respectively. Formate and propionate were identified as reduction products from acetate reduction where no products were identified from formate

reduction. Ethanol and methanol were theoretically assumed as reduction products from acetate and methanol, respectively. However, due to lack of chemical analytical tools at the time, these products were not qualified or quantified. Similar experiments without the use of bacteria did not show any substrate reduction suggesting their use by the bacteria.

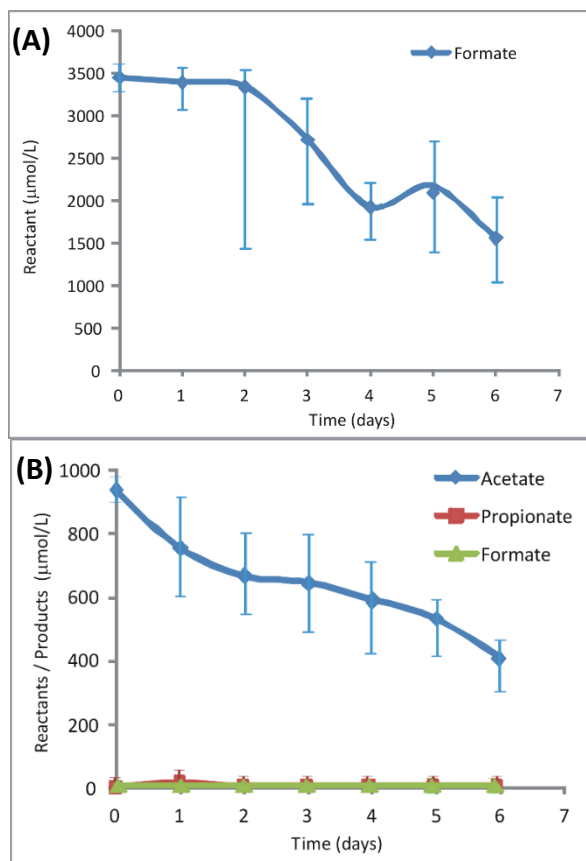


Figure 5.4: (A) Formate and (B) acetate reduction; reactants and products balances in biotic microbiological experiments using *Shewanella Oneidensis* MR-1 and H₂ as an electron donor at 30°C (n=3).

Biotic potentiostatically controlled experiments were also performed to test the ability of the bacteria to swap from using H₂ to use a solid state electrode and still perform the reactions. Figure 5.5 demonstrates the volatile fatty acid and alcohol analyses from formate and acetate reduction over time. The occurrence of methanol was realised as the main formate reduction product along traces of propionate. The formation of ethanol was found as the main acetate reduction product along traces of formic acid. Abiotic experiments did not show any volatile fatty acids, alcohol production or any substrate reduction. This suggests that the substrate reduction occurred in biotic experiments was performed by the bacteria.

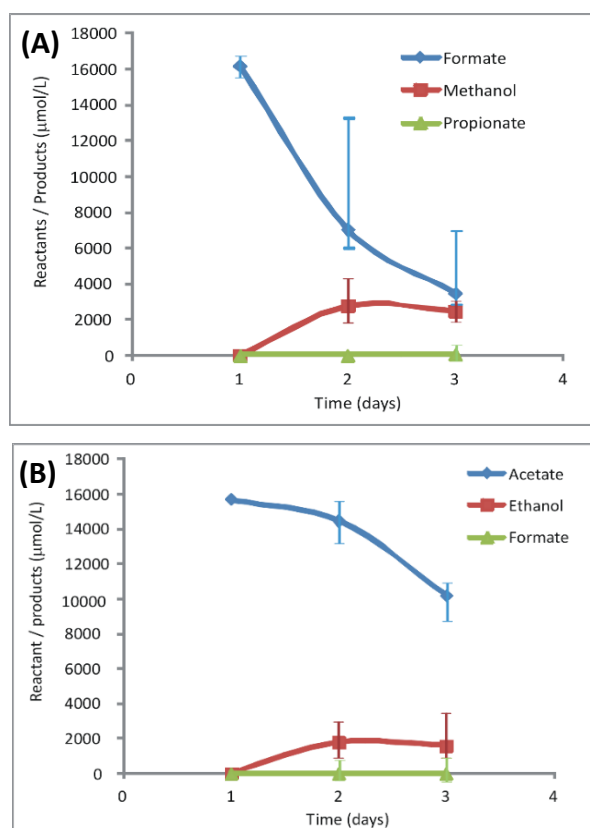


Figure 5.5: Biotic potentiostatically controlled experiments using *Shewanella Oneidensis* MR-1 with H_2 as an electron donor and (A) formate and (B) acetate as electron acceptors at $30\text{ }^\circ\text{C}$ (n=3).

Figure 5.6 shows the redox activity of the BESs with formate and acetate as substrates in duplicates. Even that a cathodic electrochemical activity was observed when formate was used, no peaks were identified. However, three formal potentials were calculated when acetate was used, at -0.18 , -0.2 and -0.58 V vs. (Ag/AgCl). These potentials agreed with *Shewanella Oneidensis* MR-1, MtrcA and OmcA, acetate to ethanol and acetate to acetaldehyde, respectively (Gerald, 2008; Meitl *et al.*, 2009) supporting the possibility of acetate reduction to a range of products biologically. However, chemical acetaldehyde qualification and quantification was not confirmed due to lack of chemical analytical tools.

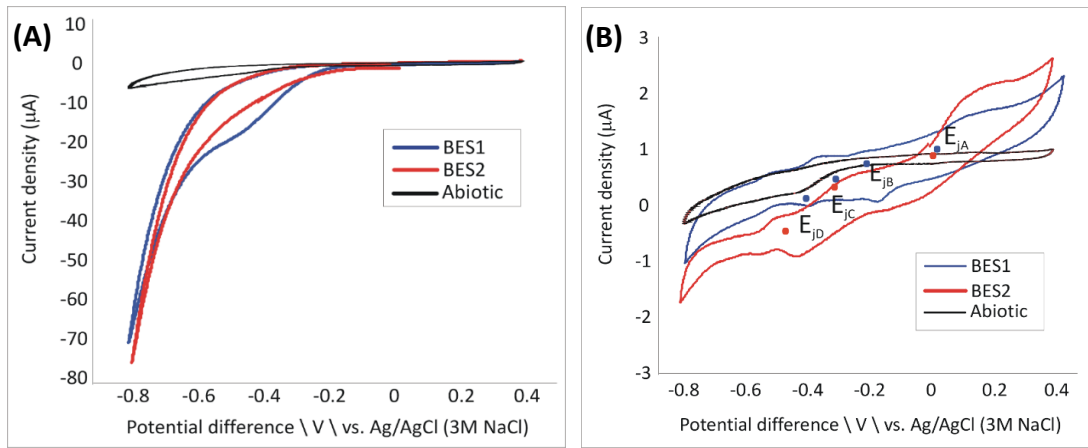


Figure 5.6: Redox activity voltammetry associated with BESs with *Shewanella Oneidensis* MR-1 using acetate as substrate. The abiotic cell voltammetry is shown as a baseline. E_j stands for the calculated redox potential of BES 1 and BES 2 using coordinated colours. The experiment was performed at 30 °C.

Total organic carbon analysis was also performed 24 hours after bioproduction for all polarizations where the organic carbon in solution varied from 18.4-147.4 mg/L (data shown in Appendix C5). Total volatile fatty acid concentration was also calculated after 24 hours of operation and was found around 0.00-204.1 µmol/L (data shown in Appendix C5). Figure 5.7 shows the total organic carbon and volatile fatty acids data versus polarization compared to abiotic experiments. Due to the large variability in the data a lack of understanding was developed. Thus to further interpret the data, a statistical analysis was performed where it was found that there was no relation between polarizations and the total organic carbon or volatile fatty acids produced in the BESs (Total organic carbon: $p=0.101$ (Kruskal-Wallis test), Volatile fatty acids: $p= 0.192$ (Kruskal-Wallis test)). This suggests that organic carbon concentrations were not affected by using different polarizations

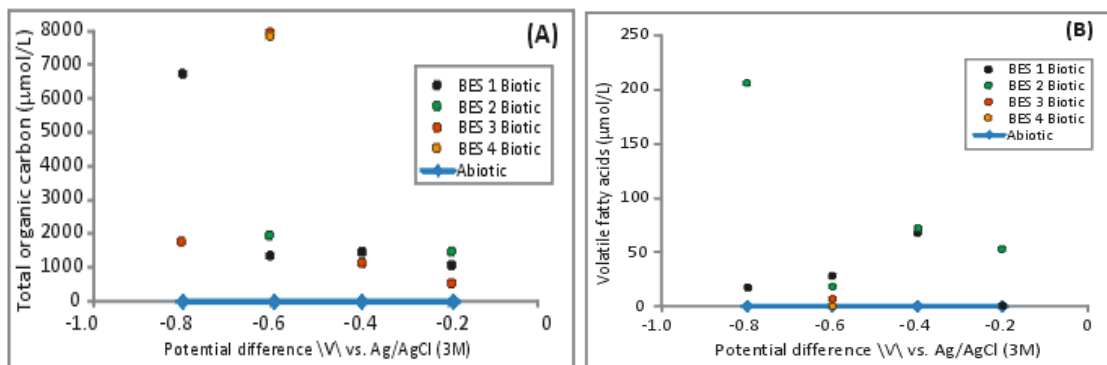


Figure 5.7: (A) Total organic carbon and (B) volatile fatty acids data versus different polarizations. BESs 1-4 are referred to a group that was polarized with different polarization potentials (1: -0.2 V, 2: -0.4 V, 3: -0.6 V and 4: -0.8 V).

5.4.2 BES performance and efficiency:

The cathode performance was evaluated in terms of cathode capture efficiency (CCE) which represents the product recovery from current at all controlled potentials. Table 5-6 shows the maximum CCEs occurred of the biotic experiments. The CCE varied throughout the different polarizations achieving a maximum of 77% at -0.2 V potential and a minimum of 13% at -0.8 V potential. A more repeatable CCE was showed when using -0.4 and -0.6 V potentials. No relation was found between CCE and polarization for biotic experiments ($p=0.682$, Kruskal-Wallis Test) proposing that the CCE was not affected by different polarizations.

Table 5-6: Cathode capture efficiency values for bioproduction obtained from CO₂ reduction using *Shewanella Oneidensis* MR-1

Polarization potentials (V)	Cathode Capture efficiency (%) - Biotic experiments
-0.2	14.37
-0.2	77.12
-0.4	57.94
-0.4	38.60
-0.6	17.47
-0.6	18.15
-0.8	50.10
-0.8	13.22

The energy efficiency relative to the electrical input was also calculated. Table 5-7 shows the total energy yield of compounds produced from biotic and abiotic experiments. The energy used for producing those compounds varied from 0.0001-0.63 % for biotic experiments suggesting that most of the energy available in the system is lost or used to produce unknown compounds.

Table 5-7: Energy efficiency values for products derived from CO₂ reduction using *Shewanella Oneidensis* MR-1 in H-shape bioelectrochemical systems

Polarization potentials (V)	Energy yield (%) -Biotic experiments	Compounds produced
-0.2	0.0018	Acetate
-0.2	0.6362	Acetate
-0.4	0.0331	Acetate
-0.4	0.0059	Acetate, Formate
-0.6	0.0007	Acetate, Formate, Valerate
-0.6	0.0001	Acetate, Formate
-0.8	0.0026	Acetate, Formate Propionate
-0.8	0.0009	Acetate, Propionate

Calculating the maximum theoretical yield of each possible produced compound, it was revealed that the most favourable compound that could be produced using a high amount of energy was formate (Table 5-8).

Table 5-8: Maximum theoretical energy efficiency obtained from products derived via MES

Polarization potentials (V)	Maximum theoretical energy yield (%) - Acetate	Maximum theoretical energy yield (%) - Formate	Maximum theoretical energy yield (%) - Valerate	Maximum theoretical energy yield (%) – Propionate
-0.2	30	170	33	40
-0.4	15	85	16	20
-0.6	10	56	11	13
-0.8	7.5	42.5	8	10

The production of valerate and propionate was further researched in literature where it was found that when Levy *et al.* (1981) investigated organic acid production from CO₂ using a mixed culture anaerobes, they obtained small amounts of byproducts such as valerate, propionate and butyrate. This finding can also support the data obtained in this paper suggesting that valerate and propionate are by-products of CO₂ reduction.

The conversion rate of carbon into the various observed products at different polarizations was also calculated and shown in Table 5-9. Similarly to CCE and energy efficiency values, the conversion rates for acetate and formate were found low. However, in the case of valerate (51%) and propionate (26.10%) production, the obtained conversion rate was higher suggesting that the formation of longer chain molecules was promising.

Table 5-9: Carbon conversion rates into organic compounds at different polarizations

Polarization potentials (V)	Occurred reactions	Maximum Conversion rates (%)
-0.2	Acetate	4.20
-0.4	Acetate	3.10
	Formate	2.33
-0.6	Acetate	2.70
	Formate	2.18
	Valerate	51.00
-0.8	Formate	2.84
	Propionate	26.10

5.4.3 CO₂ reduction: Thermodynamics description

The applied potential of -0.6 and -0.8 V (vs. Ag/AgCl), was calculated to be thermodynamically appropriate to support the transformation of HCO_3^- to acetate and it was not the cause of the limitation of this production to microscale. Similarly, using Equation 5.9 to calculate hydrogen evolution with a standard potential of E_{H_2O/H_2}^0 at -0.828 V (vs. SHE) revealed that only the applied potentials of -0.6 and -0.8 V (vs. Ag/AgCl) would allow H₂ evolution in the system. On the other hand, using -0.2 and -0.4 V (vs. Ag/AgCl) potentials were confirmed to be too high to allow H₂ evolution and acetate production. However, acetate was observed and linked to possible biochemical reactions.

Thermodynamic insights are important for metabolic reaction networks or pathways to address the reaction viability of bioprocesses (Von Stockar and Van der Wielen, 2003). Thermodynamically, the difference in Gibbs free energy fixes the driving force for any system undergoing changes. Thus, thermodynamic analysis based on the Gibbs free energy change is applied to elucidate the spontaneity and existence of driving force for the occurrence of metabolic pathways responsible for a desired product. Moreover, a pathway for which the free energy change is large and negative has an equilibrium that favours the side of products. On the other hand, a pathway for which the free energy is large and positive has an equilibrium that favours the side of reactants. Therefore, using thermodynamic tools as an approach to understand and optimise metabolic productivity can be instrumental to the selection of feasible pathways and identifying optimal cellular environment for metabolic systems (Xu *et al.*, 2009). The minimisation of Gibbs free energy change and the maximisation of productivity of desired metabolites need to work simultaneously for an overall optimal selection of pathways and set of enzymes (or proteins) responsible for these pathways.

5.5 The effect of metabolic pathway on bioproduction

The low amount of volatile fatty acids versus the amount of total organic carbon is possibly attributed to the production of other products that have yet to be identified. The low rate of bioproduction triggered the need to investigate the bacterial conditions before and after the use of CO₂ to examine the tolerance of *Shewanella Oneidensis* MR-1 with CO₂. Live/Dead analyses showed that there was no significant difference between live or dead cells before and after CO₂ addition (Wilcoxon two-sample test, Appendix C6). This ensures that the small amount of compounds produced are not due to the high dead cells number. However, microbiological experiments with dead bacteria were performed to identify whether

compounds within the *Shewanella Oneidensis* MR-1 cell can contribute to this bioproduction trend.

Figure 5.8 shows that acetate was produced by dead cells when CO₂ was used as an electron acceptor and H₂ as an electron donor. Acetate was produced on the second day of the experiment and the concentration remained stable around 20 μmol. These results were equal to the results when live cells were used (Figure 5.3(B)). This proposes the possibility that *Shewanella Oneidensis* MR-1 does not use CO₂ within its respiration process but as a biochemical process within its cytochromes. This suggests that the reduction reaction occurring in BES systems might be related to a type of process called reductive dechlorination (Mohn and Tiedje, 1992; Fetzner and Lingens, 1994). This dehalogenation reaction sometime occurs with heat killed cells and with electron donors such as H₂ (in microbiological vessels) and/or electrode (in BES systems). Picardal *et al.* (1993) showed that respiratory c-type cytochromes were responsible for the reductive dehalogenation of tetrachloromethane in *Shewanella*. With *Shewanella Oneidensis* MR-1 producing a number of cytochromes, it is likely that the porphyrins (within the proteins) these contain, ‘accidentally’ reduce a range of compounds. Similarly, this reaction could also be related to the microsome activity of the cells. Here, it is suggested that CO₂ is affecting the protein chemical composition and thus resulted to the observed bioproduction.

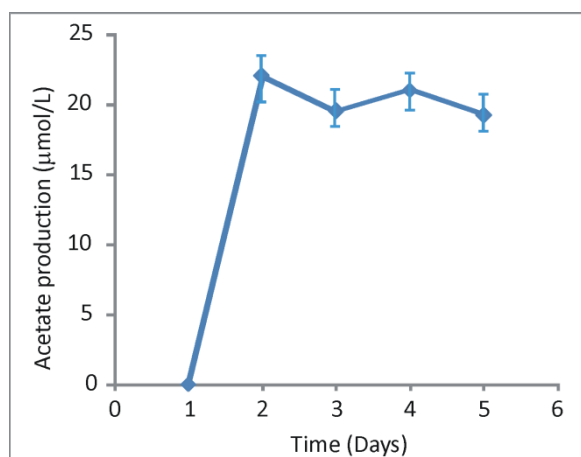


Figure 5.8: Acetate production from biotic microbiological experiments using dead *Shewanella Oneidensis* MR-1, CO₂ as an electron acceptor and H₂ as an electron donor at 30 °C (n=3).

5.5.1 Role of proteins in CO₂ reduction pathway:

To gain further insight into this anomalous effect of bioproduction, extracted proteins from *Shewanella Oneidensis* MR-1 cells were used to elucidate the CO₂ reduction pathway. Figure

5.9 (A) shows the electrochemical activity of the extracted proteins with and without CO₂. After the addition of proteins, a large spike was observed with a decrease in current density to approximately -10 μA and steadily increased to -2 μA after about 10 hours. Then again with the addition of CO₂ the electric current gradually decreased suggesting the use of CO₂ in the cathode and its possible use from proteins. Figure 5.9 (B) presents the redox activity of the cathode. Even that a reduction peak could be identified from the cyclic voltammetry, the first derivative (Figure 5.9 (C)) was used to analyse the reduction potential more clearly. In both MESs, a reduction potential of -0.81 V (vs. Ag/AgCl) was calculated and translated to -0.613 V vs. SHE which agrees with the reduction peak of CO₂ to acetate. These findings were supporting the fact that proteins have an effect on CO₂ reduction or vice versa.

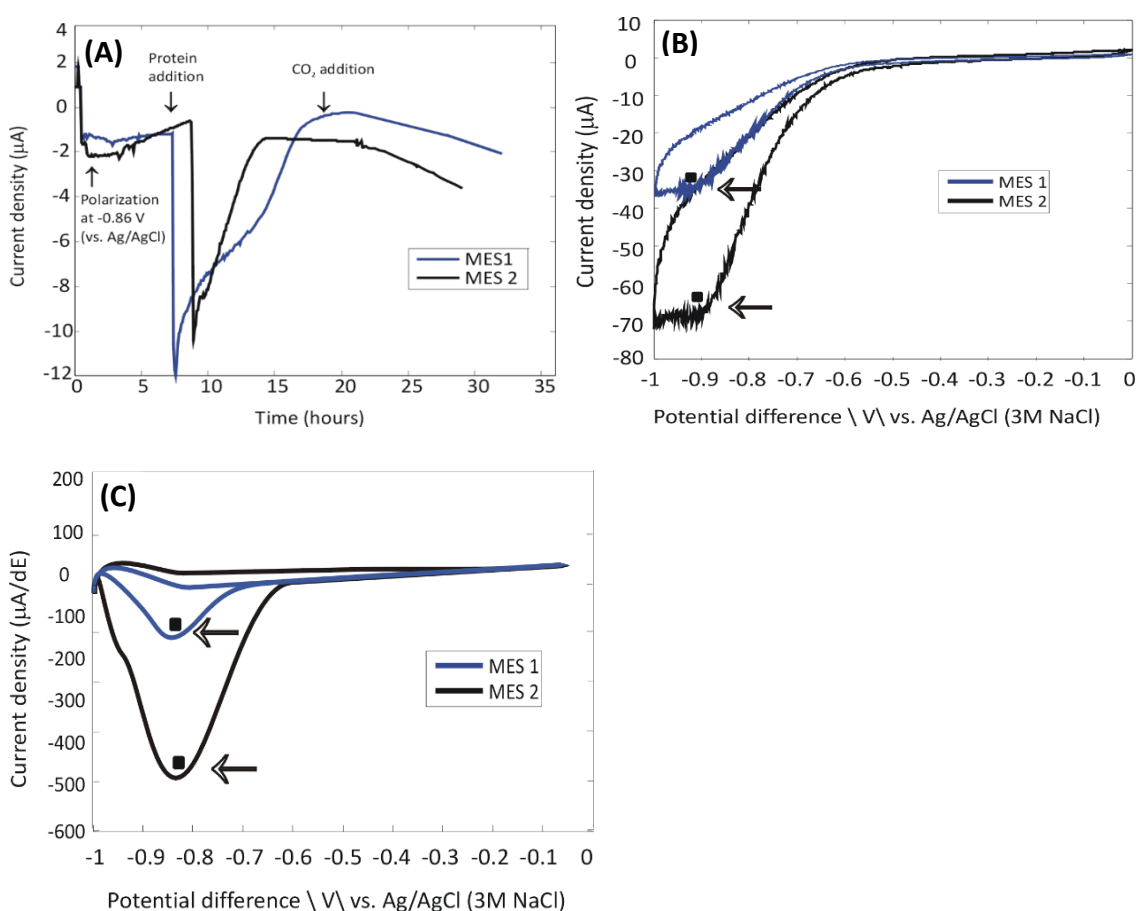


Figure 5.9: (A) Amperometric detection of MES 1 and 2 for electrochemical activity of proteins with CO₂. Polarization was performed at -0.8 V vs. Ag/AgCl. The arrows indicate the additions of proteins extracted from *Shewanella Oneidensis* MR-1 cells and CO₂. (B) Cyclic voltammetry of BESs with extracted proteins from *Shewanella* cells after with CO₂. (C) First derivative originated from the cyclic voltammetry in subfigure (B). The arrows indicate the resulted reduction peak. All electrochemical experiments were performed at pH 7.

Figure 5.10 (A) presents the concentration of acids and alcohols before and after the addition of CO₂ using different protein amounts. An increase in concentration of acids and alcohols was observed when higher amounts of proteins were used. This suggests that combining CO₂ and

polarized potentials can affect the biochemical process for product formation. To gain a deeper understanding, experiments without CO₂ were also performed. Figure 5.10 (B) shows the results of product formation using proteins and polarized potentials (without CO₂). The potential was polarized for 10 minutes, followed by the addition of proteins (time 0) and sampling which showed a total product formation; acetic and propionic acids, of ca. 150 μmol. Samples after 30 minutes of operation showed identical product formation suggesting that polarizing the electrode did not affect the protein composition. These findings match with the findings mentioned before and reported in Picardal *et al.* (1993). Experiments without the use of polarized potential did not show any acid and alcohol present in the samples. Absorbance and pH measurements remained stable showing that they did not have any effect on the changes in the system. These outcomes suggest that the presence of CO₂ in solution and the use of polarization potential have an effect in the chemical composition of proteins which lead to biochemical production.

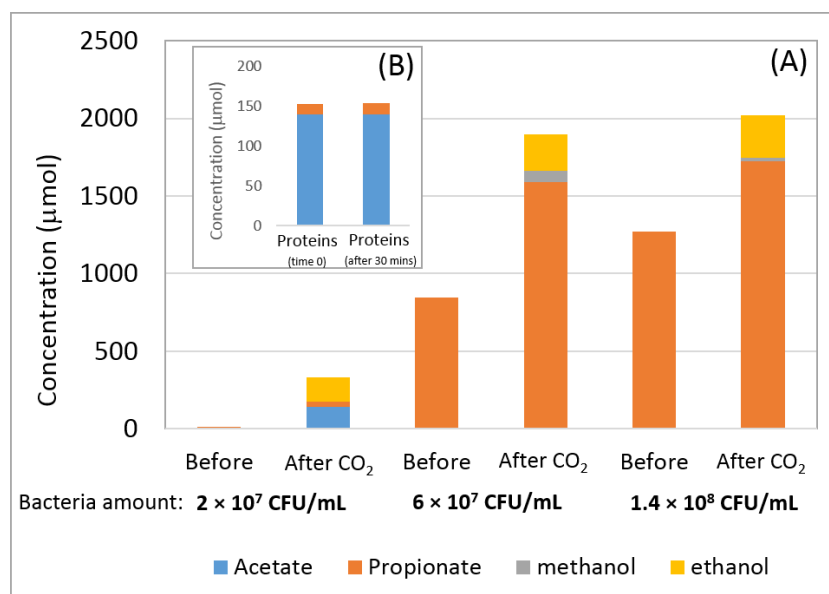


Figure 5.10: (A) Acid and alcohol concentration before and after CO₂ addition using different concentrations of proteins measured as equivalent to bacterial concentration (CFU/mL). (B) Acid concentration 10 and 30 minutes after applying a potential. The polarized potential used was -0.8 V vs. (Ag/AgCl) and the pH was measured stable at 7.

Protein molecules have shown their capability of catalysing reactions through bacteria (i.e. enzymes) for the production of enantiomerically pure amino acids and other chemicals since 1914 (Leisola *et al.*, 2002). Proteins are assumed as a growing biocatalyst industry and nowadays it involves genetically modified living cells to optimise processes and chemical productions. The idea of proteins usage to allow industrial processes to be carried out in mild conditions (i.e. low temperature and pressure) to reduce energy costs has been very attractive.

Having said this and results from this study suggest the feasibility of *Shewanella Oneidensis* MR-1 to produce chemicals under the effect of electricity and CO₂ should be further researched as it could offer an additional potential source of chemical production using the principles of green chemistry. This chemical production route could contribute to chemical production demand by reducing CO₂ emissions and add on meeting the CO₂ emission reduction target set for 2050 (CCC, 2015).

5.6 Hypothesized pathway of bioproduction

In order to establish potential chemical production pathways, the data and the identified reactions occurred in *Shewanella Oneidensis* MR-1 were presented in a hypothesized pathway which was developed based on findings (Figure 5.11). *Shewanella Oneidensis* MR-1 was capable of producing a range of compounds using a pathway starting from CO₂. A number of experiments show the formation of volatile fatty acids, aldehydes and alcohol which were identified and quantified using a range of chemical and electrochemical analytical techniques.

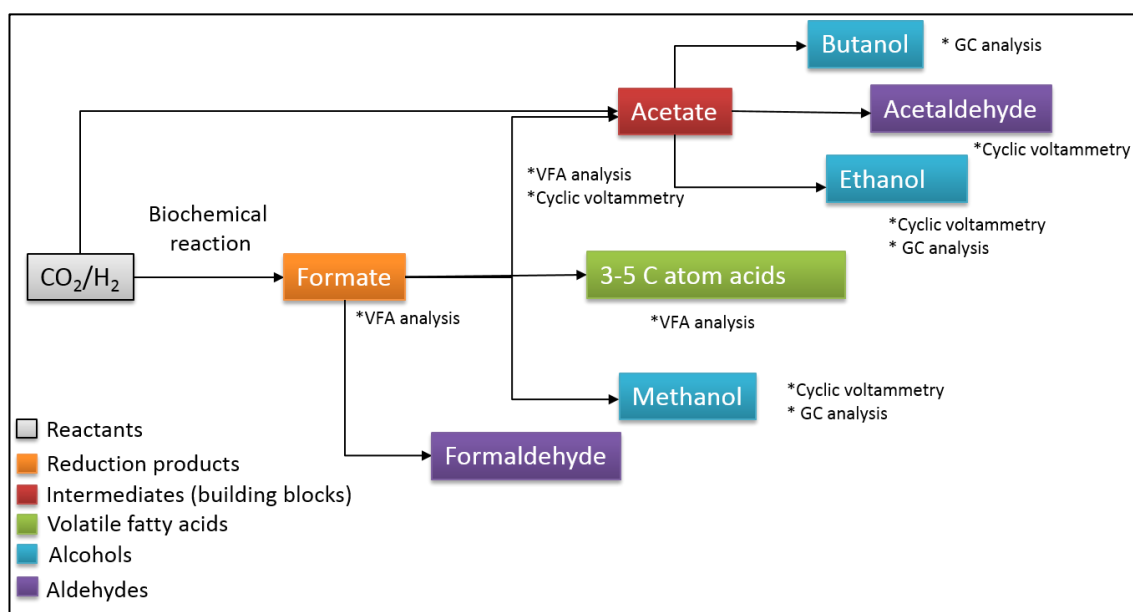


Figure 5.11: Hypothesized pathway of bioproduction using *Shewanella Oneidensis* MR-1

5.7 Conclusion:

This study confirmed that BESs' current density and lag phase was affected by the operating temperature offering limitations in biofilm development. CV scans showed a clear catalytic activity in all BESs and evidence of biofilm accumulation in two bioanodes. The redox potential of excreted riboflavin, MtrC & OmcA, and lactate to acetate reaction were identified from the CVs. Results from bioproduction under different polarization potentials showed formic, acetic, propionic and valeric acids production at the micro range scale. Statistical analyses performed regarding polarization potentials and product formation showed no correlation. These results along with low CCE and energy efficiency suggested a possible biochemical process occurred rather than respiration. Alongside, from the theoretical energy efficiency calculations, formate was identified as the most theoretically favourable product to be formed using an applied potential. Using acetate and formate as substrates to investigate the production of longer chain molecules revealed the capability of *Shewanella Oneidensis* MR-1 to respire them and produce small alcohol molecules (i.e. methanol and ethanol). The use of extracted proteins from *Shewanella Oneidensis* MR-1 showed a trend of increasing product formation with increased protein amount suggesting that CO₂ and applied polarization potentials have an effect on their chemical composition. These findings suggest the capability of *Shewanella Oneidensis* MR-1 to biosynthesize hydrocarbons from CO₂ using proteins as biocatalysts. Furthermore, a hypothesized pathway, which resulted from this work, was developed.

Chapter 6: Effect of temperature, agitation and biofilm development techniques on the performance of bioelectrochemical systems for energy and chemical production

6.1 Introduction

Microbial fuel cells (MFC) gained considerable interest on bioelectricity production (Rahimnejad *et al.*, 2015) for practical applications such as power source for small robots (Melhuish *et al.*, 2006; Ieropoulos *et al.*, 2010) and as biosensors for COD/BOD detection levels (Kim *et al.*, 2003; Kim *et al.*, 2005; Wang *et al.*, 2012). MFC is a bioelectrochemical system where inorganic and/or organic substrates are oxidised directly into energy at the presence of bacteria. Bacteria function as bio-catalysts, usually in the form of a biofilm, for the production of electrons through their metabolic activity and also perform electron transfer to the anode electrode. Bioelectricity harvesting from such systems gained an increased amount of significance as it meets practical and sustainable goals by using wastewater as substrate.

To increase and optimise MFC performance, the anodic biofilm development is highly important for an effective and vital process. Biofilm is a complex mass of bacterial communities attached to a solid substrate using self-excreted adhesive called extracellular polymeric substances. Biofilm consists mainly of water, extracellular polymeric substances and bacteria and is very often characterized by genetic diversity and complex bacterial community interactions (Sand and Gehrke, 2006). Biofilm is an important factor in electrochemical process due to the presence of high cell density on solid electrode materials (Reguera *et al.*, 2005; Gorby *et al.*, 2006). The higher the cell density on the electrode, the greater the potential is for cell- to-cell contact to stimulate electron transfer mechanisms.

The performance of MFCs and thus bioelectricity production is affected by biological, physical, chemical and mechanical component integration as well as their interactions. Operating an MFC successfully, relies strongly on its operating conditions as well as on electrode material choice (Venkata Mohan *et al.*, 2008; Feng *et al.*, 2009; Ieropoulos *et al.*, 2010). Temperature, agitation and electrode optimization treatments for MFC operation often present challenges that affect biofilm development and thus MFC performance, energy generation and chemical production (MES).

In this report, an attempt was made to study and investigate the effects that different levels of temperature and agitation have on biofilm development, bioelectricity and chemical

production. Different electrode treatments were used to optimise the process and enhance biofilm development. Electrode coverage and biofilm condition were also explored.

6.1.1 General hypothesis

Different operating conditions can affect biofilm development time, electric current, LIVE/DEAD cell count and electrode coverage.

6.1.2 Objectives

1. To evaluate the **biofilm development** from *Shewanella Oneidensis* MR-1 using different levels of **temperature** and **agitation** as well as different **electrode treatments**
2. To elucidate the effect of operating conditions on **biofilm development time (lag phase)**, **electric current production**, **LIVE/DEAD cell count** and **electrode coverage** using statistical analyses
3. To investigate how **different biofilm growth (and cell attachment)** affect **chemical production** through empirical and statistical analyses

6.2 Materials and methodology

6.2.1 Experimental set-up of BESs

Sixteen identical H-shaped BESs made of glass were set up with an anode and a cathode chamber of 80 mL working volume and 30 mL headspace (Figure 6.1). The anode and cathode chambers were separated by a 2.27 cm² proton exchange membrane (Nafion 117, Sigma Aldrich, UK). The anode chambers were stirred using a magnetic stirrer to maintain uniform flow and the temperature was maintained constant using a temperature controlled DIY incubator. The reactors were equipped with working and counter electrodes made of carbon cloth (4 cm², wet proofed 20%, Fuel Cell Earth, US) connected with titanium wire and previously immersed in ethanol for 24 hours followed by three times washes with autoclaved deionised water to ensure sterile conditions. A volume of 80 mL of anaerobic medium (0.225g K₂HPO₄, 0.225g KH₂PO₄, 0.46g NaCl, 0.225g (NH₄)₂SO₄ and 0.117g MgSO₄ per litre) was introduced in the anode and cathode chambers of the BESs while sparging with N₂ to achieve complete anaerobic conditions for the prevention of the cells to use oxygen as an electron acceptor. All equipment, glassware and solutions were autoclaved prior use unless differently stated.

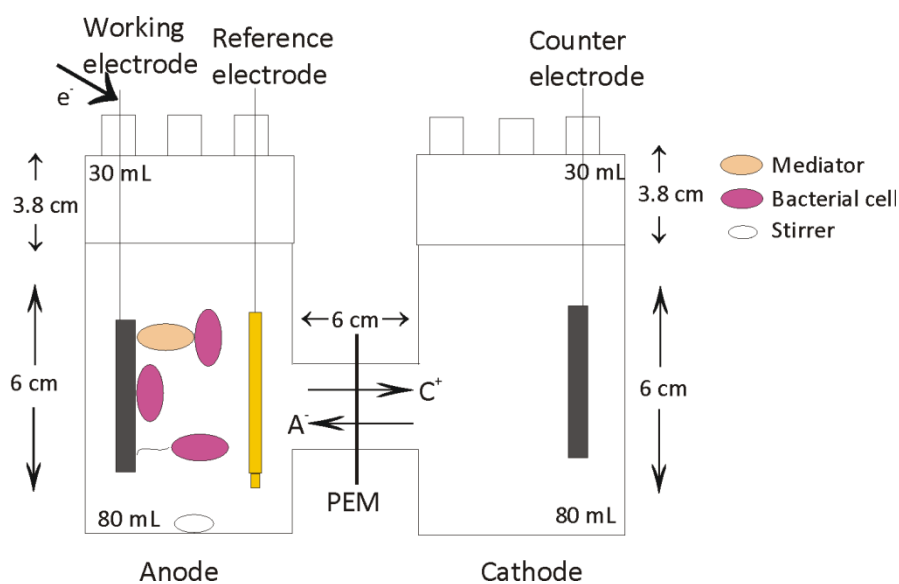


Figure 6.1: Schematics on bioelectrochemical systems' overall dimensions and operation

6.2.1.1 MFC reactors inoculation and operation

The performance of MFCs was evaluated in different operating conditions based on temperature (15 °C and 30 °C) and agitation (90 rpm and 140 rpm). The anode chamber was inoculated with pure culture of *Shewanella Oneidensis* MR-1 at $\times 10^6$ CFU/mL, anaerobic medium and the carbon cloth electrode. Lactate was used as the sole electron donor along with an oxidised potential of +0.2 V (vs. Ag/AgCl).

6.2.1.2 Fluid mechanics reactors operation

Culture medium of Luria broth (LB, 1L) was made and distributed in eight conical flasks (Erlenmeyer flasks) of 250 mL. Eight carbon cloth electrodes (4 cm²) were connected with titanium wire and immersed in the culture medium and stabilised with autoclavable foam sponge. The conical flasks were then autoclaved. After the sterilization, *Shewanella Oneidensis* MR-1 cells were added in the flasks for growth (Figure 6.2) at open circuit potential (OCP) and left for 36 hours corresponding to exponential growth/early stationary phase and an optical density (OD₆₀₀) of 1nm to be used in biofilm development experiments. The electrodes were then transferred to eight H-shaped bioelectrochemical systems including anaerobic medium. An incubator was used to accommodate the growth flasks and to fit the growth conditions. After the 36 hours of incubation the electrodes were transferred in eight H-shape BESs. These BESs were labelled as Fluid mechanics and their performance was evaluated at the same operating conditions as in MFCs using lactate as the electron donor and +0.2 V (vs. Ag/AgCl) as applied potential.

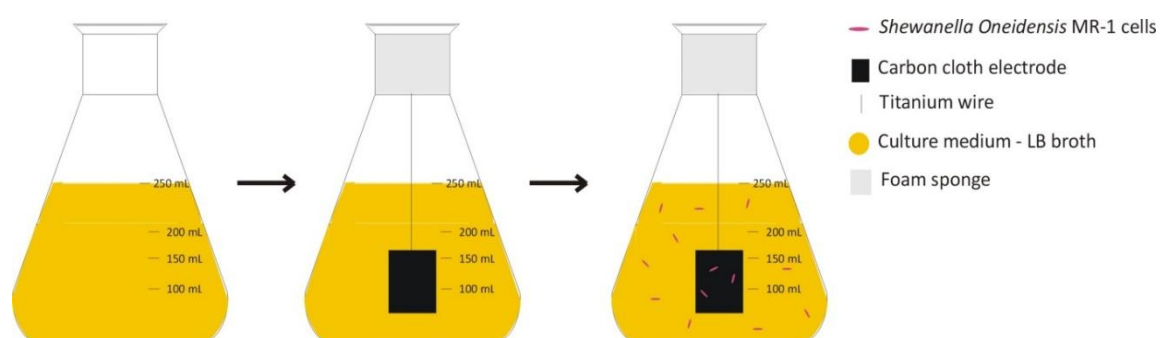


Figure 6.2: Schematic on hydrodynamic method set-up

The maximum levels were chosen due to the bacterial growth favourable growth conditions where the minimum levels were chosen due to the laboratory equipment use. All reactors were operated for a total of approximately 20 days and results were compared based on lag phase occurrence, maximum current density generation, number of live/dead cells on electrode and electrode coverage by bacteria.

6.2.2 Experimental set-up using polyHIPEs electrodes

6.2.2.1 Bacterial growth and start-up biofilm stage

Two polyHIPE electrodes were autoclaved and placed on a Petri dish. The electrodes were wetted with lactate (1 g/L) and left in an oven to dry at 30 °C for 6 hours. *Shewanella Oneidensis* MR-1 cells, previously grown in LB broth, was put onto the surface of the electrodes and left in the oven for 24 hours in OCP. Lactate was added every 2 days to enhance the growth of the biofilm. Control experiments were performed previously to identify the appropriate period needed for complete biofilm coverage (Figure 6.3). The polyHIPE were removed from the incubator after 12 days and connected to a titanium wire to be used as anode electrodes.

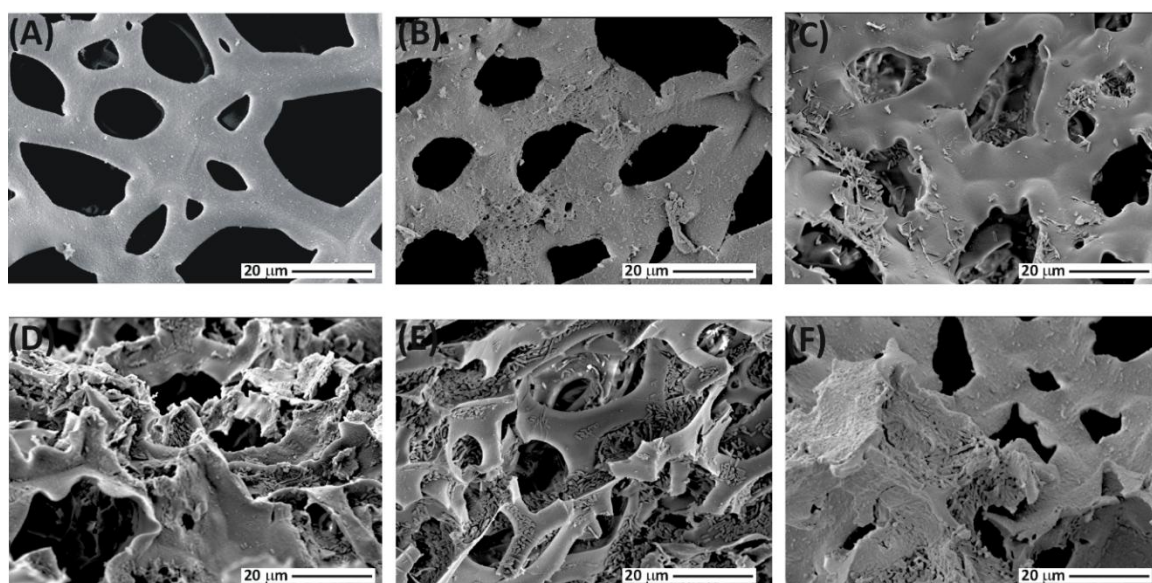


Figure 6.3: Controls of biofilm development at OCP: (A) Day 0, (B) Day 3, (C) Day 5, (D) Day 7, (E) Day 10 and (F) Day 12

6.2.2.2 Experimental set-up and operation

Two identical H-shaped BESs were prepared and set up as described previously. Here, the reactors were equipped with working electrodes made of polyHIPE material (2.45 cm², 400% hydrophilic) and counter electrodes made of carbon cloth (4 cm², wet proofed 20%, Fuel Cell Earth, US). Anodic biofilms were grown previously on the anode electrodes in a Petri dish as described earlier. For the biofilm conditioning in BESs, lactate was used as the electron donor and the electrode as the electron acceptor. The steps for the anode preparation are shown in Figure 6.4.

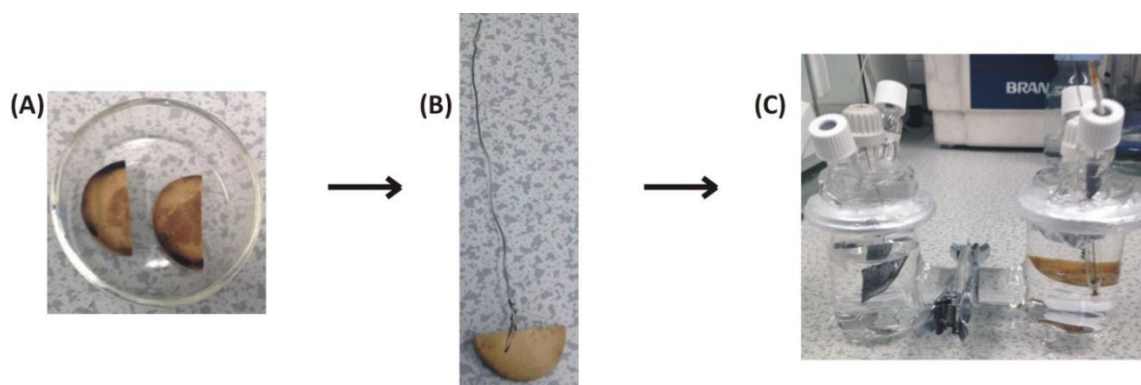


Figure 6.4: Steps of the anode electrode preparation; (A) biofilm growth on anode electrode, (B) electrode preparation, (C) bioelectrochemical system set-up

6.2.3 Cathode: Experimental set-up using carbon cloth electrodes

Six identical H-shaped BESs made of glass were set up similar to the experimental set up for anode experiments. Here, for the experimental set up, platinum counter electrodes were used instead of carbon cloth to gain better data acquisition. In addition, the anode chamber was spurge with N_2 to set anaerobic conditions and the cathode chamber was initially left aerobic until biofilm development and then switched to CO_2 as the sole electron acceptor for bioproduction.

6.2.3.1 MES reactors inoculation and operation

The performance of MESs was evaluated at best operating conditions chosen from data resulted from the anode experiments for maximum performance (30 °C and 90 rpm). The cathode chamber was inoculated with pure culture of *Shewanella Oneidensis* MR-1 at $\times 10^6$ CFU/mL, anaerobic medium and the carbon cloth electrode. Originally oxygen was used as the sole electron acceptor to enhance biofilm development followed by CO_2 addition as substrate and the only source of carbon at -0.8 V vs (Ag/AgCl). Liquid samples were then collected to test for bioproduction. Two systems were used for biofilm development; OCP and closed circuit potential (CCP). OCP biofilm were developed as stated previously for anodes where CCP biofilms were grown using free bacterial cells in solution.

6.2.4 Statistical analysis

The lag-phase, maximum electric current generation, live/dead cells count, electrode coverage and chemical production were statistically analysed for comparison using a non-parametric test, Mann-Whitney U-test with a 95% confidence level ($\alpha=0.05$).

6.2.5 Electrochemical analyses

6.2.5.1 Biofilm growth and conditioning period

The electrochemical experiments were conducted in the H-shape cells using a 3 electrode system. During the bacterial growth, the anode was polarized at +0.200 V (vs. Ag/AgCl) to act as an electron acceptor and lactate (1 g/L) was used as electron donor. For the anode operation, cyclic voltammograms were measured from -0.600 to 0.600 V (vs. Ag/AgCl) at a scan rate of 0.001 V/s. For cathode operation, cyclic voltammograms were measured from 0.0 to -1.0 V (vs. Ag/AgCl) at a scan rate of 0.001 V/s. Slow scan is used to prevent damage of the cells. In this report, we evaluate the biological systems which require the initial scans of cyclic voltammetry to avoid the effect of electrode polarization on the electrode bound protein metabolism. Thus, cyclic voltammograms reported here, refer to the second scans. Polarization curves were measured during bacterial growth based on the current obtained over time under potentiostatic polarization. All measurements and applied potential experiments were done on a PSTrace potentiostat. First derivatives of cyclic voltammetry were calculated after pre-treating the data using Matlab functions; polyfit and polyval.

6.2.6 Biofilm analysis

6.2.6.1 Scanning electron microscopy (SEM)

SEM was used to visualize features of the biomass on the electrode. Carbon cloth electrodes with biofilm were fixed with 2.5% gluteraldehyde solution in phosphate buffer, dehydrated in increasing ethanol concentrations (20, 40, 60, 80 and 100%) and subjected to critical point drying using an automated critical point dryer. The samples were sputter-coated with gold and examined by SEM (Cambridge Stereoscan 240 SEM, UK).

6.2.6.2 Confocal microscopy

Confocal microscopy analysis was used to observe the condition of the bacterial cells on the electrode. The carbon cloth electrodes were immersed in deionized water which contained two stains; SYTO9 and propidium iodide (FILMTRACER™ LIVE/DEAD^R biofilm viability kit, Thermo Fisher, UK). The samples were incubated at room temperature for 30 mins and then washed with deionised water to remove excess of dye. Confocal microscopy was used to view the samples.

Bacterial cell number was evaluated using image processing and analysis software ImageJ.

6.3 Results and discussion

6.3.1 Effect of operating temperature, agitation and electrode pre-treatment on anode performance

Figure 6.5 shows the electric current during the addition of lactate (1g/L) in the anode of MFCs and Fluid mechanics reactors at different operating conditions. All reactors were potentiostatically controlled at an oxidizing value of +0.200 V vs. (Ag/AgCl) to enhance the anode start-up. *Shewanella Oneidensis* MR-1 cells were inoculated after 10 minutes from the start-up of the reactors. After 4 hours of the inoculation of *Shewanella Oneidensis* MR-1, lactate was added in the anode compartment. A lactate spike was observed and the electric current increased in all reactors. Lactate was repeatedly added in the anode compartments at days 6 and 10 where the same effect was observed. Lactate exhaustion occurred after 2-4 days from its addition depending on the operating conditions and it was indicated by the current drop. The reactors were operated for a total of approximately 20 days.

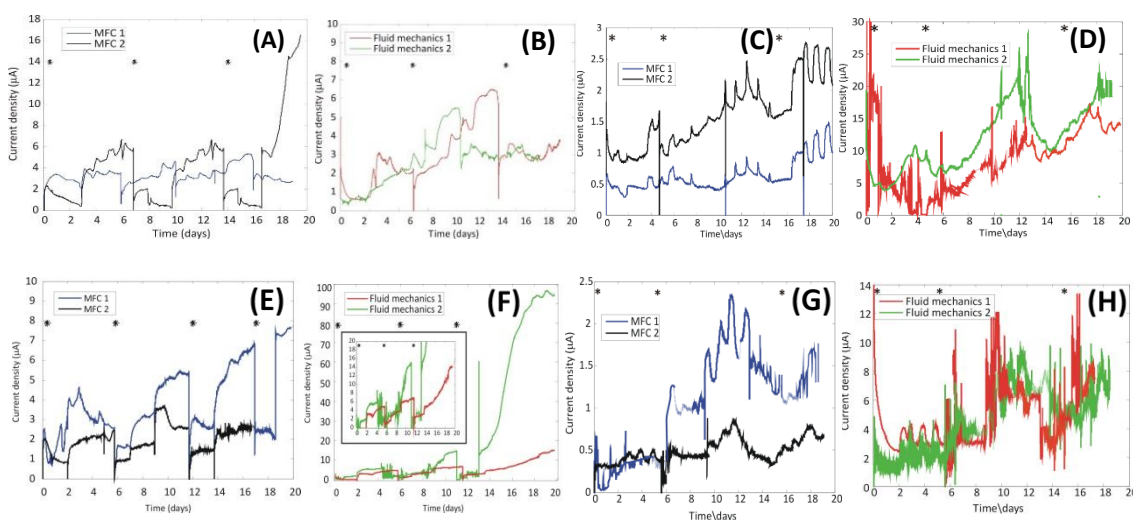


Figure 6.5: Current generation over time using *Shewanella Oneidensis* MR-1 and a polarization potential of +0.2 V (vs. Ag/AgCl); At 90 rpm and 30 °C: A and B, at 90 rpm and 15 °C: C and D, at 140 rpm and 30 °C: E and F, at 140 rpm and 15 °C: G and H. The stars (*) indicate the addition of substrate (lactate). The pH of all reactors was set at 7 with an electrical conductivity of approximately 9 mS/cm.

MFCs operating at 15 °C were observed with the presence of 4-6 days long lag-phase where MFCs operating at 30 °C showed a 1-2 days short lag-phase suggesting that temperature conditions are vital to the bacterium's metabolism for growth. Using low temperatures promotes falling of enzymatic activity within the cells, thus longer adaptation time and lower electric current generation. On the other hand, fluid mechanics reactors demonstrated a two times faster adaptation (1-2 days) and an average of 76% higher (median = 12.05 µA, n=8) electric current generation than MFCs (median = 3.05 µA, n=8). This is probably to the attachment of the bacterial cells during their exponential growth phase which contributes to

an easier transition suggesting to influence shorter lag phase ($p=0.0460$, $W=87.5$; Figure 6.6) and higher electric current generation ($p=0.0136$, $W=44$; Figure 6.6). The use of already start-up biofilms eliminates the time needed for the bacteria to move from the solution to the electrode and thus decreases the lag phase. *Shewanella Oneidensis* MR-1 is a bacterium with the ability of switching from using oxygen to use the carbon cloth anode electrode as a terminal electron acceptor in its metabolism. However, this change can be dependent on a number of factors including temperature, agitation and electrode material (electrode treatments etc.).

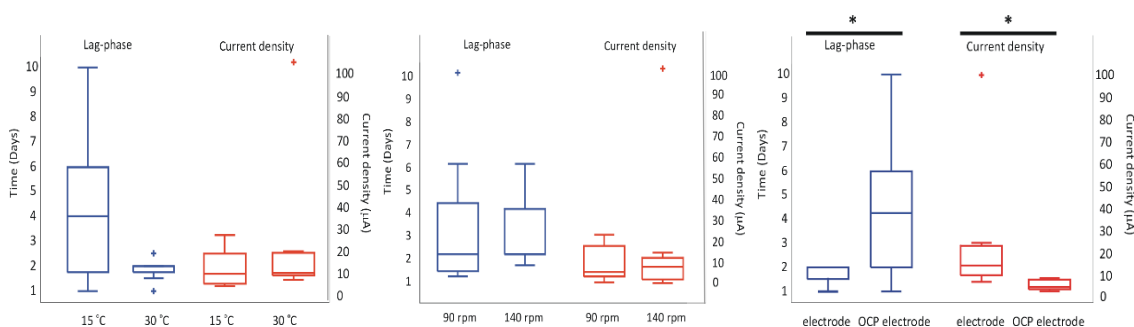


Figure 6.6: Effect of operating conditions in lag-phase and electric current generation. Left: Box plots of temperature conditions ($n=8$). Centre: Box plots of agitation rates ($n=8$). Right: Box plots of OCP treatment ($n=8$). The star (*) indicates the significant pairwise difference ($p < 0.05$).

Subsequent analytical methods were used for elucidating the effect of changes in the local redox environment to evaluate biofilm development on the electrode surface. The CV scans were performed as non-turnover conditions to study all redox-active compounds of the substrate at the electrode and the formal potential of possible extracellular electron transfer. Figure 6.7 shows the cyclic voltammetry scans of MFCs and Fluid mechanics reactors after 20 days of operation. Figure 6.7 (A), (B), (C), (E) and (F) show the electrochemical characteristics of an anodic biofilm indicating the catalytic oxidation of substrate (lactate) and heterogeneous electron transfer to the electrode. The presence of a cathodic reaction with small current generation was also shown but it was later linked to noise. Figure 6.7 (D), (G) and (H) show characteristics that suggest evidence of biomass accumulation on the electrode surface area. Higher electric current generation proposes the increase of resistance on the electrode surface area compared to the Abiotic scans. However, this will cause a possible decrease of the electrode's performance due to the built up of capacitance. The leaf shaped cyclic voltammogram scans also indicates the catalytic activity of the biofilm.

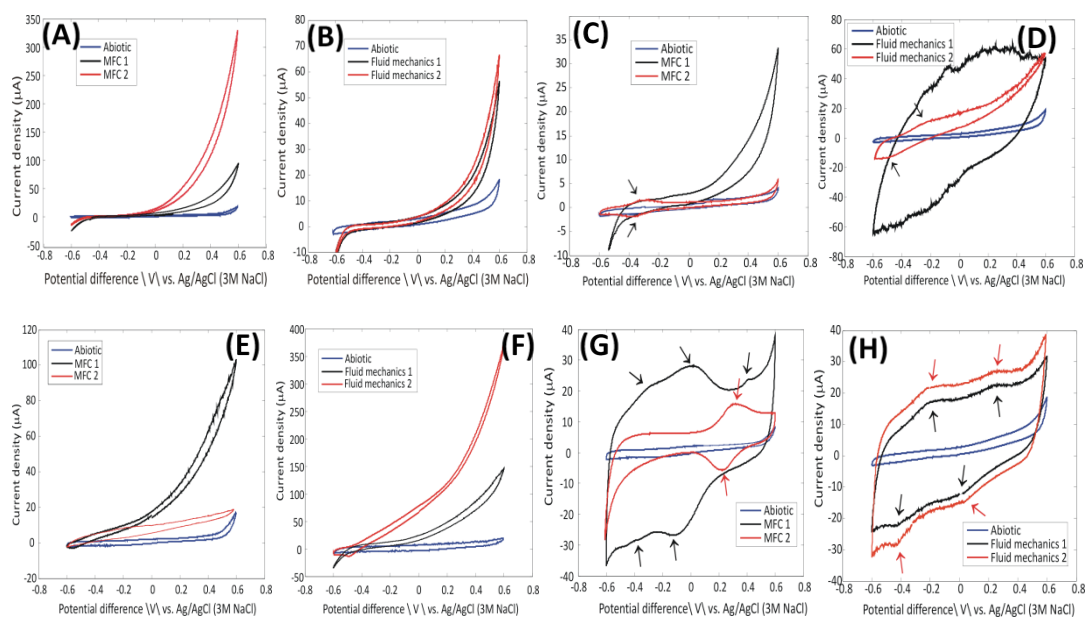


Figure 6.7: Redox activity associated with *Shewanella Oneidensis* MR-1 in MFCs and Fluid mechanic reactors at different operating conditions; At 90 rpm and 30 °C: A and B, at 90 rpm and 15 °C: C and D, at 140 rpm and 30 °C: E and F, at 140 rpm and 15 °C: G and H. The arrows indicate the identified peaks at pH 7 and electrical conductivity of approximately 9 mS/cm.

A number of broad peaks were identified from Figure 6.7 and confirmed using the first derivative. Most of the scans showed to maintain a redox peak around -0.325 to -0.375 V (vs. Ag/AgCl) which is closed to the redox potential of riboflavin which varies from -0.219 to -0.450 V (Albertas Malinauskas, 2008; Velasquez-Orta *et al.*, 2010). This fact suggests the excretion of riboflavin from the bacteria, with a shift to the left probably to pH changes. Another redox peak was also detected around 0.15 to 0.25 V (vs. Ag/AgCl) which agrees with the lactate and NAD⁺ to acetate potential slightly shifted to the left. Possible individual peak responses from MtrC and OmcA proteins might be overlapping with the riboflavin peak (Hartshorne *et al.*, 2007; Meitl *et al.*, 2009). However, due to the increased noise present in the cyclic voltammetry scans, it was very difficult to be identified.

6.4 Anodic biofilm growth

Anodic biofilm growth was observed using SEM (Figure 6.8). Although the data from SEM was used to depict electrode coverage, a relationship between biofilm growth and operating conditions could also be established. For all reactors, bacteria morphology was homogeneous with rod shape cells correlating to *Shewanella Oneidensis* MR-1 cells suggesting of a pure culture biofilm. In all SEM analyses, the formation of pilus-like nanowires was visible which are proved to be electrically conductive appendages.

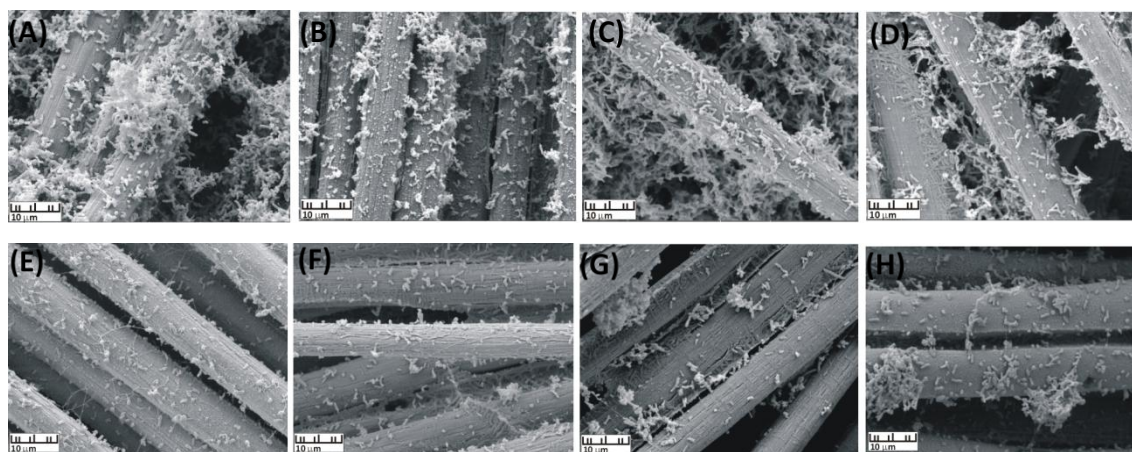


Figure 6.8: Scanning electron microscopy of MFC and Fluid mechanics reactors at different operating conditions. (A) MFC at 90 rpm and 30 °C, (B) Fluid mechanics at 90 rpm and 30 °C, (C) MFC at 140 rpm and 30 °C and (D) Fluid mechanics at 140 rpm and 30 °C. (E) MFC at 90 rpm and 15 °C, (F) Fluid mechanics at 90 rpm and 15 °C, (G) MFC at 140 rpm and 15 °C and (H) Fluid mechanics at 140 rpm and 15 °C.

MFC and Fluid mechanics reactors showed similar growth patterns at 30 °C, with 90 and 140 rpm agitation rates (Figure 6.8 A-D). The majority of the electrode was covered and colonization was described as relatively good. Even that some ‘clumpy’ growth could be seen, the majority of the biomass appeared to have a uniform biofilm formation. MFC and Fluid mechanics reactors showed different patterns at 15 °C, with 90 and 140 rpm agitation rates (Figure 6.8 E-H). While some ‘clumpy’ growth was also present, more dispersed patterns were observed throughout the electrode. Even though, no significant effect was observed when different agitation rates ($p=0.95$, $W=69$, Figure 6.9) and OCP treatments ($p=0.71$, $W=64$, Figure 6.9) were used for biofilm growth, using 30 °C as an operating temperature showed 3.3 times (median=35.29%, $n=8$) more coverage ($p= 0.0009$, $W=36$, Figure 6.9) than low operating temperature (median=10.83%, $n=8$). Higher biomass accumulation it was expected with higher temperatures as it is a more vital environment for bacterial growth.

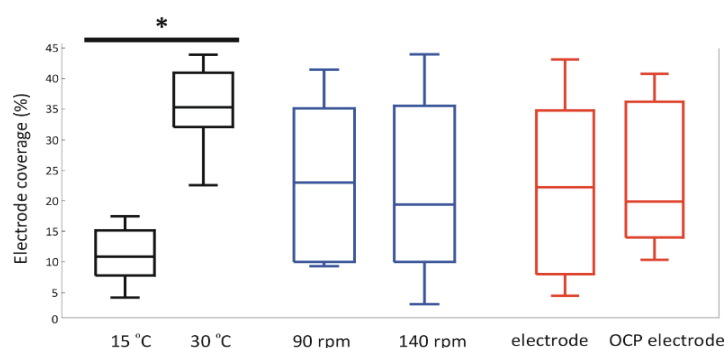


Figure 6.9: Effect of operating conditions in electrode coverage. Box plots of temperature, agitation and OCP treatment ($n=8$). The star (*) indicates the significant pairwise difference ($p < 0.05$).

Confocal microscopy images showed the surface of the anode electrode with viable (green) and non-viable bacterial colonies (red) during the period evaluated (Figure 6.10). In all reactors, the bacteria growth was located on the carbon cloth fibres forming a thin layer of biofilm. MFC and fluid mechanic reactors operated at 15 and 30 °C and 90 rpm showed comparable live/dead bacterial conditions (Figure 6.10A, B, E and F). For further verification of these data, the results were compared with Figure 6.5A, B, E and F where it was found that the electric current production was similar. However, for fluid mechanic reactors operated at 15 and 30 °C with 140 rpm agitation rate, the biomass accumulation was greater and spread also around the fibres (Figure 6.10D and H). With higher accumulation of bacterial growth, higher electric current production was expected and matched with the data shown in Figure 6.5D and H. MFC reactors operated at 15 and 30 °C and 140 rpm (Figure 6.10C and G) were observed with minor live cells number and scattered bacterial growth confirming the low electric current produced (Figure 6.5C and G).

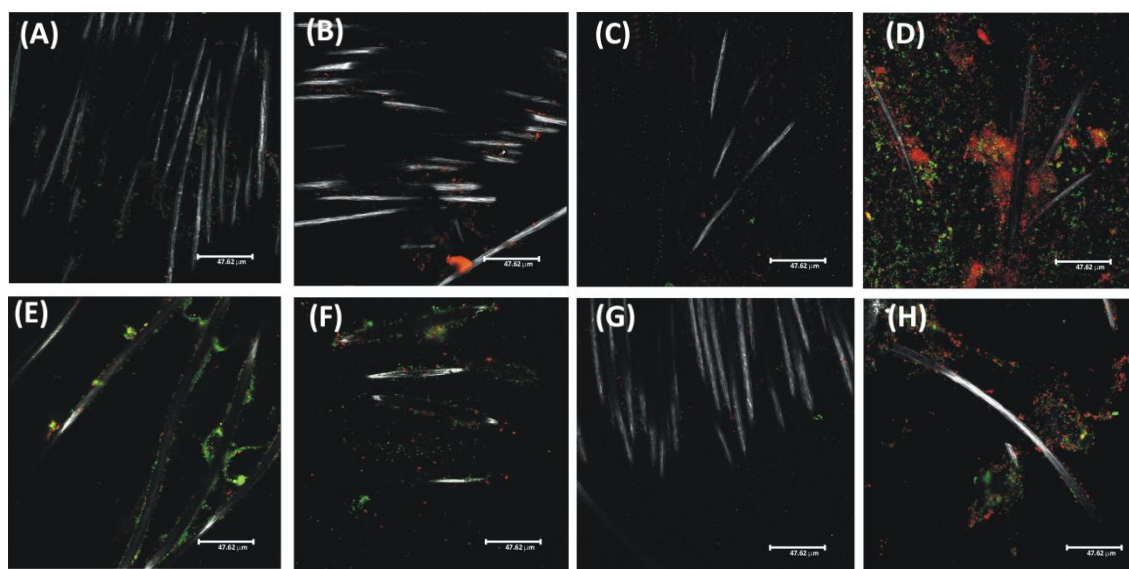


Figure 6.10: Live Dead analyses of MFC and Fluid mechanic reactors at different operating conditions. (A) MFC at 90 rpm and 30 °C, (B) Fluid mechanics at 90 rpm and 30 °C, (C) MFC at 140 rpm and 30 °C and (D) Fluid mechanics at 140 rpm and 30 °C. (E) MFC at 90 rpm and 15 °C, (F) Fluid mechanics at 90 rpm and 15 °C, (G) MFC at 140 rpm and 15 °C and (H) Fluid mechanics at 140 rpm and 15 °C.

By assessing the bacterial condition on the electrode surface area, not only correlations between outputs were found but the effects of different operating conditions and electrode treatment were elucidated. Using an operating temperature of 30 °C had a significant effect ($p=0.0181$, $W=45$, Figure 6.11) on the live cells count. The amount of live bacteria was increased almost 3.2 times (median= 2.3×10^6 , $n=8$) compared to low temperature (median= 0.7×10^6 , $n=8$). As said previously, the use of 30 °C offers a vital environment for bacterial growth and promotes a healthy biofilm formation. On the other hand, the presence of high dead cells was significant ($p=0.0181$, $W=45$, Figure 6.11) when 140 rpm agitation

(median= 1.4×10^6 , $n=8$) was used compared to 90 rpm agitation (median= 0.6×10^6 , $n=8$). Reactors at high agitation rates were least productive with suppressed biofilm growth probably due to lack of nutrients capture and biofilm detachment (Ieropoulos *et al.*, 2010; Kim *et al.*, 2013). Even that the use of OCP electrode did not have any significant effect on the live/dead cells number, an increased amount of dead cells can be seen probably due to the lack of nutrients capture by the bacteria (Figure 6.10 and Figure 6.11).

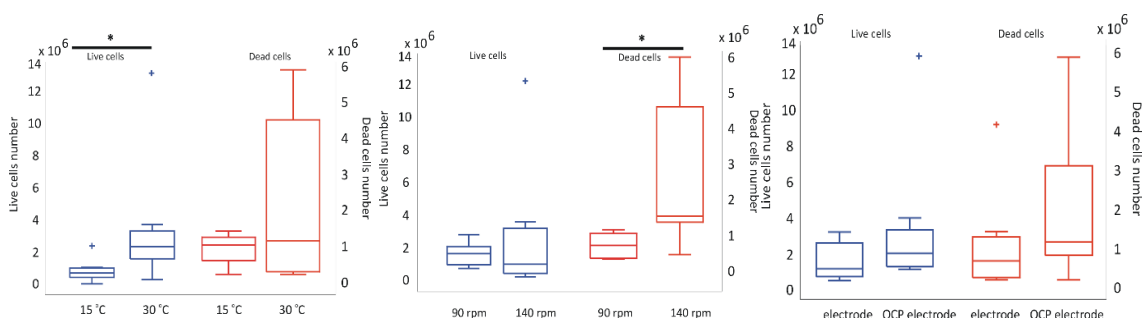


Figure 6.11: Effect of operating conditions in live and dead cells number. Left: Box plots of temperature conditions ($n=8$). Centre: Box plots of agitation rates ($n=8$). Right: Box plots of OCP treatment ($n=8$). The star (*) indicates the significant pairwise difference ($p < 0.05$).

The operating conditions were analysed individually, though the effect of possible interactions should be also evaluated. In this study two way interaction plots were used to analyse any possible effect, however due to the insufficient sample size and the non-normality and non-homogeneity of the variances only assumptions could be made (Appendices D3-D5). In order to evaluate whether there is a real interaction between factors, more data are needed. Same principle applies for three way interaction analyses.

6.4.1 *Shewanella Oneidensis* MR-1 cultivation on PolyHipe anodes and reactor performance

The use of different MFC configurations (Liu and Logan, 2004), electrode materials (HaoYu *et al.*, 2007; Jiang and Li, 2009) and operational conditions (Ieropoulos *et al.*, 2010) has been proven to improve electric current production and bacterial adhesion. One way to achieve a higher electric current production is to enhance the contact between bacteria and electrodes. More attached bacteria should enable more electron transfer (Logan, 2005). One of the most common electrode materials is carbon cloth which is very often expensive and impractical for large scale applications. Figure 6.12 shows the electrochemical analyses of a new electrode material made of conductive polymers (polyHIPEs). The PolyHipe electrodes were previously immobilized with *Shewanella Oneidensis* MR-1 cells at OCP to enhance the anode start up and improve bacteria adhesion. Results showed that the polyHIPE electrodes slightly increased the electric current production after 5 days of operation (Figure 6.12A). This increase might be caused by the electron transfer mechanisms used by the bacteria for using the lactate.

However, after 10 days the electric current of both MFCs decreased over time and stayed near zero without any obvious electroactive activity occurred. The addition of lactate on 15th day did not enhance the electric current production.

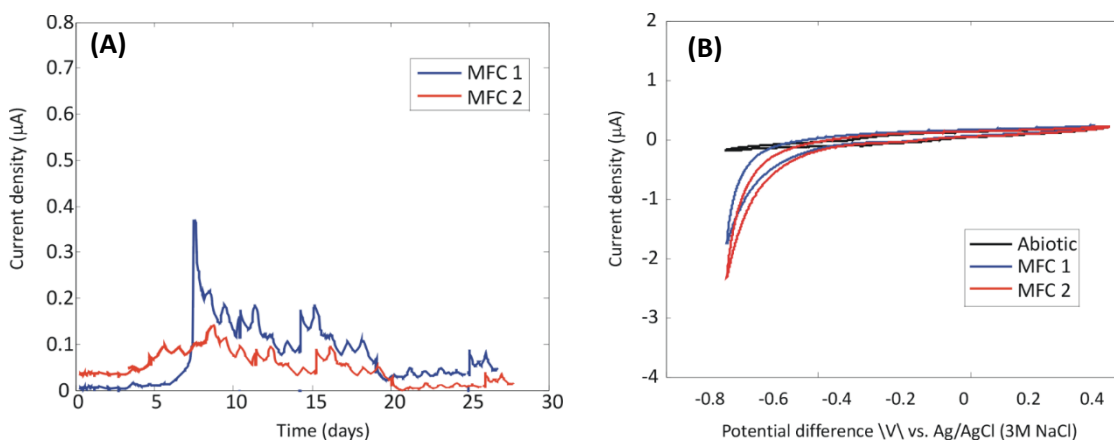


Figure 6.12: (A) Amperometric detection of PolyHIPE electrodes at +0.2 V (vs. Ag/AgCl). (B) Cyclic voltammetry of PolyHIPE electrode at a scan rate of 0.001 V/s.

To further study this effect, cyclic voltammetry was used to identify the state of the bacteria. Figure 6.12B shows the cyclic voltammetry scans of the polyHIPE electrodes in relation with an Abiotic reactor. No peaks were identified and all three scans were of similar activity suggesting that bacteria could probably be inactive. In order to confirm this, SEM and confocal microscopy analyses were used. Figure 6.13 shows the SEM and confocal microscopy images to describe the conditions of the bacterial cells. The SEM images showed very low bacteria growth scattered around the polyHIPE. Due to the structure of the material, confocal microscopy did not show clear results. However, the majority of the visible cells were dead confirming the low electric current. The surface of the electrode was covered with 15% of the total bacteria cells number and 85% with dead bacteria. However, when a depth analysis was performed, 95% of dead bacteria were count. The reason bacteria within the electrode are dead is believed to be because of the characteristics of the polyHIPE. The polyHIPE is highly hydrophilic by nature. Since it is used in an aqueous environment, then it is always fully saturated. When substrate is added in the reactor, it cannot be absorbed by the polyHIPE resulting to the starvation of the cells followed by death and detachment.

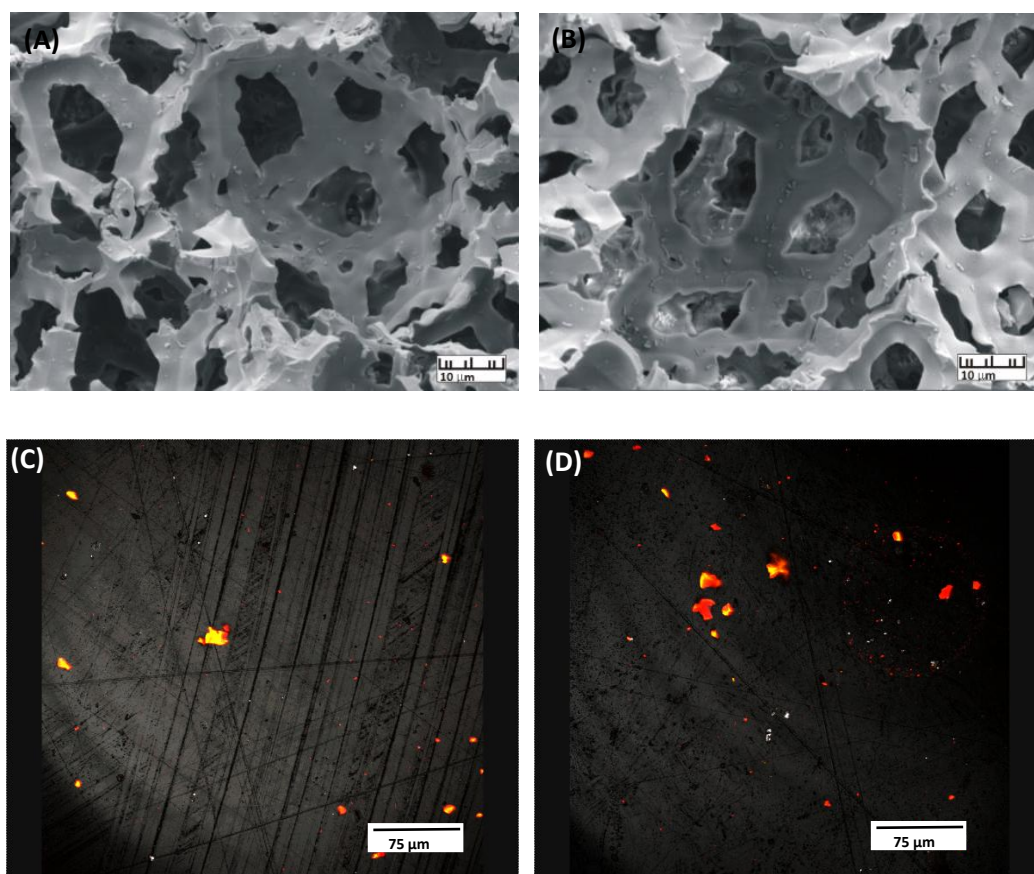


Figure 6.13: Scanning electron microscopy on PolyHIPE electrodes; (A) MFC 1 and (B) MFC 2. Confocal microscopy on PolyHIPE electrodes: (C) MFC 1 and (D) MFC 2.

Even that the polyHIPE material did not seem to be suitable as an electrode material in MFCs due to its hydrophilic nature, it seems to be suitable for accommodating biofilm growth in solid/dry state and can be used for other applications such as tissue engineering and bioprocess (Akay, 2004). The hydrophilic polyHIPE polymers can be used in solid state fermentation cultures so that the moisture from air (gases as substrates) can be adsorbed by the support and utilized by the bacteria. Other applications consist of plant/cell/bacteria growth medium, as an ion exchange medium or bioremediation. Due to their high water absorbing capability and ability to release functional groups, they can be used in agriculture, horticulture, landscaping, reforestation and land reclamation and plant transportation/storage. The use polyHIPEs in the field can reduce the irrigation systems frequency, soil aeration etc. (Akay *et al.*, 2010). PolyHIPEs can also be used as a three dimensional connective support for plant cells, mammalian cells or bacteria. Their hydrophilic nature ensures nutrient and cell penetration into the support system without any pressure application which can decrease process costs intensification (Akay *et al.*, 2010).

6.4.2 Effect of electrode pre-treatment on cathode performance and chemical production

Figure 6.14 shows the electric current during saturated conditions of O_2 in the cathode of OCP (Figure 6.14 (A)) and CCP (Figure 6.14 (B)) biofilm reactors. All reactors were potentiostatically controlled at a reductive value of -0.800 V vs. (Ag/AgCl) to enhance the cathode start-up. In Figure 6.14 (A) *Shewanella Oneidensis* MR-1 cells were inoculated after 10 minutes from the start-up of the reactors where in Figure 6.14 (B) the biofilm was already developed prior its use in the MES reactors. Both systems; CCP and OCP, showed a decrease in current density when oxygen was used as a substrate. This suggests the ability of the biofilm to perform electron transfer from the electrode to the bacterial cell followed by the final electron acceptor (i.e. oxygen). All reactors were assumed steady state when the current density remained stable for over 1.5 days followed by the addition of CO_2 as the sole carbon in the system. A rapid increase in the current density was obtained suggesting the effect of CO_2 in the reactors' environment probably due to pH changes. The pH of the reactors was set at 7.4 during biofilm development where after the addition of CO_2 the pH moved to 6.9. However, when OCP biofilms were used, the current density seemed to decrease again after 2 days of operation. The fact that current density was produced in both environments; oxygenated and anaerobic (with CO_2), suggests the ability of the biofilms to adapt with different substrates (or electron acceptor) or to change from one substrate to another. On the other hand, the current density after the CO_2 addition did not recover or start decreasing for the CCP biofilm system suggesting that more stabilization time is needed. Studies have shown that biofilms obtained with OCP have been shown that are healthier than CCP which could eventually affect their performance after substrate changes (Larrosa-Guerrero *et al.*, 2010).

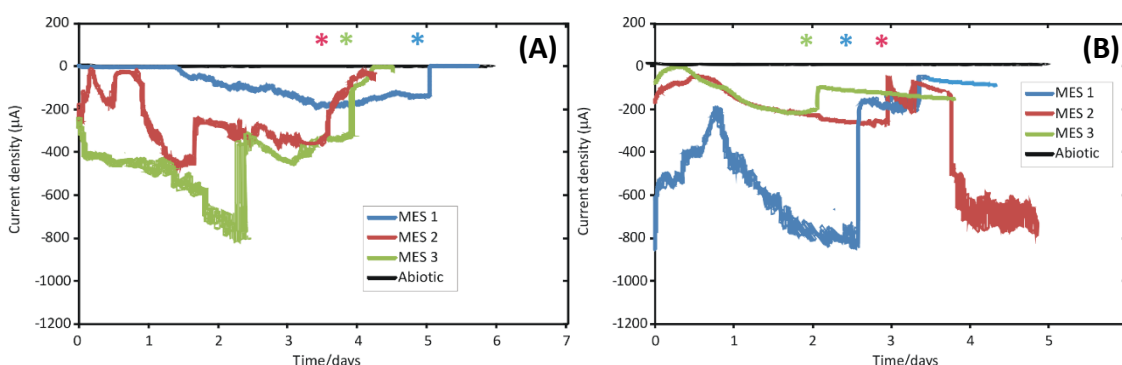


Figure 6.14: Current generation over time using *Shewanella Oneidensis* MR-1 and a polarization potential of -0.8 V (vs. Ag/AgCl) at 90 rpm and 30 °C at (A) CCP (n=3) and (B) OCP (n=3) systems. The colour coordinated stars indicate the addition of CO_2 .

CCP biofilm systems were observed with the presence of 0.2 – 1.5 days (mean = 0.9, STD=0.37, n=3) of lag-phase where OCP biofilm systems demonstrated an 11% faster adaptation (0.5 – 1 days, mean = 0.8, STD=0.08, n=3). There was no major difference observed on the lag phase time suggesting that both systems would operate similarly. However, CCP biofilm systems obtained an average of 1.65 times higher (mean = -467 μ A, STD= 306 μ A, n=3) electric current generation than OCP biofilm systems (mean= -410 μ A, STD= 338 μ A, n=3). CCP biofilm systems, apart from creating a biofilm on the electrode, they also consist of suspended bacterial cells in solution which contributes to the current density production. In contrast, OCP biofilm systems only operate with the amount of bacteria already grown on the electrode which is confirmed to a disadvantage over the CCP biofilm systems.

In addition, for understanding the effect that different biofilm development methods and substrates have on the MES reactors, CV scans were performed. Figure 6.15 presents the redox activity observed in CCP (Figure 6.15 (A)) and OCP (Figure 6.15 (B)) biofilm systems in the presence of oxygen and CO₂. Abiotic reactors were used as the blanks. The presence of a cathodic reaction was shown confirming the operation of a cathode biofilm. In Figure 6.15 (A), no peaks were identified for the abiotic reactors, however one peak at -0.405 V vs. (Ag/AgCl) was observed when bacteria were added and oxygen was used as the electron acceptor which falls within the potentials of riboflavin as reported in literature (Velasquez-Orta *et al.*, 2010). When CO₂ was added as the electron acceptor, two peaks were observed; -0.465 and -0.28 V vs. (Ag/AgCl). The first peak was explained as the riboflavin potential with a shift due to the pH changes mentioned before. The second peak agrees with the potentials obtained for the cell proteins produced by *Shewanella Oneidensis* MR-1 (Hartshorne *et al.*, 2007; Meitl *et al.*, 2009).

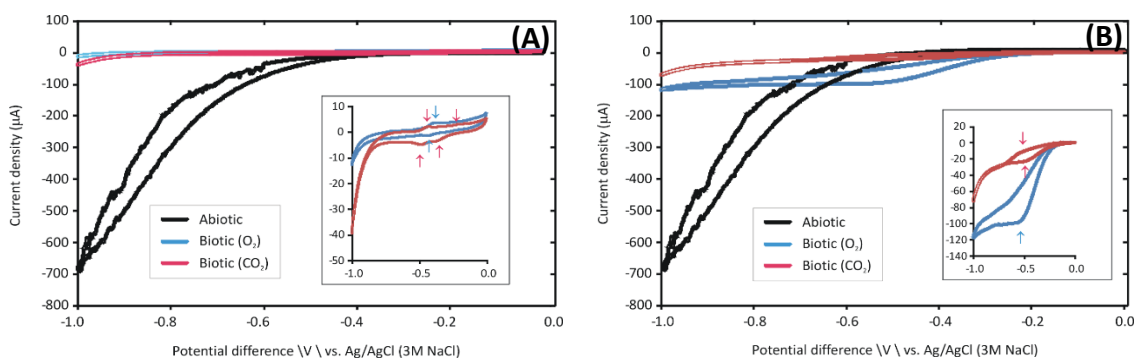


Figure 6.15: Redox activity associated with *Shewanella Oneidensis* MR-1 in (A) CCP and (B) OCP systems at different at 90 rpm and 30 °C. The colours coordinated arrows indicate the identified peaks at pH 7. The arrows indicate the identified peaks.

Similarly to Figure 6.15 (A), the abiotic reactor in Figure 6.15 (B) did not show any peaks compared to the biotic reactors. A reduction peak was observed when oxygen was used as the substrate at -0.56 V vs. (Ag/AgCl) which has not been yet related to any reduction compound. However, a peak with a midpoint at -0.485 V vs. (Ag/AgCl) came into agreement with the potential of riboflavin. The occurrence of peaks in the presence of oxygen and CO₂ as well as either CCP or OCP biofilm development, suggests that the bacterial cell is active. The fact that peaks were identified in either biofilm systems confirms that *Shewanella Oneidensis* MR-1 is capable of a diverse array of respiratory capabilities and its ability to thrive at redox interfaces as well as its plasticity for electron transfer (Heidelberg *et al.*, 2002).

Volatile fatty acid and total organic carbon analyses were used to determine chemical production in CCP and OCP biofilm systems after CO₂ addition. Figure 6.16 represents the chemical production in terms of carbon content within the produced compounds after 48 hours of operations. It should be noted that time 0 (seconds after adding CO₂), no organic carbon was identified in either systems. The CCP biofilm system shown to produced almost 100 mg/L (n=3, STD = 30.04) of organic carbon which the majority was translated into ethanol (mean=0.58 mM \approx 64.73 mg/L of organic carbon, STD = 64.73) at a 40% conversion rate. Acetic acid (mean=0.17 mM \approx 24.52 mg/L of organic carbon, STD = 1.87) and methanol (mean=0.11 mM \approx 4.23 mg/L of organic carbon STD = 3.60) were also present at 15.29% and 2.60% conversion rates, respectively. A value of 6.17 mg/L of organic carbon was unidentified supporting the fact that other chemical compounds are yet to be qualified and quantified. In contrast, in OCP biofilm system, 47.6 mg/L (n=3, STD = 25.32) of organic carbon was quantified however, none of this available carbon was qualified as product confirming the previous statement about other chemical compounds present in the system. According to the CV analyses, part of this unknown carbon should contain the riboflavin excreted from the bacterial cells.

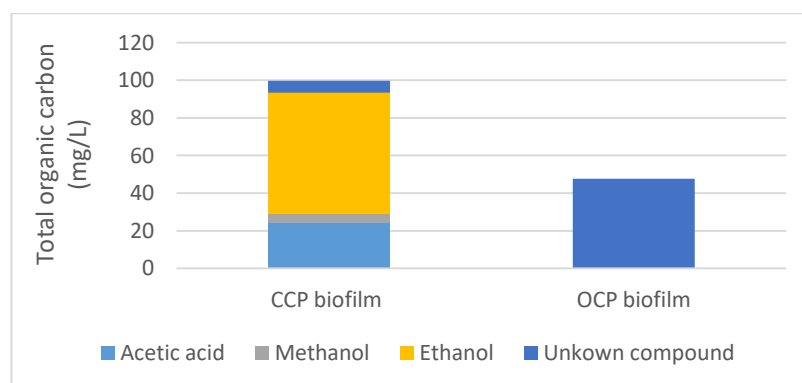


Figure 6.16: Total organic carbon production from CCP (n=3, STD = 30.04) and OCP (n=3, STD = 25.32) biofilm systems after 48 hours of operation using CO₂ as a reactant.

The chemical production results showed that the biofilm development method has an effect on the chemical production. This fact suggests that the growth of a biofilm using CCP and OCP conditions impacts differently to environmental changes. Acclimatizing an MES using CCP, allows the biofilm to reach steady state cell potential according to Babauta *et al.* (2012). On the other hand, the acclimatization of a biofilm under an OCP allows the potential to reach steady state by using natural redox processes. Thus OCP biofilms are more likely to respond better to different environments (i.e. different substrates, aerobic to anaerobic conditions etc.) compared to CCP biofilms. Consequently, CCP biofilm would stimulate more protein synthesis for adapting to environmental changes followed by an effect to the chemical production concentration compared to OCP biofilms explaining its lower chemical production. It has been previously demonstrated that the chemical production is not necessarily dependent on the reduction degree but to the metabolic pathways that are derived from (Kracke and Krömer, 2014). Having said this, it is very possible that CCP biofilm systems might select a different metabolic pathway than OCP biofilm systems when CO₂ is used as an electron acceptor in an anaerobic system. This theory also supports the fact of higher current density in OCP than CCP biofilm system but not directly explained as higher product yield. However, more extended research is needed to fully understand the metabolic pathways occurring in such systems.

A cell's metabolic pathway is a complex network of a series of enzyme catalysed reactions that precisely transform the given substrate to biomass or an end product (Xu *et al.*, 2009). This chemical transformation is central to cellular biochemical activities, which channel substrate metabolites into the production of energy, building blocks for biosynthesis, energy reserves, to eliminate waste products and for recycling reducing equivalents (Nolan *et al.*, 2006). In this line, to quantify the intracellular reaction steps, the occurred pathways and to infer the objectives of cellular metabolic systems, rational optimization strategies need to be developed for manipulating cell properties and thus productivity (Xu *et al.*, 2008; Xu *et al.*, 2009). There are several theoretical approaches to assign metabolic priorities through engineered cells and are mentioned in detail in Xu *et al.* (2008) and (Xu *et al.*, 2009). Using the multi-objective optimisation approach more information could be obtained to contribute to the optimization and understanding of the systems explored in this study.

The morphology of the bacteria and thus the biofilm was observed as homogeneous using SEM analysis as shown in Figure 6.17 (A) and (B). This suggested that no contamination was occurred during biofilm growth and development in either substrates used; oxygen or CO₂. In terms of electrode coverage, it was assessed that biofilms developed with OCP, had an

electrode coverage of 38.73% (STD=4.51, n=3), similar to the coverage achieved by CCP biofilms (mean=37.33, STD=6.43, n=3) suggesting that the method did not affect electrode coverage. For evaluating the life status of the biofilm and thus its operation in MES systems, LIVE/DEAD analysis was used (Figure 6.17 (C) and (D)). CCP biofilms showed to have more than 3 times less live bacteria count (mean= 6425866, STD=8529583, n=3) than the OCP biofilms (mean=20781210, STD=11501396, n=3). On the other hand, dead bacteria count was evaluated to be 22% lower for CCP biofilms (mean=8326198, STD=13035146, n=3) than OCP biofilms (mean=10691818, STD=11989422, n=3). This proposes that using the OCP biofilm development technique favours both live and dead bacterial cell count most probably as a results of environment change from OCP to closed circuit.

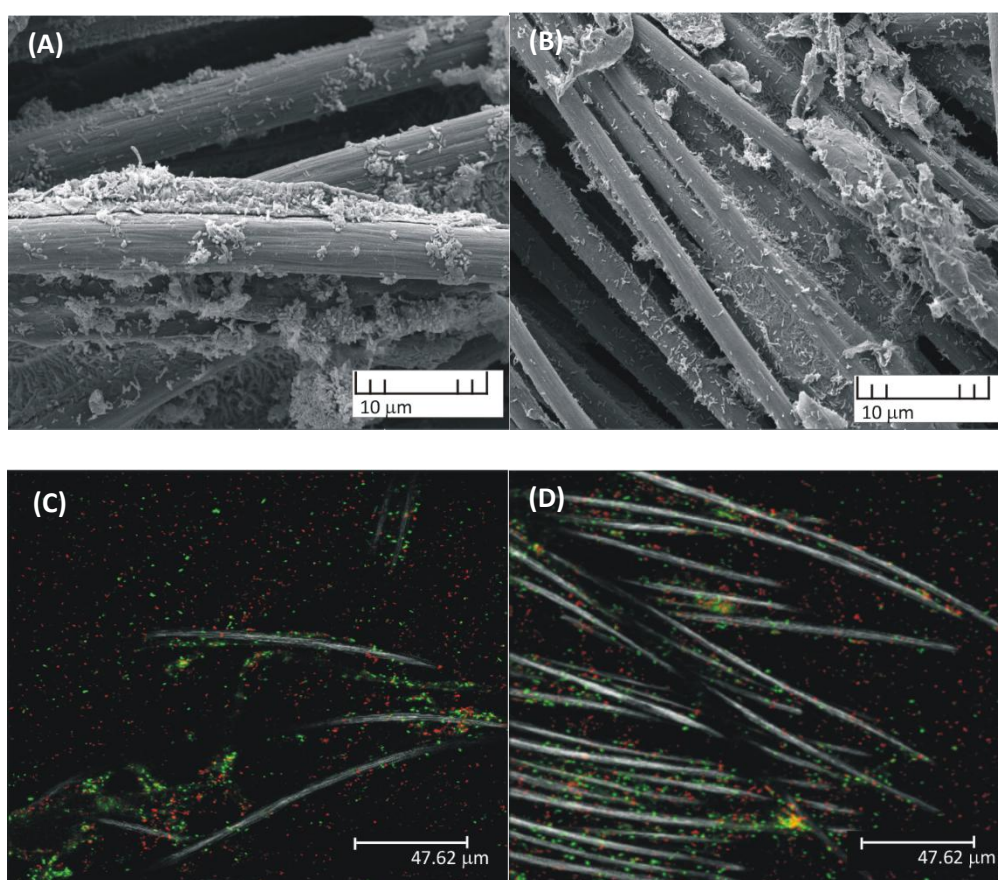


Figure 6.17: Scanning electron microscopy on biofilm development on cathode electrodes using; (A) CCP and (B) OCP. Confocal microscopy on biofilm development on cathodes using; (C) CCP and (D) OCP.

Amperometric detection and CV analysis did not show any critical difference on electric current production suggesting that both systems had similar number of active bacteria. Better biofilm development should show higher amount of live bacteria reflected to lower electric current production and thus higher chemical production. Here, it was observed that CCP biofilms produced almost twice more organic carbon than OCP biofilms confirming that CCP and OCP biofilms are using different metabolic pathways to reduce CO_2 into other compounds.

6.5 Conclusions

For developing a good quality biofilm that can result in high electric current generation and maximum electrode coverage with minimum lag phase and dead cells count, the temperature must be set at 30 °C. In order to prevent extensive dead cells count within the biofilm slow agitation levels have to be used at 90 rpm flow rates. However, for forming a biofilm with maximum live cells count high temperature is needed (30 °C). Finally, for achieving high electric current generation and short lag-phase, electrode pre-treatment is required at open circuit potential prior its use in bioelectrochemical systems. The use of already start-up biofilms might eliminate the time needed for the bacteria to move from the solution to the electrode in terms of anodic growth however when it comes to cathodic growth the biofilm development technique is insignificant. The use of PolyHipe material in BESs did not seem to be suitable as an anode electrode material; however, its capability of accommodating biofilm growth in solid/dry state materials was confirmed. CCP and OCP biofilm systems for cathode operation and chemical production showed that there was no major difference between the two different biofilm development methods in terms of current density and live/dead counts. However, chemical production was affected suggesting that the use of OCP or CCP triggers different metabolic pathways and thus different protein production that could contribute on product formation.

Chapter 7: Conclusions & Future work

7.1 Conclusion

This research was centred on investigating, economically and experimentally, the performance of MES for chemical production from CO₂ and. Its potential for scale up and industrial intake was evaluated economically in terms of production costs, investment costs, pay-back period and discounted cash flow rate of return. Experimentally, the use of a pure strain of *Shewanella Oneidensis* MR-1 was tested for bioproduction in MES by altering different electron transfer mechanisms and different polarization potentials. In addition, the performance of bioelectrochemical systems for energy and chemical production and how it was affected by different temperature, agitation and electrode treatments was assessed. In order to evaluate each of these aspects, four different studies were designed and performed. The following subsections describe the conclusions drawn from each of the studies.

7.1.1 Economic evaluation for acetic acid production using MES

It is highly important that new technologies are economically assessed to identify their capability and feasibility for industrial intake. An economic analysis of MES and AF for acetic acid production has been presented and assessed based on production and investment costs. The results from Chapter 3 showed that using CO₂ offers environmental benefits over chemical processes, but embeds high costs due to its thermodynamic stability. It was revealed that low production rates (100 t/y) from MES and AF caused expensive investment and production costs compared to conventional processes. The research findings of this study have provided evidence that MES and AF cannot be used as stand-alone processes with the current production rates; however, an integration between them can give complementary advantages on economics by reducing production costs (0.24 £/kg), avoiding CO₂ emission in the environment, and increasing overall process efficiency performance by widening the production rates (200 t/y). The performance of additional economic evaluations on MES as a stand-alone process exposed that the production of formic and propionic acids are highly profitable projects. This suggested that MES, as a technology, should currently focus on high value products of small demand.

7.1.2 Investigation of bioproduction

Experiments conducted in this thesis used biofilm and mediator driven systems to study their effect on bioproduction. *Shewanella Oneidensis* MR-1 was used as the biocatalyst; and CO₂ as the sole carbon source in Chapter 4. When Mediated Systems were used, higher electric current densities (max. 11 μA) were produced than Biofilm Systems (max. 3 μA). This indicated that the use of exogenous mediator affects the electric density output. The main product formed in both systems was acetate (0.03-0.66 mmol) along with traces of formic, propionic and butyric acids. Unknown carbon was also present in solution suggesting the formation of other products to be yet identified. Gas analyses also showed hydrocarbons presence in the reactor's headspace for the mediated systems only confirming that the use of mediators improves electron transfer and thus product formation. These outcomes suggest the capability of *Shewanella Oneidensis* MR-1 to biosynthesize hydrocarbons from CO₂.

Biofilm driven systems were utilised to further investigate bioproduction using different polarization potentials. Biofilm driven systems were chosen upon mediated systems to eliminate the potential of any other product present in the reactor to act as electron acceptors. The results from Chapter 5 showed formic (2.74-39 μmol), acetic (9.80-53.86 μmol), propionic (204.11-270.9 μmol) and valeric (383.8 μmol) acids production at the micro range scale during different polarization. However, no correlation was identified regarding polarization potentials and product formation. These results along with low CCE (14-77%) and energy efficiency (0.0001-0.63%) suggested a possible biochemical process occurred within the biocatalyst's proteins rather than respiration. The use of extracted proteins from *Shewanella Oneidensis* MR-1 showed a trend of increasing product formation with increased protein amount suggesting that CO₂ and applied polarization potentials have an effect on their chemical composition and thus reflected in as chemical production. These findings suggest the possibility of *Shewanella Oneidensis* MR-1 to biosynthesize hydrocarbons from CO₂ using proteins as biocatalysts. This study was also used to develop a hypothesized pathway.

7.1.3 Investigation of factors affecting energy and chemical production

Temperature, agitation and electrode treatments were assessed as factors affecting energy and chemical production. Initially, Chapter 6 describes the energy production investigation where it was found that temperature must set at 30 °C for achieving maximum electric current generation, live cells number and electrode coverage (biofilm). Furthermore, slow agitation levels are needed to prevent extensive dead cells number. Using, OCP biofilms showed to offer additional advantages such as shorter lag phase. Regarding to cathodic growth, OCP and CCP

biofilm systems were operating similarly in terms of electric current production, lag-phase period and live/dead cells count. However, chemical production was affected suggesting that the use of OCP or CCP triggers different metabolic pathways and thus different protein production that could contribute to product formation.

7.2 Summary

The findings presented in this study revealed the drawbacks of MES to scale up and offer an understanding on actions to take place for the optimization of such a technology to become market compatible. Moreover, experimental studies confirmed the feasibility of *Shewanella Oneidensis MR-1* for bioproduction using CO₂ through biochemical processing (i.e. proteins). Furthermore, electric current, bacterial cell life status, electrode coverage and lag-phase period were affected by agitation, temperature and different biofilm development methods (i.e. OCP and CCP) in anodic processes but not in cathodic process. In contrast, OCP and CCP biofilm methods affect chemical production due to the use of different metabolic pathways for electron transfer.

7.3 Future research

- The evaluation of the economic aspects of MES was assessed in terms of production and investment costs, pay-back period and discounted cash flow rate of return. In this study, variables based on the main reaction only were considered thus further research and evaluations should be done on an MES plant including total variable costs. In addition, detailed analysis on fixed costs should be performed to identify limitations and reduce operating costs.
- The understanding and optimization of bioproduction from CO₂ using *Shewanella Oneidensis MR-1* will continue to be a subject of development. However, this should be directed towards gene modification, molecular microbiology and synthetic biology fields to obtain a deep understanding of the metabolic pathway used and the proteins involved.
- The effect of different parameters on energy and chemical production was analysed individually using *Shewanella Oneidensis MR-1*, though the effect of possible interactions should also be evaluated. In this study, two way-interaction plots were

used to analyse possible effect, however, due to the insufficient sample size, the non-normality and non-homogeneity of the variances only assumptions could be made. Thus strictly designed experiments should be performed to add on to the conclusions of this thesis and also to verify assumptions that were drawn. In addition, theoretical approaches should be used, such as the multi- objective optimisation tool, to assign metabolic priorities through engineered cells for further understanding and optimizing this systems.

- To further investigate energy and chemical production, other biofilm development techniques should be used apart from OCP and CCP biofilms. 3D electrodes could be used to increase the electrode surface area and thus increase the number of cells and consequently the rate of reactions; either for energy or chemical production(Jourdin *et al.*, 2015a). Moreover, the use of glue-like materials is essential to control bacterial cell number for statistical tests based on increasing bacterial cell concentration.

References

- Abboud, R., Popa, R., Souza-Egipsy, V., Giometti, C.S., Tollaksen, S., Mosher, J.J., Findlay, R.H. and Neilson, K.H. (2005) 'Low-temperature growth of *Shewanella oneidensis* MR-1', *Applied and Environmental Microbiology*, 71(2), pp. 811-816.
- Aelterman, P., Freguia, S., Keller, J., Verstraete, W. and Rabaey, K. (2008) 'The anode potential regulates bacterial activity in microbial fuel cells', *Applied Microbiology and Biotechnology*, 78(3), pp. 409-418.
- Aelterman, P., Rabaey, K., Pham, H.T., Boon, N. and Verstraete, W. (2006) 'Continuous electricity generation at high voltages and currents using stacked microbial fuel cells', *Environmental Science and Technology*, 40(10), pp. 3388-3394.
- Akay, G. (2004) 'Method and apparatus for processing flowable material and polyhipe polymers'. Google Patents. Available at: <http://www.google.com/patents/WO2004004880A3?cl=en>.
- Akay, G., Noor, Z.Z., Calkan, O.F., Ndlovu, T.M. and Burke, D.R. (2010) 'Process for preparing a functionalised polyHIPE polymer'. Google Patents. Available at: <http://www.google.ch/patents/US7820729>.
- Albertas Malinauskas (2008) 'Electrochemical study of riboflavin adsorbed on a graphite electrode', *Chemija*, 19(2), pp. 1–3
- Amiri-Jami, M. and Griffiths, M.W. (2010) 'Recombinant production of omega-3 fatty acids in *Escherichia coli* using a gene cluster isolated from *Shewanella baltica* MAC1', *Journal of Applied Microbiology*, 109(6), pp. 1897-1905.
- Amiri-Jami, M., Lapointe, G. and Griffiths, M.W. (2014) 'Engineering of EPA/DHA omega-3 fatty acid production by *Lactococcus lactis* subsp. *cremoris* MG1363', *Applied Microbiology and Biotechnology*, 98(7), pp. 3071-3080.
- Anastas, P. and Warner, J. (1998) 'Green Chemistry: Theory and Practice', in Oxford University Press: New York.
- Angenent, L.T. and Rosenbaum, M.A. (2013) 'Microbial electrocatalysis to guide biofuel and biochemical bioprocessing', *Biofuels*, 4(2), pp. 131-134.
- APIC (2015) *Acetyls Chains - World Market Overview*.
- Arthur, N. (2014) *Wind power is cheapest energy, EU analysis finds* (Accessed: 09/09/2015).
- ATCC (2015) *The Global Bioresource Centre* (Accessed: 29/11/2015).
- Aulenta, F., Reale, P., Canosa, A., Rossetti, S., Panero, S. and Majone, M. (2010) 'Characterization of an electro-active biocathode capable of dechlorinating trichloroethene and cis-dichloroethene to ethene', *Biosensors and Bioelectronics*, 25(7), pp. 1796-1802.
- Aulenta, F., Reale, P., Catervi, A., Panero, S. and Majone, M. (2008) 'Kinetics of trichloroethene dechlorination and methane formation by a mixed anaerobic culture in a bio-electrochemical system', *Electrochimica Acta*, 53(16), pp. 5300-5305.
- Babauta, J., Renslow, R., Lewandowski, Z. and Beyenal, H. (2012) 'Electrochemically active biofilms: Facts and fiction. A review', *Biofouling*, 28(8), pp. 789-812.
- Bard, A.J. (1985) *Standard potentials in aqueous solution*.
- Bard, A.J. and Faulkner, L.R. (2001) *Electrochemical Methods: fundamentals and applications*. John Wiley & Sons, Inc.
- Battle-Vilanova, P., Puig, S., Gonzalez-Olmos, R., Vilajeliu-Pons, A., Balaguer, M.D. and Colprim, J. (2015) 'Deciphering the electron transfer mechanisms for biogas upgrading to biomethane within a mixed culture biocathode', *RSC Advances*, 5(64), pp. 52243-52251.
- Behera, M., Jana, P.S. and Ghangrekar, M.M. (2010) 'Performance evaluation of low cost microbial fuel cell fabricated using earthen pot with biotic and abiotic cathode', *Bioresource Technology*, 101(4), pp. 1183-1189.

- Bennetto, H.P., Stirling, J.L., Tanaka, K. and Vega, C.A. (1983) 'Anodic reactions in microbial fuel cells', *Biotechnology and Bioengineering*, 25(2), pp. 559-568.
- Blanchet, E., Duquenne, F., Rafrafi, Y., Etcheverry, L., Erable, B. and Bergel, A. (2015) 'Importance of the hydrogen route in up-scaling electrosynthesis for microbial CO₂ reduction', *Energy and Environmental Science*, 8(12), pp. 3731-3744.
- BMI Research (2014) *Saudi Arabia's LPG demand surging as ethane supply strains* (Accessed: 09/09/2015).
- Bond, D.R. and Lovley, D.R. (2003) 'Electricity production by *Geobacter sulfurreducens* attached to electrodes', *Applied and Environmental Microbiology*, 69(3), pp. 1548-1555.
- Bounaceur, R., Lape, N., Roizard, D., Vallieres, C. and Favre, E. (2006) 'Membrane processes for post-combustion carbon dioxide capture: A parametric study', *Energy*, 31(14), pp. 2556-2570.
- BP (2014) 'BP Energy Outlook 2035 shows global energy demand growth slowing, despite increases driven by emerging economies' *Energy Outlook 2035*. bp.com/en/global/corporate/press/press-releases/energy-outlook-2035.html.
- Bretschger, O., Obratsova, A., Sturm, C.A., In, S.C., Gorby, Y.A., Reed, S.B., Culley, D.E., Reardon, C.L., Barua, S., Romine, M.F., Zhou, J., Beliaev, A.S., Bouhenni, R., Saffarini, D., Mansfeld, F., Kim, B.H., Fredrickson, J.K. and Nealson, K.H. (2007) 'Current production and metal oxide reduction by *Shewanella oneidensis* MR-1 wild type and mutants', *Applied and Environmental Microbiology*, 73(21), pp. 7003-7012.
- Brunetti, A., Scura, F., Barbieri, G. and Drioli, E. (2010) 'Membrane technologies for CO₂ separation', *Journal of Membrane Science*, 359(1-2), pp. 115-125.
- Busalmen, J.P. and De Sánchez, S.R. (2005) 'Electrochemical polarization-induced changes in the growth of individual cells and biofilms of *Pseudomonas fluorescens* (ATCC 17552)', *Applied and Environmental Microbiology*, 71(10), pp. 6235-6240.
- Cao, X., Huang, X., Liang, P., Boon, N., Fan, M., Zhang, L. and Zhang, X. (2009a) 'A completely anoxic microbial fuel cell using a photo-biocathode for cathodic carbon dioxide reduction', *Energy and Environmental Science*, 2(5), pp. 498-501.
- Cao, X., Huang, X., Liang, P., Xiao, K., Zhou, Y., Zhang, X. and Logan, B.E. (2009b) 'A new method for water desalination using microbial desalination cells', *Environmental Science and Technology*, 43(18), pp. 7148-7152.
- CCC (2015) *The Fifth Carbon Budget - The next step towards a low-carbon economy*. www.theccc.org.uk/publication/the-fifth-carbon-budget-the-next-step-towards-a-low-carbon-economy/.
- CEAE (2014) *Redox half reaction reductions potentials and free energies* (Accessed: 20/07/2016).
- Centi, G. and Perathoner, S. (2009) 'Opportunities and prospects in the chemical recycling of carbon dioxide to fuels', *Catalysis Today*, 148(3-4), pp. 191-205.
- Chae, K.J., Choi, M., Ajayi, F.F., Park, W., Chang, I.S. and Kim, I.S. (2008) 'Mass transport through a proton exchange membrane (Nafion) in microbial fuel cells', *Energy and Fuels*, 22(1), pp. 169-176.
- Chandrasekaran, M. (2012) *Valorization of Food processing By-products*. CRC Press. pp 559-588.
- Chang, I.S., Moon, H., Bretschger, O., Jang, J.K., Park, H.I., Nealson, K.H. and Kim, B.H. (2006) 'Electrochemically active bacteria (EAB) and mediator-less microbial fuel cells', *Journal of Microbiology and Biotechnology*, 16(2), pp. 163-177.
- Chen, G.W., Choi, S.J., Lee, T.H., Lee, G.Y., Cha, J.H. and Kim, C.W. (2008) 'Application of biocathode in microbial fuel cells: Cell performance and microbial community', *Applied Microbiology and Biotechnology*, 79(3), pp. 379-388.
- Cheng, K.Y., Ho, G. and Cord-Ruwisch, R. (2010) 'Cathodic oxygen reduction', *Environmental Science and Technology*, 44(1), pp. 518-525.

- Cheng, S., Xing, D., Call, D.F. and Logan, B.E. (2009) 'Direct biological conversion of electrical current into methane by electromethanogenesis', *Environmental Science and Technology*, 43(10), pp. 3953-3958.
- Cheng, W. and Kung, H.H. (1994) *Methanol production and use*. New York: Marcel Dekker, Inc. p. 176-184.
- Chenier, P.J. (2002) *Survey of Industrial Chemistry*. 3rd edn. Springer US, p. 151.
- Cheung, H., Tanke, R.S. and Torrence, G.P. (2000) 'Acetic Acid', in *Ullmann's Encyclopedia of Industrial Chemistry*. Wiley-VCH Verlag GmbH & Co. KGaA.
- Cho, E.J. and Ellington, A.D. (2007) 'Optimization of the biological component of a bioelectrochemical cell', *Bioelectrochemistry*, 70(1), pp. 165-172.
- Choi, O. and Sang, B.I. (2016) 'Extracellular electron transfer from cathode to microbes: Application for biofuel production', *Biotechnology for Biofuels*.
- Clauwaert, P., Desloover, J., Shea, C., Nerenberg, R., Boon, N. and Verstraete, W. (2009) 'Enhanced nitrogen removal in bio-electrochemical systems by pH control', *Biotechnology Letters*, 31(10), pp. 1537-1543.
- Clauwaert, P., Rabaey, K., Aelterman, P., De Schampelaire, L., Pham, T.H., Boeckx, P., Boon, N. and Verstraete, W. (2007a) 'Biological denitrification in microbial fuel cells', *Environmental Science and Technology*, 41(9), pp. 3354-3360.
- Clauwaert, P., Tolêdo, R., van der Ha, D., Crab, R., Verstraete, W., Hu, H., Udert, K.M. and Rabaey, K. 57 (2008) 'Combining biocatalyzed electrolysis with anaerobic digestion' *Water Science and Technology*. pp. 575-579. Available at: <http://www.scopus.com/inward/record.url?eid=2-s2.0-42549151516&partnerID=40&md5=32e6a53aa964a355fcf770e232e6fee8>.
- Clauwaert, P., Van Der Ha, D., Boon, N., Verbeken, K., Verhaege, M., Rabaey, K. and Verstraete, W. (2007b) 'Open air biocathode enables effective electricity generation with microbial fuel cells', *Environmental Science and Technology*, 41(21), pp. 7564-7569.
- Cournet, A., Délia, M.L., Bergel, A., Roques, C. and Bergé, M. (2010) 'Electrochemical reduction of oxygen catalyzed by a wide range of bacteria including Gram-positive', *Electrochemistry Communications*, 12(4), pp. 505-508.
- CSI market (2016) 'Chemical manufacturing sector'. 01/09/2016. http://csimarket.com/Industry/industry_ManagementEffectiveness.php?ind=101.
- Davey, M.E. and O'Toole, G.A. (2000) 'Microbial Biofilms: from Ecology to Molecular Genetics', *Microbiology and Molecular Biology Reviews*, 64(4), pp. 847-867.
- DECC (2015) *Energy and emissions projections and DECC update-Autumn 2015* (Accessed: 05/02/2016).
- Ditzig, J., Liu, H. and Logan, B.E. (2007) 'Production of hydrogen from domestic wastewater using a bioelectrochemically assisted microbial reactor (BEAMR)', *International Journal of Hydrogen Energy*, 32(13), pp. 2296-2304.
- Du, Z., Li, H. and Gu, T. (2007) 'A state of the art review on microbial fuel cells: A promising technology for wastewater treatment and bioenergy', *Biotechnology Advances*, 25(5), pp. 464-482.
- Duan, J., Higuchi, M., Krishna, R., Kiyonaga, T., Tsutsumi, Y., Sato, Y., Kubota, Y., Takata, M. and Kitagawa, S. (2014) 'High CO₂/N₂/O₂/CO separation in a chemically robust porous coordination polymer with low binding energy', *Chemical Science*, 5(2), pp. 660-666.
- Dumas, C., Basseguy, R. and Bergel, A. (2008) 'Microbial electrocatalysis with *Geobacter sulfurreducens* biofilm on stainless steel cathodes', *Electrochimica Acta*, 53(5), pp. 2494-2500.
- Eggleston, C.M., Vörös, J., Shi, L., Lower, B.H., Droubay, T.C. and Colberg, P.J.S. (2008) 'Binding and direct electrochemistry of OmcA, an outer-membrane cytochrome from an iron reducing bacterium, with oxide electrodes: A candidate biofuel cell system', *Inorganica Chimica Acta*, 361(3), pp. 769-777.

- El-Naggar, M.Y., Wanger, G., Leung, K.M., Yuzvinsky, T.D., Southam, G., Yang, J., Lau, W.M., Nealson, K.H. and Gorby, Y.A. (2010) 'Electrical transport along bacterial nanowires from *Shewanella oneidensis* MR-1', *Proceedings of the National Academy of Sciences of the United States of America*, 107(42), pp. 18127-18131.
- ElMekawy, A., Hegab, H.M., Mohanakrishna, G., Elbaz, A.F., Bulut, M. and Pant, D. (2016) 'Technological advances in CO₂ conversion electro-biorefinery: A step toward commercialization', *Bioresource Technology*, 215, pp. 357-370.
- Erable, B., Vandecandelaere, I., Faimali, M., Delia, M.L., Etcheverry, L., Vandamme, P. and Bergel, A. (2010) 'Marine aerobic biofilm as biocathode catalyst', *Bioelectrochemistry*, 78(1), pp. 51-56.
- European Wind Energy Association (2014) *Onshore wind cheaper than coal, gas and nuclear, according to European Commission report* (Accessed: 16/02/2015).
- Feng, Y., Lee, H., Wang, X. and Liu, Y. (2009) *Asia-Pacific Power and Energy Engineering Conference, APPEEC*. Available at: <http://www.scopus.com/inward/record.url?eid=2-s2.0-84869985170&partnerID=40&md5=9d854690d0f479db343a3a6d14260423>.
- Fetzner, S. and Lings, F. (1994) 'Bacterial dehalogenases: Biochemistry, genetics, and biotechnological applications', *Microbiological Reviews*, 58(4), pp. 641-685.
- Fredrickson, J.K., Romine, M.F., Beliaev, A.S., Auchtung, J.M., Driscoll, M.E., Gardner, T.S., Nealson, K.H., Osterman, A.L., Pinchuk, G., Reed, J.L., Rodionov, D.A., Rodrigues, J.L.M., Saffarini, D.A., Serres, M.H., Spormann, A.M., Zhulin, I.B. and Tiedje, J.M. (2008) 'Towards environmental systems biology of *Shewanella*', *Nature Reviews Microbiology*, 6(8), pp. 592-603.
- Freguia, S., Rabaey, K., Yuan, Z. and Keller, J. (2008) 'Sequential anode-cathode configuration improves cathodic oxygen reduction and effluent quality of microbial fuel cells', *Water Research*, 42(6-7), pp. 1387-1396.
- Freguia, S., Tsujimura, S. and Kano, K. (2010) 'Electron transfer pathways in microbial oxygen biocathodes', *Electrochimica Acta*, 55(3), pp. 813-818.
- Ganigué, R., Puig, S., Batlle-Vilanova, P., Balaguer, M.D. and Colprim, J. (2015) 'Microbial electrosynthesis of butyrate from carbon dioxide', *Chemical Communications*, 51(15), pp. 3235-3238.
- GCO (2013) *Towards Sound Management of Chemicals* (Accessed: 27/11/2015).
- Gebrezgabher, S.A., Meuwissen, M.P.M., Prins, B.A.M. and Lansink, A.G.J.M.O. (2010) 'Economic analysis of anaerobic digestion—A case of Green power biogas plant in The Netherlands', *NJAS - Wageningen Journal of Life Sciences*, 57(2), pp. 109-115.
- Gerald, K. (2008) *Cell and Molecular Biology*. 5th edn. Wiley.
- Gorby, Y.A., Caccavo Jr, F. and Bolton Jr, H. (1998) 'Microbial reduction of cobalt(III)EDTA- in the presence and absence of manganese(IV) oxide', *Environmental Science and Technology*, 32(2), pp. 244-250.
- Gorby, Y.A., Yanina, S., McLean, J.S., Rosso, K.M., Moyses, D., Dohnalkova, A., Beveridge, T.J., Chang, I.S., Kim, B.H., Kim, K.S., Culley, D.E., Reed, S.B., Romine, M.F., Saffarini, D.A., Hill, E.A., Shi, L., Elias, D.A., Kennedy, D.W., Pinchuk, G., Watanabe, K., Ishii, S., Logan, B., Nealson, K.H. and Fredrickson, J.K. (2006) 'Electrically conductive bacterial nanowires produced by *Shewanella oneidensis* strain MR-1 and other microorganisms', *Proceedings of the National Academy of Sciences of the United States of America*, 103(30), pp. 11358-11363.
- Gregory, K.B., Bond, D.R. and Lovley, D.R. (2004) 'Graphite electrodes as electron donors for anaerobic respiration', *Environmental Microbiology*, 6(6), pp. 596-604.
- Gregory, K.B. and Lovley, D.R. (2005) 'Remediation and recovery of uranium from contaminated subsurface environments with electrodes', *Environmental Science and Technology*, 39(22), pp. 8943-8947.
- HaoYu, E., Cheng, S., Scott, K. and Logan, B. (2007) 'Microbial fuel cell performance with non-Pt cathode catalysts', *Journal of Power Sources*, 171(2), pp. 275-281.

- Harnisch, F., Rosa, L.F.M., Kracke, F., Viridis, B. and Krömer, J.O. (2015) 'Electrifying White Biotechnology: Engineering and Economic Potential of Electricity-Driven Bio-Production', *ChemSusChem*, 8(5), pp. 758-766.
- Harnisch, F., Wirth, S. and Schröder, U. (2009) 'Effects of substrate and metabolite crossover on the cathodic oxygen reduction reaction in microbial fuel cells: Platinum vs. iron(II) phthalocyanine based electrodes', *Electrochemistry Communications*, 11(11), pp. 2253-2256.
- Hartshorne, R.S., Jepson, B.N., Clarke, T.A., Field, S.J., Fredrickson, J., Zachara, J., Shi, L., Butt, J.N. and Richardson, D.J. (2007) 'Characterization of Shewanella oneidensis MtrC: A cell-surface decaheme cytochrome involved in respiratory electron transport to extracellular electron acceptors', *Journal of Biological Inorganic Chemistry*, 12(7), pp. 1083-1094.
- Hau, H.H. and Gralnick, J.A. 61 (2007a) 'Ecology and biotechnology of the genus Shewanella' *Annual Review of Microbiology*. pp. 237-258. Available at: <http://www.scopus.com/inward/record.url?eid=2-s2.0-34848889237&partnerID=40&md5=9dbca96aa82a9c782b90fc501479a2cf>.
- Hau, H.H. and Gralnick, J.A. 61 (2007b) 'Ecology and biotechnology of the genus Shewanella'. pp. 237-258. Available at: <http://www.scopus.com/inward/record.url?eid=2-s2.0-34848889237&partnerID=40&md5=9dbca96aa82a9c782b90fc501479a2cf>.
- Heidelberg, J.F., Paulsen, I.T., Nelson, K.E., Gaidos, E.J., Nelson, W.C., Read, T.D., Eisen, J.A., Seshadri, R., Ward, N., Methe, B., Clayton, R.A., Meyer, T., Tsapin, A., Scott, J., Beanan, M., Brinkac, L., Daugherty, S., DeBoy, R.T., Dodson, R.J., Durkin, A.S., Haft, D.H., Kolonay, J.F., Madupu, R., Peterson, J.D., Umayam, L.A., White, O., Wolf, A.M., Vamathevan, J., Weidman, J., Impraim, M., Lee, K., Berry, K., Lee, C., Mueller, J., Khouri, H., Gill, J., Utterback, T.R., McDonald, L.A., Feldblyum, T.V., Smith, H.O., Craig Venter, J., Neelson, K.H. and Fraser, C.M. (2002) 'Genome sequence of the dissimilatory metal ion-reducing bacterium Shewanella oneidensis', *Nature Biotechnology*, 20(11), pp. 1118-1123.
- Henstra, A.M. and Stams, A.J.M. (2011) 'Deep Conversion of Carbon Monoxide to Hydrogen and Formation of Acetate by the Anaerobic Thermophile Carboxydotherrmus hydrogenoformans', *International Journal of Microbiology*, 2011, p. 4.
- Holtmann, D., Hannabel, A. and Schrader, J. (2014) 'Microbial Electrosynthesis', *Encyclopedia of Applied Electrochemistry*, pp. 1268-1275.
- Hosea, C., Robin, S. and Paul, G. (2005) 'Acetic acid', in *Ullmann's Encyclopedia of Industrial Chemistry*. Weinheim: Wiley-VCH.
- Hromatka, O. and Ebner, H. (1949) 'Investigations on vinegar fermentation: Generator for vinegar fermentation and aeration procedures', *Enzymologia*, 13, p. 369.
- Huang, L. and Angelidaki, I. (2008) 'Effect of humic acids on electricity generation integrated with xylose degradation in microbial fuel cells', *Biotechnology and Bioengineering*, 100(3), pp. 413-422.
- Huang, L., Chen, J., Quan, X. and Yang, F. (2010) 'Enhancement of hexavalent chromium reduction and electricity production from a biocathode microbial fuel cell', *Bioprocess and Biosystems Engineering*, 33(8), pp. 937-945.
- Huang, L., Regan, J.M. and Quan, X. (2011) 'Electron transfer mechanisms, new applications, and performance of biocathode microbial fuel cells', *Bioresour. Technol.*, 102(1), pp. 316-323.
- ICIS (2016) *Energy*. www.icis.com/energy/.
- ICIS Chemical Business (2006) *Chemical profile: Formic acid* (Accessed: 11/11/2016).
- ICIS Chemical Business (2007) *Chemical profile: Propionic acid* (Accessed: 11/11/2016).
- Ieropoulos, I., Winfield, J. and Greenman, J. (2010) 'Effects of flow-rate, inoculum and time on the internal resistance of microbial fuel cells', *Bioresour. Technol.*, 101(10), pp. 3520-3525.

- IPCC (2007) *Summary for Policymakers. In: Climate Change 2007: The Physical Science Basis. Contribution of Working Group I to the Fourth Assessment Report of the Intergovernmental Panel on Climate Change.*
- Jacobson, K.S., Drew, D.M. and He, Z. (2011) 'Efficient salt removal in a continuously operated upflow microbial desalination cell with an air cathode', *Bioresource Technology*, 102(1), pp. 376-380.
- Jang, Y.S., Kim, B., Shin, J.H., Choi, Y.J., Choi, S., Song, C.W., Lee, J., Park, H.G. and Lee, S.Y. (2012) 'Bio-based production of C2-C6 platform chemicals', *Biotechnology and Bioengineering*, 109(10), pp. 2437-2459.
- Jenkins, R.W., Sargeant, L.A., Whiffin, F.M., Santomauro, F., Kaloudis, D., Mozzanega, P., Bannister, C.D., Baena, S. and Chuck, C.J. (2015) 'Cross-Metathesis of Microbial Oils for the Production of Advanced Biofuels and Chemicals', *ACS Sustainable Chemistry and Engineering*, 3(7), pp. 1526-1535.
- Jia, H., Azlina, H., Wei, S. and Ghasem, N. (2007) 'Clostridium aceticum—A potential organism in catalyzing carbon monoxide to acetic acid: Application of response surface methodology', *Enzyme and Microbial Technology*, 40(5), pp. 1234-1243.
- Jiang, D. and Li, B. 59 (2009) 'Novel electrode materials to enhance the bacterial adhesion and increase the power generation in microbial fuel cells (MFCs)' *Water Science and Technology* [Article]. pp. 557-563. Available at: <http://www.scopus.com/inward/record.url?eid=2-s2.0-62849104654&partnerID=40&md5=87cf0157abe8dde88780cda6f30d73b1>.
- Jiang, Y., Su, M., Zhang, Y., Zhan, G., Tao, Y. and Li, D. (2013) 'Bioelectrochemical systems for simultaneously production of methane and acetate from carbon dioxide at relatively high rate', *International Journal of Hydrogen Energy*, 38(8), pp. 3497-3502.
- Johannes, T., Simurdiak, M.R. and Zhao, H. (2006) *Biocatalysis*. (5 vols). New York: Taylor & Francis. pp. 101-110.
- Jones, J.H. (2000) 'The Cativa® Process for the Manufacture of Acetic Acid', *Platinum Metals Review*, 44(3), pp. 94-105.
- Jourdin, L., Freguia, S., Donose, B.C. and Keller, J. (2015a) 'Autotrophic hydrogen-producing biofilm growth sustained by a cathode as the sole electron and energy source', *Bioelectrochemistry*, 102, pp. 56-63.
- Jourdin, L., Freguia, S., Flexer, V. and Keller, J. (2016a) 'Bringing High-Rate, CO₂-Based Microbial Electrosynthesis Closer to Practical Implementation through Improved Electrode Design and Operating Conditions', *Environmental Science and Technology*, 50(4), pp. 1982-1989.
- Jourdin, L., Grieger, T., Monetti, J., Flexer, V., Freguia, S., Lu, Y., Chen, J., Romano, M., Wallace, G.G. and Keller, J. (2015b) 'High Acetic Acid Production Rate Obtained by Microbial Electrosynthesis from Carbon Dioxide', *Environmental Science and Technology*, 49(22), pp. 13566-13574.
- Jourdin, L., Lu, Y., Flexer, V., Keller, J. and Freguia, S. (2016b) 'Biologically Induced Hydrogen Production Drives High Rate/High Efficiency Microbial Electrosynthesis of Acetate from Carbon Dioxide', *ChemElectroChem*.
- Karpinets, T.V., Romine, M.F., Schmoyer, D.D., Kora, G.H., Syed, M.H., Leuze, M.R., Serres, M.H., Park, B.H., Samatova, N.F. and Uberbacher, E.C. (2010) 'Shewanella knowledgebase: integration of the experimental data and computational predictions suggests a biological role for transcription of intergenic regions', *Database : the journal of biological databases and curation*, 2010.
- Khunjar, W.O., Sahin, A., West, A.C., Chandran, K. and Banta, S. (2012) 'Biomass Production from Electricity Using Ammonia as an Electron Carrier in a Reverse Microbial Fuel Cell', *PLoS ONE*, 7(9).
- Kiefer, D.M. (2002) 'Soda Ash, Solvay Style', *Todays' Chemist at Work*, 11(2), pp. 87-88, 90 [Online]. Available at:

<http://pubs.acs.org/subscribe/journals/tcaw/11/i02/html/02chemchron.html>

(Accessed: 29/02/2016).

- Kim, B.H., Park, H.S., Kim, H.J., Kim, G.T., Chang, I.S., Lee, J. and Phung, N.T. (2004) 'Enrichment of microbial community generating electricity using a fuel-cell-type electrochemical cell', *Applied Microbiology and Biotechnology*, 63(6), pp. 672-681.
- Kim, H.J., Park, H.S., Hyun, M.S., Chang, I.S., Kim, M. and Kim, B.H. (2002) 'A mediator-less microbial fuel cell using a metal reducing bacterium, *Shewanella putrefaciens*', *Enzyme and Microbial Technology*, 30(2), pp. 145-152.
- Kim, J., Kim, H.S., Han, S., Lee, J.Y., Oh, J.E., Chung, S. and Park, H.D. (2013) 'Hydrodynamic effects on bacterial biofilm development in a microfluidic environment', *Lab on a Chip - Miniaturisation for Chemistry and Biology*, 13(10), pp. 1846-1849.
- Kim, J.R., Min, B. and Logan, B.E. (2005) 'Evaluation of procedures to acclimate a microbial fuel cell for electricity production', *Applied Microbiology and Biotechnology*, 68(1), pp. 23-30.
- Kim, J.R., Premier, G.C., Hawkes, F.R., Rodríguez, J., Dinsdale, R.M. and Guwy, A.J. (2010) 'Modular tubular microbial fuel cells for energy recovery during sucrose wastewater treatment at low organic loading rate', *Bioresource Technology*, 101(4), pp. 1190-1198.
- Kim, M., Youn, S.M., Shin, S.H., Jang, J.G., Han, S.H., Hyun, M.S., Gadd, G.M. and Kim, H.J. (2003) 'Practical field application of a novel BOD monitoring system', *Journal of Environmental Monitoring*, 5(4), pp. 640-643.
- Kouzuma, A., Meng, X.Y., Kimura, N., Hashimoto, K. and Watanabe, K. (2010) 'Disruption of the putative cell surface polysaccharide biosynthesis Gene SO3177 in *Shewanella oneidensis* MR-1 enhances adhesion to electrodes and current generation in microbial fuel cells', *Applied and Environmental Microbiology*, 76(13), pp. 4151-4157.
- Kracke, F. and Krömer, J.O. (2014) 'Identifying target processes for microbial electrosynthesis by elementary mode analysis', *BMC Bioinformatics*, 15(1).
- Kracke, F., Vassilev, I. and Krömer, J.O. (2015) 'Microbial electron transport and energy conservation - The foundation for optimizing bioelectrochemical systems', *Frontiers in Microbiology*, 6(JUN).
- Larrosa-Guerrero, A., Scott, K., Katuri, K.P., Godinez, C., Head, I.M. and Curtis, T. (2010) 'Open circuit versus closed circuit enrichment of anodic biofilms in MFC: Effect on performance and anodic communities', *Applied Microbiology and Biotechnology*, 87(5), pp. 1699-1713.
- Laurinavicius, V., Razumiene, J., Ramanavicius, A. and Ryabov, A.D. (2004) 'Wiring of PQQ-dehydrogenases', *Biosensors and Bioelectronics*, 20(6), pp. 1217-1222.
- Lefebvre, O., Tan, Z., Shen, Y. and Ng, H.Y. (2013) 'Optimization of a microbial fuel cell for wastewater treatment using recycled scrap metals as a cost-effective cathode material', *Bioresource Technology*, 127, pp. 158-164.
- Leisola, M., Jokela, J., Pastinen, O., Turunen, O. and Schoemaker, H. (2002) 'Industrial Use of Enzymes', in *Encyclopedia of Life Support Systems (EOLSS)*. Oxford, UK: EOLSS Publishers Co.
- Levy, P.F., Barnard, G.W. and Garcia-Martinez, D.V. (1981) 'Organic acid production from CO₂/H₂ and CO/H₂ by mixed-culture anaerobes', *Biotechnology and Bioengineering*, 23(10), pp. 2293-2306.
- Li, H., Opgenorth, P.H., Wernick, D.G., Rogers, S., Wu, T.Y., Higashide, W., Malati, P., Huo, Y.X., Cho, K.M. and Liao, J.C. (2012) *AIChE Annual Meeting, Conference Proceedings*.
- Li, Z., Rosenbaum, M.A., Venkataraman, A., Tam, T.K., Katz, E. and Angenent, L.T. (2011) 'Bacteria-based and logic gate: A decision-making and self-powered biosensor', *Chemical Communications*, 47(11), pp. 3060-3062.
- Liang, P., Fan, M., Cao, X. and Huang, X. (2009) 'Evaluation of applied cathode potential to enhance biocathode in microbial fuel cells', *Journal of Chemical Technology and Biotechnology*, 84(5), pp. 794-799.

- Lies, D.P., Hernandez, M.E., Kappler, A., Mielke, R.E., Gralnick, J.A. and Newman, D.K. (2005) 'Shewanella oneidensis MR-1 uses overlapping pathways for iron reduction at a distance and by direct contact under conditions relevant for biofilms', *Applied and Environmental Microbiology*, 71(8), pp. 4414-4426.
- Liu, C., Gorby, Y.A., Zachara, J.M., Fredrickson, J.K. and Brown, C.F. (2002) 'Reduction kinetics of Fe(III), Co(III), U(VI), Cr(VI), and Tc(VII) in cultures of dissimilatory metal-reducing bacteria', *Biotechnology and Bioengineering*, 80(6), pp. 637-649.
- Liu, H. and Logan, B.E. (2004) 'Electricity generation using an air-cathode single chamber microbial fuel cell in the presence and absence of a proton exchange membrane', *Environmental Science and Technology*, 38(14), pp. 4040-4046.
- Liu, H., Ramnarayanan, R. and Logan, B.E. (2004) 'Production of Electricity during Wastewater Treatment Using a Single Chamber Microbial Fuel Cell', *Environmental Science and Technology*, 38(7), pp. 2281-2285.
- Logan, B. (2008) *Microbial Fuel Cells*. New Jersey: John Wiley & Sons. pp. 1-11.
- Logan, B.E. 52 (2005) 'Simultaneous wastewater treatment and biological electricity generation' *Water Science and Technology* [Article]. pp. 31-37. Available at: <http://www.scopus.com/inward/record.url?eid=2-s2.0-25144508500&partnerID=40&md5=552262ef87f9cd4b2ee7d61c62fab99e>.
- Logan, B.E. (2009) 'Exoelectrogenic bacteria that power microbial fuel cells', *Nature Reviews Microbiology*, 7(5), pp. 375-381.
- Logan, B.E. (2010) 'Scaling up microbial fuel cells and other bioelectrochemical systems', *Applied Microbiology and Biotechnology*, 85(6), pp. 1665-1671.
- Logan, B.E., Call, D., Cheng, S., Hamelers, H.V.M., Sleutels, T.H.J.A., Jeremiase, A.W. and Rozendal, R.A. (2008) 'Microbial electrolysis cells for high yield hydrogen gas production from organic matter', *Environmental Science and Technology*, 42(23), pp. 8630-8640.
- Logan, B.E., Hamelers, B., Rozendal, R., Schröder, U., Keller, J., Freguia, S., Aelterman, P., Verstraete, W. and Rabaey, K. (2006) 'Microbial fuel cells: Methodology and technology', *Environmental Science and Technology*, 40(17), pp. 5181-5192.
- Lovley, D.R. (2003) 'Cleaning up with genomics: Applying molecular biology to bioremediation', *Nature Reviews Microbiology*, 1(1), pp. 35-44.
- Lovley, D.R. (2006) 'Erratum: Bug juice: Harvesting electricity with microorganisms (Nature Reviews Microbiology (2006) vol. 4 (497-508) doi:10.1038/nrmicro1442)', *Nature Reviews Microbiology*, 4(10), p. 797.
- Lovley, D.R. (2008) 'The microbe electric: conversion of organic matter to electricity', *Current Opinion in Biotechnology*, 19(6), pp. 564-571.
- Lovley, D.R. (2011) 'Powering microbes with electricity: Direct electron transfer from electrodes to microbes', *Environmental Microbiology Reports*, 3(1), pp. 27-35.
- Lovley, D.R. and Nevin, K.P. (2013) 'Electrobiocommodities: powering microbial production of fuels and commodity chemicals from carbon dioxide with electricity', *Current Opinion in Biotechnology*.
- Lowy, D.A., Tender, L.M., Zeikus, J.G., Park, D.H. and Lovley, D.R. (2006) 'Harvesting energy from the marine sediment-water interface II. Kinetic activity of anode materials', *Biosensors and Bioelectronics*, 21(11), pp. 2058-2063.
- Luo, Q., Wang, H., Zhang, X. and Qian, Y. (2005) 'Effect of direct electric current on the cell surface properties of phenol-degrading bacteria', *Applied and Environmental Microbiology*, 71(1), pp. 423-427.
- Marshall, C.W., Ross, D.E., Fichot, E.B., Norman, R.S. and May, H.D. (2012) 'Electrosynthesis of commodity chemicals by an autotrophic microbial community', *Applied and Environmental Microbiology*, 78(23), pp. 8412-8420.
- Marshall, C.W., Ross, D.E., Fichot, E.B., Norman, R.S. and May, H.D. (2013) 'Long-term operation of microbial electrosynthesis systems improves acetate production by

- autotrophic microbiomes', *Environmental Science and Technology*, 47(11), pp. 6023-6029.
- Marsili, E., Baron, D.B., Shikhare, I.D., Coursolle, D., Gralnick, J.A. and Bond, D.R. (2008) 'Shewanella secretes flavins that mediate extracellular electron transfer', *Proceedings of the National Academy of Sciences of the United States of America*, 105(10), pp. 3968-3973.
- Massey, R. and Jacobs, M. (2011) 'Global Chemicals Outlook, Pillar I: Trends and Indicators'. McGraw-Hill Higher Education (2003) *Plant design and Economics for Chemical Engineers* (Accessed: 15/01/2015).
- Mehanna, M., Kiely, P.D., Call, D.F. and Logan, B.E. (2010) 'Microbial electro dialysis cell for simultaneous water desalination and hydrogen gas production', *Environmental Science and Technology*, 44(24), pp. 9578-9583.
- Meitl, L.A., Eggleston, C.M., Colberg, P.J.S., Khare, N., Reardon, C.L. and Shi, L. (2009) 'Electrochemical interaction of Shewanella oneidensis MR-1 and its outer membrane cytochromes OmcA and MtrC with hematite electrodes', *Geochimica et Cosmochimica Acta*, 73(18), pp. 5292-5307.
- Melhuish, C., Ieropoulos, I., Greenman, J. and Horsfield, I. (2006) 'Energetically autonomous robots: Food for thought', *Autonomous Robots*, 21(3), pp. 187-198.
- Meshulam-Simon, G., Behrens, S., Choo, A.D. and Spormann, A.M. (2007) 'Hydrogen metabolism in Shewanella oneidensis MR-1', *Applied and Environmental Microbiology*, 73(4), pp. 1153-1165.
- MMSA (2013) *Acetic acid: Global Insight, Asian Perspective* (Accessed: 19/01/2015).
- Mohanakrishna, G., Vanbroekhoven, K. and Pant, D. (2015) 'Imperative role of applied potential and inorganic carbon source on acetate production through microbial electrosynthesis', *Journal of CO2 Utilization*.
- Mohn, W.W. and Tiedje, J.M. (1992) 'Microbial reductive dehalogenation', *Microbiological Reviews*, 56(3), pp. 482-507.
- Mordor Intelligence (2015) *Global Acetic Acid Market - Segmented by Application, and Geography - Trends and Forecasts (2015-2020)*. <http://www.reportlinker.com/p03281926-summary/Global-Acetic-Acid-Market-Segmented-by-Application-and-Geography-Trends-and-Forecasts.html>.
- Myers, C.R. and Myers, J.M. (2004) 'Shewanella oneidensis MR-1 restores menaquinone synthesis to a menaquinone-negative mutant', *Applied and Environmental Microbiology*, 70(9), pp. 5415-5425.
- Myers, C.R. and Nealson, K.H. (1988) 'Bacterial manganese reduction and growth with manganese oxide as the sole electron acceptor', *Science*, 240(4857), pp. 1319-1321.
- Nealson, K.H. and Scott, J. (2005) *Ecophysiology of the genus Shewanella*. New York: Springer-Verlag.
- Nevin, K.P., Hensley, S.A., Franks, A.E., Summers, Z.M., Ou, J., Woodard, T.L., Snoeyenbos-West, O.L. and Lovley, D.R. (2011) 'Electrosynthesis of organic compounds from carbon dioxide is catalyzed by a diversity of acetogenic microorganisms', *Applied and Environmental Microbiology*, 77(9), pp. 2882-2886.
- Nevin, K.P., Richter, H., Covalla, S.F., Johnson, J.P., Woodard, T.L., Orloff, A.L., Jia, H., Zhang, M. and Lovley, D.R. (2008) 'Power output and coulombic efficiencies from biofilms of Geobacter sulfurreducens comparable to mixed community microbial fuel cells', *Environmental Microbiology*, 10(10), pp. 2505-2514.
- Nevin, K.P., Woodard, T.L., Franks, A.E., Summers, Z.M. and Lovley, D.R. (2010) 'Microbial electrosynthesis: Feeding microbes electricity to convert carbon dioxide and water to multicarbon extracellular organic compounds', *mBio*, 1(2).
- Newman, D.K. and Kolter, R. (2000) 'A role for excreted quinones in extracellular electron transfer', *Nature*, 405(6782), pp. 94-97.

- Ng, K.S., Zhang, N. and Sadhukhan, J. (2013) 'Techno-economic analysis of polygeneration systems with carbon capture and storage and CO₂ reuse', *Chemical Engineering Journal*, 219, pp. 96-108.
- Nguyen, T.A., Lu, Y., Yang, X. and Shi, X. (2007) 'Carbon and steel surfaces modified by *Leptothrix discophora* SP-6: Characterization and implications', *Environmental Science and Technology*, 41(23), pp. 7987-7996.
- Nielsen, L.P., Risgaard-Petersen, N., Fossing, H., Christensen, P.B. and Sayama, M. (2010) 'Electric currents couple spatially separated biogeochemical processes in marine sediment', *Nature*, 463(7284), pp. 1071-1074.
- NOAA (2010) *Carbon Cycle Science* (Accessed: 26/11/2015).
- NOAA (2012) *Global analysis - Annual 2012* (Accessed: 30/11/2015).
- NOAA (2015) *Global Analysis - October 2015* (Accessed: 30/11/2015).
- Nolan, R.P., Fenley, A.P. and Lee, K. (2006) 'Identification of distributed metabolic objectives in the hypermetabolic liver by flux and energy balance analysis', *Metabolic Engineering*, 8(1), pp. 30-45.
- NRC (2010) *Advancing the Science of Climate Change* (Accessed: 26/11/2015).
- Oak Ridge National Laboratory *New Tools of Analysis: Systems biology enables a leap forward in understanding life*. (Accessed: 30/09/2014).
- Osman, M.H., Shah, A.A. and Walsh, F.C. (2011) 'Recent progress and continuing challenges in bio-fuel cells. Part I: Enzymatic cells', *Biosensors and Bioelectronics*, 26(7), pp. 3087-3102.
- Pant, D., Singh, A., Van Bogaert, G., Gallego, Y.A., Diels, L. and Vanbroekhoven, K. (2011) 'An introduction to the life cycle assessment (LCA) of bioelectrochemical systems (BES) for sustainable energy and product generation: Relevance and key aspects', *Renewable and Sustainable Energy Reviews*, 15(2), pp. 1305-1313.
- Pant, D., Singh, A., Van Bogaert, G., Irving Olsen, S., Singh Nigam, P., Diels, L. and Vanbroekhoven, K. (2012) 'Bioelectrochemical systems (BES) for sustainable energy production and product recovery from organic wastes and industrial wastewaters', *RSC Advances*, 2(4), pp. 1248-1263.
- Pant, D., Van Bogaert, G., Diels, L. and Vanbroekhoven, K. (2010) 'A review of the substrates used in microbial fuel cells (MFCs) for sustainable energy production', *Bioresource Technology*, 101(6), pp. 1533-1543.
- Parameswaran, P., Zhang, H., Torres, C.I., Rittmann, B.E. and Krajmalnik-Brown, R. (2010) 'Microbial community structure in a biofilm anode fed with a fermentable substrate: The significance of hydrogen scavengers', *Biotechnology and Bioengineering*, 105(1), pp. 69-78.
- Patent US 3769329 (1973) *Production of carboxylic acids and esters* (Accessed: 05/02/2015).
- Patent US 5160412 (1991) *Dehydration of acetic acid by azeotropic distillation* (Accessed: 19/01/2015).
- Patil, S.A., Arends, J.B.A., Vanwonterghem, I., Van Meerbergen, J., Guo, K., Tyson, G.W. and Rabaey, K. (2015) 'Selective Enrichment Establishes a Stable Performing Community for Microbial Electrosynthesis of Acetate from CO₂', *Environmental Science and Technology*, 49(14), pp. 8833-8843.
- Pei, P., Korom, S.F., Ling, K. and Nasah, J. (2016) 'Cost comparison of syngas production from natural gas conversion and underground coal gasification', *Mitigation and Adaptation Strategies for Global Change*, 21(4), pp. 629-643.
- Peters, V., Janssen, P.H. and Conrad, R. (1999) 'Transient Production of Formate During Chemolithotrophic Growth of Anaerobic Microorganisms on Hydrogen', *Current Microbiology*, 38(5), pp. 285-289.
- Petrovskis, E.A., Vogel, T.M. and Adriaens, P. (1994) 'Effects of electron acceptors and donors on transformation of tetrachloromethane by *Shewanella putrefaciens* MR-1', *FEMS Microbiology Letters*, 121(3), pp. 357-363.

- Pham, T.H., Rabaey, K., Aelterman, P., Clauwaert, P., De Schampelaire, L., Boon, N. and Verstraete, W. (2006) 'Microbial fuel cells in relation to conventional anaerobic digestion technology', *Engineering in Life Sciences*, 6(3), pp. 285-292.
- Picardal, F., Arnold, R.G. and Huey, B.B. (1995) 'Effects of electron donor and acceptor conditions on reductive dehalogenation of tetrachloromethane by *Shewanella putrefaciens* 200', *Applied and Environmental Microbiology*, 61(1), pp. 8-12.
- Picardal, F.W., Arnold, R.G., Couch, H., Little, A.M. and Smith, M.E. (1993) 'Involvement of cytochromes in the anaerobic biotransformation of tetrachloromethane by *Shewanella putrefaciens* 200', *Applied and Environmental Microbiology*, 59(11), pp. 3763-3770.
- Pinchuk, G.E., Hill, E.A., Geydebrekht, O.V., de Ingeniis, J., Zhang, X., Osterman, A., Scott, J.H., Reed, S.B., Romine, M.F., Konopka, A.E., Beliaev, A.S., Fredrickson, J.K. and Reed, J.L. (2010) 'Constraint-based model of *Shewanella oneidensis* MR-1 metabolism: A tool for data analysis and hypothesis generation', *PLoS Computational Biology*, 6(6), pp. 1-8.
- Pirbadian, S., Barchinger, S.E., Leung, K.M., Byun, H.S., Jangir, Y., Bouhenni, R.A., Reed, S.B., Romine, M.F., Saffarini, D.A., Shi, L., Gorby, Y.A., Golbeck, J.H. and El-Naggar, M.Y. (2014a) '*Shewanella oneidensis* MR-1 nanowires are outer membrane and periplasmic extensions of the extracellular electron transport components', *Proceedings of the National Academy of Sciences of the United States of America*, 111(35), pp. 12883-12888.
- Pirbadian, S., Barchinger, S.E., Leung, K.M., Byun, H.S., Jangir, Y., Bouhenni, R.A., Reed, S.B., Romine, M.F., Saffarini, D.A., Shi, L., Gorby, Y.A., Golbeck, J.H. and El-Naggar, M.Y. (2014b) '*Shewanella oneidensis* MR-1 nanowires are outer membrane and periplasmic extensions of the extracellular electron transport components', *Proceedings of the National Academy of Sciences*, 111(35), pp. 12883-12888.
- Puig, S., Serra, M., Coma, M., Balaguer, M.D. and Colprim, J. (2011) 'Simultaneous domestic wastewater treatment and renewable energy production using microbial fuel cells (MFCs)', *Water Science and Technology*, 64(4), pp. 904-909.
- Q. Smejkal, D. Linke and M. Baerns (2005) 'Energetic and economic evaluation of the production of acetic acid via ethane oxidation', *Chemical Engineering and Processing*, 44, pp. 421-428.
- Rabaey, K., Boon, N., Höfte, M. and Verstraete, W. (2005a) 'Microbial phenazine production enhances electron transfer in biofuel cells', *Environmental Science and Technology*, 39(9), pp. 3401-3408.
- Rabaey, K., Girguis, P. and Nielsen, L.K. (2011) 'Metabolic and practical considerations on microbial electrosynthesis', *Current Opinion in Biotechnology*, 22(3), pp. 371-377.
- Rabaey, K., Largus Angenent, Uwe Schroder and Keller, J. (eds.) (2010) *Bioelectrochemical Systems: from extracellular electron transfer to biotechnological application*. London, UK: IWA Publishing.
- Rabaey, K., Ossieur, W., Verhaege, M. and Verstraete, W. 52 (2005b) 'Continuous microbial fuel cells convert carbohydrates to electricity'. pp. 515-523. Available at: <http://www.scopus.com/inward/record.url?eid=2-s2.0-19444374840&partnerID=40&md5=4f41828db5917cf17f49d0e937dd61a6>.
- Rabaey, K., Read, S.T., Clauwaert, P., Freguia, S., Bond, P.L., Blackall, L.L. and Keller, J. (2008) 'Cathodic oxygen reduction catalyzed by bacteria in microbial fuel cells', *ISME Journal*, 2(5), pp. 519-527.
- Rabaey, K. and Rozendal, R.A. (2010) 'Microbial electrosynthesis - Revisiting the electrical route for microbial production', *Nature Reviews Microbiology*, 8(10), pp. 706-716.
- Rahimnejad, M., Adhami, A., Darvari, S., Zirepour, A. and Oh, S.-E. (2015) 'Microbial fuel cell as new technology for bioelectricity generation: A review', *Alexandria Engineering Journal*, 54(3), pp. 745-756.

- Reda, T., Plugge, C.M., Abram, N.J. and Hirst, J. (2008) 'Reversible interconversion of carbon dioxide and formate by an electroactive enzyme', *Proceedings of the National Academy of Sciences of the United States of America*, 105(31), pp. 10654-10658.
- Reguera, G., McCarthy, K.D., Mehta, T., Nicoll, J.S., Tuominen, M.T. and Lovley, D.R. (2005) 'Extracellular electron transfer via microbial nanowires', *Nature*, 435(7045), pp. 1098-1101.
- Rinaldi, A., Mecheri, B., Garavaglia, V., Licocchia, S., Di Nardo, P. and Traversa, E. (2008) 'Engineering materials and biology to boost performance of microbial fuel cells: A critical review', *Energy and Environmental Science*, 1(4), pp. 417-429.
- Rismani-Yazdi, H., Carver, S.M., Christy, A.D. and Tuovinen, O.H. (2008) 'Cathodic limitations in microbial fuel cells: An overview', *Journal of Power Sources*, 180(2), pp. 683-694.
- Roller, S.D., Bennetto, H.P., Delaney, G.M., Mason, J.R., Stirling, J.L. and Thurston, C.F. (1984) 'Electron-transfer coupling in microbial fuel cells: 1. Comparison of redox-mediator reduction rates and respiratory rates of bacteria', *Journal of chemical technology and biotechnology. Biotechnology*, 34 B(1), pp. 3-12.
- Rozendal, R.A., Hamelers, H.V.M. and Buisman, C.J.N. (2006a) 'Effects of membrane cation transport on pH and microbial fuel cell performance', *Environmental Science and Technology*, 40(17), pp. 5206-5211.
- Rozendal, R.A., Hamelers, H.V.M., Euverink, G.J.W., Metz, S.J. and Buisman, C.J.N. (2006b) 'Principle and perspectives of hydrogen production through biocatalyzed electrolysis', *International Journal of Hydrogen Energy*, 31(12), pp. 1632-1640.
- Rozendal, R.A., Hamelers, H.V.M., Rabaey, K., Keller, J. and Buisman, C.J.N. (2008a) 'Towards practical implementation of bioelectrochemical wastewater treatment', *Trends in Biotechnology*, 26(8), pp. 450-459.
- Rozendal, R.A., Jeremiasse, A.W., Hamelers, H.V.M. and Buisman, C.J.N. (2008b) 'Hydrogen production with a microbial biocathode', *Environmental Science and Technology*, 42(2), pp. 629-634.
- Ruebush, S.S., Brantley, S.L. and Tien, M. (2006) 'Reduction of soluble and insoluble iron forms by membrane fractions of *Shewanella oneidensis* grown under aerobic and anaerobic conditions', *Applied and Environmental Microbiology*, 72(4), pp. 2925-2935.
- Sadhukhan, J., Lloyd, J.R., Scott, K., Premier, G.C., Yu, E.H., Curtis, T. and Head, I.M. (2016) 'A critical review of integration analysis of microbial electrosynthesis (MES) systems with waste biorefineries for the production of biofuel and chemical from reuse of CO₂', *Renewable and Sustainable Energy Reviews*, 56, pp. 116-132.
- Sadhukhan, J., Ng, K.S. and Martinez-Hernandez, E. (2015) 'Process Systems Engineering Tools for Biomass Polygeneration Systems with Carbon Capture and Reuse', in *Process Design Strategies for Biomass Conversion Systems*. John Wiley & Sons, Ltd, pp. 215-245.
- Saeed, H.M., Hussein, G.A., Yousef, S., Saif, J., Al-Asheh, S., Abu Fara, A., Azzam, S., Khawaga, R. and Aidan, A. (2015) 'Microbial desalination cell technology: A review and a case study', *Desalination*, 359, pp. 1-13.
- Sand, W. and Gehrke, T. (2006) 'Extracellular polymeric substances mediate bioleaching/biocorrosion via interfacial processes involving iron(III) ions and acidophilic bacteria', *Research in Microbiology*, 157(1), pp. 49-56.
- Sano, K.i., Uchida, H. and Wakabayashi, S. (1999) 'A new process for acetic acid production by direct oxidation of ethylene', *Catalysis Surveys from Japan* 3(1), pp. 55-60.
- Satomi, M. (2013) 'The family shewanellaceae', in *The Prokaryotes: Gammaproteobacteria*. pp. 597-625.
- Shea, C., Clauwaert, P., Verstraete, W. and Nerenberg, R. 58 (2008) 'Adapting a denitrifying biocathode for perchlorate reduction'. pp. 1941-1946. Available at: <http://www.scopus.com/inward/record.url?eid=2-s2.0-58949095688&partnerID=40&md5=9967576e1f04f2fba66a7365cf99914>.

- Shi, L., Squier, T., Zachara, J.M. and Fredrickson, J.K. (2007a) 'Respiration of metal (hydr)oxides by Shewanella and Geobacter: a key role for multihaem c-type cytochromes', *Molecular Microbiology*, 65(1), pp. 12-20.
- Shi, L., Squier, T.C., Zachara, J.M. and Fredrickson, J.K. (2007b) 'Respiration of metal (hydr)oxides by Shewanella and Geobacter: A key role for multihaem c-type cytochromes', *Molecular Microbiology*, 65(1), pp. 12-20.
- Shindell, D.T., Faluvegi, G., Stevenson, D.S., Krol, M.C., Emmons, L.K., Lamarque, J.F., Pétron, G., Dentener, F.J., Ellingsen, K., Schultz, M.G., Wild, O., Amann, M., Atherton, C.S., Bergmann, D.J., Bey, I., Butler, T., Cofala, J., Collins, W.J., Derwent, R.G., Doherty, R.M., Drevet, J., Eskes, H.J., Fiore, A.M., Gauss, M., Hauglustaine, D.A., Horowitz, L.W., Isaksen, I.S.A., Lawrence, M.G., Montanaro, V., Müller, J.F., Pitari, G., Prather, M.J., Pyle, J.A., Rast, S., Rodriguez, J.M., Sanderson, M.G., Savage, N.H., Strahan, S.E., Sudo, K., Szopa, S., Unger, N., van Noije, T.P.C. and Zeng, G. (2006) 'Multimodel simulations of carbon monoxide: Comparison with observations and projected near-future changes', *Journal of Geophysical Research: Atmospheres*, 111(D19), pp. n/a-n/a.
- Siegert, M., Li, X.F., Yates, M.D. and Logan, B.E. (2015) 'The presence of hydrogenotrophic methanogens in the inoculum improves methane gas production in microbial electrolysis cells', *Frontiers in Microbiology*, 6(JAN).
- Sigma Aldrich (2016) *Nafion® perfluorinated membrane* (Accessed: 28/11/2016).
- Sinnott, R.K. (2005) *Chemical Engineering design*. Fourth edn. Elsevier Butterworth-Heinemann: Coulson and Richardson's.
- Sleutels, T.H.J.A., Hamelers, H.V.M., Rozendal, R.A. and Buisman, C.J.N. (2009) 'Ion transport resistance in Microbial Electrolysis Cells with anion and cation exchange membranes', *International Journal of Hydrogen Energy*, 34(9), pp. 3612-3620.
- Smejkal, Q., Linke, D. and Baerns, M. (2005) 'Energetic and economic evaluation of the production of acetic acid via ethane oxidation', *Chemical Engineering and Processing*, 44, pp. 421-428.
- Soliman, M., Al-Zeghayer Y., S. Al-Awadi A. and Al-Mayman S. (2012) 'Economics of Acetic Acid Production by Partial Oxidation of Ethane', *APCBEE Procedia*, 3, pp. 200-208.
- Srikanth, S., Maesen, M., Dominguez-Benetton, X., Vanbroekhoven, K. and Pant, D. (2014) 'Enzymatic electrosynthesis of formate through CO₂ sequestration/reduction in a bioelectrochemical system (BES)', *Bioresource Technology*, 165, pp. 350-354.
- Strik, D.P.B.T.B., Hamelers, H.V.M. and Buisman, C.J.N. (2010) 'Solar energy powered microbial fuel cell with a reversible bioelectrode', *Environmental Science and Technology*, 44(1), pp. 532-537.
- Strik, D.P.B.T.B., Timmers, R.A., Helder, M., Steinbusch, K.J.J., Hamelers, H.V.M. and Buisman, C.J.N. (2011) 'Microbial solar cells: Applying photosynthetic and electrochemically active organisms', *Trends in Biotechnology*, 29(1), pp. 41-49.
- Strycharz-Glaven, S.M., Glaven, R.H., Wang, Z., Zhou, J., Vora, G.J. and Tender, L.M. (2013) 'Electrochemical investigation of a microbial solar cell reveals a nonphotosynthetic biocathode catalyst', *Applied and Environmental Microbiology*, 79(13), pp. 3933-3942.
- Strycharz, S.M., Gannon, S.M., Boles, A.R., Franks, A.E., Nevin, K.P. and Lovley, D.R. (2010) 'Reductive dechlorination of 2-chlorophenol by Anaeromyxobacter dehalogenans with an electrode serving as the electron donor', *Environmental Microbiology Reports*, 2(2), pp. 289-294.
- Strycharz, S.M., Woodard, T.L., Johnson, J.P., Nevin, K.P., Sanford, R.A., Löffler, F.E. and Lovley, D.R. (2008) 'Graphite electrode as a sole electron donor for reductive dechlorination of tetrachlorethene by *Geobacter lovleyi*', *Applied and Environmental Microbiology*, 74(19), pp. 5943-5947.
- Sun, M., Sheng, G.P., Mu, Z.X., Liu, X.W., Chen, Y.Z., Wang, H.L. and Yu, H.Q. (2009) 'Manipulating the hydrogen production from acetate in a microbial electrolysis cell-microbial fuel cell-coupled system', *Journal of Power Sources*, 191(2), pp. 338-343.

- Sund, C.J., McMasters, S., Crittenden, S.R., Harrell, L.E. and Sumner, J.J. (2007) 'Effect of electron mediators on current generation and fermentation in a microbial fuel cell', *Applied Microbiology and Biotechnology*, 76(3), pp. 561-568.
- Tandukar, M., Huber, S.J., Onodera, T. and Pavlostathis, S.G. (2009) 'Biological chromium(VI) reduction in the cathode of a microbial fuel cell', *Environmental Science and Technology*, 43(21), pp. 8159-8165.
- Tang, H., Cao, T., Wang, A., Liang, X., Salley, S.O., McAllister Ii, J.P. and Ng, K.Y.S. (2007) 'Effect of surface modification of silicone on Staphylococcus epidermidis adhesion and colonization', *Journal of Biomedical Materials Research - Part A*, 80(4), pp. 885-894.
- Teal, T.K., Lies, D.P., Wold, B.J. and Newman, D.K. (2006) 'Spatio-metabolic Stratification of Shewanella oneidensis Biofilms', *Applied and Environmental Microbiology*, 72(11), pp. 7324-7330.
- Thormann, K.M., Duttler, S., Saville, R.M., Hyodo, M., Shukla, S., Hayakawa, Y. and Spormann, A.M. (2006) 'Control of formation and cellular detachment from Shewanella oneidensis MR-1 biofilms by cyclic di-GMP', *Journal of Bacteriology*, 188(7), pp. 2681-2691.
- Thormann, K.M., Saville, R.M., Shukla, S., Pelletier, D.A. and Spormann, A.M. (2004) 'Initial phases of biofilm formation in Shewanella oneidensis MR-1', *Journal of Bacteriology*, 186(23), pp. 8096-8104.
- Thormann, K.M., Saville, R.M., Shukla, S. and Spormann, A.M. (2005) 'Induction of rapid detachment in Shewanella oneidensis MR-1 biofilms', *Journal of Bacteriology*, 187(3), pp. 1014-1021.
- Thrash, J.C. and Coates, J.D. (2008) 'Review: Direct and indirect electrical stimulation of microbial metabolism', *Environmental Science and Technology*, 42(11), pp. 3921-3931.
- Thrash, J.C., Van Trump, J.I., Weber, K.A., Miller, E., Achenbach, L.A. and Coates, J.D. (2007) 'Electrochemical stimulation of microbial perchlorate reduction', *Environmental Science and Technology*, 41(5), pp. 1740-1746.
- Tolker-Nielsen, T. and Molin, S. (2000) 'Spatial Organization of Microbial Biofilm Communities', *Microbial ecology*, 40(2), pp. 75-84.
- Tranier, S., Mortier-Barrière, I., Ilbert, M., Birck, C., Iobbi-Nivol, C., Méjean, V. and Samama, J.P. (2002) 'Characterization and multiple molecular forms of TorD from Shewanella massilia, the putative chaperone of the molybdoenzyme TorA', *Protein Science*, 11(9), pp. 2148-2157.
- Tremblay, P.L., Höglund, D., Koza, A., Bonde, I. and Zhang, T. (2015) 'Adaptation of the autotrophic acetogen Sporomusa ovata to methanol accelerates the conversion of CO₂ to organic products', *Scientific Reports*, 5.
- UK gov (2016) *Corporation Tax rates and reliefs* (Accessed: 15/12/2016).
- van Eerten-Jansen, M.C.A.A., Jansen, N.C., Plugge, C.M., de Wilde, V., Buisman, C.J.N. and ter Heijne, A. (2015) 'Analysis of the mechanisms of bioelectrochemical methane production by mixed cultures', *Journal of Chemical Technology and Biotechnology*, 90(5), pp. 963-970.
- Velasquez-Orta, S.B., Head, I.M., Curtis, T.P., Scott, K., Lloyd, J.R. and Von Canstein, H. (2010) 'The effect of flavin electron shuttles in microbial fuel cells current production', *Applied Microbiology and Biotechnology*, 85(5), pp. 1373-1381.
- Venkata Mohan, S., Veer Raghavulu, S. and Sarma, P.N. (2008) 'Influence of anodic biofilm growth on bioelectricity production in single chambered mediatorless microbial fuel cell using mixed anaerobic consortia', *Biosensors and Bioelectronics*, 24(1), pp. 41-47.
- Venkateswaran, K., Moser, D.P., Dollhopf, M.E., Lies, D.P., Saffarini, D.A., MacGregor, B.J., Ringelberg, D.B., White, D.C., Nishijima, M., Sano, H., Burghardt, J., Stackebrandt, E. and Nealson, K.H. (1999) 'Polyphasic taxonomy of the genus Shewanella and description of Shewanella oneidensis sp. nov.', *International Journal of Systematic Bacteriology*, 49(2), pp. 705-724.

- Villano, M., Aulenta, F., Ciucci, C., Ferri, T., Giuliano, A. and Majone, M. (2010) 'Bioelectrochemical reduction of CO₂ to CH₄ via direct and indirect extracellular electron transfer by a hydrogenophilic methanogenic culture', *Bioresource Technology*, 101(9), pp. 3085-3090.
- Viridis, B., Rabaey, K., Yuan, Z. and Keller, J. (2008) 'Microbial fuel cells for simultaneous carbon and nitrogen removal', *Water Research*, 42(12), pp. 3013-3024.
- Viridis, B., Read, S.T., Rabaey, K., Rozendal, R.A., Yuan, Z. and Keller, J. (2011) 'Biofilm stratification during simultaneous nitrification and denitrification (SND) at a biocathode', *Bioresource Technology*, 102(1), pp. 334-341.
- Von Canstein, H., Ogawa, J., Shimizu, S. and Lloyd, J.R. (2008) 'Secretion of flavins by *Shewanella* species and their role in extracellular electron transfer', *Applied and Environmental Microbiology*, 74(3), pp. 615-623.
- Von Stockar, U. and Van der Wielen, L.A.M. (2003) 'Back to Basics: Thermodynamics in Biochemical Engineering', in von Stockar, U., van der Wielen, L.A.M., Bruggink, A., Cabral, J.M.S., Enfors, S.O., Fernandes, P., Jenne, M., Mauch, K., Prazeres, D.M.F., Reuss, M., Schmalzriedt, S., Stark, D., von Stockar, U., Straathof, A.J.J. and van der Wielen, L.A.M. (eds.) *Process Integration in Biochemical Engineering*. Berlin, Heidelberg: Springer Berlin Heidelberg, pp. 1-17.
- Wackett, L. and Gralnick, J.A. (2012) *Co-cultured Synechococcus and Shewanella Produce Hydrocarbons without Cellulosic Feedstock* (Accessed: 29/11/2016).
- Walsh, C. (1980) 'Flavin coenzymes: at the crossroads of biological redox chemistry', *Accounts of Chemical Research* 13, pp. 148-155.
- Wang, H. and Ren, Z.J. (2013) 'A comprehensive review of microbial electrochemical systems as a platform technology', *Biotechnology Advances*, 31(8), pp. 1796-1807.
- Wang, Y.P., Liu, X.W., Li, W.W., Li, F., Wang, Y.K., Sheng, G.P., Zeng, R.J. and Yu, H.Q. (2012) 'A microbial fuel cell-membrane bioreactor integrated system for cost-effective wastewater treatment', *Applied Energy*, 98, pp. 230-235.
- Ward, M.J., Fu, Q.S., Rhoads, K.R., Yeung, C.H.J., Spormann, A.M. and Criddle, C.S. (2004) 'A derivative of the menaquinone precursor 1,4-dihydroxy-2-naphthoate is involved in the reductive transformation of carbon tetrachloride by aerobically grown *Shewanella oneidensis* MR-1', *Applied Microbiology and Biotechnology*, 63(5), pp. 571-577.
- Watanabe, K., Manefield, M., Lee, M. and Kouzuma, A. (2009) 'Electron shuttles in biotechnology', *Current Opinion in Biotechnology*, 20(6), pp. 633-641.
- Watson, V.J. and Logan, B.E. (2010) 'Power production in MFCs inoculated with *Shewanella oneidensis* MR-1 or mixed cultures', *Biotechnology and Bioengineering*, 105(3), pp. 489-498.
- Weber, K.A., Achenbach, L.A. and Coates, J.D. (2006) 'Microorganisms pumping iron: Anaerobic microbial iron oxidation and reduction', *Nature Reviews Microbiology*, 4(10), pp. 752-764.
- WEO (2015) *Energy and Climate Change* (Accessed: 27/11/2015).
- White, D. (1999) 'Electron transport', in M.C.D. Flickinger, S.W. (ed.) *Encyclopedia of bioprocess technology-fermentation, biocatalysis and bioseparation*. New York: John Wiley & Sons.
- Wildung, R.E., Gorby, Y.A., Krupka, K.M., Hess, N.J., Li, S.W., Plymale, A.E., McKinley, J.P. and Fredrickson, J.K. (2000) 'Effect of electron donor and solution chemistry on products of dissimilatory reduction of technetium by *Shewanella putrefaciens*', *Applied and Environmental Microbiology*, 66(6), pp. 2451-2460.
- Worden, R.M., Bredwell, M.D. and Grethlein, A.J. (1997) 'Engineering Issues in Synthesis-Gas Fermentations', in *Fuels and Chemicals from Biomass*. American Chemical Society, pp. 320-335.
- Workman, D.J., Woods, S.L., Gorby, Y.A., Fredrickson, J.K. and Truex, M.J. (1997) 'Microbial reduction of vitamin B₁₂ by *Shewanella* alga strain BrY with subsequent

- transformation of carbon tetrachloride', *Environmental Science and Technology*, 31(8), pp. 2292-2297.
- Xu, M., Bhat, S., Smith, R., Stephens, G. and Sadhukhan, J. (2009) 'Multi-objective optimisation of metabolic productivity and thermodynamic performance', *Computers & Chemical Engineering*, 33(9), pp. 1438-1450.
- Xu, M., Smith, R. and Sadhukhan, J. (2008) 'Optimization of Productivity and Thermodynamic Performance of Metabolic Pathways', *Industrial & Engineering Chemistry Research*, 47(15), pp. 5669-5679.
- Xu, S.-w., Lu, Y., Li, J., Jiang, Z.-y. and Wu, H. (2006) 'Efficient Conversion of CO₂ to Methanol Catalyzed by Three Dehydrogenases Co-encapsulated in an Alginate-Silica (ALG-SiO₂) Hybrid Gel', *Industrial & Engineering Chemistry Research*, 45(13), pp. 4567-4573.
- Yang, X., Beyenal, H., Harkin, G. and Lewandowski, Z. (2000) 'Quantifying biofilm structure using image analysis', *Journal of Microbiological Methods*, 39(2), pp. 109-119.
- Yi, H., Nevin, K.P., Kim, B.C., Franks, A.E., Klimes, A., Tender, L.M. and Lovley, D.R. (2009) 'Selection of a variant of *Geobacter sulfurreducens* with enhanced capacity for current production in microbial fuel cells', *Biosensors and Bioelectronics*, 24(12), pp. 3498-3503.
- Yoneda, N., Kusano, S., Yasui, M., Pujado, P. and Wilcher, S. (2001) 'Recent advances in processes and catalysts for the production of acetic acid', *Applied Catalysis A: General*, 221(1-2), pp. 253-265.
- You, S.J., Ren, N.Q., Zhao, Q.L., Wang, J.Y. and Yang, F.L. (2009) 'Power generation and electrochemical analysis of biocathode microbial fuel cell using graphite fibre brush as cathode material', *Fuel Cells*, 9(5), pp. 588-596.
- Zhao, F., Slade, R.C.T. and Varcoe, J.R. (2009) 'Techniques for the study and development of microbial fuel cells: An electrochemical perspective', *Chemical Society Reviews*, 38(7), pp. 1926-1939.
- Zhao, H.-Z., Zhang, Y., Chang, Y.-Y. and Li, Z.-S. (2012) 'Conversion of a substrate carbon source to formic acid for carbon dioxide emission reduction utilizing series-stacked microbial fuel cells', *Journal of Power Sources*, 217, pp. 59-64.
- Zhao, J.S., Spain, J., Thiboutot, S., Ampleman, G., Greer, C. and Hawari, J. (2004) 'Phylogeny of cyclic nitramine-degrading psychrophilic bacteria in marine sediment and their potential role in the natural attenuation of explosives', *FEMS Microbiology Ecology*, 49(3), pp. 349-357.
- Zuo, Y., Cheng, S., Call, D. and Logan, B.E. (2007) 'Tubular membrane cathodes for scalable power generation in microbial fuel cells', *Environmental Science and Technology*, 41(9), pp. 3347-3353.

Appendices

A1 - Operating costs

Table 0-1: Variables details of chemical processes; methanol carbonylation and ethane direct oxidation, and biological processes; MES and AF

		Chemical Processes	Bioprocesses
Fixed cost	Maintenance (labour & materials)	3% of fixed capital cost	5% of fixed capital cost
	Operating labour	20 men of £25,000 per year each	2 man of £30,000 per year (small plants thus one man plus one extra man allowed on days)
	Laboratory costs	20% of operating labour	20% of operating labour
	Supervision	4 people of £50,000 per year each	No supervision will be needed
	Plant overheads	50% of operating labour	50% of operating labour
	Capital charges	6% of fixed capital cost	10% of fixed capital cost
	Rates (taxes)	2% of fixed capital cost	2% of fixed capital cost
	Insurance	1% of fixed capital cost	1% of fixed capital cost
	Licence fees	1% of fixed capital cost	1% of fixed capital cost
Variable cost	Miscellaneous materials	10% of maintenance cost	5% of maintenance cost
	Raw materials (Inc. catalyst)	Dependent of the process	Dependent of the process
	Utilities	Dependent of the process	Dependent of the process (only electricity)
	Shipping & packaging	Negligible	Negligible

A2 – Investment and production costs

Investment and Production costs of Microbial electrosynthesis and Anaerobic fermentation

clear

```
%Material Balance for determining raw material cost for Microbial
%electrosynthesis
%Main Reaction: 2CO2 + 6H2O + 8e- = CH3COOH + 4H2O + 2O2
%Assumptions:
%1:Process Plant is runs in batches, each batch lasts for 3.66 days
and the plant operates for 100 batches per year
%2:Acetic acid is lost during process units thus 6.5% acetic acid is
targeted in the reactor
%3:Selectivity for CO2=58.8% and for H2O=90%
%4:Conversion rate to yield: CO2=88% and H2O=90%
%5:No side reactions are occurring

%Calculations for how much of reactants are required for a 100 ton/y
production of acetic acid
AceticAcid_mol= 16652.78; %For 1 tonne production in 3.66 days
assuming 100 tonne production in 1 year,targeted flowarate 2664.44 M
CO2_mol= 2 * AceticAcid_mol; %2 moles of CO2 are required for 1 mole
of Acetic acid production
H2O_mol= 6 * AceticAcid_mol; %6 moles of H2O are required for 1 mole
of Acetic acid production
H2O_mol_product= 4 * AceticAcid_mol; %4 moles of H2O are produced for
1 mole of Acetic acid production

%Selectivity calculations: Selectivity of reactant(s)=reactant
converted to Acetic acid/ total reactant converted
CO2_converted=88;
H2O_converted=90;
CO2_selectivity= (100/CO2_converted)*CO2_mol;
H2O_selectivity= (100/H2O_converted)*H2O_mol;

%Conversion of reactants
%Yield(%)=Selectivity * Conversion
CO2_conv_rate=58.5; % 58.5% is the average conversion achieved
experimentally (Marshall et.al, Electrosynthesis of Commodity
Chemicals by an Autotrophic Microbial Community)
H2O_conv_rate=90;
%Total reactant conversion per batch
CO2_total= CO2_selectivity/(CO2_conv_rate/100);
H2O_total= H2O_selectivity/(H2O_conv_rate/100);
%Convert to kg per batch
CO2_total_kg= (CO2_total*44.01)/1000; %CO2 molecular mass= 44.01
H2O_total_kg= (H2O_total*18)/1000; %H2O molecular mass= 18
CO2_total_ton= (CO2_total_kg/1000)*100; % to convert to tonnes/year,
1600 tonnes/year =1 year
H2O_total_ton= (H2O_total_kg/1000)*100; % to convert to tonnes/year,
1600 tonnes/year =1 year

%Material Costing
CO2_cost= (CO2_total_ton*100)*0; %CO2 is free of charge
H2O_cost= (H2O_total_ton*100)*0.76;% Process water costs 0.76 p/t

%Energy balance for determining electricity costs for Microbial
%electrosynthesis
%Assumptions:
```

```

%1: The reactors inlet and outlet are to be maintained isothermally at
%operating temperature of 25oC thus no temperature changes to the
reactants
%and products
% Microbial electrosynthesis is assumed as batch process

%cost=0.13; % cost of energy 130£/MWh
cost=0.08; %wind energy
%cost estimation for applying a constant current (for 10t/y)
Energy_tonne= AceticAcid_mol*96485*8; %96485 Coulombs/mol/e, 8
mol/e/acetate, Coulombs in the acetate produced
Energy1_tonne = Energy_tonne* 1.31; %Total coulombs consumed,
coulombic efficiency 69%
Electricity_tonne = ((Energy1_tonne*0.393)/1000)*0.000278)*cost;
%Electricity amount kWh

%cost estimation for applying a constant current (for 1000t/y)
Energy_year = ((AceticAcid_mol*100)*96485*8)*1.31; %96485
Coulombs/mol/e, 8 mol/e/acetate, Coulombs in the acetate produced,
coulombic efficiency 69%(Total coulombs consumed)
Electricity_year = ((Energy_year*0.393)/1000)*0.000278)*cost;
%Electricity amount and cost, kWh

%Energy needed to heat the reactor liquid per batch (19.20 tonnes of
%reaction medium)
m=H2O_mol*18; %reaction medium
c=4.2; %4.2 J/g
dT= 25-16; %degrees needed to increase the temperature
Q_mes=(((m*c*dT)*100)/1e+9)*277.778*cost;%1000 tonnes per year,
277.778 to convert GJ to kW

%Capital cost of Microbial electrosynthesis
%Purchased equipment cost for main process units for microbial
electrosynthesis (3 items)(PCE)
%Estimated using graphical figures. CEPCI index for 2015 547.2
(Cheical
%engineering Journal 2016)
Distillation = 13251.24; %Distillation columns, column diameter=1.5m,
carbon steel sieve trays = 20
Membrane = 1700; %2 m2 membrane
Reactor = 13821; % 1.8m3, 316 stainless steel
Filter = 899 + 1099; % vaccum pump + filter-cartridge 3 m3
Mixing = 15242;% 1.8m3, stainless steel
Electrode = 830 * 4.6; % Marshall et al 2013 used 30 grams of carbon
graphite for the production of 0.017 M per days thus, 4.6 tonnes of
graphite electrode was estimated to be needed per batch. Cost per
tonne is £830
PCE = Distillation + Membrane + Reactor + Filter + Electrode + Mixing;

%Calculating direct cost using Lang factors for capital cost
Lang_factors= [[0.4,0.3];[0.7,0];[0.2,0.1];[0.1,0];[0.15,0];[0.05,0]];
%Create a matrix with Lang factors, 1t column=direct costs, 2nd
column=indirect costs

sum(Lang_factors); %Adding the rows of each column
v =sum(Lang_factors);
PCC_direct= PCE*(1+v(1)); %Total purchase of major equipment cost
FCC= PCC_direct*(1+v(2)); %Total physical plant cost

```

```

%Calculating working capital
Working_capital= FCC*0.05;

%Calculating total investment cost
Total_investment_cost= FCC + Working_capital;

%Annual operating costs,Operating time, allowing for plant attainment
=365*0.95 = 347 d/y, 347*24 = 8328 h/y, 8000 working hours.
%Calculating operating costs
Y=[[ (FCC*0.05), (H2O_cost)]; [60000, (Electricity_year+Q_mes)]; [(60000*0.2), ((FCC*0.05)*0.05)]; [0,350]; [60000*0.5*0.02,0]; [(FCC*0.1),0]; [(FCC*0.01),0]; [(FCC*0.02),0]];

sum(Y); %Adding the rows of each column together, 1st column=Fixed Cost, 2nd column=Variable Cost
cost= sum(Y);
Operating_cost= sum(cost,2);

%Acetic acid price
Acetic_Acid_price=Operating_cost/100000;

clear
%ANAEROBIC FERMENTATION process
%Main Reaction: 4CO + 2H2O = CH3COOH + 2CO2
%Assumptions:
%1:Process Plant is continuous, runs 24/7, for 8000 hours
%2:Acetic acid is lost during process units thus 6.5% acetic acid is targeted in the reactor
%3:Selectivity for CO=90% and for H2O=99%
%4:Conversion rate to yield: CO=88% and H2O=90%
%5:No side reactions are occurring
AceticAcid_mol_fer= 16652.78; %For 1 hour of operation for a 1 tonne production in 3.66 days assuming 100 tonne production in 1 year,targeted flowarate 189.42 M
CO_mol_fer= 4 * AceticAcid_mol_fer; %4 moles of CO are required for 1 mole of Acetic acid production
H2O_mol_fer= 2 * AceticAcid_mol_fer; %2 moles of H2O are required for 1 mole of Acetic acid production
CO2_fer = 2 * AceticAcid_mol_fer; %2 moles of CO2 are produced with 1 mole of acetic acid

%Selectivity calculations: Selectivity of reactant(s)=reactant converted to Acetic acid/ total reactant converted
CO_converted_fer=99;
H2O_converted_fer=99;
CO_selectivity_fer= (100/CO_converted_fer)*CO_mol_fer;
H2O_selectivity_fer= (100/H2O_converted_fer)*H2O_mol_fer;

%Conversion of reactants
%Yield(%)=Selectivity * Conversion
CO_conv_rate_fer=99;% 100% conversion is achieved at a specific CO pressure experimentally (Sim et.al 2007, Clostridium aceticum-A potential organism in catalysing carbon monoxide to acetic acid: Application of response surface methodology)
H2O_conv_rate_fer=90;
%Total reactant conversion
CO_total_fer= CO_selectivity_fer/(CO_conv_rate_fer/100);%For mol/h
H2O_total_fer= H2O_selectivity_fer/(H2O_conv_rate_fer/100); %For mol/h

```



```

%Convert to kg/s
CO_total_kg_fer= (CO_total_fer*28.01)/1000; %CO molecular mass= 28.01
H2O_total_kg_fer= (H2O_total_fer*18)/1000; %H2O molecular mass= 18
CO_total_ton_fer= (CO_total_kg_fer/1000)*8000; % to convert to
tonnes/year, 8000 working hours =1 year
H2O_total_ton_fer= (H2O_total_kg_fer/1000)*8000; % to convert to
tonnes/year, 8000 working hours =1 year

%Material Costing
CO_cost_fer= CO_total_ton_fer*18.95; %CO is £18.95 per ton
H2O_cost_fer= H2O_total_ton_fer*0.76;% Process water costs 0.76 p/t

% Energy balances
%Energy consumed by acetate production = energy in products leaving
the
%fermenter
DH_CO = 283; % Enthalpy of CO, KJ/mol
DH_H2O = 285; % Enthalpy of H2O, KJ/mol
Cp_acetate=0.123; %Heat capacity constant, KJ/mol
Cp_CO2=0.0372;
T1=15; %datum temperature

T_out =
15+((CO_mol_fer*DH_CO)+(H2O_mol_fer*DH_H2O))/((AceticAcid_mol_fer*Cp_a
cetate)+ (CO2_fer*Cp_CO2)); %Temperature coming out of reactor

%Amount of cooling water needed
%Heat load (Q) = Qh = Qc
%Qc = rate of heat loss by hot fluid
%Qh = heat gain by cold fluid
%Qc = mCpDT=mCp(Tin-Tout)
%Qh = mCpDt = mCp (Tout-Tin)
Cp_acetate=2.043; %KJ/Kg.K
Cp_water=4.187; %KJ/Kg.K

Qc=AceticAcid_mol_fer*Cp_acetate*(8910.15-59);
m = (Qc/(86-59))/Cp_water; %mass of cooling water, Kg/batch

%cost of cooling water
cooling_water_cost=(m*(8*10^-5))*100;% for a yearly supply

%Capital cost of anaerobic fermentation
%Purchased equipment cost for main process units for microbial
electrosynthesis (3 items)(PCE)
%Estimated using graphical figures. CEPCI index for 2015 547.2
(Cheical
%engineering Journal 2016)
Distillation = 13251.24; %Distillation columns, column diameter=1.5m,
carbon steel sieve trays = 20
Membrane = 1000+(350*2); %2 m2 membrane
Reactor = 17262; % 0.6m3, 316 stainless steel
Filter = 899 + 1099; % vacuum pump + filter-cartridge 3 m3
Mixing= 7621; % Mixing tank, stainless steel, 0.6 m3
PCE = Distillation + Membrane + Reactor + Filter + Mixing;

%Calculating direct cost using Lang factors for capital cost
Lang_factors= [[0.4,0.3];[0.7,0];[0.2,0.1];[0.1,0];[0.15,0];[0.05,0]];
%Create a matrix with Lang factors, 1t column=direct costs, 2nd
column=indirect costs

```

```

sum(Lang_factors); %Adding the rows of each column
v =sum(Lang_factors);
PCC_direct= PCE*(1+v(1)); %Total purchase of major equipment cost
FCC= PCC_direct*(1+v(2)); %Total physical plant cost

%Calculating working capital
Working_capital= FCC*0.05;

%Calculating total investment cost
Total_investment_cost= FCC + Working_capital;

%Annual operating costs, Operating time, allowing for plant attainment
=365*0.95 = 347 d/y, 347*24 = 8328 h/y, 8000 working hours.
%Calculating operating costs
Y=[[ (FCC*0.05), (H2O_cost_fer+CO_cost_fer)]; [60000, (cooling_water_cost)
]; [ (60000*0.2), ((FCC*0.05)*0.05)]; [0,330]; [60000*0.5*0.02,0]; [(FCC*0.1
),0]; [(FCC*0.01),0]; [(FCC*0.02),0]];

sum(Y); %Adding the rows of each column together, 1st column=Fixed
Cost, 2nd column=Variable Cost
cost= sum(Y);
Operating_cost= sum(cost,2);

%Acetic acid price
Acetic_Acid_price=Operating_cost/100000;

```

Investment and Production costs of Integrated process 200 t/y

```

clear
%Purchased equipment cost for main process units for the integrated
process of anaerobic fermentation and microbial electrosynthesis (PCE)
%Estimated using graphical figures
Distillation = 13251.24; %Distillation columns, column diameter=1.5m,
carbon steel sieve trays = 20
Membrane = 2000; %2 m2 membrane
Reactor = 17262; % 0.12m3, 316 stainless steel
Filter = 899 + 1099; % vacuum pump + filter-cartridge 3 m3
Mixing= 7621+15242; % Mixing tank, stainless steel, 0.38 m3
Electrode = 830 * 4.6; % Marshall et al 2013 used 30 grams of carbon
graphite for the production of 0.017 M per days thus, 4.6 tonnes of
graphite electrode was estimated to be needed per batch. Cost per
tonne is £830
Recycle=13821; %The microbial electrosynthesis reactor will work as
the CO2 recycling unit
PCE = Distillation + Membrane + Reactor + Filter + Electrode + Mixing
+ Recycle;

%Calculating direct cost using Lang factors
Lang_factors= [[0.4,0.3];[0.7,0];[0.2,0.1];[0.1,0];[0.15,0];[0.05,0]];
%Create a matrix with Lang factors, 1st column=direct costs, 2nd
column=indirect costs

sum(Lang_factors); %Adding the rows of each column
v =sum(Lang_factors);
PCC_direct= PCE*(1+v(1)); %Total purchase of major equipment cost
FCC= PCC_direct*(1+v(2)); %Total physical plant cost

```

```

%Calculating working capital
Working_capital= FCC*0.05;

%Calculating total investment cost
Total_investment_cost= FCC + Working_capital;

%Annual operating costs, Operating time, allowing for plant attainment
=365*0.95 = 347 d/y, 347*24 = 8328 h/y.
%Calculating operating costs
Y=[[ (FCC*0.05), (1.6875e+04)+(2.9269e+05) ]; [60000, (2.4161e+04)+(2.1310e
+04) ]; [ (60000*0.2), ((FCC*0.05)*0.05) ]; [0, 350+330]; [60000*0.5*0.02, 0]; [
(FCC*0.1), 0]; [(FCC*0.01), 0]; [(FCC*0.02), 0]];
%((1.6875e+04)+350+(2.4161e+04)) = Feedstock, biocatalyst and energy
prices for MES
%((3.2597e+05)+350+20) = Feedstock, biocatalyst and energy prices for
anaerobic fermentation

sum(Y); %Adding the rows of each column together, 1st column=Fixed
Cost, 2nd column=Variable Cost
cost= sum(Y);
Operating_cost= sum(cost,2);

%Acetic acid price
Acetic_Acid_price=Operating_cost/2e+6;% operating cost/production rate
(in kg)

```

MES- Acetic acid production 1000 t/y

```

clear
%Material Balance for determining raw material cost for Microbial
%electrosynthesis
%Main Reaction: 2CO2 + 6H2O + 8e- = CH3COOH + 4H2O + 2O2
%Assumptions:
%1:Process Plant is runs in batches, each batch lasts for 3.66 days
and the plant operates for 100 batches per year
%2:Acetic acid is lost during process units thus 6.5% acetic acid is
targeted in the reactor
%3:Selectivity for CO2=58.8% and for H2O=90%
%4:Conversion rate to yield: CO2=88% and H2O=90%
%5:No side reactions are occurring

%Calculations for how much of reactants are required for a 1000 ton/y
production of acetic acid
AceticAcid_mol= 166527.9; %For 10 tonne production in 3.66 days
assuming 1000 tonne production in 1 year, targeted flowrate 2664.44 M
CO2_mol= 2 * AceticAcid_mol; %2 moles of CO2 are required for 1 mole
of Acetic acid production
H2O_mol= 6 * AceticAcid_mol; %6 moles of H2O are required for 1 mole
of Acetic acid production
H2O_mol_product= 4 * AceticAcid_mol; %4 moles of H2O are produced for
1 mole of Acetic acid production

%Selectivity calculations: Selectivity of reactant(s)=reactant
converted to Acetic acid/ total reactant converted
CO2_converted=88;
H2O_converted=90;
CO2_selectivity= (100/CO2_converted)*CO2_mol;
H2O_selectivity= (100/H2O_converted)*H2O_mol;

```

```

%Conversion of reactants
%Yield(%)=Selectivity * Conversion
CO2_conv_rate=58.5; % 58.5% is the average conversion achieved
experimentally (Marshall et.al, Electrosynthesis of Commodity
Chemicals by an Autotrophic Microbial Community)
H2O_conv_rate=90;
%Total reactant conversion per batch
CO2_total= CO2_selectivity/(CO2_conv_rate/100);
H2O_total= H2O_selectivity/(H2O_conv_rate/100);
%Convert to kg per batch
CO2_total_kg= (CO2_total*44.01)/1000; %CO2 molecular mass= 44.01
H2O_total_kg= (H2O_total*18)/1000; %H2O molecular mass= 18
CO2_total_ton= (CO2_total_kg/1000)*100; % to convert to tonnes/year,
1600 tonnes/year =1 year
H2O_total_ton= (H2O_total_kg/1000)*100; % to convert to tonnes/year,
1600 tonnes/year =1 year

%Material Costing
CO2_cost= (CO2_total_ton*100)*0; %CO2 is free of charge
H2O_cost= (H2O_total_ton*100)*0.76;% Process water costs 0.76 p/t

%Energy balance for determining electricity costs for Microbial
%electrosynthesis
%Assumptions:
%1: The reactors inlet and outlet are to be maintained isothermally at
%operating temperature of 25oC thus no temperature changes to the
reactants
%and products
% Microbial electrosynthesis is assumed as batch process

%cost=0.13; % cost of energy 130£/MWh
cost=0.08; %wind energy
%cost estimation for applying a constant current (for 10t/y)
Energy_tonne= AceticAcid_mol*96485*8; %96485 Coulombs/mol/e, 8
mol/e/acetate, Coulombs in the acetate produced
Energy1_tonne = Energy_tonne* 1.31; %Total coulombs consumed,
coulombic efficiency 69%
Electricity_tonne = (((Energy1_tonne*0.393)/1000)*0.000278)*cost;
%Electricity amount KWh

%cost estimation for applying a constant current (for 1000t/y)
Energy_year = ((AceticAcid_mol*100)*96485*8)*1.31; %96485
Coulombs/mol/e, 8 mol/e/acetate, Coulombs in the acetate produced,
coulombic efficiency 69%(Total coulombs consumed)
Electricity_year = (((Energy_year*0.393)/1000)*0.000278)*cost;
%Electricity amount and cost, KWh

%Energy needed to heat the reactor liquid per batch (19.20 tonnes of
%reaction medium)
m=H2O_mol*18; %reaction medium
c=4.2; %4.2 J/g
dT= 25-16; %degrees needed to increase the temperature
Q_mes=(((m*c*dT)*100)/1e+9)*277.778*cost;%1000 tonnes per year,
277.778 to convert GJ to kW

%Purchased equipment cost for main process units for microbial
electrosynthesis (3 items)(PCE)

```

```

%Estimated using graphical figures. CEPCI index for 2015 547.2
(Cheical
%engineering Journal 2016)
Distillation = 13251.24; %Distillation columns, column diameter=1.5m,
carbon steel sieve trays = 20
Membrane = (350*2); %2 m2 membrane
Reactor = 49789*4; % 4.5m3, 316 stainless steel
Filter = 899 + 1099; % vacuum pump + filter-cartridge 3 m3
Electrode = 830 * 4.6; % Marshall et al 2013 used 30 grams of carbon
graphite for the production of 0.017 M per days thus, 4.6 tonnes of
graphite electrode was estimated to be needed per batch. Cost per
tonne is £830
Mixing = 48838;% 18m3, stainless steel
PCE = Distillation + Membrane + Reactor + Filter + Electrode + Mixing;

%calculating direct cost using Lang factors for capital cost
Lang_factors= [[0.4,0.3];[0.7,0];[0.2,0.1];[0.1,0];[0.15,0];[0.05,0]];
%Create a matrix with Lang factors, 1t column=direct costs, 2nd
column=indirect costs

sum(Lang_factors); %Adding the rows of each collumn
v =sum(Lang_factors);
PCC_direct= PCE*(1+v(1)); %Total purchahse of major equipment cost
FCC= PCC_direct*(1+v(2)); %Total physical plant cost

%Calculating working capital
Working_capital= FCC*0.05;

%Calculating total investment cost
Total_investment_cost= FCC + Working_capital;

%Annual operating costs, Operating time, allowing for plant attainment
=365*0.95 = 347 d/y, 347*24 = 8328 h/y, 8000 working hours.
%calculating operating costs
Y=
[[ (FCC*0.05), (H2O_cost)]; [30000*0.2, ((FCC*0.05)*0.05)]; [(30000*0.5), (Q
_mes+Electricity_year)]; [30000*0.1,0]; [FCC*0.02,0]; [(FCC*0.01),0]; [(FC
C*0.01),0]];

sum(Y); %Adding the rows of each column together, 1st column=Fixed
Cost, 2nd column=Variable Cost
cost= sum(Y);
Operating_cost= sum(cost,2);

%Acetic acid price
Acetic_Acid_price=Operating_cost/1000000;

```

MES- Formic acid production 1000 t/y

```
clear
%Energy balance for determining electricity costs for Microbial
%electrosynthesis
%Assumptions:
%1: The reactors inlet and outlet are to be maintained isothermally at
%operating temperature of 25oC thus no temperature changes to the
reactants
%and products
% Microbial electrosynthesis is assumed as batch process

%Material Balance for determining raw material cost for Microbial
%electrosynthesis
%Main Reaction: CO2 + 2H2O + 2e- = HCOOH + H2O +0.5O2
%Assumptions:
%1:Process Plant is runs in batches, each batch lasts for 3.66 days
and the plant operates for 100 batches per year
%2:Formic acid is lost during process units thus 6.5% formic acid is
targeted in the reactor
%3:Selectivity for CO2=58.8% and for H2O=90%
%4:Conversion rate to yield: CO2=88% and H2O=90%
%5:No side reactions are occurring

%Calculations for how much of reactants are required for a 1000 ton/y
production of formic acid
Formicacid_mol= 217273.2; %For 1 tonne production in 3.66 days
assuming 1000 tonne production in 1 year, targeted flowrate 347634 M
CO2_mol= 1 * Formicacid_mol; %2 mole of CO2 are required for 1 mole of
formic acid production
H2O_mol= 2 * Formicacid_mol; %4 moles of H2O are required for 1 mole
of formic acid production
H2O_mol_product= 1 * Formicacid_mol; %1 mole of H2O are produced for 1
mole of formic acid production

%Selectivity calculations: Selectivity of reactant(s)=reactant
converted to formic acid/ total reactant converted
CO2_converted=88;
H2O_converted=90;
CO2_selectivity= (100/CO2_converted)*CO2_mol;
H2O_selectivity= (100/H2O_converted)*H2O_mol;

%Conversion of reactants
%Yield(%)=Selectivity * Conversion
CO2_conv_rate=58.5; % 58.5% is the average conversion achieved
experimentally (Marshall et.al, Electrosynthesis of Commodity
Chemicals by an Autotrophic Microbial Community)
H2O_conv_rate=90;
%Total reactant conversion per batch
CO2_total= CO2_selectivity/(CO2_conv_rate/100);
H2O_total= H2O_selectivity/(H2O_conv_rate/100);
%Convert to kg per batch
CO2_total_kg= (CO2_total*44.01)/1000; %CO2 molecular mass= 44.01
H2O_total_kg= (H2O_total*18)/1000; %H2O molecular mass= 18
CO2_total_ton= (CO2_total_kg/1000)*100; % to convert to tonnes/year,
1600 tonnes/year =1 year
H2O_total_ton= (H2O_total_kg/1000)*100; % to convert to tonnes/year,
1600 tonnes/year =1 year

%Material Costing
CO2_cost= (CO2_total_ton*100)*0; %CO2 is free of charge
```

```

H2O_cost= (H2O_total_ton*100)*0.76;% Process water costs 0.76 p/t

%Energy needed to heat the reactor liquid per batch (19.20 tonnes of
%reaction medium)
m=H2O_mol*18; %reaction medium
c=4.2; %4.2 J/g
dT= 25-15; %degrees needed to increase the temperature
%cost=0.13; % cost of energy 130£/MWh
cost=0.08; %wind energy
Q_mes=((m*c*dT)*100)/1e+9)*277.778*cost;%1000 tonnes per year,
277.778 to convert GJ to kW

%cost estimation for applying a constant current (for 10t/y)
Energy_tonne= Formicacid_mol*96485*2; %96485 Coulombs/mol/e, 8
mol/e/acetate, Coulombs in the acetate produced
Energy1_tonne = Energy_tonne* 1.31; %Total coulombs consumed,
coulombic efficiency 69%clear
Electricity_tonne = (((Energy1_tonne*0.203)/1000)*0.000278)*cost;
%Electricity amount kWh
%cost estimation for applying a constant current (for 1000t/y)
Energy_year = ((Formicacid_mol*100)*96485*2)*1.31; %96485
Coulombs/mol/e, 8 mol/e/acetate, Coulombs in the acetate produced,
coulombic efficiency 69%(Total coulombs consumed)
Electricity_year = (((Energy_year*0.203)/1000)*0.000278)*cost;
%Electricity amount and cost, kWh

%Capital cost of Microbial electrosynthesis
N=4; %functional units
Q=1600; %plant capacity (t/y)
s=1; %reactor conversion
C=170*N*(Q/s)^0.675);

%Purchased equipment cost for main process units for microbial
electrosynthesis (3 items)(PCE)
%Estimated using graphical figures. CEPCI index for 2015 547.2
(Cheical
%engineering Journal 2016)
Distillation = 13251.24; %Distillation columns, column diameter=1.5m,
carbon steel sieve trays = 20Membrane = 350*2;
Membrane = 350*2; %2 m2 membrane
Reactor = 66607; % 7.8m3, 316 stainless steel
Filter = 899 + 1099; % vacuum pump + filter-cartridge 3 m3
Electrode = 830 * 4.6; % Marshall et al 2013 used 30 grams of carbon
graphite for the production of 0.017 M per days thus, 4.6 tonnes of
graphite electrode was estimated to be needed per batch. Cost per
tonne is £830
Electrode = 300;
Mixing=30879;%7.8m3
PCE = Distillation + Membrane + Reactor + Filter + Electrode+Mixing ;

%Calculating direct cost using Lang factors for capital cost
Lang_factors= [[0.4,0.3];[0.7,0];[0.2,0.1];[0.1,0];[0.15,0];[0.05,0]];
%Create a matrix with Lang factors, 1st column=direct costs, 2nd
column=indirect costs
sum(Lang_factors); %Adding the rows of each column
v =sum(Lang_factors);
PCC_direct= PCE*(1+v(1)); %Total purchase of major equipment cost
FCC= PCC_direct*(1+v(2)); %Total physical plant cost

%Calculating working capital
Working_capital= FCC*0.05;

```

```

%Calculating total investment cost
Total_investment_cost= FCC + Working_capital;

%Annual operating costs,Operating time, allowing for plant attainment
=365*0.95 = 347 d/y, 347*24 = 8328 h/y, 8000 working hours.
%Calculating operating costs
Y=[[ (FCC*0.05), (H2O_cost)];[30000, ((FCC*0.05)*0.05)];[(30000*0.2), (Q_m
es+
Electricity_year)];[30000*0.5,0];[30000*0.1,0];[FCC*0.02,0];[(FCC*0.01
),0];[(FCC*0.01),0]];

sum(Y); %Adding the rows of each column together, 1st column=Fixed
Cost, 2nd column=Variable Cost
cost= sum(Y);
Operating_cost= sum(cost,2);

%Acetic acid price
Formic_Acid_price=Operating_cost/1000000;

```

MES- Propionate production 1000 t/y

```

clear
%Material Balance for determining raw material cost for microbial
%electrosynthesis
%Main Reaction: 3CO2 + 10H2O + 6e- = CH3CH2CHOOH + 5H2O +
%Assumptions:
%1:Process Plant is runs in batches, each batch lasts for 3.66 days
and the plant operates for 100 batches per year
%2:Propionic acid is lost during process units thus 6.5% propionic
acid is targeted in the reactor
%3:Selectivity for CO2=58.8% and for H2O=90%
%4:Conversion rate to yield: CO2=88% and H2O=90%
%5:No side reactions are occurring

%Calculations for how much of reactants are required for a 1000 ton/y
production of propionic acid
Propionic_mol= 134992.8; %For 10 tonne production in 3.66 days
assuming 1600 tonne production in 1 year, targeted flowrate 215986 M
CO2_mol= 3 * Propionic_mol; %3 moles of CO2 are required for 1 mole of
propionic acid production
H2O_mol= 10 * Propionic_mol; %10 moles of H2O are required for 1 mole
of propionic acid production
H2O_mol_product= 5 * Propionic_mol; %7 moles of H2O are produced for 1
mole of propionic acid production

%Selectivity calculations: Selectivity of reactant(s)=reactant
converted to propionic acid/ total reactant converted
CO2_converted=88;
H2O_converted=90;
CO2_selectivity= (100/CO2_converted)*CO2_mol;
H2O_selectivity= (100/H2O_converted)*H2O_mol;

%Conversion of reactants
%Yield(%)=Selectivity * Conversion
CO2_conv_rate=58.5; % 58.5% is the average conversion achieved
experimentally (Marshall et.al, Electrosynthesis of Commodity
Chemicals by an Autotrophic Microbial Community)
H2O_conv_rate=90;

```



```

%Total reactant conversion per batch
CO2_total= CO2_selectivity/(CO2_conv_rate/100);
H2O_total= H2O_selectivity/(H2O_conv_rate/100);
%Convert to kg per batch
CO2_total_kg= (CO2_total*44.01)/1000; %CO2 molecular mass= 44.01
H2O_total_kg= (H2O_total*18)/1000; %H2O molecular mass= 18
CO2_total_ton= (CO2_total_kg/1000)*100; % to convert to tonnes/year,
1600 tonnes/year =1 year
H2O_total_ton= (H2O_total_kg/1000)*100; % to convert to tonnes/year,
1600 tonnes/year =1 year

%Material Costing
CO2_cost= (CO2_total_ton*100)*0; %CO2 is free of charge
H2O_cost= (H2O_total_ton*100)*0.76;% Process water costs 0.76 p/t

%Energy balance for determining electricity costs for Microbial
%electrosynthesis
%Assumptions:
%1: The reactors inlet and outlet are to be maintained isothermally at
%operating temperature of 25oC thus no temperature changes to the
reactants
%and products
% Microbial electrosynthesis is assumed as batch process

%cost=0.13; % cost of energy 130£/MWh
cost=0.08; %Wind energy
%cost estimation for applying a constant current (for 1t/y)
Energy_tonne= Propionic_mol*96485*6; %96485 Coulombs/mol/e, 8
mol/e/acetate, Coulombs in the acetate produced
Energy1_tonne = Energy_tonne* 1.31; %Total coulombs consumed,
coulombic efficiency 69%
Electricity_tonne = (((Energy1_tonne*0.29)/1000)*0.000278)*cost;
%Electricity amount KWh

%cost estimation for applying a constant current (for 100t/y)
Energy_year = ((Propionic_mol*100)*96485*6)*1.31; %96485
Coulombs/mol/e, 8 mol/e/acetate, Coulombs in the acetate produced,
coulombic efficiency 69%(Total coulombs consumed)
Electricity_year = (((Energy_year*0.29)/1000)*0.000278)*cost;
%Electricity amount and cost, KWh

%Energy needed to heat the reactor liquid per batch (19.20 tonnes of
%reaction medium)
m=H2O_mol*18; %reaction medium
c=4.2; %4.2 J/g
dT= 25-15; %degrees needed to increase the temperature
Q_mes= ((m*c*dT)*100)/1e+9)*277.778*cost;%1600 tonnes per year,
277.778 to convert GJ to kW

%Capital cost of Microbial electrosynthesis
N=4; %functional units
Q=1600; %plant capacity (t/y)
s=1; %reactor conversion
C=170*N*( (Q/s)^0.675);

%Purchased equipment cost for main process units for microbial
electrosynthesis (3 items)(PCE)
%Estimated using graphical figures. CEPCI index for 2015 547.2
(Cheical

```

```

%engineering Journal 2016)
Distillation = 9937.46; %Distillation columns, column diameter=1.5m,
carbon steel sieve trays = 10
Membrane = 350*2; %2 m2 membrane
Reactor = 69271*3; % 8.3m3, 316 stainless steel (x4 reactors)
Filter = 899 + 1099; % vacuum pump + filter-cartridge 3 m3
Electrode = 830 * 4.6; % Marshall et al 2013 used 30 grams of carbon
graphite for the production of 0.017 M per days thus, 4.6 tonnes of
graphite electrode was estimated to be needed per batch. Cost per
tonne is £830
Mixing =58475; %25m3
PCE = Distillation + Reactor + Filter + Electrode +Mixing ;

%Calculating direct cost using Lang factors for capital cost
Lang_factors= [[0.4,0.3];[0.7,0];[0.2,0.1];[0.1,0];[0.15,0];[0.05,0]];
%Create a matrix with Lang factors, 1st column=direct costs, 2nd
column=indirect costs

sum(Lang_factors); %Adding the rows of each column
v =sum(Lang_factors);
PCC_direct= PCE*(1+v(1)); %Total purchase of major equipment cost
FCC= PCC_direct*(1+v(2)); %Total physical plant cost

%Calculating working capital
Working_capital= FCC*0.05;

%Calculating total investment cost
Total_investment_cost= FCC + Working_capital;

%Annual operating costs, Operating time, allowing for plant attainment
=365*0.95 = 347 d/y, 347*24 = 8328 h/y, 8000 working hours.
%Calculating operating costs
Y=[[ (FCC*0.05), (H2O_cost)];[30000, ((FCC*0.05)*0.05)];[(30000*0.2), (Q_m
es+Electricity_year)];[30000*0.5,0];[30000*0.1,0];[FCC*0.02,0];[(FCC*0
.01),0];[(FCC*0.01),0]];

sum(Y); %Adding the rows of each column together, 1st column=Fixed
Cost, 2nd column=Variable Cost
cost= sum(Y);
Operating_cost= sum(cost,2);

%Acetic acid price
Propionic_Acid_price=Operating_cost/1000000;

```

MES- Ethanol production 1000 t/y

```

clear
%Material Balance for determining raw material cost for Microbial
%electrosynthesis
%Main Reaction: 2CO2 + 9H2O + 18e- = CH3CH2OH + 6H2O + 3O2
%Assumptions:
%1:Process Plant is runs in batches, each batch lasts for 3.66 days
and the plant operates for 100 batches per year
%2:Ethanol is lost during process units thus 6.5% ethanol is targeted
in the reactor
%3:Selectivity for CO2=58.8% and for H2O=90%
%4:Conversion rate to yield: CO2=88% and H2O=90%

```

```

%5:No side reactions are occurring

%Calculations for how much of reactants are required for a 1000 ton/y
%production of ethanol
Ethanol_mol= 217070.4; %For 10 tonne production in 3.66 days assuming
1000 tonne production in 1 year, targeted flowrate 347309 M
CO2_mol= 2 * Ethanol_mol; %2 moles of CO2 are required for 1 mole of
ethanol production
H2O_mol= 9*Ethanol_mol; %for 10% of ethanol production
H2O_mol_product= 6*Ethanol_mol;

%Selectivity calculations: Selectivity of reactant(s)=reactant
converted to ethanol/ total reactant converted
CO2_converted=88;
H2O_converted=90;
CO2_selectivity= (100/CO2_converted)*CO2_mol;
H2O_selectivity= (100/H2O_converted)*H2O_mol;

%Conversion of reactants
%Yield(%)=Selectivity * Conversion
CO2_conv_rate=58.5; % 58.5% is the average conversion achieved
experimentally (Marshall et.al, Electrosynthesis of Commodity
Chemicals by an Autotrophic Microbial Community)
H2O_conv_rate=90;
%Total reactant conversion per batch
CO2_total= CO2_selectivity/(CO2_conv_rate/100);
H2O_total= H2O_selectivity/(H2O_conv_rate/100);
%Convert to kg per batch
CO2_total_kg= (CO2_mol*44.01)/1000; %CO2 molecular mass= 44.01
H2O_total_kg= (H2O_mol*18)/1000; %H2O molecular mass= 18
CO2_total_ton= (CO2_total_kg/1000)*100; % to convert to tonnes/year,
1600 tonnes/year =1 year
H2O_total_ton= (H2O_total_kg/1000)*100; % to convert to tonnes/year,
1600 tonnes/year =1 year

%Material Costing
CO2_cost= (CO2_total_ton*100)*0; %CO2 is free of charge
H2O_cost= (H2O_total_ton*100)*0.76;% Process water costs 0.76 p/t

%Energy balance for determining electricity costs for Microbial
%electrosynthesis
%Assumptions:
%1: The reactors inlet and outlet are to be maintained isothermally at
%operating temperature of 25oC thus no temperature changes to the
reactants
%and products
% Microbial electrosynthesis is assumed as batch process

%cost=0.13; % cost of energy 130£/MWh
cost=0.08; %wind energy
%cost estimation for applying a constant current (for 1t/y)
Energy_tonne= Ethanol_mol*96485*18; %96485 Coulombs/mol/e, 8
mol/e/acetate, Coulombs in the acetate produced
Energy1_tonne = Energy_tonne* 1.31; %Total coulombs consumed,
coulombic efficiency 69%
Electricity_tonne = (((Energy1_tonne*0.335)/1000)*0.000278)*cost;
%Electricity amount KWh

%cost estimation for applying a constant current (for 100t/y)

```

```

Energy_year      =      ((Ethanol_mol*100)*96485*18)*1.31;      %96485
Coulombs/mol/e, 8 mol/e/acetate, Coulombs in the acetate produced,
coulombic efficiency 69%(Total coulombs consumed)
Electricity_year      =      (((Energy_year*0.335)/1000)*0.000278)*cost;
%Electricity amount and cost, kWh

%Energy needed to heat the reactor liquid per batch (19.20 tonnes of
%reaction medium)
m=H2O_mol*18; %reaction medium
c=4.2; %4.2 J/g
dT= 25-15; %degrees needed to increase the temperature
Q_mes=(((m*c*dT)*100)/1e+9)*277.778*cost;%1600 tonnes per year,
277.778 to convert GJ to kW

%Capital cost of Microbial electrosynthesis
N=4; %functional units
Q=1600; %plant capacity (t/y)
s=1; %reactor conversion
C=170*N*((Q/s)^0.675);

%Purchased equipment cost for main process units for microbial
electrosynthesis (3 items)(PCE)
%Estimated using graphical figures
Distillation = 19214.02; %Distillation columns, column diameter=1.5m,
carbon steel sieve trays = 20Membrane = 350*2;
Membrane = 350*2; %2 m2 membrane
Reactor = 44243*10; % 3.6m3, 316 stainless steel
Filter = 899 + 1099; % vacuum pump + filter-cartridge 3 m3
Electrode = 830 * 4.6; % Marshall et al 2013 used 30 grams of carbon
graphite for the production of 0.017 M per days thus, 4.6 tonnes of
graphite electrode was estimated to be needed per batch. Cost per
tonne is £830
Mixing=48838*2;%18me
PCE = Distillation + Membrane + Reactor + Filter + Electrode+Mixing ;

%Calculating direct cost using Lang factors
Lang_factors      =
[[0.4,0.3];[0.7,0];[0.2,0.1];[0.1,0];[0.15,0];[0.05,0]]; %Create a
matrix with Lang factors, 1t column=direct costs, 2nd column=indirect
costs

sum(Lang_factors); %Adding the rows of each collumn
v =sum(Lang_factors);
PCC_direct= PCE*(1+v(1)); %Total purchahse of major equipment cost
FCC= PCC_direct*(1+v(2)); %Total physical plant cost

%Calculating working capital
Working_capital= FCC*0.05;

%Calculating total investment cost
Total_investment_cost= FCC + Working_capital;

%Annual operating costs,Operating time, allowing for plant attainment
=365*0.95 = 347 d/y, 347*24 = 8328 h/y, 8000 working hours.
%Calculating operating costs
Y=
[[ (FCC*0.05), (H2O_cost) ]; [30000, ((FCC*0.05)*0.05) ]; [ (30000*0.2), (Q_mes

```

```

+Electricity_year)];[30000*0.5,0];[30000*0.1,0];[FCC*0.02,0];[(FCC*0.0
1),0];[(FCC*0.01),0]];

sum(Y); %Adding the rows of each column together, 1st column=Fixed
Cost, 2nd column=Variable Cost
cost= sum(Y);
Operating_cost= sum(cost,2);

%Acetic acid price
Ethanol=Operating_cost/1000000;

```

MES- Methanol production 1000 t/y

```

clear
%Material Balance for determining raw material cost for microbial
%electrosynthesis
%Main Reaction: CO2 + 3H2O + 6e- = CH3OH + H2O + 0.5O2
%Assumptions:
%1:Process Plant is runs in batches, each batch lasts for 3.66 days
and the plant operates for 100 batches per year
%2:methanol is lost during process units thus 6.5% methanol is
targeted in the reactor
%3:Selectivity for CO2=58.8% and for H2O=90%
%4:Conversion rate to yield: CO2=88% and H2O=90%
%5:No side reactions are occurring

%Calculations for how much of reactants are required for a 1000 ton/y
production of methanol
Methanol_mol= 312109.8; %For 10 tonne production in 3.66 days assuming
1000 tonne production in 1 year, targeted flowrate 499375 M
CO2_mol= 1 * Methanol_mol; %1 mole of CO2 are required for 1 mole of
methanol production
H2O_mol= 9*Methanol_mol; %3 moles of H2O are required for 1 mole of
methanol production
H2O_mol_product= 8*Methanol_mol; %1 mole of H2O are produced for 1
mole of methanol production

% %Selectivity calculations: Selectivity of reactant(s)=reactant
converted to methanol/ total reactant converted
% CO2_converted=88;
% H2O_converted=90;
% CO2_selectivity= (100/CO2_converted)*CO2_mol;
% H2O_selectivity= (100/H2O_converted)*H2O_mol;
%
% %Conversion of reactants
% %Yield(%)=Selectivity * Conversion
% CO2_conv_rate=58.5; % 58.5% is the average conversion achieved
experimentally (Marshall et.al,Electrosynthesis of Commodity Chemicals
by an Autotrophic Microbial Community)
% H2O_conv_rate=90;
% %Total reactant conversion per batch
% CO2_total= CO2_selectivity/(CO2_conv_rate/100);
% H2O_total= H2O_selectivity/(H2O_conv_rate/100);
%Convert to kg per batch
CO2_total_kg= (CO2_mol*44.01)/1000; %CO2 molecular mass= 44.01
H2O_total_kg= (H2O_mol*18)/1000; %H2O molecular mass= 18
CO2_total_ton= (CO2_total_kg/1000)*100; % to convert to tonnes/year,
1600 tonnes/year =1 year

```

```

H2O_total_ton= (H2O_total_kg/1000)*100; % to convert to tonnes/year,
1600 tonnes/year =1 year

%Material Costing
CO2_cost= (CO2_total_ton*100)*0; %CO2 is free of charge
H2O_cost= (H2O_total_ton*100)*0.76;% Process water costs 0.76 p/t

%Energy balance for determining electricity costs for Microbial
%electrosynthesis
%Assumptions:
%1: The reactors inlet and outlet are to be maintained isothermally at
%operating temperature of 25oC thus no temperature changes to the
reactants
%and products
% Microbial electrosynthesis is assumed as batch process

%cost=0.13; % cost of energy 130£/MWh
cost=0.08;
%cost estimation for applying a constant current (for 1t/y)
Energy_tonne= Methanol_mol*96485*6; %96485 Coulombs/mol/e, 8
mol/e/acetate, Coulombs in the acetate produced
Energy1_tonne = Energy_tonne* 1.31; %Total coulombs consumed,
coulombic efficiency 69%
Electricity_tonne = (((Energy1_tonne*0.390)/1000)*0.000278)*cost;
%Electricity amount KWh

%cost estimation for applying a constant current (for 100t/y)
Energy_year = ((Methanol_mol*100)*96485*6)*1.31; %96485
Coulombs/mol/e, 8 mol/e/acetate, Coulombs in the acetate produced,
coulombic efficiency 69%(Total coulombs consumed)
Electricity_year = (((Energy_year*0.390)/1000)*0.000278)*cost;
%Electricity amount and cost, KWh

%Energy needed to heat the reactor liquid per batch (19.20 tonnes of
%reaction medium)
m=H2O_mol*18; %reaction medium
c=4.2; %4.2 J/g
dT= 25-15; %degrees needed to increase the temperature
Q_mes=(((m*c*dT)*100)/1e+9)*277.778*cost;%1600 tonnes per year,
277.778 to convert GJ to kW

%Capital cost of Microbial electrosynthesis
N=4; %functional units
Q=1600; %plant capacity (t/y)
s=1; %reactor conversion
C=170*N*(Q/s)^0.675);

%Purchased equipment cost for main process units for microbial
electrosynthesis (3 items)(PCE)
%Estimated using graphical figures
Distillation = 13251.24; %Distillation columns, column diameter=1.5m,
carbon steel sieve trays = 20
Membrane = 350*2; %2 m2 membrane
Reactor = 52643*10; % 5m3, 316 stainless steel (x10 reactors)
Filter = 899 + 1099; % vacuum pump + filter-cartridge 3 m3
Electrode = 830 * 4.6; % Marshall et al 2013 used 30 grams of carbon
graphite for the production of 0.017 M per days thus, 4.6 tonnes of

```

```

graphite electrode was estimated to be needed per batch. Cost per
tonne is £830
Mixing = 58475*2; %25m3 (2 tanks)
PCE = Distillation + Membrane + Reactor + Filter + Electrode ;

%Calculating direct cost using Lang factors
Lang_factors= [[0.4,0.3];[0.7,0];[0.2,0.1];[0.1,0];[0.15,0];[0.05,0]];
%Create a matrix with Lang factors, 1st column=direct costs, 2nd
column=indirect costs

sum(Lang_factors); %Adding the rows of each column
v =sum(Lang_factors);
PCC_direct= PCE*(1+v(1)); %Total purchase of major equipment cost
FCC= PCC_direct*(1+v(2)); %Total physical plant cost

%Calculating working capital
Working_capital= FCC*0.05;

%Calculating total investment cost
Total_investment_cost= FCC + Working_capital;

%Annual operating costs, Operating time, allowing for plant attainment
=365*0.95 = 347 d/y, 347*24 = 8328 h/y, 8000 working hours.
%Calculating operating costs
Y=[[ (FCC*0.05), (H2O_cost)];[30000, ((FCC*0.05)*0.05)];[(30000*0.2), (Q_m
es+Electricity_year)];[30000*0.5,0];[30000*0.1,0];[FCC*0.02,0];[(FCC*0
.01),0];[(FCC*0.01),0]];

sum(Y); %Adding the rows of each column together, 1st column=Fixed
Cost, 2nd column=Variable Cost
cost= sum(Y);
Operating_cost= sum(cost,2);

%Acetic acid price
Methanol_price=Operating_cost/1000000;

```

Table 0-2: Example of Lang factors calculation for acetic acid production (100 t/y) via MES using the purchased equipment cost.

Bare erected	Factors	Cost (£/t)	External Capital	Factors	Cost (£/t)
Equipment erection	0.4	199.32	Design and Engineering and Contractor's fee	0.3	358.77
Piping	0.7	348.81	Contingency	0.1	119.59
Instrumentation	0.2	99.66	Total	0.4	478.36
Electrical	0.1	49.83			
Building and Civil	0.15	74.745			
Civil	0.05	24.91			
Total	1.6	797.28			

- The major purchased equipment cost was used to calculate the total physical plant and fixed capital costs as shown below:
 - Total physical plant cost= purchased equipment cost × Total bare erected factors
 - Total physical plant cost= $49830 \times (1+1.6) = 129560$ £
 - Fixed capital cost = Total physical plant cost × Total external capital factors
 - Fixed capital cost = $129560 \times (1+0.4) = 181380$ £
- The total investment cost was calculated by summing the fixed capital cost and the working capital cost
 - Working capital cost was assumed as 0.05% of the fixed capital cost
 - Total investment cost = $181,380 \times (181,380 \times 0.05) = 190,450$ or 1,904 £/t

A3 – Selectivity and conversion rates

To calculate the reactants flowrate and obtain final reactants quantities the values in Table 0-3 were used.

Table 0-3: Selectivity and conversion rates

	Methanol Carbonylation	Ethane Oxidation	AF	MES
Selectivity (%)	$CH_3OH=99.5$ $CO=94$	$CH_3CH_3=99$ $O_2=94$	$CO=94$ $H_2O=99$	$CO_2=94$ $H_2O=99$
Conversion rate to yield (%)	$CH_3OH=90.5$ $CO=88.35$	$CH_3CH_3=90$ $O_2=88$	$CO=99$ $H_2O=90$	$CO_2=58.5$ $H_2O=90$

A4: Energy and acetic acid production costs

Table 0-4: Energy costs per MWh from different technologies and acetic acid production costs (£/kg) of the Integrated process

Energy sources	Cost (£/MWh)	Acetic acid production cost from Integrated process (£/kg)
Onshore wind	80	0.233
Gas	130	0.24
Nuclear	105	0.238
Coal	128-184	0.24-0.27
Offshore wind	147	0.25
Solar photovoltaics	171	0.26

A5: Energy values and costs

Table 0-5: Energy values of MES

Process Units	Acetic acid (100 t/y)	Acetic acid (1000 t/y)	Formic acid (1000 t/y)	Propionic acid (1000 t/y)	Ethanol (1000 t/y)	Methanol (1000 t/y)
	Energy (kWh)					
Mixer	1861	18611	4722	30555	56666	16666
MES reactor	20285	1379722	666111	856111	4641111	2586111
Gas separator/ membrane	12972	129722	84722	157777	169166	121388
Rectification unit	4001111	40011111	2110555	35814444	1347222	1331388

Table 0-6: Energy values of anaerobic fermentation and Integrated process

Process Units	Anaerobic fermentation (100 t/y)	Integrated Process (200 t/y)
	Energy (kWh)	
Mixer	1861	3722
Reactor	NA	20285
Gas separator/ membrane	12972	25944
Rectification unit	4001111	4001111

Table 0-7: Investment, operating and production costs and rate of return of formic and propionic acids and methanol and alcohol using MES (1000 t/y) including full utility costs. Chemical such as: acetic, formic and propionic acids, and alcohols; methanol and ethanol were assessed for plant capacities of 1000 t/y.

Products	Total investment cost (£)	Operating cost (£ p.a.)	Production costs (£/kg)	Production cost using renewable energy (£/kg)	Market price (£/kg) (ICIS, 2016)	Discounted cash flow rate of return (%)
Acetic acid	1,009,300	5,743,200	5.74	3.84	0.48	NA
Formic acid	434700	493,170	0.49	0.30	0.38	21
Propionic acid	1,066,500	5,167,000	5.16	3.46	1.01	NA
Methanol	2,074,100	1,153,300	1.15	0.77	0.23	NA
Ethanol	2,149,200	1,318,300	1.31	0.88	1.09	14

A6: Mass flow rates

Table 0-8: Mass flow rates of MES plant for acetic acid production (100 t/y)

Acetic acid (100 t/y)		In (t/y)		Out (t/y)
Mixer	Water	222.22	Water	222.22
	CO ₂	283.27	CO ₂	283.27
Bioreactor	CO ₂	283.27	CO ₂	116.70
	Water	222.22	Water	142.22
	Product	0	Product	100
	Oxygen	0	Oxygen	106.57
Gas Separator	CO ₂	116.70	CO ₂	116.70
	Oxygen	106.57	Oxygen	106.57
Rectification Unit	Water	142.22	Water	142.22
	Product	100	Product	100
Storage Tank	Product	100	Product	100

Table 0-9: Mass flow rates of AF plant for acetic acid production (100 t/y)

Acetic acid (100 t/y)		In (t/y)		Out (t/y)
Mixer	Water	67.28	Water	67.28
	CO	190.36	CO	190.36
Fermenter	CO	190.36	CO	4.64
	Water	67.28	Water	1.02
	Product	0	Product	100
	CO ₂	0	CO ₂	146.58
Gas Separator	CO	4.64	CO	4.64
	CO ₂	146.58	CO ₂	146.58
Rectification Unit	Water	1.02	Water	1.02
	Product	100	Product	100
Storage Tank	Product	100	Product	100

Table 0-10: Mass flow rates of integrated process (MES and AF) plant for acetic acid production (200 t/y)

Acetic acid (200 t/y)		In (t/y)		Out (t/y)
Mixer (MES)	Water	222.22	Water	222.22
	CO ₂	283.27	CO ₂	283.27
Mixer (AF)	Water	67.28	Water	67.28
	CO	190.36	CO	190.36
Bioreactor	CO ₂	283.27	CO ₂	116.70
	Water	222.22	Water	142.22
	Product	0	Product	100
	Oxygen	0	Oxygen	106.57
Fermenter	CO	190.36	CO	4.64
	Water	67.28	Water	1.02
	Product	0	Product	100
	CO ₂	0	CO ₂	146.58
Gas Separator	CO ₂	263.28	CO ₂	263.28
	Oxygen	106.57	Oxygen	106.57
	CO	4.64	CO	4.64
Rectification Unit	Water	143.24	Water	143.24
	Product	200	Product	200
Storage Tank	Product	200	Product	200

Table 0-11: Mass flow rates of MES plant for acetic acid production (1000 t/y)

Acetic acid (1000 t/y)		In (t/y)		Out (t/y)
Mixer	Water	2222.22	Water	2222.22
	CO ₂	2832.75	CO ₂	2832.75
Bioreactor	CO ₂	2832.75	CO ₂	1167.09
	Water	2222.22	Water	1422.22
	Product	0	Product	1000
	Oxygen	0	Oxygen	1065.78
Gas Separator	CO ₂	1167.09	CO ₂	1167.09
	Oxygen	1065.78	Oxygen	1065.78
Rectification Unit	Water	1422.22	Water	1422.22
	Product	1000	Product	1000
Storage Tank	Product	1000	Product	1000

Table 0-12: Mass flow rates of MES plant for formic acid production (1000 t/y)

Formic acid (1000 t/y)		In (t/y)		Out (t/y)
Mixer	Water	966.45	Water	966.45
	CO ₂	1847.96	CO ₂	1847.96
Bioreactor	CO ₂	1847.96	CO ₂	761.36
	Water	966.45	Water	488.06
	Product	0	Product	1000
	Oxygen	0	Oxygen	347.63
Gas Separator	CO ₂	761.36	CO ₂	761.36
	Oxygen	347.63	Oxygen	347.63
Rectification Unit	Water	488.06	Water	488.06
	Product	1000	Product	1000
Storage Tank	Product	1000	Product	1000

Table 0-13: Mass flow rates of MES plant for propionic acid production (1000 t/y)

Propionic acid (1000 t/y)		In (t/y)		Out (t/y)
Mixer	Water	3002.26	Water	3002.26
	CO ₂	3444.38	CO ₂	3444.38
Bioreactor	CO ₂	3444.38	CO ₂	1419.08
	Water	3002.26	Water	2002.50
	Product	0	Product	1000
	Oxygen	0	Oxygen	2807.77
Gas Separator	CO ₂	1419.08	CO ₂	1419.08
	Oxygen	2807.77	Oxygen	2807.77
Rectification Unit	Water	2002.50	Water	2002.50
	Product	1000	Product	1000
Storage Tank	Product	1000	Product	1000

Table 0-14: Mass flow rates of MES plant for methanol production (1000 t/y)

Methanol (1000 t/y)		In (t/y)		Out (t/y)
Mixer	Water	2082.46	Water	2082.46
	CO ₂	2654.60	CO ₂	2654.60
Bioreactor	CO ₂	2654.60	CO ₂	1093.70
	Water	2082.46	Water	770.51
	Product	0	Product	1000
	Oxygen	0	Oxygen	1498.12
Gas Separator	CO ₂	1093.70	CO ₂	1093.70
	Oxygen	1498.12	Oxygen	1498.12
Rectification Unit	Water	770.51	Water	770.51
	Product	1000	Product	1000
Storage Tank	Product	1000	Product	1000

Table 0-15: Mass flow rates of MES plant for ethanol production (1000 t/y)

Ethanol (1000 t/y)		In (t/y)		Out (t/y)
Mixer	Water	4344.83	Water	4344.83
	CO ₂	3692.35	CO ₂	3692.35
Bioreactor	CO ₂	3692.35	CO ₂	1521.25
	Water	4344.83	Water	2780.70
	Product	0	Product	1000
	Oxygen	0	Oxygen	2083.78
Gas Separator	CO ₂	1521.25	CO ₂	1521.25
	Oxygen	2083.78	Oxygen	2083.78
Rectification Unit	Water	2780.70	Water	2780.70
	Product	1000	Product	1000
Storage Tank	Product	1000	Product	1000

B1: Growth curves in aerobic conditions

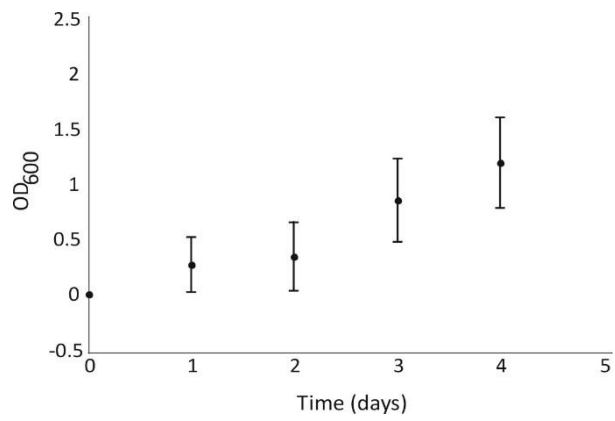


Figure 0.1 : *Shewanella Oneidensis* MR-1 growth curves in Luria broth medium under aerobic conditions. The experiment was performed in quadruplicates (n=4).

B2: Medium compositions

Table 0-16: Medium A

Chemical Description	FW	g/L	Molecular Formula	Conc. in final medium prep.(mM)
•PIPES buffer	302.4	0.91	C ₈ H ₁₈ N ₂ O ₆ S ₂	3.00
•Dipotassium phosphate	174.2	0.225	K ₂ HPO ₄	1.30
•Monopotassium phosphate	136.08	0.225	KH ₂ PO ₄	1.60
•Sodium chloride	58.44	0.46	NaCl	7.80
•Ammonium sulphate	132.14	0.225	(NH ₄) ₂ SO ₄	1.70
•Magnesium sulphate	120.366	0.117	MgSO ₄	9.72 × 10 ⁻⁴
•Minerals solution, 100X stock		10 mL	-	see below
•Vitamins solution, 100X stock		10 mL	--	see below
•Amino acid solution, 100X stock		10 mL		see below
•Fumaric acid (for growth in anaerobic conditions)	160.1	4.8	C ₄ H ₂ O ₄ Na ₂	30
•Sodium lactate, 60%(w/w) syrup(@) (for bacterial growth)	112.1	11.206	C ₃ H ₅ O ₃ Na	100

Table 0-17: Medium B

Chemical Description	FW	g/L	Molecular Formula	Conc. in final medium prep. (mM)
•HEPES	238.30	4.766	C ₈ H ₁₈ N ₂ O ₄ S	20
•Dipotassium phosphate	174.2	0.884	K ₂ H ₂ PO ₄	5.08
•Monopotassium phosphate	136.08	0.397	K ₂ HPO ₄	2.92
•Sodium chloride	58.44	29.22	NaCl	500
•Ammonium sulphate	132.14	4.757	(NH ₄) ₂ SO ₄	36
•Sodium bicarbonate	84.007	4.757	NaHCO ₃	8
•Calcium chloride	147.014	0.0713	CaCl ₂ .2H ₂ O	0.485
•Minerals solution, 100X stock		10 mL	-	see below
•Vitamins solution, 100X stock		10 mL	--	see below
•Amino acid solution, 100X stock		10 mL		see below
•Fumaric acid (for growth in anaerobic conditions)	160.1	4.8	C ₄ H ₂ O ₄ Na ₂	30
•Sodium lactate, 60%(w/w) syrup(@) (for bacterial growth)	112.1	11.206	C ₃ H ₅ O ₃ Na	100

Table 0-18: Medium C

Chemical Description	FW	g/L	Formula	Conc. in final medium (mM)
•PIPES buffer	302.4	0.91	C ₈ H ₁₈ N ₂ O ₆ S ₂	3
•Sodium hydroxide	40.00	0.3	NaOH	7.5
•Ammonium chloride	53.49	1.5	NH ₄ Cl	28.04
•Potassium chloride	74.55	0.1	KCl	1.34
•Sodium phosphate monobasic	138.0	0.6	NaH ₂ PO ₄ H ₂ O	4.35
•Sodium chloride	58.44	1.75	NaCl	30
•Minerals solution, 100X stock		10 mL		see below
•Vitamins solution, 100X stock		10 mL		see below
•Amino acid solution, 100X stock		10 mL		see below
•Fumaric acid (for growth in anaerobic conditions)	160.1	4.8	C ₄ H ₂ O ₄ Na ₂	30
•Sodium lactate, 60%(w/w) syrup(@) (for bacterial growth)	112.1	11.206	C ₃ H ₅ O ₃ Na	100

Table 0-19: Vitamin mix

Chemical Description	FW	mg/L (100X stock)	Formula	Final conc. in medium (nM)
•biotin (d-biotin)	244.3	0.002	C ₁₀ H ₁₆ N ₂ O ₃ S	81.87
•folic acid	441.1	0.002	C ₁₉ H ₁₉ N ₇ O ₆	45.34
•pyridoxine HCl	205.6	0.010	C ₈ H ₁₂ ClNO ₃	486.38
•riboflavin	376.4	0.005	C ₁₇ H ₂₀ N ₄ O ₆	132.84
•thiamine HCl 1.0 H ₂ O	355.3	0.005	C ₁₈ H ₁₈ Cl ₂ N ₄ OS	140.73
•nicotinic acid	123.1	0.005	C ₆ H ₅ NO ₂	406.17
•d-pantothenic acid, hemicalcium salt	238.3	0.005	C ₉ H ₁₆ NO ₅ · 1/2Ca	209.82
•B12	1355.4	0.0001	C ₆₃ H ₈₈ CoN ₁₄ O ₁₄ P	0.74
•p-aminobenzoic acid	137.13	0.005	C ₇ H ₇ NO ₂	364.62
•thioctic acid	206.3	0.005	C ₈ H ₁₄ O ₂ S ₂	242.37

Table 0-20: Mineral mix

Chemical Description	FW	g/L (100X stock)	Formula	Final conc. in medium (μM)
•nitrilotriacetic acid(a)	191.1	1.5	C ₆ H ₉ NO ₃	78.49

(dissolve with NaOH to pH 8)				
•magnesium sulfate heptahydrate	246.48	3	MgSO ₄ 7H ₂ O	121.71
•manganese sulfate monohydrate	169.02	0.5	MnSO ₄ H ₂ O	29.58
•sodium chloride	58.44	1	NaCl	171.12
•ferrous sulfate heptahydrate	277.91	0.1	FeSO ₄ 7H ₂ O	3.60
•calcium chloride dihydrate	146.99	0.1	CaCl ₂ 2H ₂ O	6.80
•cobalt chloride hexahydrate	237.93	0.1	CoCl ₂ 6H ₂ O	4.20
•zinc chloride	136.28	0.13	ZnCl ₂	9.54
•cupric sulfate pentahydrate	249.68	0.01	CuSO ₄ 5H ₂ O	0.40
•aluminum potassium disulfate dodecahydrate	474.38	0.01	AlK(SO ₄) ₂ 12H ₂ O	0.21
•boric acid	61.83	0.01	H ₃ BO ₃	1.62
•sodium molybdate dihydrate	241.95	0.025	Na ₂ MoO ₄ 2H ₂ O	1.03
•nickel chloride hexahydrate	237.6	0.024	NiCl ₂ 6H ₂ O	1.01
•sodium tungstate	329.86	0.025	Na ₂ WO ₄ 2H ₂ O	0.76

Table 0-21: Amino acids mix

	g/L (100X stock)	Final conc. in medium (mg/L)
L-glutamic acid	2	2
L-arginine	2	2
DL-Serine	2	2

B3: Growth curves in different anaerobic mediums

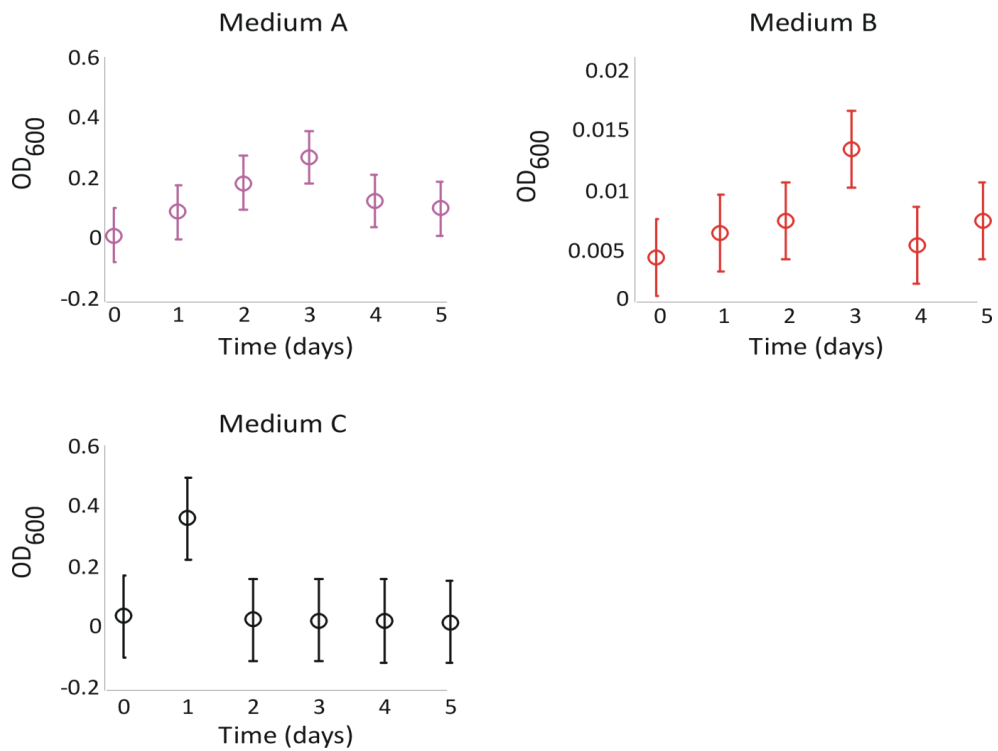
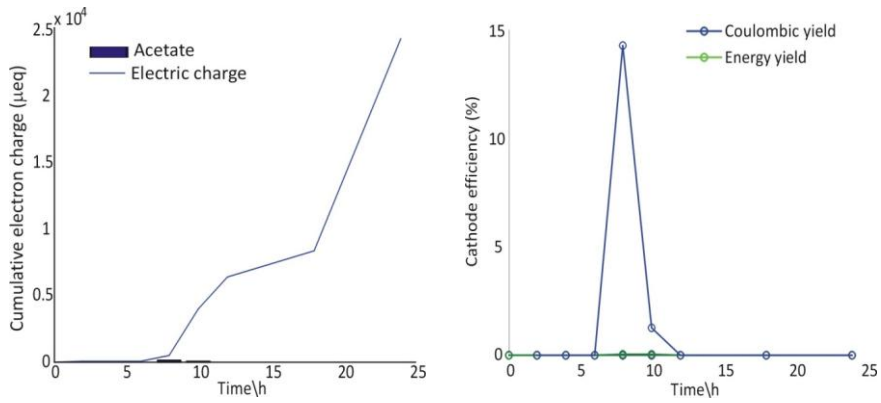


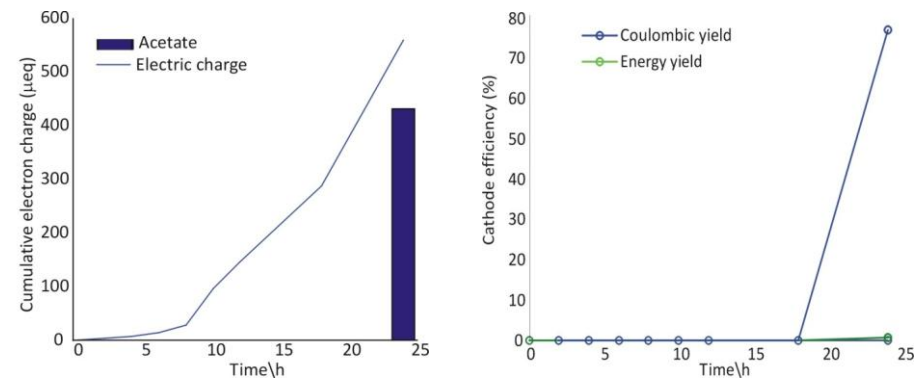
Figure 0.2: *Shewanella Oneidensis* MR-1 growth curves in three different anaerobic growth mediums. Each experiment was performed in quadruplicates (n=4).

C1 – Bioproduction at -0.2 V polarization

BES1:

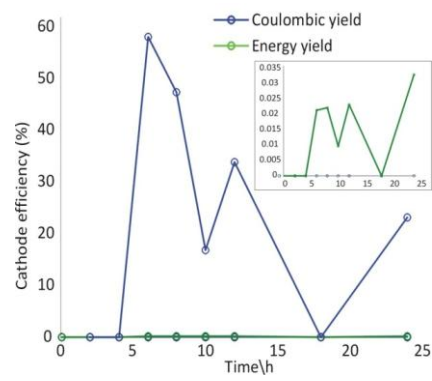
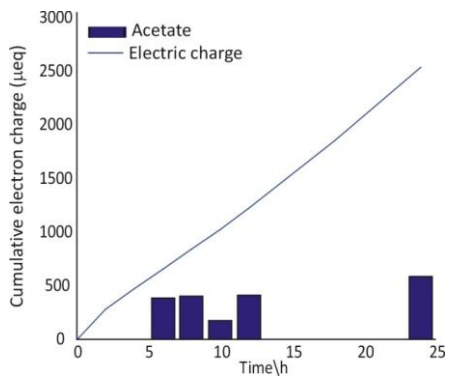


BES2:

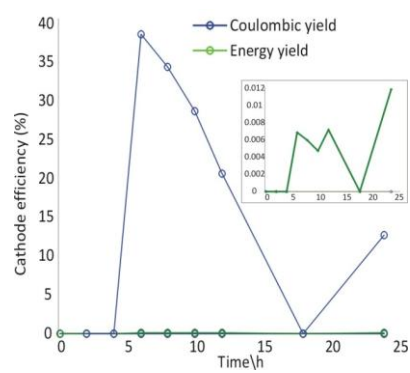
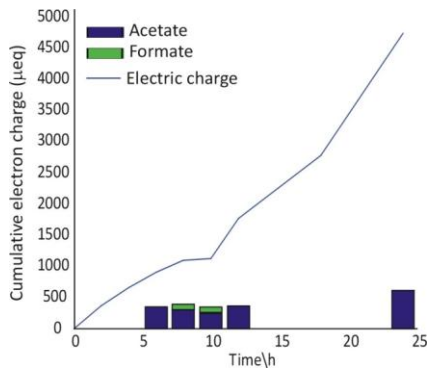


C2 – Bioproduction at -0.4 V polarization

BES1:

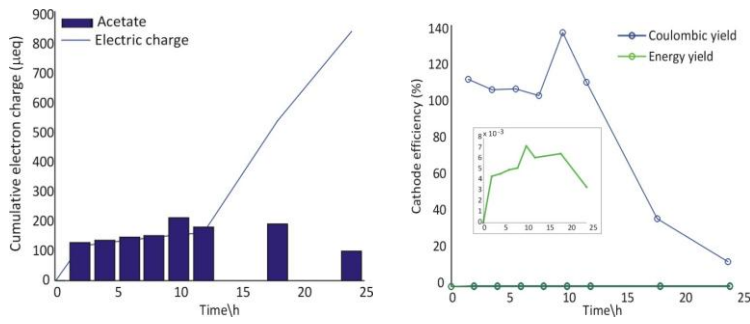


BES2:

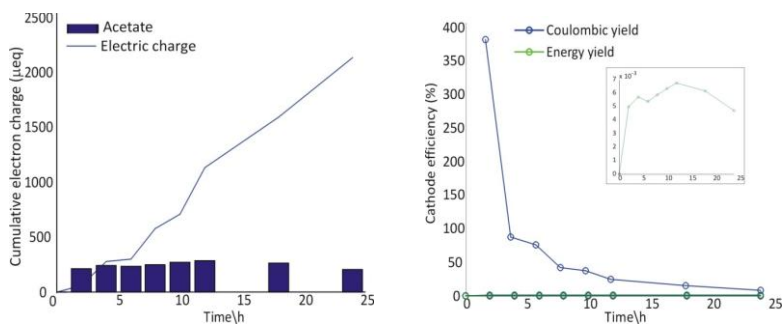


C3 – Bioproduction at -0.6 V polarization

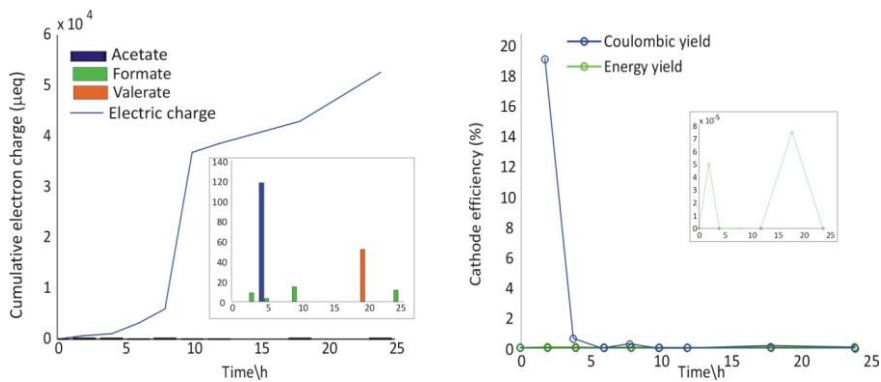
BES1:



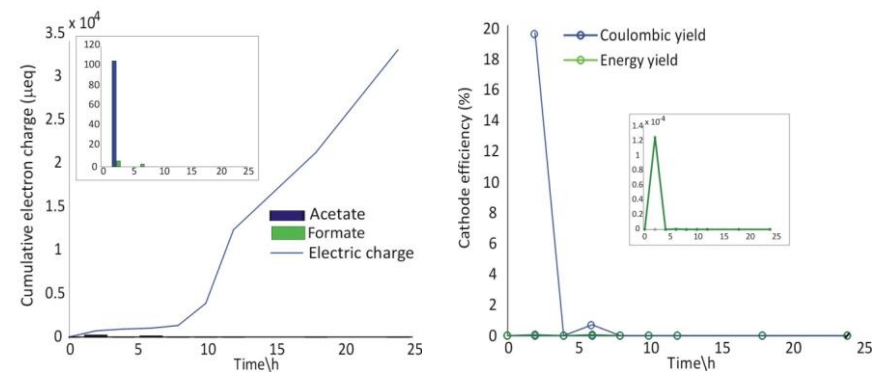
BES2:



BES3:

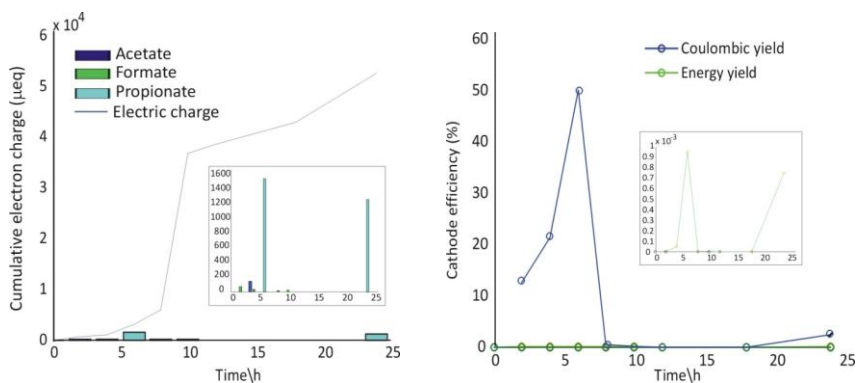


BES4:

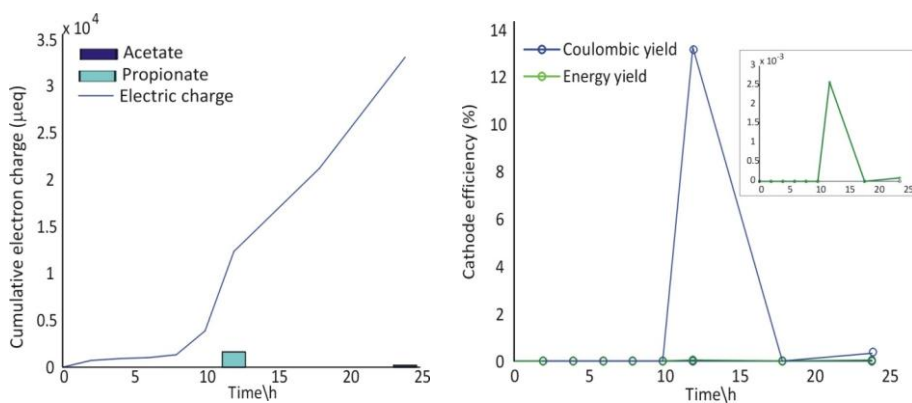


C4 – Bioproduction at -0.8 V polarization

BES1:



BES2:



C5 – Total organic carbon and volatile fatty acid bioproduction

Table 0-22: Total organic carbon and volatile fatty acids analyses based on different polarizations

Polarization potentials	TOC (mg/L)	VFA ($\mu\text{mol/L}$)
-200	13.550	0.000
-200	8.291	53.860
-400	20.520	73.390
-400	18.380	75.390
-600	19.420	24.811
-600	146.400	12.250
-600	28.560	6.510
-600	147.800	0.000
-800	81.700	12.840
-800	23.500	204.108

C6 – Live/Dead analysis

Table 0-23: Live/Dead cells count before and after CO₂ addition

Reactors	Live/before	Live/after	Dead/before	Dead/after
BES 1	333	340	229	157
	171	38	137	36
	18	43	57	46
	26	45	62	48
	20	11	94	82
	77	20	54	104
	17	36	21	74
BES 2	282	208	115	558
	17	75	69	135
	26	30	75	40
	50	11	150	148
	67	10	160	259
	34	15	170	135

D1: Mann Whitney U-test and p-values

Table 0-24: Mann Whitney U-test of operating conditions and electrode pre-treatment effect on lag phase, electric current generation, live/dead cells count and electrode coverage. The 'p' values and Wilcoxon test values are at a confidence level of 95% ($\alpha=0.05$)

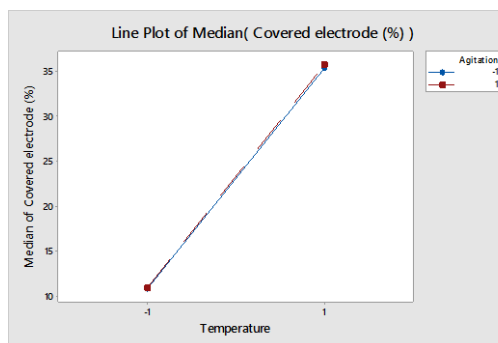
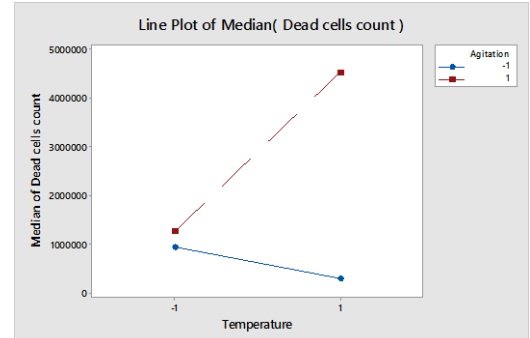
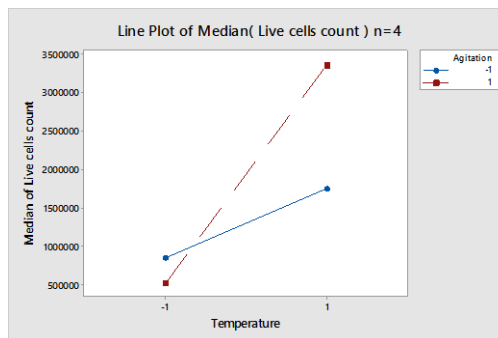
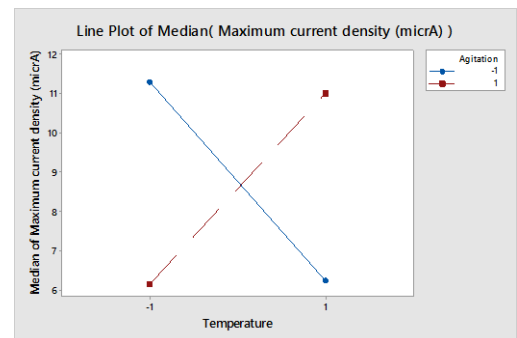
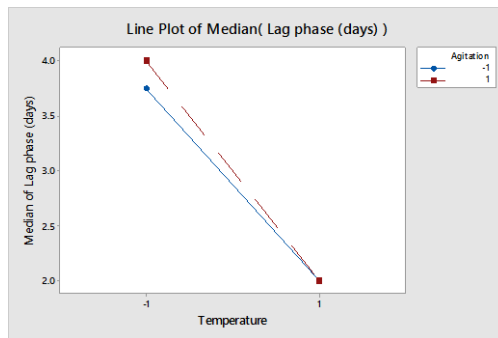
(n=8)	Lag phase (days)	Current generation (μA)	Live cells count (cells)	Dead cells count (cells)	Electrode coverage (%)
Temperature 15 °C vs. 30 °C	Md _{150C} =4	Md _{150C} =6.30	Md _{150C} =743481	Md _{150C} =1051305	Md _{150C} =10.83
	Md _{300C} =2 p=0.2701	Md _{300C} =6.75 p=0.4309	Md _{300C} =2360477 p=0.0181	Md _{300C} =1167382 p=0.6365	Md _{300C} =35.29 p=0.0009
Agitation 90 rpm vs. 140 rpm	Md _{90rpm} =2	Md _{90rpm} =6.25	Md _{90rpm} =1617732	Md _{90rpm} =611976	Md _{90rpm} =23.55
	Md _{140rpm} =2 p=0.7527	Md _{140rpm} =8.50 p=0.9581	Md _{140rpm} =909515 p=0.7132	Md _{140rpm} =1442881 p=0.0054	Md _{140rpm} =19.99 p=0.9581
Pre-treatment: Closed circuit vs. Open circuit	Md _{CC} =4.25	Md _{CC} =3.05	Md _{CC} =785357	Md _{CC} =712625	Md _{CC} =22.46
	Md _{OC} =2 p=0.0460	Md _{OC} =12.05 p=0.0136	Md _{OC} =1692667 p=0.1563	Md _{OC} =1194565 p=0.4309	Md _{OC} =19.99 p=0.7132

D2: Electrochemical analysis

Table 0-25: Peaks identified from cyclic voltammetry

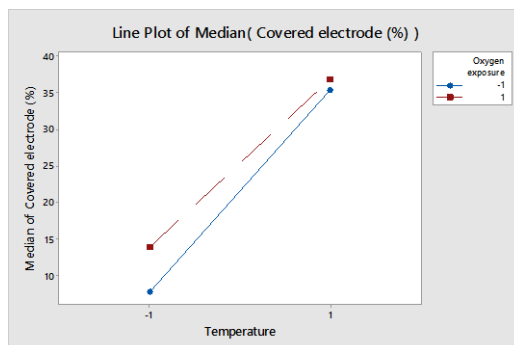
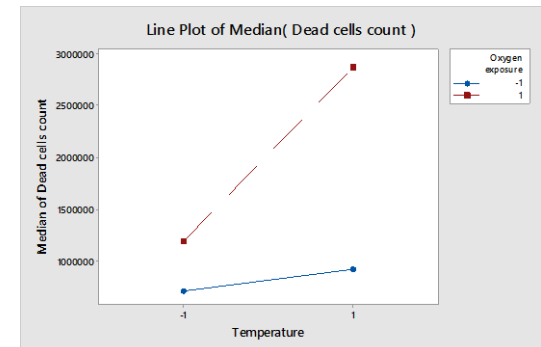
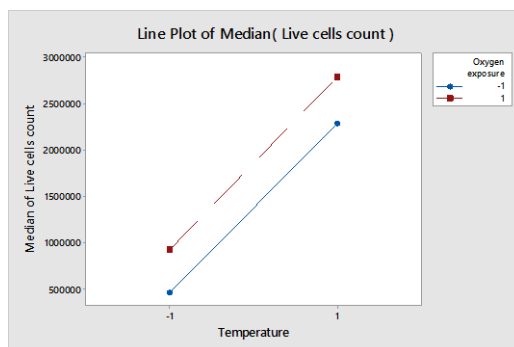
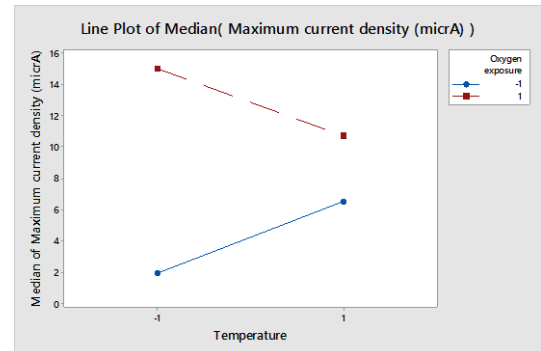
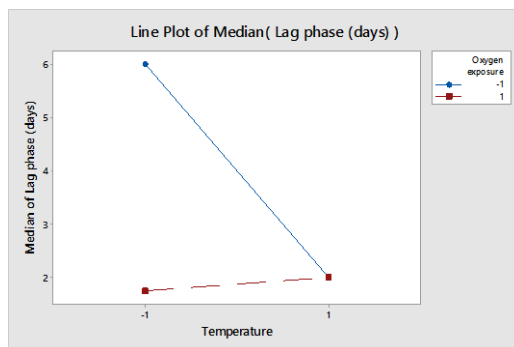
	90 rpm and 30 °C		90 rpm and 15 °C		140 rpm and 30 °C		140 rpm and 15 °C	
	E _c	E _A	E _c	E _A	E _c	E _A	E _c	E _A
MFC reactors	none	none	none	none	none	none	-0.35	-0.3
	none	none	none	none	none	none	0.2	0.3
Fluid mechanics reactors	none	none	-	0.3	none	none	0.1	0.2
	none	none	-	0.54	none	none	-0.45	-0.3
	none	none	-	none	none	none	0.1	0.2
							-0.45	-0.3

D3: Two way interaction tests: Temperature & agitation



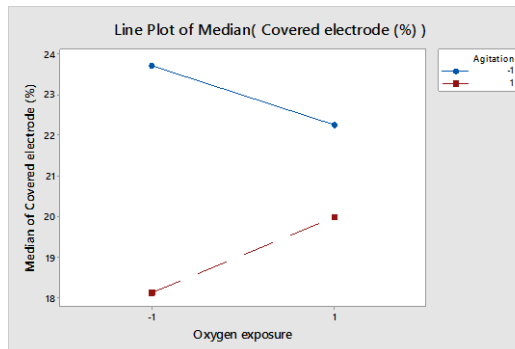
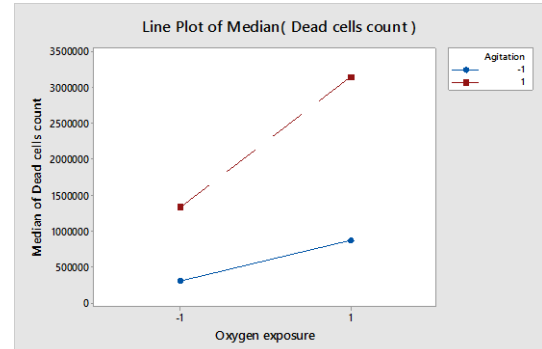
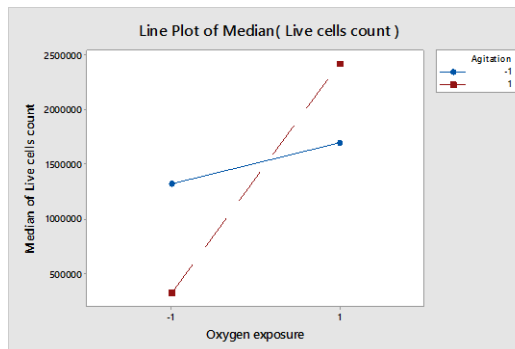
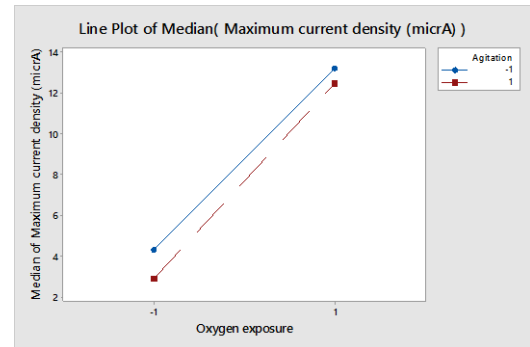
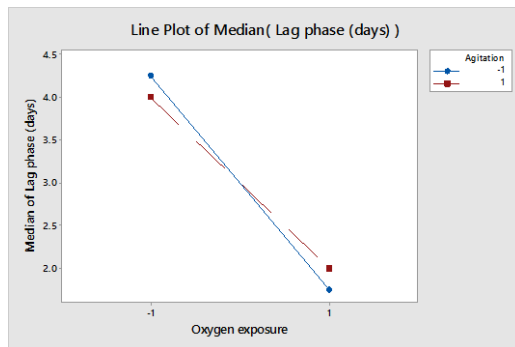
- With the data we have we can see trends that temperature and agitation might affect live cells count, current density and dead cells count
- More data needed to evaluate whether there is a real interaction between temperature and agitation

D4: Two way interaction tests: Temperature & oxygen exposure



- With the data we have we can see trends that temperature and oxygen exposure might affect lag phase, current density and dead cells count
- More data needed to evaluate whether there is a real interaction between temperature and oxygen exposure

D5: Two way interaction tests: Agitation & oxygen exposure



- With the data we have we can see trends that oxygen exposure and agitation might affect lag phase, live and dead cells count, current density and electrode coverage
- More data needed to evaluate whether there is a real interaction between temperature and agitation